COORDINATING AUTHOR'S PREFACE

ALWYN WILLIAMS
[University of Glasgow]

The first edition of Part H, Brachiopoda, of the *Treatise on Invertebrate Paleontology* predated, by months rather than years, the publication of ZUCKERKANDL and PAULING's proposition (1965) that genetic macromolecules are "documents of evolutionary history" (p. 357), HENNIG's *Phylogenetic Systematics* (1966), and the results of the earliest electron microscopic studies of the brachiopod shell (SASS, MONROE, & GERACE, 1965; TOWE & HARPER, 1966; WILLIAMS, 1966). The limitations imposed on our understanding of the phylum by the unavailability of these revolutionary methods of classifying and studying organisms are well illustrated by the first edition itself. Cluster analysis had been used sporadically (WILLIAMS, 1965, p. 243; WILLIAMS & WRIGHT, 1965, p. 301) to identify trends in stratigraphic distributions of fossil assemblages and in the modal morphologies of orthidines. The structure of the shell in relation to its secreting mantle had also been widely studied to ascertain taxonomically important changes in the skeletal fabric of extinct and living species. Moreover, the section on shell composition (JOPE, 1965) is now hailed as a pioneer systematic exploration of the degradation of the organic residues (episemantic molecules of ZUCKERKANDL & PAULING, 1965, p. 358) of representative living and fossil shells of marine invertebrates. These methods, however, hardly compare with the sophisticated protocols afforded by computers, electron microscopes, and amino-acid analyzers, which are among the wide range of facilities used in the preparation of this revision.

Yet crucial as these facilities have been to the continuing advancement of the natural sciences as a whole, the prime source of upsurge in recent brachiopod research has been the first edition itself, which was the first comprehensive account of all brachiopod genera since the ZITTEL series (1880, *et seq.*). Its publication in 1965 was most opportune, as the number of brachiopod genera had increased fivefold over those recognized by HALL and CLARKE (1892–1894) to nearly 1,700. Monographs and catalogues of the phylum appearing between 1894 and 1965 indicate that new genera were being proposed at a fairly steady rate of just under 20 per year, with new discoveries being described at about one-half the rate of those created by continual taxonomic revision (WILLIAMS, 1957). In contrast, between 1965 and March 1995 (the generally observed deadline for the retrieval of taxonomic data for inclusion in the revision) about 2,000 new genera were proposed. Even assuming an abnormally high proportion of invalid or synonymous genera, the annual rate of creation has been four to five times that obtaining prior to the publication of the first edition. Moreover, a casual scrutiny of post-1965 literature confirms that many of the new taxa were long-established species upgraded to generic rank to conform with the taxonomic practices of the first edition. However, significant numbers of new genera were also erected for specimens recovered from previously poorly known geological successions in Australia, North Africa, and especially Asia, where Chinese and Russian colleagues have not only collaborated in revising many brachiopod groups but also willingly provided all contributors with relevant translations and illustrations that would otherwise have remained inaccessible.

These extraordinary increases in new genera were not the only consideration prompting a thorough revision of the 1965 edition. Brachiopod evolution and biology have also attracted keen interest among scientists other than taxonomists. Brachiopods are probably unique among metazoans in the continuity and diversity of their geologic record. They were well represented among the earliest

Cambrian fossil assemblages and quickly dominated most ecological niches available for sedentary benthos. By Ordovician times, they had attained maximum diversity in those stem groups determining the main lines of phyletic descent and had reached the peak of generic proliferation by the Devonian. Thereafter, these ciliary suspension filter feeders, notwithstanding their lower oxygen consumption rates, were increasingly displaced by the more efficient, filter-feeding and deposit-feeding molluscs as the dominant shellfish of most benthic environments. There is some evidence that brachiopod diversity, as measured by fluctuations in the numbers of contemporaneous genera recorded throughout the geological column, has been increasing since the end of the Mesozoic. Even so, fewer than 4 percent of the genera currently assigned to the phylum are represented by living species.

Living brachiopods, however, are modest only in the number of described species as they are cosmopolitan in distribution and intertidal to abyssal in habit. Moreover, although they have been sidetracked within the protostomous mainstream of metazoan phylogeny, which accounts for their comparative neglect by biologists throughout much of the twentieth century, their ubiquity in time and space has stimulated multidisciplinary research into evolutionary aspects of many of the biological systems of brachiopods. Within the last two decades there have been significant new biochemical, ecological, embryological, genetic, and physiological investigations that have radically changed our understanding of the phylum. Accounts of brachiopod anatomy and embryology were included in the first edition. They were, however, largely based on the studies of the great Victorian naturalists in Europe and North America. Unsurprisingly, many of these classical investigations have stood the test of time; but they were necessarily limited in scope (especially at the cytological level) and selective in their coverage of the main groups of living species.

Anatomical studies in particular have been used by paleontologists to understand the biological significance of fossil morphology and thereby furnish reconstructions of ancient life forms. Such enterprise can, however, lead to a blurring of the distinction between observation and interpretation. Even BEECHER's classification (1892), based on the nature of the pedicle opening, was founded on a mixture of published accounts of the embryology of the living shell and assumptions on the anatomical significance of the delthyrial structures of long extinct stocks.

This widespread practice is understandable as the overwhelming weight of evidence for brachiopod evolution is the shell morphology of extinct groups. But it raises presentational problems when one is attempting to cover the natural history of the phylum as a whole. Should the fossilized shell and the inferred secreting epithelium of extinct strophomenides, for example, be discussed in the context of mantle anatomy or primarily as a chemicostructural variant of the biomineralized component of the integument? The issue was addressed during the preparation of the first edition. It was agreed that skeletal morphology, the variability of which is dominated by extinct features, should be described separately from the anatomy of the shell. This separation has been criticized as a "regrettable symptom of the divorce between neontology and palaeontology" (RUDWICK, 1970, p. 10), without any apparent awareness of the importance of distinguishing between fact and inference. The issue was reconsidered when the layout of the revision was being formulated and no overriding reason emerged to break with precedence.

In the broader perspective of affording brachiopodologists access to both neontological and paleontological methods, the range of specialties of current contributors should be reassuring. Only one of the 19 authors of the first edition was not a paleontologist-taxonomist compared with ten of the 45 contributors to the revision. These

transdisciplinary investigations of all aspects of the phylum have already made their mark even on a classification founded on shell morphology, with familial lineages as well as the broad-frame taxonomic hierarchy being reviewed in the light of genomic studies. Indeed the multidisciplinary nature of much recent research on the phylum and its constituent species can be shown in a brief review of the changes in content and topic of this *Treatise* compared with the 1965 edition.

The anatomy section has been entirely rewritten to include the main features of post-1965 investigations, which account for more than two-thirds of the cited references. Basic advances have been made in our understanding of most aspects of brachiopod anatomy, not least of which are the digestive system and gametogenesis. Especially noteworthy for their impact on phylogenetic studies, however, are the processes of mantle secretion and the elucidation of crucial phases in the development of the craniid larva.

The section on the brachiopod genome, not surprisingly, is even more modern in conception and execution. The earliest known paper on brachiopod genetics did not appear until 1975 (Ayala & others, 1975), and of the hundred or so cited references only one work earlier than 1965 merits special mention—Darwin's *Origin of Species* (1859b). Indeed, the research into the genetic constitution of 30 brachiopod species, which was undertaken and described by the authors of the section, was not conceived until 1987. It has, therefore, been a noteworthy feat to have obtained results in time for their use in the preparation of a broad-frame classification of the phylum as well as for inclusion in this first volume of the revision.

The section on physiology and metabolism is new, not through neglect of the topics in the first edition but as a result of a recent burgeoning interest in the way brachiopods live, as is confirmed by the fact that 90 percent of cited references were published in 1965 or later. Much of this interest has been stimulated by a growing desire to know how extinct groups functioned. Accordingly, research has tended to concentrate on those activities such as physiology of growth, musculature, and feeding that are more readily recognized as indicators of the life-styles and habits of fossil species.

Skeletal biochemistry and shell structure, in contrast, were described in the first edition, although they, too, are essentially modern studies so that the reviews herein are based largely on research undertaken since 1965. The brachiopod exoskeleton is rich in a wide range of organic polymers occurring as intracrystalline and intercrystalline components of differently structured apatitic and calcitic shells. This chemicostructural differentiation of the shell is now being chronicled throughout brachiopod phylogeny, as recounted in those sections of this volume.

The section on morphology has changed the least since its publication in 1965. The heart of the section is the glossary of morphological terms. When these terms were collated for the first edition, more than 700 were found scattered throughout the literature. Many of them were being used idiosyncratically, and a large number were redundant to our understanding of shell morphology and even obscured homologous relationships. Spurred (and stung) by the comment that it is "habitual with paleontologists to create a formidable terminology to cover every minute detail of extinct exoskeletons" (Hyman, 1959b, p. 525), authors heavily pruned the list, although about 500 terms survived—almost as many words as in the basic English vocabulary! Moreover, a few contributors refused to accept any economy of jargon and continued to use a personal vocabulary, to the detriment of the first edition. In preparing the revision, four versions of a continually revised glossary were circulated in the largely realized hope of achieving unanimity on the definition and selection of approved terms. Even so, nearly 500 of over 800 terms have survived scrutiny and are used in this edition. With respect to

the general part of the morphology section, the most significant improvements include the scrapping of a labyrinthine terminology to describe the loop based on generic names and intelligible to only a few specialists; a rationalization of terms used for homologous parts of various articulatory devices; and the application of a better understanding of shell structure to elucidate the growth and function of various features.

In revising the section on ecology, an important policy decision had to be made. The 1965 review touched upon brachiopods in their past and present habitats with an emphasis on autecological aspects. At the time it was recognized that the almost total neglect by zoologists of brachiopod ecology had left paleoecological studies without any rigorous comparative standards. As a result, much of what was then being reported in this field was of "dubious validity" (RUDWICK, 1965a, p. 199) and would have to be discarded in due course. Since 1965, there has been a most welcome interest in the ecology of living species although accompanied by a disproportionate increase in paleoecological studies. Some of the latter will undoubtedly prove to be based on sound inferences. Most, however, have been founded on more tenuous speculation, and their merits have yet to be rigorously tested by further evidence. Such literature is, therefore, potentially ephemeral, and it would presently be fortuitous to single out those studies that will emerge as models for future investigations. In these circumstances it was decided to restrict the ecological section of the revision to those interpretations, mainly autecological, that are firmly upheld by field and laboratory observations of living inarticulated as well as articulated species.

The organization of the rest of the revision has been changed in line with the sequence of processing the taxonomic data. The remaining volumes of this revision will carry brief forewords. In addition, the systematic descriptions of Volume 2 will be prefaced by an account of the classification of the phylum as a whole, while those of the final volume will end with sections on evolution and stratigraphic distribution that cannot be completed until the diagnoses and geological ranges of all taxa are known. Such reviews will benefit from the many novel studies published over the last thirty years that have further clarified the scope and pace of phylogenetic diversification, proliferation, and extinction. On the other hand, the greatest challenge of the entire revision has been to produce a classification that is compatible with brachiopod genealogy while facilitating routine identification, one of the main aims of the *Treatise.*

The classification used in this revision is a hybrid device. When the revision was launched in 1989, contributors recruited for the project were assigned genera in groups delineated in the original volume. In effect, the empirical classification of 1965, based on morphological comparison at successive levels in the hierarchy, determined the taxonomic content and structure of assignments. At the time it was confidently believed that most of these suprageneric packages would prove to be monophyletic. In contrast, ordinal relationships within the Brachiopoda had already become controversial (HENNIG, 1966; ROWELL, 1982; GORJANSKY & POPOV, 1986). It was therefore decided to erect a classification in two stages. First, contributors would be responsible for grouping genera up to the superfamilial or subordinal rank. Second, the coordinating author and deputies (A. WILLIAMS, S. J. CARLSON, and C. H. C. BRUNTON) would provide a broad-frame classification for all higher taxa founded on genera. At the outset it was agreed that classifications at all hierarchical levels would be phylogenetically structured. With this in mind, an essay review of phylogenetic systematics was circulated in 1991 among all contributors by S. J. CARLSON in the hope that those who were unfamiliar with phylogenetic analysis would be encouraged to adopt such techniques in classifying and describing their assigned taxa.

The outcome has been mixed, with some contributors using phylogenetic methods

(PAUP, MacClade) in processing their data (Carlson, 1993b; Popov & others, 1993; Williams & Brunton, 1993) and others relying on qualitative procedures (Baker, 1990; Carter & others, 1994; Rong & Cocks, 1994). Such a cautious reaction is understandable, as many of the morphological features used in brachiopod classification have evolved repeatedly in the past and have, thereby, introduced a high level of homoplasy into the intraordinal classification of extinct groups. Even so, the information freely made available by all contributors was so comprehensive as to afford a unique opportunity to test the versatility of the revised, supraordinal classification (Williams & others, 1996). This broad-frame classification, which is mainly based on the anatomy and skeleton of living species, is compatible not only with orders erected on shell morphology for extinct groups throughout the geological record but also with the brachiopod genome as it is presently known. Whether new biological or paleontological evidence will prompt such profound reinterpretation of the homology or polarity of characters as to undermine this supraordinal classification remains to be seen. For the present, at least, the systematic descriptions presented in this revision of Part H on the Brachiopoda are set in a classification consistent with our current understanding of brachiopod phylogeny.

ACKNOWLEDGMENTS

This revision of Part H on the Brachiopoda was completed over a period of about eight years, by 45 contributors from thirteen countries. During that time all of us, almost without exception, enjoyed the support of various institutions—mainly our places of employment—universities, museums, marine stations, geological (and other) surveys and so on. We are indebted to such centers for providing the wide-ranging facilities that enabled us to complete our assignments. Most contributors have also benefitted from advice and gifts and loans of materials received from a host of experts and have had access to type collections throughout the world. These invaluable sources of information are too numerous to be listed here. Specific acknowledgments will be made in the forewords to the remaining volumes and, with regard to illustrations and loaned specimens, at the appropriate places in the text of the systematic descriptions.

There are a few persons and institutions meriting special mention at this juncture for their notable contributions to the progression of the project as a whole. Pride of place goes to Mr. R. A. Doescher of the Smithsonian Institution, Washington, D.C. and Mrs. S. Ogden at the University of Glasgow. Rex Doescher maintained the unique, computerized database on brachiopod taxa and literature (SIBIC, Smithsonian International Brachiopod Information Center), which owes its origin to Dr. G. Arthur Cooper and his wife Josephine, who for decades translated Russian (and other) taxonomic descriptions of brachiopods for general use by any student of the phylum. The database has ensured that all contributors, directly or through Glasgow, have been provided with the essential data on every proposed brachiopod genus. Sue Ogden maintained a continually updated variant of SIBIC in Glasgow, with the genera grouped into families and superfamilies and packaged according to assignments. She compiled annual returns for four years as integrated reports for circulation among contributors, which gave snapshot views of the progress of work in all its aspects. The accuracy and expedition of this revision are a testament to the dedication of these two colleagues.

In addition to institutional support, many contributors have also been awarded grants by research councils, foundations, learned societies, philanthropic trusts, and industry to undertake research and to visit museums and universities at home and abroad in connection with their *Treatise* assignments. Among the awards made in support of research programs were National Science Foundation grants (BSR 8717424 and DEB 9221453) to S. J. Carlson; grants from the

Swedish Natural Science Research Council, the Royal Swedish Academy of Sciences, and the Swedish Institute to L. Holmer and L. Popov; a grant from the University of Kansas Paleontological Institute to E. Owen; grants from the Royal Society to G. B. Curry, M. Cusack, and A. Williams; a grant from Natural Sciences and Engineering Research Council of Canada to P. Copper; grants from the Natural Environment Research Council to B. L. Cohen, G. B. Curry, M. Cusack, and A. Williams; grants from the Leverhulme Trust (F 179Z) and British Petroleum plc to A. Williams; a grant from the Richard Lounsberry Foundation to G. B. Curry; and a grant from the International Science Foundation, Washington, D.C., to T. Smirnova.

Awards toward expenses of travel and accommodation incurred during *Treatise* business included a grant from the Swedish Natural Science Research Council to M. Bassett, J. Laurie, and L. Popov; grants from the Natural Environment Research Council to nine British contributors; grants from the Royal Society of New Zealand to D. Lee; grants from the Royal Society of London to S. Lazarev, M. Mancenido, and A. Williams; grants from the University of Kansas Paleontological Institute and the Smithsonian Institution to N. Savage and from the latter source to L. Popov; and grants from the Consejo Nacional de Investigaciones Cientificas y Tecnicas of Argentina (CONICET) to M. Mancenido and the Royal Society of Edinburgh and the Carnegie Trust to A. Williams.

ANATOMY

ALWYN WILLIAMS[1], MARK A. JAMES[2], CHRISTIAN C. EMIG[3], SARAH MACKAY[1], and MELISSA C. RHODES[4]

[1University of Glasgow; 2Ministry of Agriculture, Fisheries, and Food, London; 3Centre d'Océanologie de Marseille; 4Academy of Natural Sciences, Philadelphia]

GENERAL CHARACTERS

The soft parts of all living brachiopods (HANCOCK, 1859) are enclosed by a shell consisting of a pair of valves that typically are bilaterally symmetrical but dissimilar in size, shape, and even ornamentation. Posteriorly, the shell usually bears a variably developed fleshy stalk, the **pedicle,** which normally emerges from the **ventral** (or pedicle) **valve** (Fig. 1). The opposing valve, the **dorsal** (or brachial) **valve,** is generally smaller than the ventral valve. The body occupies the posterior part of the space inside the shell, and its wall is prolonged forward and folded as a pair of **mantles** that line the anterior inner surfaces of the valves to enclose the **mantle** (or brachial) **cavity** (Fig. 2). The body space (**coelomic cavity**) accommodates the digestive, excretory, and reproductive organs as well as muscle systems, some of which are responsible for movements of the valves relative to each other, including the opening of the shell (**gape**). The mantle cavity is separated from the body by the **anterior body wall** and contains the feeding organ or **lophophore** (Fig. 1–2). A nervous system and a primitive circulatory system are present.

Although the Brachiopoda are well defined as a phylum, living species segregate into three groups differing fundamentally in their development, anatomy, and gross morphology. **Articulated brachiopods** have invariably calcitic shells, with valves

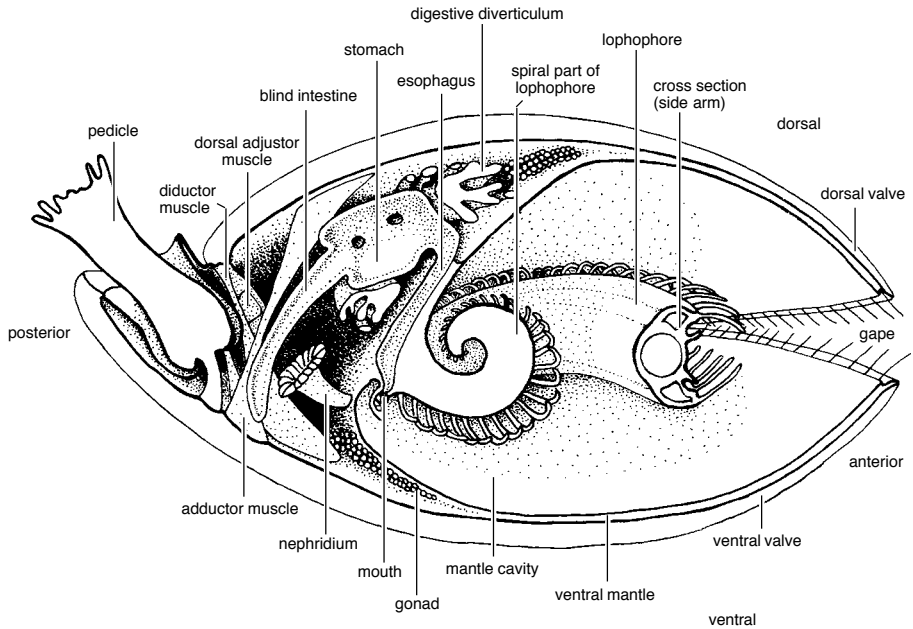

FIG. 1. Diagrammatic representation of the principal organs of the brachiopod as typified by *Terebratulina* (Williams & Rowell, 1965a).

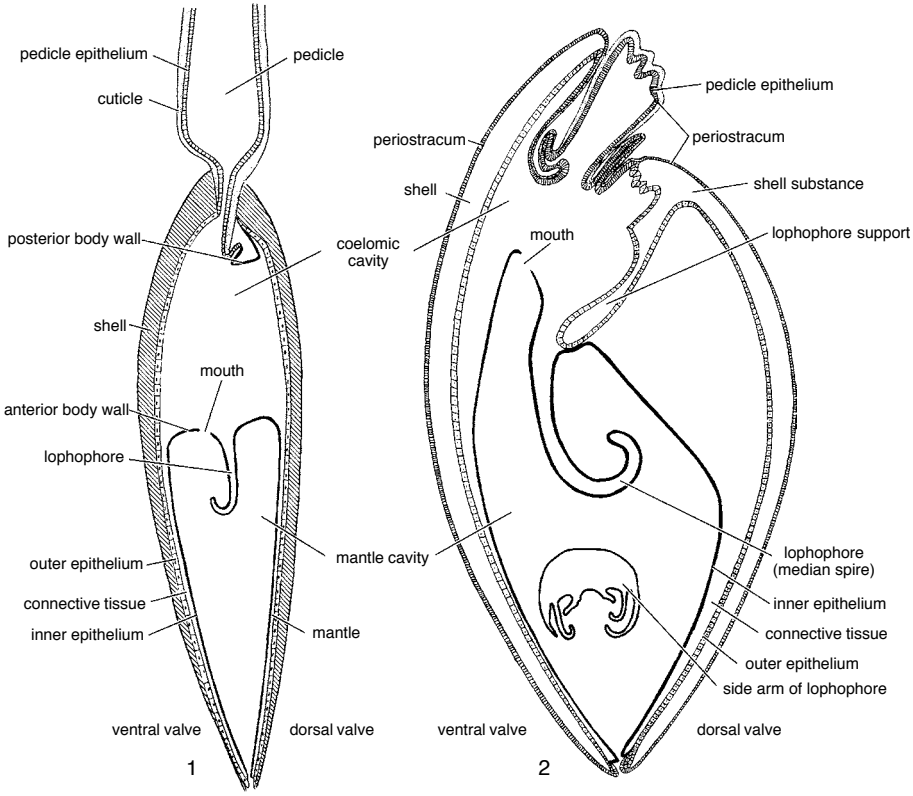

FIG. 2. Generalized representation of the distribution of epithelium *1,* in lingulids (Williams & Rowell, 1965a) and *2,* in terebratulids (Williams, 1956).

interlocking by **complementary teeth** and **sockets;** the dorsal valve is commonly equipped with outgrowths forming lophophore supports (Fig. 2.2). All organophosphatic-shelled brachiopods (lingulides and discinides) and the carbonate-shelled craniides are inarticulated with no biomineralized outgrowths developed for articulation or lophophore support. The lack of articulation permits rotation in the plane of the margins or **commissure,** and the musculature of inarticulated species is usually relatively complex. Other internal differences are even more profound. The pedicle of living articulated brachiopods develops from a primary segment of the larva, while that of the lingulides and discinides arises from evaginations of the ventral mantle. Living craniides lack even a rudimentary pedicle. The lingulides and discinides and the craniides are also distinguishable from one another as well as from articulated species in other respects. The biomineral constituents of their shells are apatite and calcite respectively with further significant differences in the organic content, especially the presence of chitin and collagen in the lingulide shell. Distinguishing features of the development and anatomy of the soft parts include differently disposed intestines (NIELSEN, 1991) and the loss of the anus among living articulated brachiopods.

In contrast to the wide diversity of most other anatomical features, the body wall of all brachiopods consists of an outer layer of ectodermal **epithelium** resting on a thin connective-tissue layer coated internally by a ciliated coelomic epithelium (peritoneum). In the mantles, coelomic epithelium is restricted in distribution, being limited to sinuses of the coelomic space permeating the

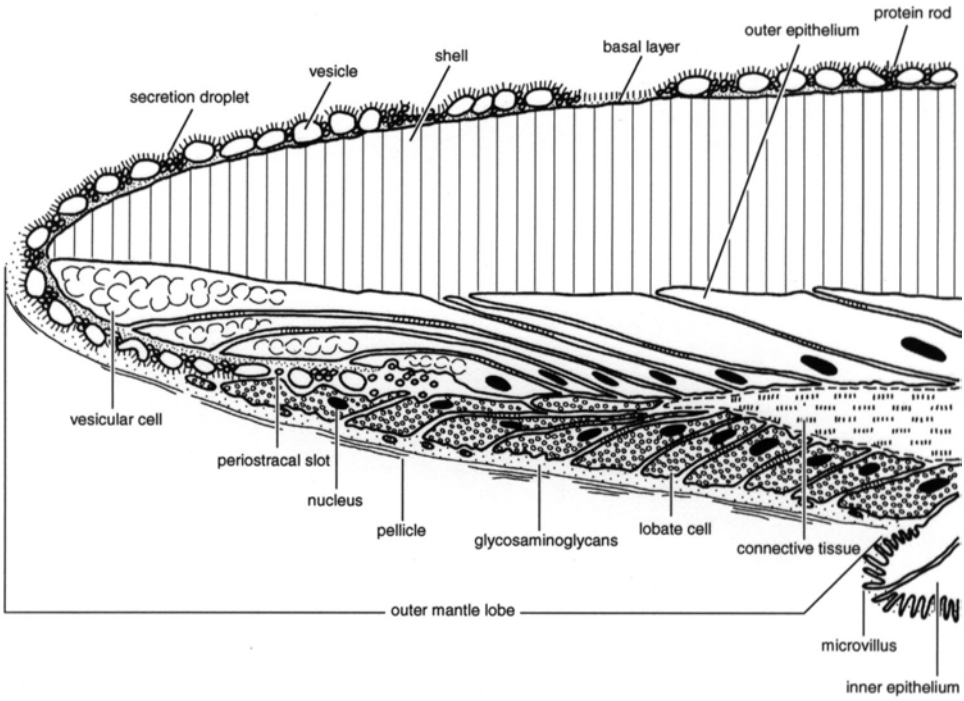

FIG. 3. Diagrammatic sagittal section of a valve of the terebratulide *Calloria* to show the outer mantle lobe in relation to the vesicles and basal layer of the periostracum and the underlying calcareous shell (adapted from Williams, 1990).

connective tissue (**mantle canals**) and unconnected marginal sinuses just within the mantle edges of organophosphatic brachiopods. The ectodermal epithelium is morphologically and functionally differentiated into a number of distinctive types. Posteriorly, it underlies and secretes a cuticular cover for the pedicle and is known as **pedicle epithelium** (Fig. 2). The zones responsible for the secretion of the biomineralized valves are referred to as **outer epithelium.** They are separated from the **inner epithelium** lining the mantle cavity by narrow strips of highly modified epithelium (**vesicular** and **lobate cells**) secreting various organic compounds, which occupy the hinge of the fold at the margins of both mantles. Within the mantle cavity, the inner epithelium is continuous with the selectively ciliated lophophore epithelium.

The adaptation of the ectoderm to secrete a biomineralized shell with outgrowths commonly of a complex nature occurred very early in the Phanerozoic so that the brachiopod phylum is well represented by a more or less continuous, fossilized skeletal record. Accordingly, it seems appropriate to begin this account of brachiopod anatomy with a description of the morphology and function of the ectodermal epithelium.

MANTLES AND BODY WALLS

The outer epithelium, which underlies the brachiopod shell and envelops its outgrowths, is continuous with the inner epithelium along the mantle margin. The junction almost invariably lies in a groove between two asymmetrical mantle lobes just within the shell edge (Fig. 3) and is a reference-datum horizon in describing the differentiation of the mantle. These epithelial sheets are separated by a layer of connective tissue that is invaded to a varying degree by extensions (mantle sinuses or canals) of the coelom and further modified to facilitate storage and stiffening.

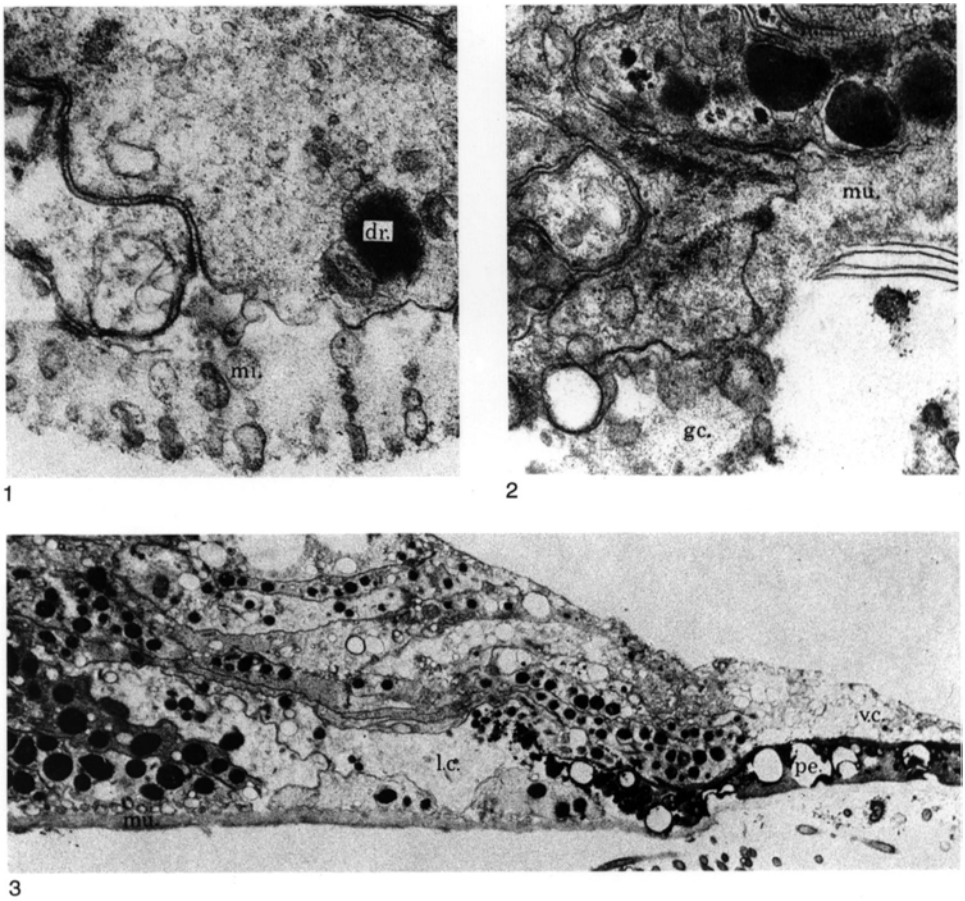

FIG. 4. TEM micrograph of mantle edge and periostracum of *Calloria inconspicua* (SOWERBY); *1,* inner epithelial cells (adjacent to lobate cells) bearing short microvilli (*mi*) and electron-dense droplets (*dr*), ×36,000; *2,* detail of the inner epithelium-lobate cell junction showing the disappearance of microvilli from the lobate cell apical plasmalemma and the continuation of the glycocalyx (*gc*) into the GAGs film (*mu*) of the lobate cells with pellicles to the exterior, ×36,000; *3,* sagittal section of the mantle edge showing the periostracum (*pe*) emerging from a slot between the lobate cells (*l.c.*) secreting a GAGs film (*mu*) and the vesicular cells (*v.c.*), ×3,600 (Williams & Mackay, 1978).

INNER EPITHELIUM AND CONNECTIVE TISSUE

The **inner lobe** at the mantle margin is a circumferential fold of inner epithelium. This layer typically consists of cuboidal, microvillous, monociliated cells with plasmalemmas disposed in folds especially adjacent to the basal lamina and well-developed, smooth endoplasmic reticulum, mitochondria, and Golgi complexes (Fig. 4.1). Vesicles and membrane-bound droplets of varying electron density, representing glycoproteins, lipids, and glycosaminoglycans (GAGs), are common. These inclusions, together with the products of widely distributed mucous cells are constantly exocytosed so that the fibrillar coats of the microvilli are always impregnated with a glycocalyx of variable electron density. The columnar cells of the inner mantle lobe lack cilia and are commonly distended with crowded vesicles of mucus (the gland cells of *Lingula* and *Discinisca*) but are regularly microvillous and represent marginal folds of inner epithelium (Fig. 4.1).

The connective tissue, enclosed within the basal laminae of both inner and outer

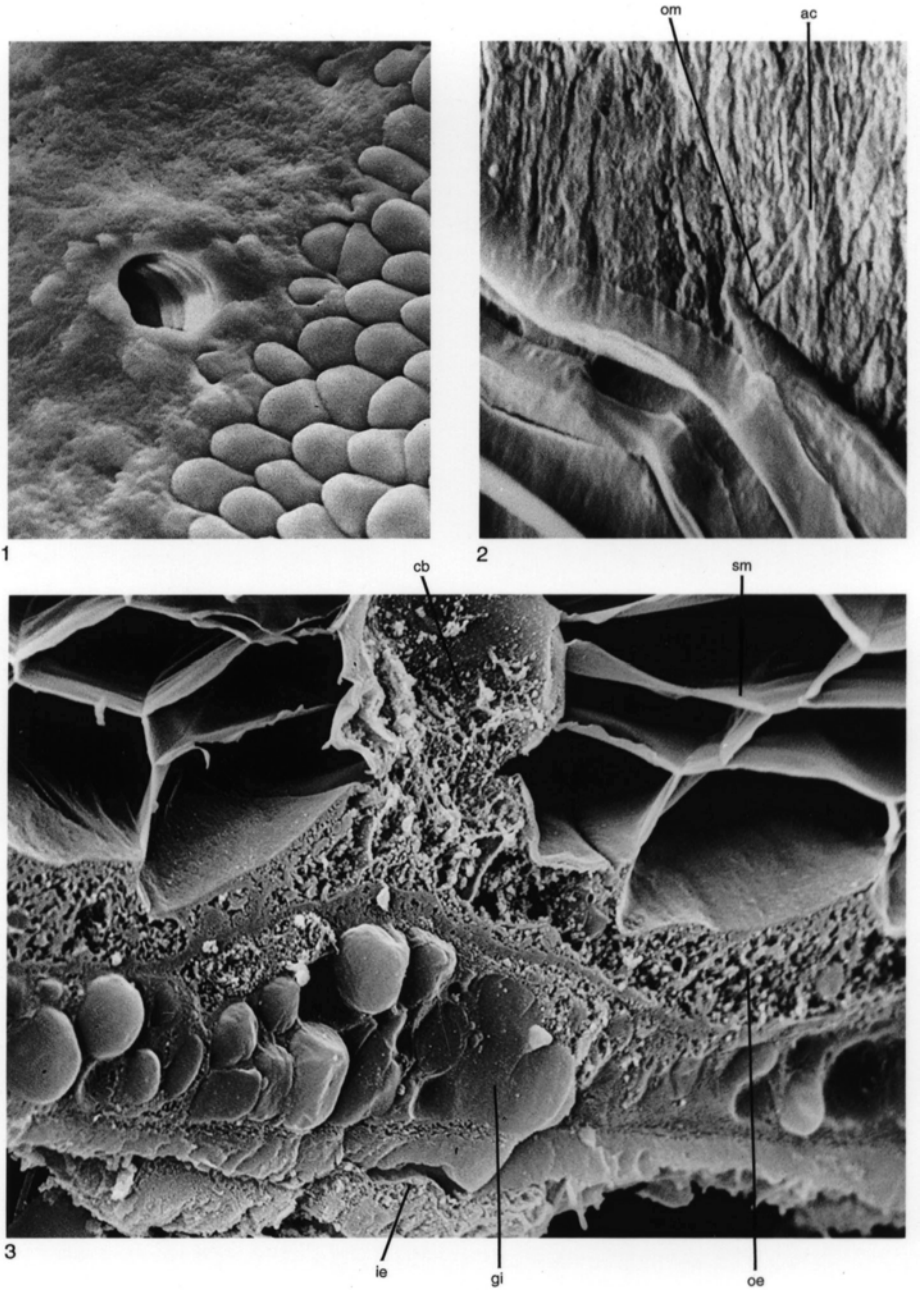

FIG. 5. Terebratulide secondary shell. *1,* SEM micrograph of the internal edge of a dorsal valve of *Gryphus vitreus* (BÖRN) showing the primary-secondary shell junction with incipient fibers forming on the granular primary layer to the left, especially around the puncta, ×1,235; *2,* SEM micrograph of an etched submedian longitudinal section of the shell of *Liothyrella neozelanica* THOMSON showing acicular crystallites (*ac*) of the primary shell terminating at oblique, smooth boundaries representing the onset (*om*) of the membranes sheathing the secondary fibers below, ×6,840; *3,* SEM micrograph of cryoprotected and etched fracture surface of the mantle underlying a caecal base (*cb*) and the surrounding shell of *Calloria inconspicua,* showing interconnected membranes (*sm*) of the fibrous secondary layer and the collagenous storage zone with glycoprotein inclusions (*gi*), with the connective tissue between outer (*oe*) and inner (*ie*) epithelium, ×3,895 (new).

epithelia, is the typical extracellular matrix composed mainly of GAGs and fibrous collagens. The alignment of collagens is normally determined by localized stresses set up, for example, by penetrating distributaries of the mantle canal systems or by biomineralized bodies (**spicules**) secreted by clusters of mesenchymous cells (scleroblasts). Distension by such cavities and bodies tends to pack collagens into concentric swarms; and, where large sinuses are developed (as in the *vascula genitalia*), the connective tissue is compacted into columns subtended between the bounding epithelia. The most distinctive feature of the connective tissue in the brachiopod mantle, however, is a highly collagenous zone beneath the outer epithelium (HARO, 1963). Numerous lacunae within this zone usually contain membrane-free glycoproteins, glycogen granules, and, in *Glottidia* at least, other granules of a biomineral nature (PAN & WATABE, 1988a). The zone is evidently an important storage site (Fig. 5.3).

OUTER EPITHELIUM: OUTER MANTLE LOBE

The **outer mantle lobe** is a fold of outer epithelium that underlies the edge of the valve and forms the circumferential hinge of the mantle. The lobe controls the expansion of the mantle that lines a valve and, therefore, the peripheral growth of the valve itself. An outer lobe is composed of variously specialized secretory cells that are best illustrated by describing how components of a terebratulide integument are deposited in successive layers by the outer mantle lobe of *Calloria.*

In *Calloria* (WILLIAMS & MACKAY, 1978) the proximal inner surface of the outer mantle lobe is composed of a band of lobate cells, 10 to 12 deep in sagittal section. The lobate cells are distinguishable from adjacent inner epithelium: their secretory plasmalemmas are not regularly microvillous but disposed as irregular folds and protuberances, up to 0.5 μm long (Fig. 4.2–4.3; 6.2). They contain small and large vesicles, well-developed Golgi systems, and an increased number of electron-dense, membrane-bound droplets that are prominent among the constituents exocytosed at the apical plasmalemmas as a film of mucus bounded externally by impersistent, lightly fibrillar sheets lying in parallel packs. The film rolls forward to the edge of the outer mantle lobe and covers the **periostracum** proper.

The periostracum arises in a slot, up to 20 μm deep, separating the more distant lobate cells from four or five elongate vesicular cells that occupy the hinge of the outer mantle lobe (Fig. 4.3; 6.3). These cells overlap one another as tonguelike extensions and are distinguishable from the lobate cells in being crowded with vesicles that usually culminate in one, large structure immediately beneath the apical plasmalemma. In other respects, lobate and vesicular cells are very much alike, being characterized by an abundance of glycogen, the folded and cylindroid extensions of their secretory plasmalemmas, and the rarity of tight junctions between crudely fitting adjacent cells.

The **periostracal slot** is variably developed in other brachiopod groups. It is deeply inserted between vesicular and lobate cells in thecideidines (WILLIAMS, 1973) but is only a superficial indentation separating the vesicular and lobate cells of the rhynchonellide outer mantle lobe (WILLIAMS, 1977). The inarticulated lingulids also lack a periostracal slot but have previously been described as having a few lobate cells (WILLIAMS, 1977). In fact, these lobate cells are distinguishable

FIG. 6. TEM micrographs of the periostraca of various terebratulide brachiopods; *1,* periostracum of young *Calloria inconspicua* showing the basal layer (*b.l.*), vesicle (*ve*) surrounded by amalgamated droplets and the outer fringe of electron-dense rods (*rd*), ×36,000; *2,* periostracum of *Gwynia capsula* (JEFFREYS) arising between lobate cells (*l.c.*) and vesicular cells (*v.c.*) and consisting of a basal layer (*b.l.*) and an isoclinally folded, sheeted superstructure (*s.s.*), ×36,000; *3,* vesicular cells (*v.c.*) at the mantle edge of *Terebratulina retusa* (LINNÉ) bounded externally with periostracum (*pe*) extended into curled sheets (*cs*), within folds of a film of GAGs (*mu*) with an external polymerized pellicle (*pl*), ×9,000 (Williams & Mackay, 1978).

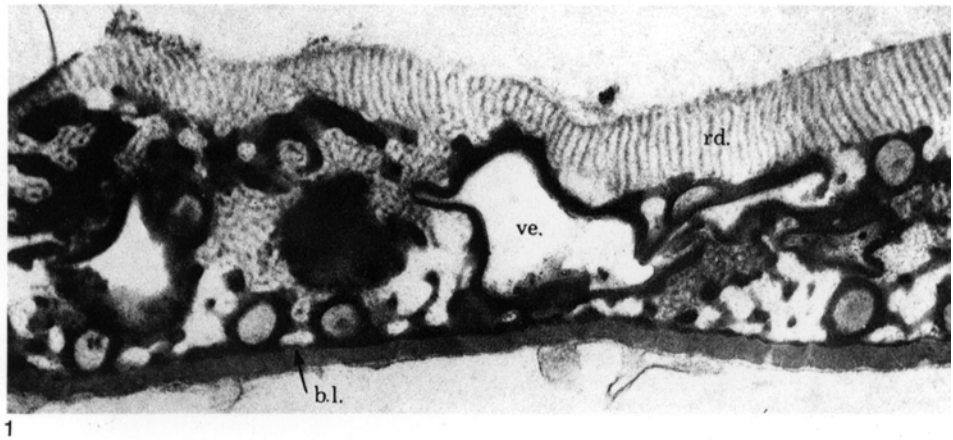

1

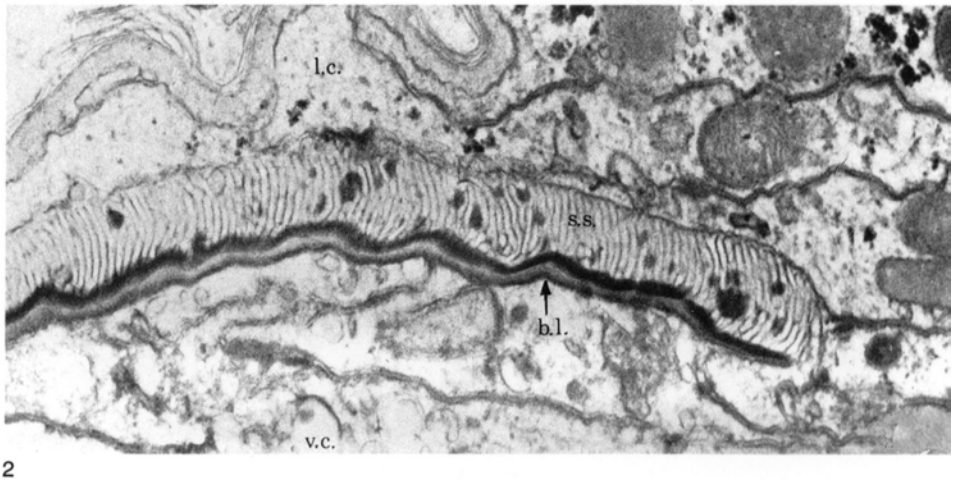

2

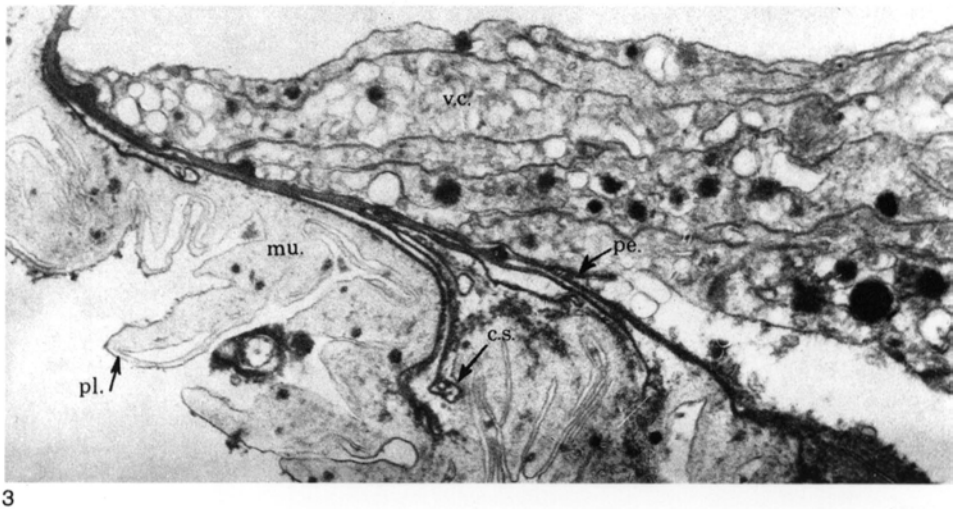

3

FIG. 6. *(For explanation, see facing page.)*

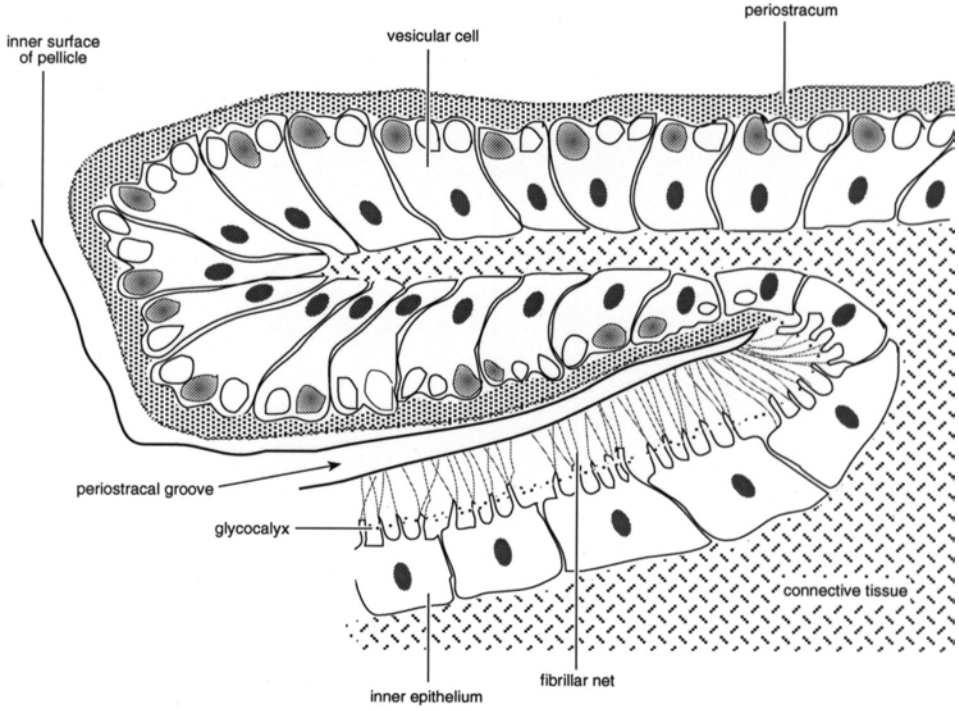

FIG. 7. Diagrammatic sagittal section of the edge of a valve of *Glottidia pyramidata* (STIMPSON) illustrating the differentiation of the periostracal lobe in relation to the inner epithelium (new).

from inner epithelium only in having shorter microvilli. Moreover, in discinids as well as lingulids, these cells act in unison with the inner epithelium in secreting the external surface of the pellicle, which is made up of fibrous constituents streaming from all microvillous plasmalemmas (Fig. 7–8). On balance, they are probably a modified fringe of inner epithelium along the junction with vesicular cells. This is also true of the inarticulated craniids (WILLIAMS & MACKAY, 1979).

The periostracum is a highly variable structure. In *Calloria,* the vesicular cells secrete a basal, electron-dense layer that thickens anteriorly away from its zone of origin by accretion on its proximal surface, which is consequently more irregular and less sharply defined than the distal surface (Fig. 3; 4.3). Indeed, the distal surface tends to be delineated as an electron-dense boundary underlain by a light layer to simulate a unit membrane about 20 nm thick. The entire layer ultimately attains a thickness of 100 nm before its proximal surface becomes the seeding sheet for the first-formed calcite crystallites of the primary carbonate layer of the shell.

As this basal layer is being exuded, large vesicles and clusters of smaller droplets accumulate on the inner surface (Fig. 6.1). The vesicles, which may be up to 1 μm in diameter, are usually stacked in densely packed groups so that they assume distorted outlines in sections. They are exocytosed through the plasmalemmas of the lobate cells forming the inner boundary to the periostracal slot. As the periostracum matures, the accumulating droplets tend to be emptied of their contents, which form accretionary layers of variable thickness around the vesicles and the droplets to give a labyrinthine aspect to these amalgamated bodies. In addition, the labyrinths are filled by an exudation that quickly polymerizes into regular, closely packed hex-

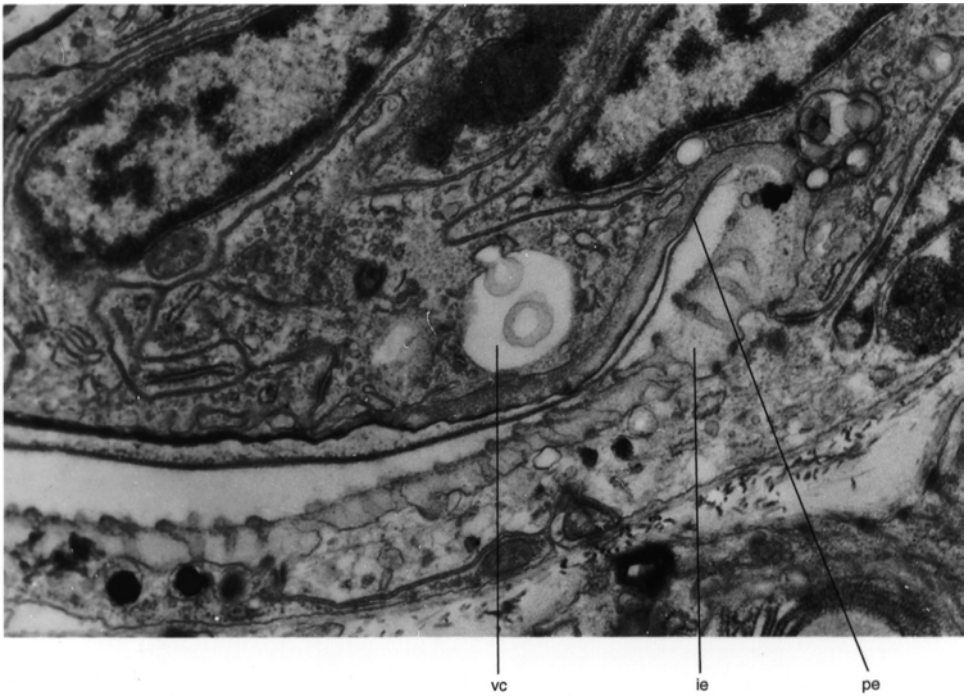

FIG. 8. TEM micrograph of the periostracal groove of *Lingula anatina* LAMARCK showing the origin of the double-layered pellicle (*pe*) secreted by inner epithelium (*ie*) and vesicular cells (*vc*), and the underlying periostracum, ×24,000 (new).

agonal rays of medium, electron-dense rods. The rods bear signs of being spirally constructed and of being joined to one another by fine fibrillar webs. This fibrillar matrix seems to be exuded by lobate cells in adults (WILLIAMS & MACKAY, 1978), but STRICKER and REED (1985a) have not ruled out the possibility that it can also be secreted (as can some vesicles) by vesicular cells, at least in juveniles.

Either way, a periostracum of varying complexity is continuously built up beneath the outer mucous film and is conveyed forward to the very edge of the outer mantle lobe. In *Calloria* and other terebratelloids, the periostracal succession is, therefore, a diachronous one consisting of a labyrinthine superstructure and a thickening basal layer that are secreted simultaneously on the outer and inner surfaces of the first-formed membranous component by the lobate and vesicular cells respectively (Fig. 9). It is noteworthy, however, in view of the limited variability of the periostracum of living species, that the terebratelloid labyrinthine superstructure, although characteristic of adult *Terebratalia,* is absent from the protegular periostracum, which is nothing more than a thin, amorphous, basal layer bearing a few electron-dense spheroidal bodies (STRICKER & REED, 1985b).

The terebratelloid periostracal succession is among the most complex so far known in living brachiopods as both superstructure and basal layer have been found to be variable (Fig. 9), although not below superfamilial rank (WILLIAMS & MACKAY, 1979). Thus, the superstructure may be absent as in the lingulids, craniids, rhynchonellids, and thecideidines. It is also absent from the periostracum of *Terebratulina,* which consists essentially of successions of sheets of the basal layer (Fig. 6.3), although in *Liothyrella* small, electron-dense secretion droplets are

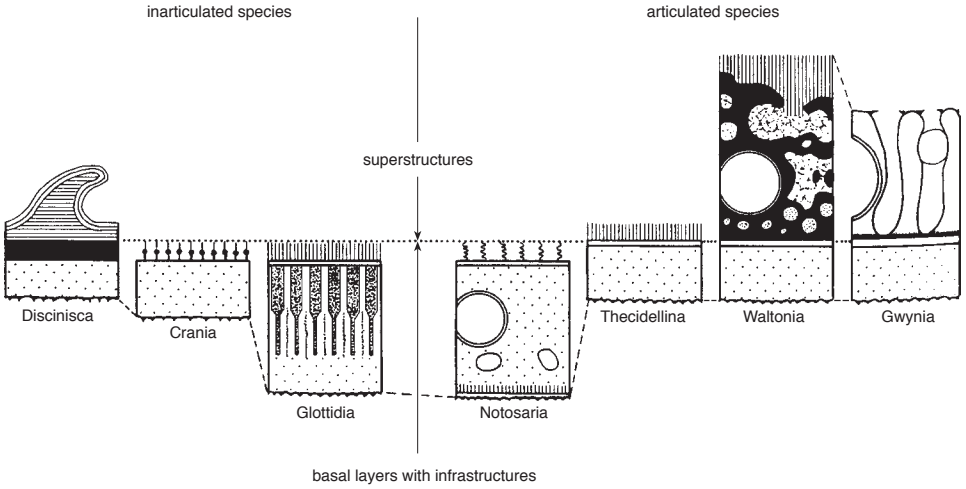

FIG. 9. The main types of periostraca characterizing inarticulated and articulated brachiopods (Williams & Mackay, 1979).

sporadically distributed on the external surface (comparable with the protegular periostracum of *Terebratalia*) and are secreted by lobate cells in the same way as the elaborate superstructure of *Calloria.* Moreover, both the enigmatic terebratulide *Gwynia* and the organophosphatic discinids have complex superstructures consisting respectively of folded proteinaceous sheets disposed normal to the basal layer (Fig. 6.2) and of concentric bands with thickened bases composed of up to 100 or so, electron-dense, fibrillar sheets disposed almost parallel with the basal layer (Fig. 10.1).

The basal layer can also consist of a variety of proteinaceous compounds, which, when banded, form chronological successions. The basal layer of the thecideidines consists of a simple, thickened membrane. That of the craniids is also essentially little more than a membrane with an outer coat of bulbous-tipped, fibrillar rods up to 30 nm high. In lingulids the distal surface of the basal layer polymerizes almost immediately after exudation into a coarsely fibrillar, unit membrane bounding a gradually thickening, medium, electron-dense, finely textured layer. When this inner layer attains a thickness of about 250 nm, internal differentiation takes place (Fig. 10.2). Linear arrangements of electron-dense bodies disposed at high angles to the external surface polymerize out of the matrix and, as polymerization spreads inwardly, the thickening periostracum becomes three layered. In a fully developed periostracum, which may be 5 or 6 μm thick, the outer layer consists of hexagonally stacked, electron-dense rods separated by partitions, while a medium, electron-dense layer shares an irregular, interdigitating boundary with an inner, electron-light, somewhat fibrillar layer. The composition and distribution of these different components have not yet been determined although the lingulid periostracum is reported as being mainly a glycine-poor protein with some traces of chitin and hydroxyproline (JOPE, 1965). The basal layer of the rhynchonellid *Notosaria,* which may be up to 1 μm thick, is also differentiated. It consists of an outer, bounding, unit membrane with coiled fibrils in rhombic arrays; a main layer composed mainly of GAGs with scattered membrane-bounded vesicles; and vertically arranged fibrils and an inner bounding membrane.

In calcareous-shelled brachiopods, secretion of the periostracum is completed by the time it has been conveyed to the edge of the

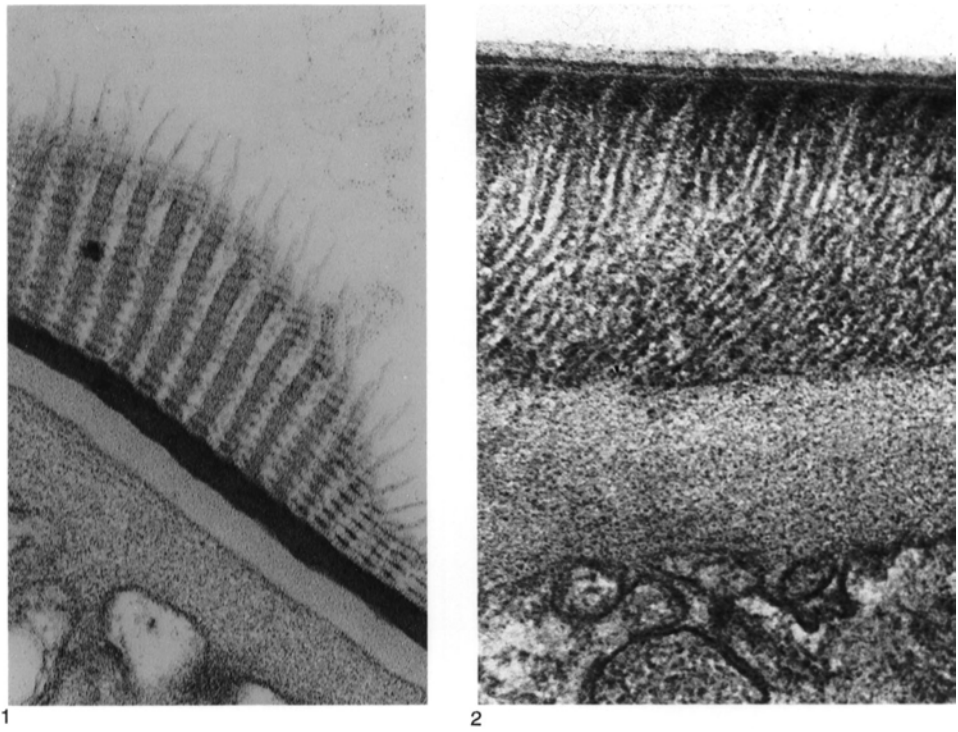

FIG. 10. TEM micrographs of the periostraca of organophosphatic brachiopods; *1,* periostracum of *Discina striata* (SCHUMACHER) consisting of a sheeted superstructure and thickened, electron-dense basal layer underlain by the beginnings of a mainly organic primary layer secreted by protuberances of the apical plasmalemma, ×32,550; *2,* periostracum of mature *Glottidia pyramidata* showing the outer (top) layer of hexagonally stacked, electron-dense rods separated by partitions becoming less well defined internally and sharing an irregular boundary with an inner, electron-light layer being secreted by protuberances of the apical plasmalemmas (bottom), ×98,580 (new).

outer mantle lobe. As it rotates around the hinge of the mantle to become an integral part of the expanding shell, isolated calcite rhombs are secreted on the proximal surface of the basal layer. The subsequent sequence in the secretion of the brachiopod integument is well known through the studies of the craniids (WILLIAMS & WRIGHT, 1970), the thecideidines (WILLIAMS, 1973), terebratulides including *Calloria* (WILLIAMS, 1968b; WILLIAMS & MACKAY, 1978; STRICKER & REED, 1985a, 1985b), and especially the rhynchonellide *Notosaria,* which, on account of the simplicity of the succession, may be taken as the standard sequence (WILLIAMS, 1968d).

As calcite rhombs continue to increase in number and size through further nucleation and accretion, they amalgamate with one another to form a layer of inclined crystallites with sporadic lenticular patches (Fig. 11). This is the **primary shell layer,** which is featureless except for **growth banding** and high-angled breaks presumably corresponding to intercellular spaces in the secreting plasmalemmas. No organic traces other than those related to the retraction and advance of the mantle edge have yet been seen, but that does not preclude the existence of intracrystalline, water-soluble compounds. The cells responsible for the secretion of this layer form a well-defined band transitional between the elongate vesicular cells and the typical cuboidal cells of outer epithelium. In addition to being less elongate than the vesicular cells, those underlying the primary

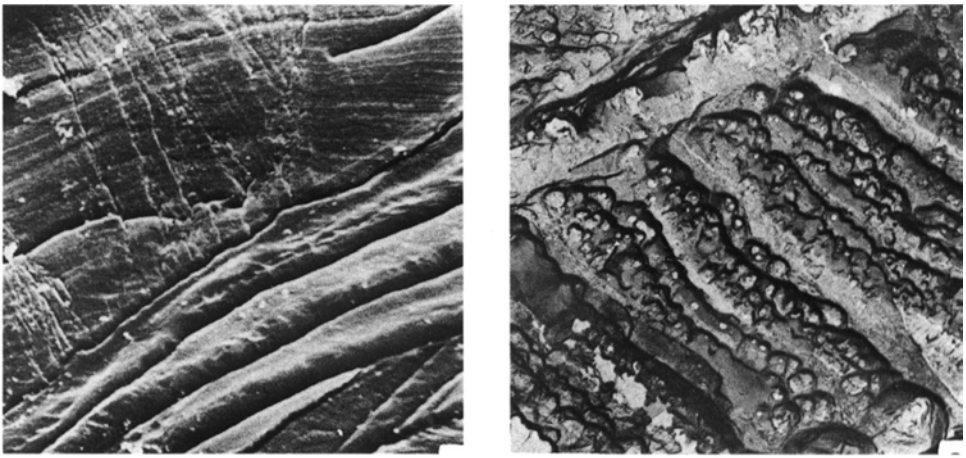

1 2

FIG. 11. SEM and TEM micrographs of the primary layer of *Notosaria nigricans* (SOWERBY); *1,* section showing the growth banding in the primary shell and its junction with secondary fibers, ×2,500; *2,* external surface immediately below the periostracum, ×6,800 (Williams, 1971a).

shell have fewer membrane-bound vesicles and smoother secretory plasmalemmas (Fig. 12).

OUTER EPITHELIUM OF CALCITIC SHELLS

As deposition of the primary layer proceeds, the secreting cells become increasingly separated from the periostracum. At a given distance behind the edge of the outer mantle lobe, however, the outer epithelial cells start secreting the organocalcitic secondary layer. The distance within the valve margin, at which secretion of the secondary layer is initiated, determines the thickness of the primary layer. The thickness varies not only from one species to another but also during ontogeny. In *Notosaria* the maximum thickness of the primary layer has been calculated as increasing more or less steadily from the umbo by about 12 μm per mm of surface length (WILLIAMS, 1971a).

The first sign of **secondary shell** deposition on the internal surface of a valve is the occurrence of impersistent membranous strips adhering to the carbonate surface (Fig. 5.1). Each strip is the first-formed part of a membrane, about 10 nm thick, exuded along an arcuate anterior zone of the secreting plasmalemma of a cell. The membrane acts as a seeding sheet for calcite being secreted by the posterior part of the plasmalemma. Moreover, the outer epithelium underlying the secondary layer consists of outwardly inclined, cuboidal cells regularly arranged in alternating rows. Consequently, the membranes, spun out by adjacent cells, join up with one another so that the calcite of the secondary cell becomes segregated into a series of **fibers** (Fig. 5.2), each ensheathed in interconnected membranes (Fig. 5.3) and with its terminal face contained by the posterior part of the apical plasmalemma. The fibers are usually inclined at about 10° to the diachronous interface with the primary layer. They each have a distinctive, anvil-shaped cross section reflecting the posterior concavity of the secreting plasmalemma and occur in characteristically stacked series. The microtexture of a fiber is typically granular with a rough, pitted terminal face in complement to the microscopic protuberances of the apical plasmalemma (WILLIAMS, 1968a; GASPARD, 1986) and with smoothed surfaces corresponding to enclosing membranous sheaths.

Fibers continue to lengthen so long as their controlling cells continue to secrete

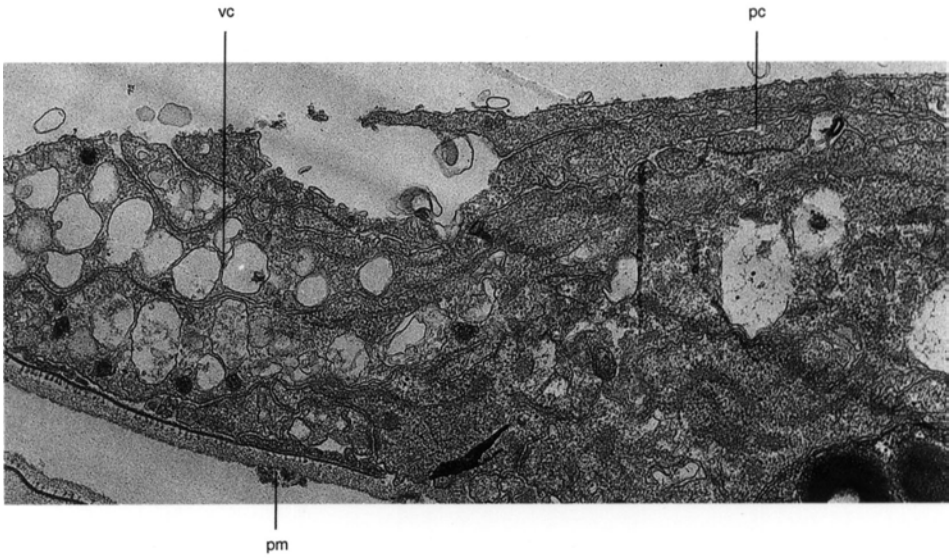

FIG. 12. TEM of the mantle edge of *Notosaria nigricans* showing the cells (*pc*) secreting primary shell (removed by decalcification of the section) in relation to vesicular vells (*vc*) and periostracum (*pm*), ×7,500 (new).

protein and calcite (WILLIAMS, 1966, 1968a; GASPARD, 1986). Accordingly, the secondary layer is normally thickest posteromedially at the site of the oldest cells. All internal skeletal features (except spicules, described below) are composed of secondary shell.

The apical plasmalemma of a typical, outer epithelial cell, which secretes the secondary layer, is devoid of cilia and regular microvilli. It is, however, normally studded with an anterior arc of hemidesmosomes (Fig. 13). These are terminations of bundles of filaments extending to the basal lamina. Their fibrous constituents are probably incorporated into the proteinaceous membranes ensheathing the calcitic fibers, to which they are attached. Posteriorly, the apical plasmalemma is usually ruffled into low-lying protuberances, up to 150 nm long, with an adherent, discontinuous membrane. Membrane-bound droplets of glycoprotein and GAGs occur but less frequently than in the inner epithelium, while rough, endoplasmic reticulum is normally much more conspicuous than the smooth.

The skeletal succession and outer epithelium just described are characteristic of most living brachiopods with calcitic fibrous shell. There are, however, two groups with significantly different secretory regimes, as revealed in changes in the outer epithelium as well as the integument.

The carbonate skeleton of the living thecideidines, *Lacazella* and *Thecidellina,* mainly consists of a primary layer of acicular and granular calcite with growth banding bearing frequent signs of interrupted accretion or absorption and widely distributed microscopic features, such as tubercles and closely packed rhombic blocks, on the internal surfaces of mature shells (Fig. 14). The only traces of orthodoxly stacked secondary fibers with proteinaceous sheaths occur on the teeth and socket ridges and the tubercles (WILLIAMS, 1973). The outer epithelium secreting this persistent primary layer consists of flat, cuboidal cells with large composite inclusions of glycoprotein, and it varies greatly in thickness, being attenuated and thickened over tubercles and mantle canals respectively (Fig. 15.1). A conspicuous feature of the secretory surface of the outer epithelium is the presence of a medium electron-dense discontinuous layer about as

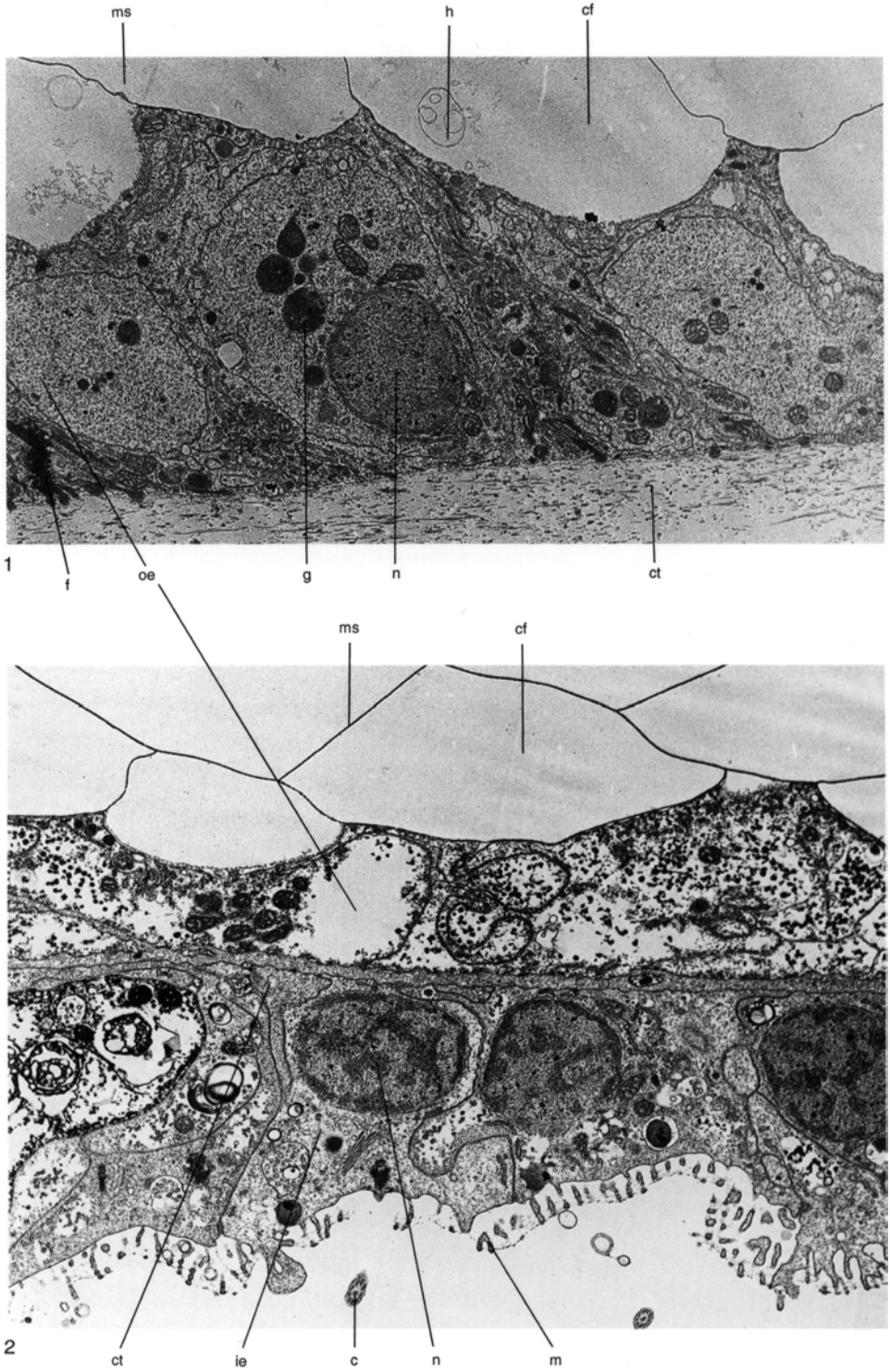

FIG. 13. *(For explanation, see facing page.)*

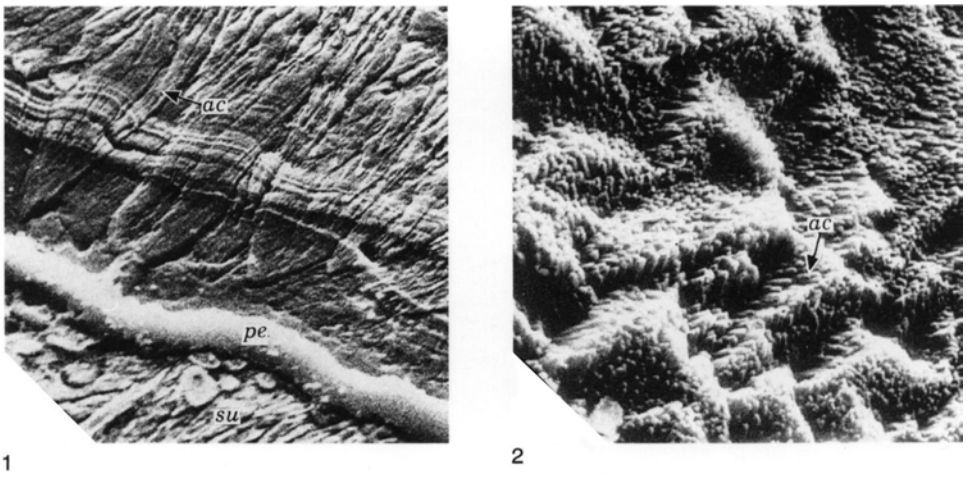

FIG. 14. SEM micrographs of the shell of *Thecidellina barretti* (DAVIDSON); *1,* etched section showing the attachment of the periostracum (*pe*) to the substrate (*su*) with the overlying primary layer displaying growth bands and acicular crystallites (*ac*), ×1,500; *2,* internal surface of a dorsal valve showing acicular crystallites (*ac*) in rhombic arrays, ×3,000 (Williams, 1973).

thick as the underlying plasmalemma to which it is attached by hemidesmosomes continuous with intracellular filaments (Fig. 15.2). As no comparable organic sheets are secreted within the carbonate shell, this discontinuous layer possibly represents a persistent organic mesh marking the external limit of a liquid film, about 100 nm thick, saturated with Ca^{2+} and HCO^{-}_{3}. The discontinuous layer may be a general feature of the epithelium responsible for the secretion of the primary layer as it is also well developed in the terebratulid *Liothyrella,* and traces of it have been found in *Notosaria.*

In contrast to the virtual suppression of the secondary layer in living thecideidines, such terebratulids as *Liothyrella* and *Gryphus* (MACKINNON & WILLIAMS, 1974) develop a continuous, **tertiary** layer. This consists of discrete units (prisms) that represent terminal faces of fibers growing normal to the surface of accretion (see Fig. 255). Sections of decalcified mantle show that the epithelium secreting the tertiary layer is like that underlying the secondary shell except that it does not exude proteinaceous sheets between prisms (Fig. 16.1). A continuous proteinaceous sheet, up to 10 nm thick, however, persists about 20 nm external to the secreting plasmalemma to which it is attached by septate and fibrillar hemidesmosomes (Fig. 16.2). This monolayer, like that associated with the outer epithelium secreting the primary layer or the calcitic face of the secondary fiber, is interpreted as the outer boundary to a film of extracellular fluid sustaining carbonate secretion. The reason the tertiary layer consists of discrete prisms instead of one continuous sheet like the primary layer is presently unknown. Amalgamation of prisms may be inhibited either by sheets of water-soluble, organic compounds or by crystallographic incompatibility through the nonalignment of lattice structures. Shell sections normally show depositional continuity from the acicular primary shell through the

FIG. 13. TEM micrographs of *Calloria inconspicua* showing the relationship of outer epithelium (*oe*) with the membranous sheaths (*ms*) enclosing secondary calcitic fibers (*cf*) and with the underlying connective tissue (*ct*) and inner epithelium (*ie*); cilia (*c*), filaments (*f*), glycoprotein inclusions (*g*), hemidesmosomes (*h*), microvilli (*m*), and nuclei (*n*) are prominent; sections of *1,* decalcified integuments of the shell, ×8,000; and *2,* descending lamella of the loop, ×17,000 (new).

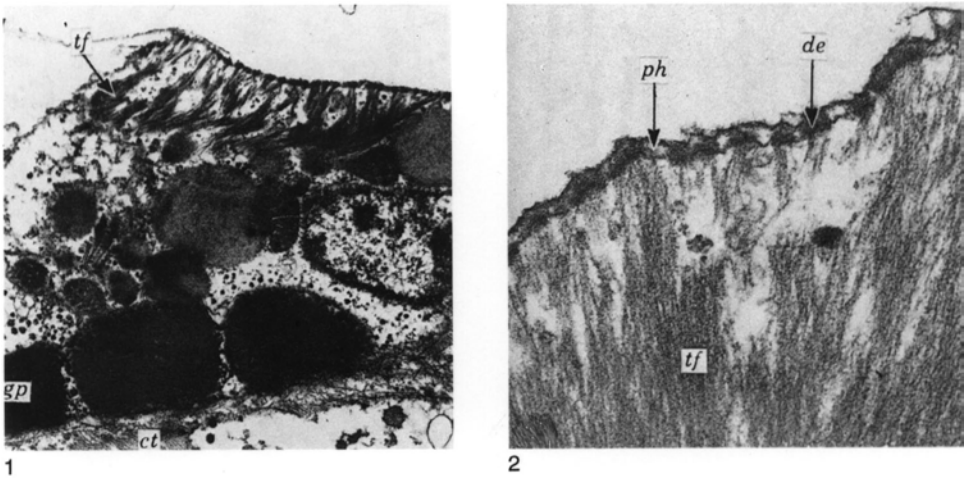

FIG. 15. TEM micrographs of sections of the outer epithelium of *Thecidellina barretti; 1,* bundles of filaments (*tf*) within the cell containing glycoprotein inclusions (*gp*); *ct,* connective tissue, ×11,000; *2,* their association with hemidesmosomes (*de*) attached to a discontinuous external membrane (*ph*) at the apical plasmalemma, ×68,700 (Williams, 1973).

fibrous secondary layer to the tertiary prisms (WILLIAMS, 1968a; MACKINNON & WILLIAMS, 1974).

Although the calcitic shell of the craniides, as represented by living *Neocrania,* is separable into primary and secondary layers, both are different from those of the rhynchonellides, the latter profoundly so (SCHUMANN, 1970; WILLIAMS & WRIGHT, 1970).

The primary layer normally consists of crystallites inclined at about 45° to the isochronous growth surfaces within the succession; here and there crystallites may amalgamate to form impersistent lenticles of

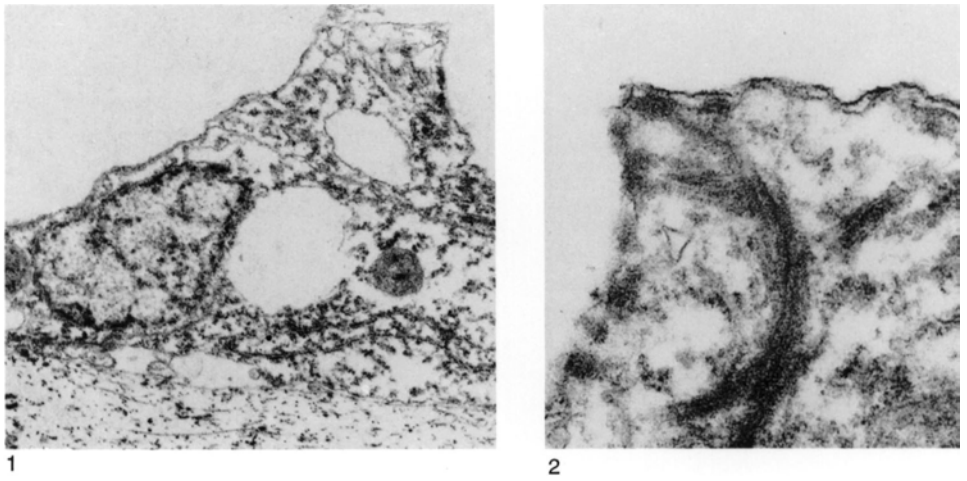

FIG. 16. TEM micrographs of decalcified sections of the outer epithelium underlying the tertiary shell of *Liothyrella neozelanica* showing *1,* the absence of fibrous membranes distal of the apical plasmalemma, ×8,200, and *2,* a detail of the apical plasmalemma with an external membrane attached by hemidesmosomes at the distal ends of bundles of filaments, ×55,000 (MacKinnon & Williams, 1974).

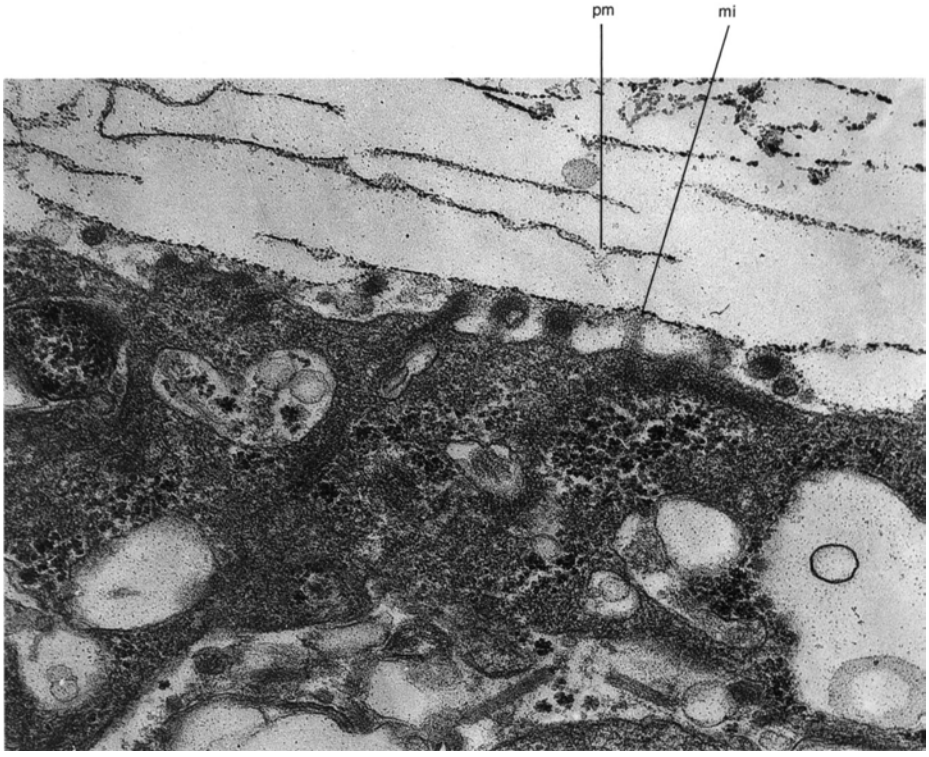

FIG. 17. TEM micrograph of decalcified section of the outer epithelium of *Neocrania anomala* (MÜLLER) showing the apical plasmalemma in relation to proteinaceous membranes (*pm*) covering calcitic laminae with short microvilli (*mi*), containing the ends of bundles of filaments extending through a zone presumably filled with extrapallial fluid; the zone occurs at different levels consistent with a section through spirally growing laminae, ×41,000 (Williams, 1970b).

calcite. The main changes, however, occur in a narrow, transitional zone marking the boundary between the primary and secondary layers. Here the crystallites tend to form tabular aggregates that grade inwardly into uniformly thinner laminae. Both types form regular successions of overlapping tiles with comarginal edges scalloped in rhombohedral angles of 75° or 105°.

The secondary shell, which is not developed in the attached pedicle valve, is distinguishable from the transitional zone in that the **laminae,** about 250 nm thick and up to 15 μm across, are ensheathed in interconnecting proteinaceous sheets. The laminae are disposed as rhombohedral or dihexagonal tablets and are stepped in single- or double-screw dislocations (see Fig. 248) indicating that the secondary layer thickens by spiral growth. An outer epithelial cell, contributing to the growth of secondary shell, contains numerous vesicles of glycoprotein and bundles of filaments (Fig. 17). At the secretory plasmalemma, groups of fibrils occupy cylindroid protuberances up to 200 nm long and become continuous through the membrane with clusters of hemidesmosomal fibrils. The fibrils pervade a narrow zone of variable electron density to connect with a membrane that represents the innermost proteinaceous sheet of the secondary shell. This zone intervenes everywhere between outer epithelium and shell and contains discarded vesicle membranes and finely divided particles. The zone presumably contains materials being used in the synthesis of proteinaceous membranes and a liquid saturated with Ca^{2+} and HCO_3^- ions that, on

precipitation, maintain the lateral expansion of laminae over newly forming membranes.

OUTER EPITHELIUM OF APATITIC SHELLS

The mantle and phosphatic integument of organophosphatic brachiopods are fundamentally different from those of carbonate-shelled species, micromorphologically, structurally, and biochemically. Recent research, however, has led to conflicting conclusions on the nature of the organophosphatic secretory regime so that no single model serves as a standard for comparison. The differences can be illustrated by comparing the studies of *Lingula, Glottidia,* and *Discinisca* by IWATA (1981, 1982) with those of *Glottidia* and *Lingula* by WATABE and PAN (1984), of *Discina* by WILLIAMS, MACKAY, and CUSACK (1992), and of *Lingula* by WILLIAMS, CUSACK, and MACKAY (1994). The differences partly stem from using even such general terms as primary and secondary shell to mean different things. (In this account, the terminology is that of WILLIAMS, MACKAY, and CUSACK, 1992.) There are also disagreements on the structure and differentiation of the secreting epithelium and on the nature of the basic components of the skeletal successions. Accordingly, the lingulids and discinids will be separately described although it is evident that their secretory regimes are homologous and that the differences between them are likely to rest on misinterpretations.

PAN and WATABE (1988b) described *Glottidia* as having a thick, well-defined primary layer immediately underlying the periostracum within which crystal aggregates decrease in density toward the secondary shell. This layer is secreted by cuboidal cells containing calcium phosphate granules but relatively few organelles. The main components of the layer are apatitic spherulites consisting of acicular crystallites up to 200 nm long dispersed within a fibrous matrix consisting of proteins and GAGs.

In contrast, the inner part of the shell succession includes a number of secondary layers composed of amalgamated crystals, which are separated from one another by thicker chitinous layers. These secondary mineralized and chitinous layers are, according to PAN and WATABE (1988a, 1988b), secreted by three kinds of squamous cells. Type I cells, with relatively smooth secretory plasmalemma, contain granule-bearing vesicles that are released into an extrapallial space to form the mineralized layer. Types II and III cells have short and small, irregular microvilli respectively connecting with intracellular bundles of filaments and the extracellular chitinous layers. A noteworthy feature of the chitinous layers of *Glottidia* is the presence of arrays of long, slender rods of apatitic spherulites set at acute angles to one another (see Fig. 238).

IWATA's studies of the skeletal successions of *Lingula* and *Glottidia* (1981, 1982) suggested that they differ in many respects. He was unable to differentiate the shell succession of *Lingula* into primary and secondary layers. Instead, he described the shell as consisting of alternations of organic and mineralized layers. A typical organic layer (also referred to as the chitin layer) is distinguishable from the organic matrix of a succeeding mineralized layer in being electron dense and composed of organic fibrils less than 10 nm long that are usually disposed in a reticulate mesh. Hexosamine and some proteins are the main constituents of the organic layer. The fully developed mineralized layer was zoned by IWATA (1981, p. 41) according to the size of apatitic components (Fig. 18). Overlying an organic layer with a sharply defined interface, a thin layer composed of apatitic granules about 50 nm in size is usually developed (designated the C zone). The mineral components of the succeeding A zone are acicular crystallites up to 150 nm long arranged more or less parallel to the boundaries of the zone. In the overlying B zone, which grades into the next organic layer, the apatitic components consist of coarse, acicular crystallites up to 200 nm long, which are irregularly disposed throughout the zone. The organic matrix of all three zones is comparable to collagen but has excessive concentrations of alanine. IWATA

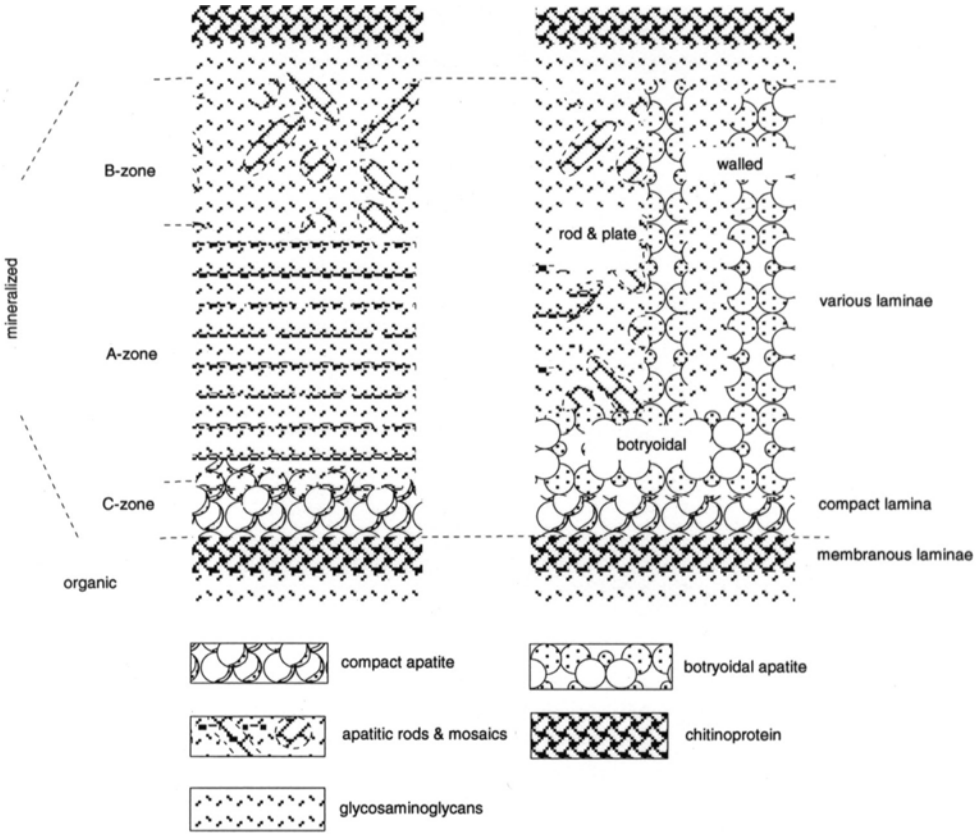

FIG. 18. A terminological correlation of a composite laminar set of the shell of *Lingula anatina* (right-hand side) as described herein with the mineralized and organic layers as understood by IWATA (1981, p. 41); laminae in the main part of the succession usually consist of botryoids, vertical walls, and rods and plates (see Fig. 235, 237 for SEMs of these laminar sets) of apatite in a GAGs matrix (adapted from Williams, Cusack, & Mackay, 1994).

(1981) noted that the *Lingula* could not be digested by chitinase and suggested that the chitin, which is known by other tests to be present, is masked by a scleroprotein.

IWATA (1981) did not find any differentiation of the outer epithelium secreting the *Lingula* shell, which consists of columnar cells with the secreting plasmalemmas forming irregular projections accommodating terminations of bundles of internal filaments. Some micrographs (IWATA, 1981, pl. 14/2) have been interpreted as showing the presence of extrapallial fluid.

IWATA (1982) confirmed that the succession of *Glottidia* consists of alternations of organic and mineralized layers but did not identify a primary layer. The mineral layers are described as being composed of rods and needlelike crystallites of apatite aligned subparallel to the shell surface. The mineral components of the organic layer, on the other hand, are slender, mineralized fibrils that are disposed within the layer in a latticelike manner. With respect to the distribution of the biomineral components in the *Glottidia* shell, IWATA drew a closer comparison with *Discinisca* rather than *Lingula.* He additionally noted that the basic apatitic component of *Discinisca* is an extremely fine granule aggregated into acicular crystallites. All three genera have a collagen-like protein as a dominant organic constituent.

In describing the skeletal succession of *Discina,* a stratiform terminology was

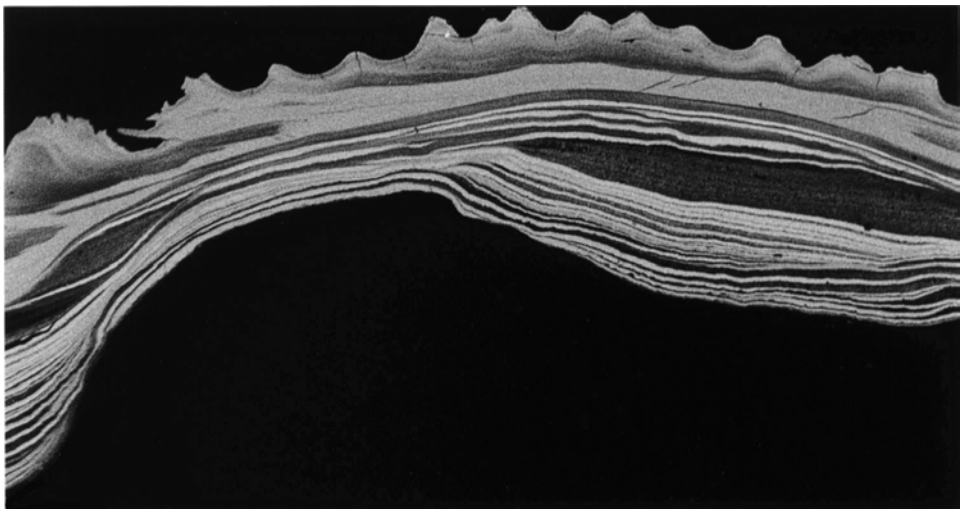

FIG. 19. Backscattered electron micrograph of a section near the dorsal umbo of *Discina striata,* digested in chitinase and papain and coated with carbon, showing the distribution of apatite (white) and organic (grey to black) components of the shell succession, ×40 (Williams, Mackay, & Cusack, 1992).

introduced (WILLIAMS, MACKAY, and CUSACK, 1992) in an attempt to standardize definitions of the various distinctive structural and biochemical units secreted by the outer epithelium (Fig. 19). A subperiostracal primary layer no more than a few microns thick is normally well defined, especially in backscattered scans for phosphate because finely granular apatite is distributed throughout the layer. The succeeding secondary layer consists of a variety of organophosphatic sheets (**laminae**) that, although normally impersistent and subject to lateral as well as vertical changes, can be categorized as one of five distinctive types. All are composed of the same basic unit: an apatitic granule between 4 and 8 nm in size with an organic coat. The units are assembled and aggregated into spherules up to 200 nm in diameter within the outer epithelium. During exocytosis, spherules are further aggregated into discoidal or spheroidal mosaics up to 1 μm or so in size, which are added incrementally to the shell succession more or less in their final, polymerized and crystallized states. The distinctiveness of each type of lamina depends on the relative proportions of its organic and biomineral components and on the aggregation of its apatitic mosaics. Typically, there is a discernible rhythmic sedimentation from a predominantly or exclusively organic to a mainly apatitic deposition, which reflects a recurrent cycle of secretion by the same group of cells.

The outer epithelium depositing these rhythmic successions consists of inclined cuboidal cells with secretory plasmalemmas prolonged as a series of prostrate tubes, 150 nm or so in diameter, which tend to form a layer up to three or four deep (Fig. 20.1–20.2). Within the cell, membrane-bound vesicles are common, and glycogen is densely distributed especially in the basal parts. Apatitic granules with medium electron-dense coats are usually distributed in varying size within and between the prostrate tubes. Such aggregates may be drawn out into rod-like structures (baculi) (Fig. 20.3–20.4). In fact, the main components of every type of lamination occur in what appears to be their final crystalline or polymerized states at the interface between the shell and outer epithelium. This kind of secretion precludes the existence of a film of extrapallial fluid

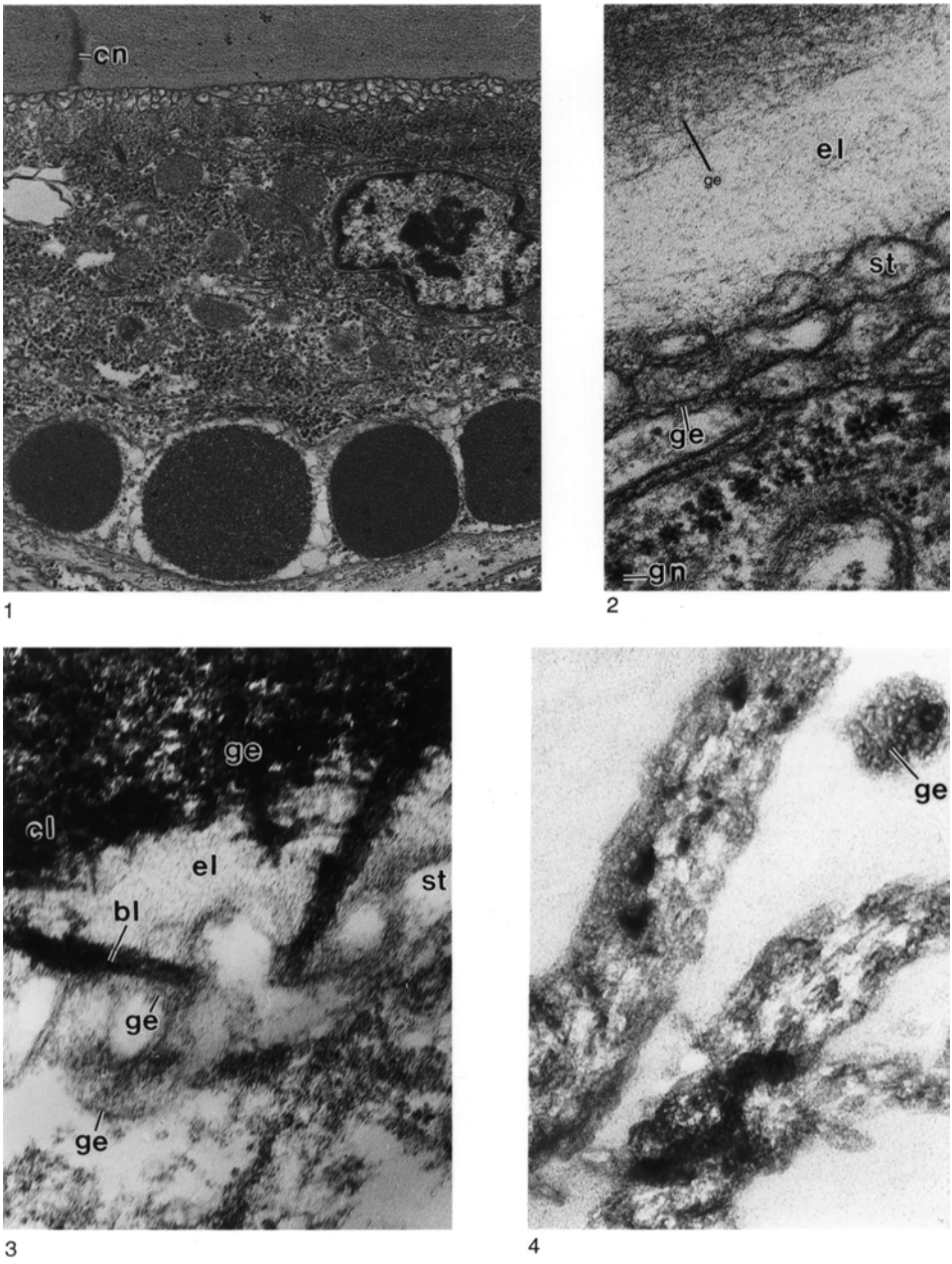

FIG. 20. TEM micrographs of shell and outer epithelium of dorsal valves of *Discina striata; 1,* general view (×9,000) and *2,* detail (×80,000) of decalcified sections of cells showing apical plasmalemmas disposed as a series of low-lying tubes (*st*), a canal (*cn*) underlying mainly organic (*1*) and stratified (*2*) laminae with apatitic granules with coats (*ge*), glycogen (*gn*), and an electron-lucent (*el*) zone with fibrils and aggregates of apatite; *3,* ×80,000, and *4,* ×130,000, sections of shell (with secreting epithelium in *3*) showing the origin of mineralized rods (baculi) and the structure of so-called acicular crystallites respectively with rods (*bl*) arising from a compact lamina (*cl*), within an electron-lucent zone containing coated apatitic granules (*ge*) being exocytosed with fibrils from plasmalemma tubes (*st*) (Williams, Mackay, & Cusack, 1992).

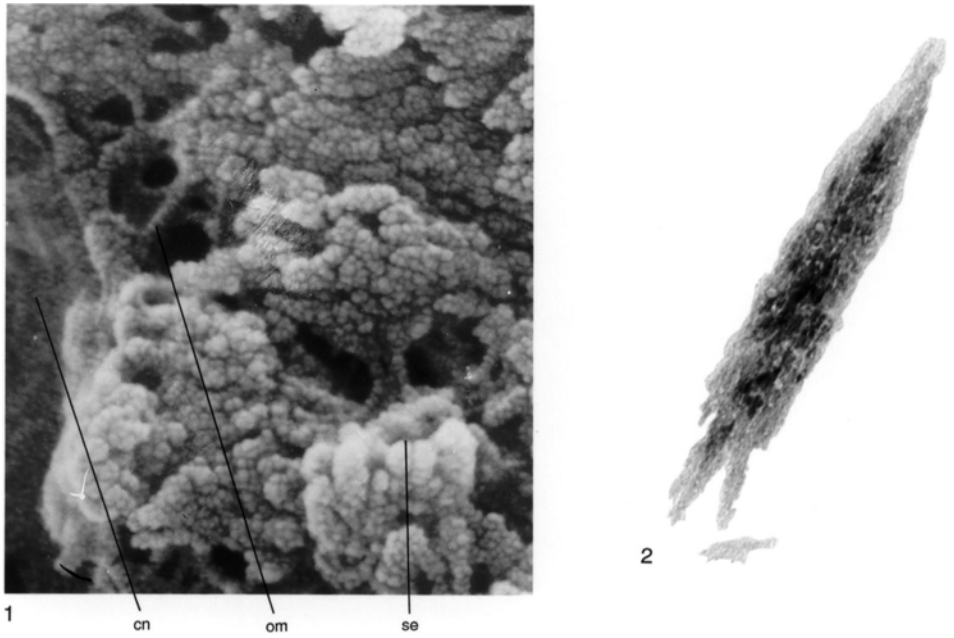

FIG. 21. Biomineral structures in the shell of *Lingula anatina; 1,* SEM micrograph of fracture section of a shell showing apatitic spherules (*se*) composed of granules adjacent to a canal (*cn*) and supported by an organic mesh (*om*) probably of chitin, collagen, or fibrous protein, ×150,000; *2,* TEM micrograph of original shell showing the structure of a so-called acicular crystallite with an electron-dense proteinaceous and chitinous matrix studded with granules, ×180,000 (new).

between newly formed shell and mantle as has been reported in lingulid brachiopods (PAN & WATABE, 1988b; IIJIMA, HIROKO, & others, 1991).

The previously reported differences in the structure and secretion of the lingulid and discinid shells also appear to be based on misinterpretations of ultrastructural features in shell and mantle (WILLIAMS, CUSACK, & MACKAY, 1994).

No evidence has been found of acicular (prismatic) crystallites constituting the basic apatitic unit in *Lingula.* The smallest apatitic unit is granular with dimensions comparable to that of the *Discina* shell (Fig. 21). This conclusion is not only at odds with the findings of IWATA (1981) and PAN and WATABE (1988b) but also appears to be incompatible with the X-ray diffraction studies of KELLY and others (1965), IIJIMA and MORIWAKI (1990), and IIJIMA, HIROKO, and others (1991). Both investigations explored the orientation of apatite relative to the organic framework of the *Lingula* shell. KELLY and others (1965, p. 339) found that the c-axes of the apatitic crystals are normally aligned parallel to the plane of the shell but vary considerably in orientation relative to the shell margins and in strength of definition (Fig. 22). In the posteromedian zone, more or less coincident with the body cavity, the c-axis may be transverse or may be disposed in two directions and even tilted to the shell surface. In the lateral areas of a valve, the c-axes tend to be disposed normal to the valve margin; in the anteromedian sector of a valve, the c-axes are as disoriented as they are in the posteromedian area. The removal of apatite by EDTA showed that the β-chitin configuration is oriented in the same way as the apatite had been so that the polysaccharide chain lies parallel with the c-axis of the apatitic component. It was noted that the reflections are generally diffuse, indicat-

ing the presence of small crystallites of the order of 20 nm, but are sharper in the lateral areas suggesting larger crystallites up to 100 nm or so. The electron microscopy done by KELLY and others (1965) confirmed that the smallest particles, at about 5 nm, are rounded and enveloped by organic material. Fractionation of the mineral components suggested that three other grades existed: needle-shaped particles with organic envelopes about 30 nm long, closely packed acicular crystallites at about 100 nm in length, and larger, rectangular aggregations.

The diagrammatic representation of the findings of IIJIMA, HIROKO, and others (1991) is closely comparable with that of KELLY and others (1965) except that they ascribed the diffuse reflections of the median area to strong organic reflection and found that the orientation of the c-axes of apatite and the fiber axes of β-chitin were closely parallel with the growth vectors of the lateral areas (Fig. 22). IIJIMA, HIROKO, and others (1991) concluded that chitin fibers grow apatite on their surfaces.

Contrary to first impressions, the disposition of the apatitic c-axes and the relative sharpness of their diffraction patterns, as described above, are actually broadly consistent with recent ultrastructural studies of the *Lingula* shell. The basic biomineral unit is invariably a granule, presumably a flattened hexagonal prism, about 4 to 8 nm in diameter. In the anteromedian sector of a valve, the granules are usually widely dispersed in spherules or small mosaics (Fig. 21.1); in the posteromedian sector, larger mosaics are closely distributed and normally aggregate into botryoidal masses. The c-axes of the apatitic components in these sectors would accordingly have weak orientations with varying inclinations to the shell surface. In the lateral areas, spherules may be aggregated into rodlike structures (Fig. 21.2) up to 400 nm long as well as into mosaics. The rods usually have a preferred orientation more or less normal to the growing edge of the valve and lie parallel to anastomosing ridges, which probably accommodate volumetric

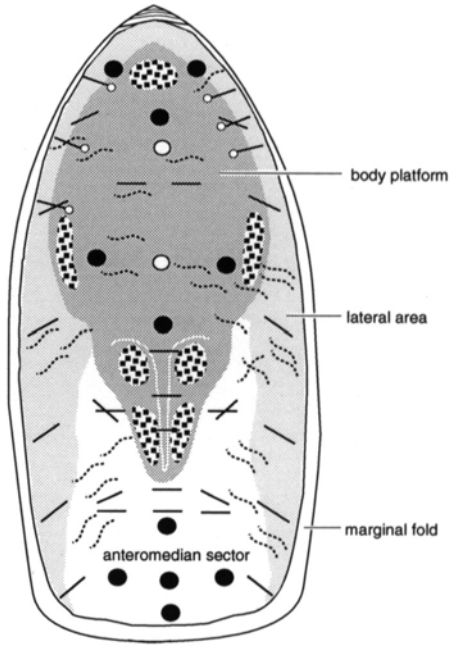

FIG. 22. The interior of a dorsal valve of *Lingula anatina* showing the orientation of apatitic crystallites, for which c-axis directions have been determined, relative to the trends of anastomosing ridges; the c-axes represented by *lines ending in circles* are those plotted by IIJIMA, MORIWAKI, and KUBOKI (1991b, p. 435), which were not coincident with those (*plain lines*) mapped by KELLY, OLIVER, and PAUTARD (1965, p. 339); the trends of the ridges are a compilation of observations of a number of interiors seen under the SEM; ●, disorientation areas; ○, strong organic reflection areas; *wavy dotted lines,* anastomosing ridge trends (Williams, Cusack, & Mackay, 1994).

changes in the mantle induced by the radial canal systems. The rods are not acicular crystallites but strings of granules that must be stacked in such a way as to have their c-axes aligned with the fiber axes of associated chitin.

As with *Discina,* the lingulid laminar succession is rhythmic as was first noted by IWATA (1982) although he did not describe its structural diversity (Fig. 18). The rhythm is initiated by the sudden bulk secretion of coated granules of apatite virtually to the exclusion of organic constituents that, however, become dominant toward the end of the cycle (Fig. 23). This increase in the organic content culminates in the secretion of

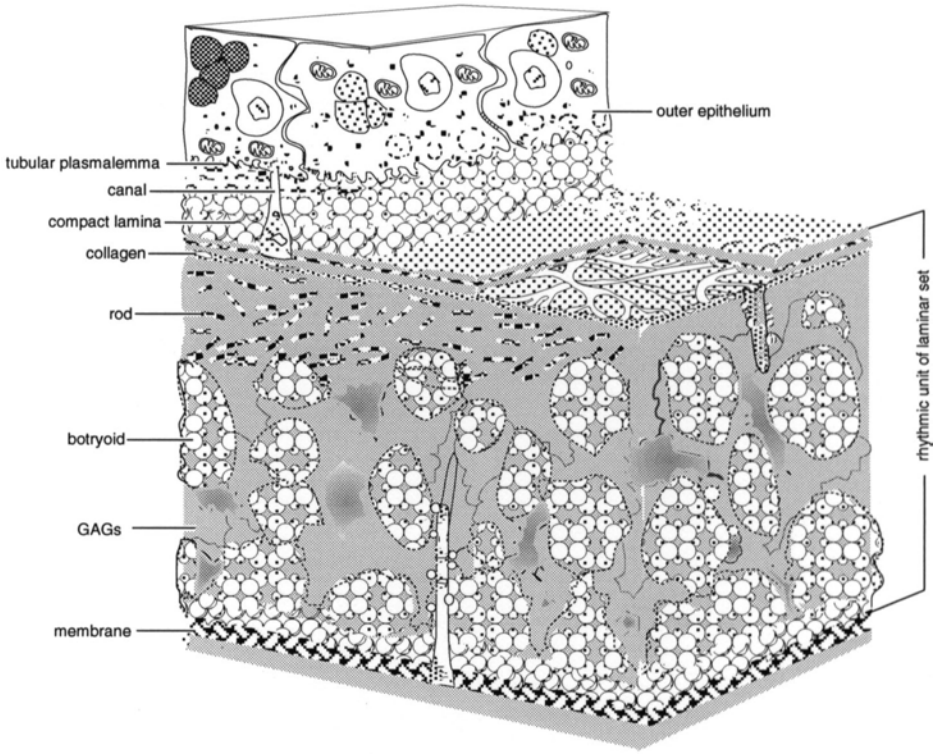

FIG. 23. Diagrammatic representation of a laminar set of the shell of *Lingula anatina* showing a complete rhythmic unit of secretion with the base of the compact lamina marking the onset of a decreasing cycle of apatitic secretion and the base of the botryoidal lamina marking the first exudation of an increasingly preponderant GAGs matrix (Williams, Cusack, & Mackay, 1994).

a chitinoproteinaceous membrane(s) that serves as the substrate for the next influx of apatite. At least ten proteins have been identified in the shell (WILLIAMS, CUSACK, & MACKAY, 1994). Some of these must be covalently attached to GAGs, the main organic matrix of the shell, while others must be associated with the chitin and fabricated into membranes and apatitic coats. Fibrillar collagens with a periodicity of about 45 nm occur mainly as sporadically developed mats within the body platform succession (Fig. 24) and as the core of the dorsal median septum. Elsewhere they appear sparingly as vertical and horizontal strands (WILLIAMS, CUSACK, & MACKAY, 1994).

The outer epithelium is normally anchored to the shell by canals (Fig. 25.1) so that a single cell can secrete in sequence that part of an entire rhythmic succession to which it is attached. Consequently, the contents of cells attached to different successions vary according to whether the principal constituents of the laminae are organic or apatitic. Thus, the typical outer epithelial cell is cuboidal (Fig. 25), about 11 μm tall, with a basal nucleus and elaborately interdigitated lateral cell membranes. The cytoskeleton is normally well developed with bundles of filaments extending through the cytosol from hemidesmosomal plaques at the basal plasmalemma to tubular extensions of the apical plasmalemma, some of which are also attached by filaments to the lateral cell membranes. The Golgi apparatus is usually identified by trails of minute vesicles, while RER and mitochondria are variably distributed. Inclusions also vary in composition and distribution. Glycogen occurs widely, but lipid droplets tend to cluster in the basal

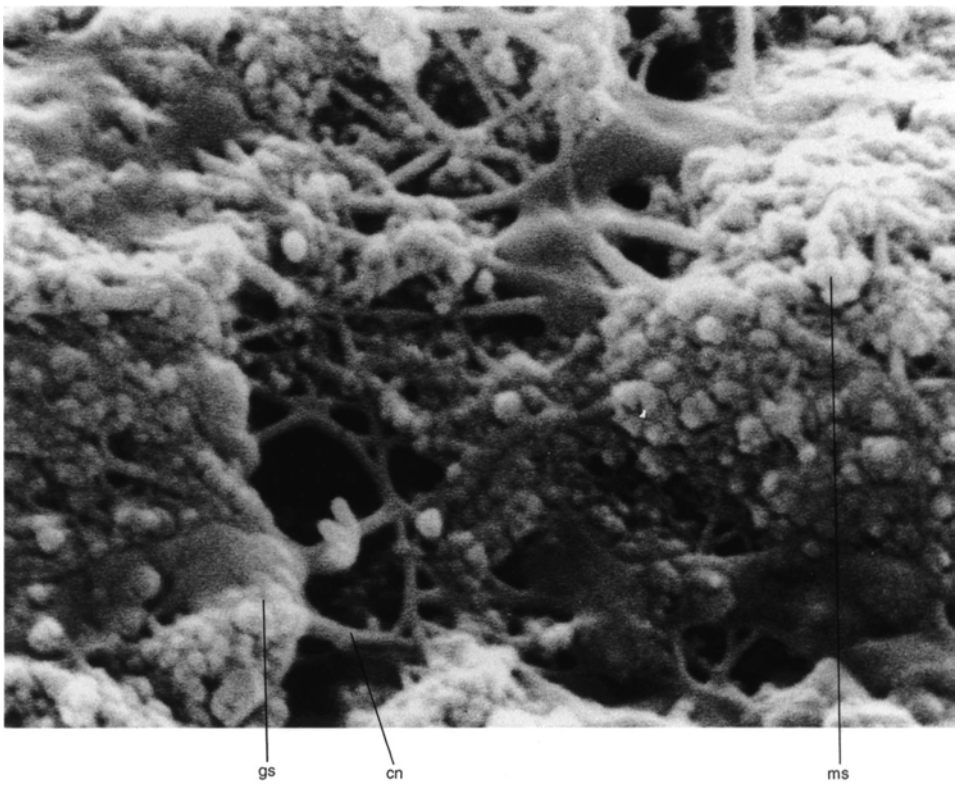

FIG. 24. SEM micrograph of an oblique fracture section of the shell of *Lingula anatina* showing the association of mosaics of apatite (*ms*) with glycosaminoglycans (*gs*) and a fibrous protein, possibly collagen (*cn*), ×24,500 (new).

regions of all cuboidal cells that are normally distorted by large, closely packed aggregates (10 μm or so in size) of differently composed vesicles, up to 1.6 μm in diameter. The large, membrane-bound vesicles in cells secreting mainly GAGs and other organic constituents, however, normally contain homogeneously electron-dense glycoprotein; mitochondria and RER are relatively rare and are much more common in the middle and basal regions of cells (Fig. 25.1). In contrast, the vesicles in cells secreting mainly apatite are mottled with electron-light granules in various stages of being reconstituted by RER; mitochondria with electron-light substrates are common within the apical region (Fig. 25.2; WILLIAMS, CUSACK, & MACKAY, 1994). It is evident that the different cell types previously observed (PAN & WATABE, 1988a, 1988b) represent phases in the secretory cycles of the basic outer epithelial cell.

MODIFICATIONS OF OUTER EPITHELIUM

The outer epithelium of brachiopods may be modified in many ways. Dense bundles of filaments attach the muscles to the floors of the valves. These traverse the outer epithelial cells to connect by hemidesmosomes proximally with basal lamina contiguous with the muscle base and distally with a proteinaceous membrane (*Thecidellina* WILLIAMS, 1973; *Liothyrella* MACKINNON, 1977; *Terebratalia* STRICKER & REED, 1985a) or a chitinous pad (*Neocrania* WILLIAMS & WRIGHT, 1970) intervening between the shell and the secretory plasmalemmas (Fig. 26–28). The emplacement of the muscle bases usually leads to partial or total suppression of secretion of the membrane within the secondary shell so that the biomineral components lose their identity and fuse into irregular plates (myotest). Even so, the epithelial cells between shell and

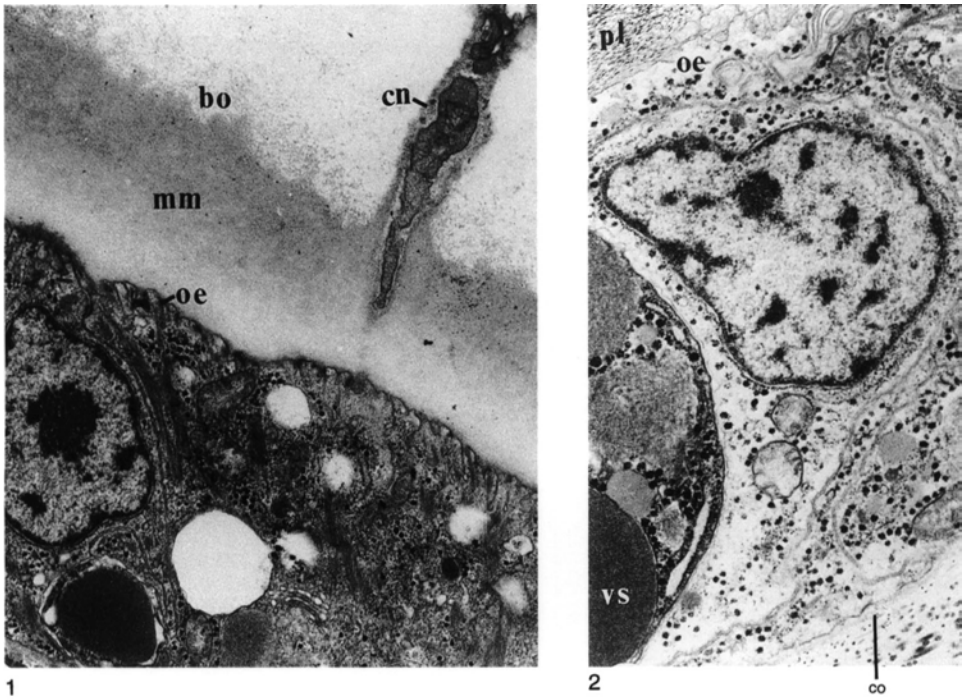

FIG. 25. TEM micrographs of sections of decalcified shell and outer epithelium of *Lingula anatina; 1,* canal (*cn*) penetrating laminae of apatitic mosaics clustered into botryoids (*bo*) and embedded in GAGs (*mm*), underlain by tubular extensions (*oe*) of the apical plasmalemmas, ×11,000; *2,* another outer epithelial cell that secreted dispersed apatitic rods (*pl*) through tubular extensions (*oe*), overlying connective tissue with fibrillar collagen (*co*) and adjacent to a cell bearing membrane-bound inclusions (*vs*), ×11,000 (Williams, Cusack, & Mackay, 1994).

muscle bases usually retain their regular, cuboidal outlines, which are commonly impressed as closely packed hexagonal casts within the muscle scars of fossil as well as living species (Fig. 26.2; 28.2–28.3).

The outer epithelium also undergoes changes to accommodate the growth of all internal skeletal features arising directly from the floors of the valves. The main changes are localized proliferations of cells as only the teeth of the ventral valve appear as features of the primary layer (STRICKER & REED, 1985a). Many of these skeletal extensions in living articulated brachiopods, however, become modified during growth by differential secretion and resorption, which processes are controlled by morphologically distinctive cells. Thus, the lamella of the loop of *Calloria* is a two-layered structure (MACKAY, MACKINNON, & WILLIAMS, 1994) consisting of a wedge of regularly stacked secondary fibers and an underlying thin layer of nonfibrous calcite (**brachiotest**) (Fig. 29). On one surface, secondary fibers predominate, but smooth, finely banded brachiotest occurs as a narrow, marginal lip upon which the secondary fibers proliferate and progressively overlap. This growing edge of the lamella is secreted by long, folded epithelial cells with fingerlike extensions to their apical plasmalemmas, which are distinguishable from the cuboidal epithelium secreting fibers and their membranous sheaths (Fig. 30.1). The other surface of the lamella consists entirely of roughened brachiotest. This surface is overlain by filamentary epithelium acting as a holdfast for the connective tissue frame of the lophophore (Fig. 30.2). The other edge of the lamella consists of truncated sections of both secondary fibers and brachiotest and

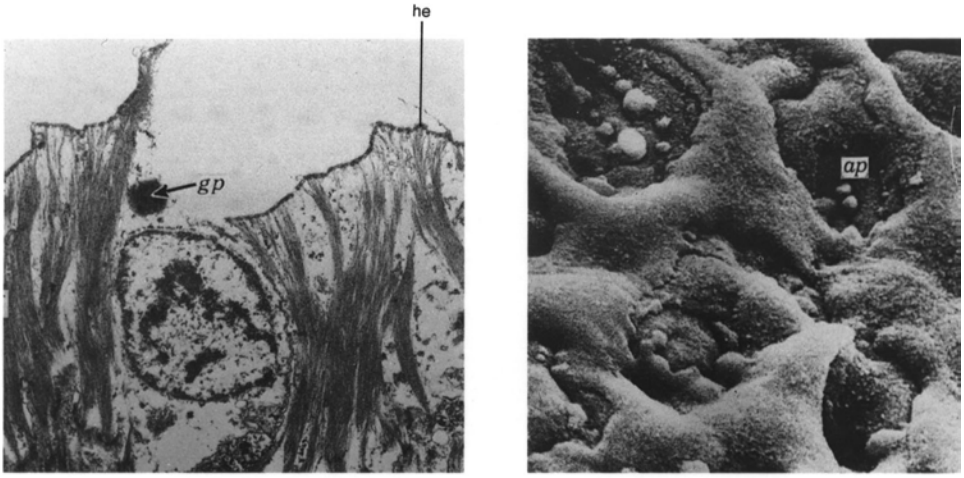

FIG. 26. Muscle attachment in *Thecidellina barretti* and *Lacazella mediterranea* (RISSO); *1,* TEM micrograph of a decalcified section of the outer epithelium permeated by bundles of filaments of a posterolateral adductor muscle showing hemidesmosomal attachment (*he*) to the apical plasmalemma and a glycoproteinaceous vesicle (*gp*), ×8,200; *2,* SEM micrograph of a muscle scar resulting from the attachment of the lophophore to the peribrachial ridge of a dorsal valve with adductor pits (*ap*) corresponding to the outline of the cuboidal outer epithelium, ×2,800 (Williams, 1973).

bears signs of resorption consistent with the degenerated state of the associated epithelium.

MANTLE EXTENSIONS

The shell of all living brachiopods, except the rhynchonellides, is pierced by perforations that are either slender cylindroids less than 1 μm in diameter (**canals**) or very much larger chambers up to 20 μm or more in diameter (**punctae**), which respectively accommodate membrane-bound secretions of the outer epithelium or papillose outgrowths of the mantle (**caeca**).

The caeca of living terebratulides, which may be simple or branched, almost penetrate the calcareous shell to connect with the periostracum by a radiating **brush** of protein-lined tubes, each about 100 nm in diameter (Fig. 31–32). The tubes permeate a canopy of primary shell about 1 μm thick (Fig. 33–34) and, together with the space between the canopy and the distal head of the caecum, are filled with GAGs (OWEN & WILLIAMS, 1969). Mature caeca are differentiated into peripheral cells, which are a flattened, cylindroid extension of the secretory outer epithelium and core cells hanging freely in a lumen occupying the basal part of the caecum. The core cells are full of inclusions of GAGs, glycoproteins, particulate glycogen, and minor lipids (Fig. 32). Their distal surfaces are extended into densely distributed microvilli (Fig. 32.1, 32.3). STRICKER and REED (1985a) have recently confirmed that, in the early stages of caecal generation at the mantle edge, microvilli give rise to the brush by being attached to the periostracum during secretion of the canopy (Fig. 35). The core cells act as storage centers for materials circulating within the mantle (OWEN & WILLIAMS, 1969).

The punctae and caeca of living thecideidines are homologous with those of the terebratulides, as is confirmed by the existence of a distal canopy penetrated by a brush of radiating canals averaging just under 300 nm in diameter and by the differentiation of the proximal part of the caeca into peripheral and core cells. The core cells of mature caeca, however, are not microvillous and are restricted to the proximal part of the punctae

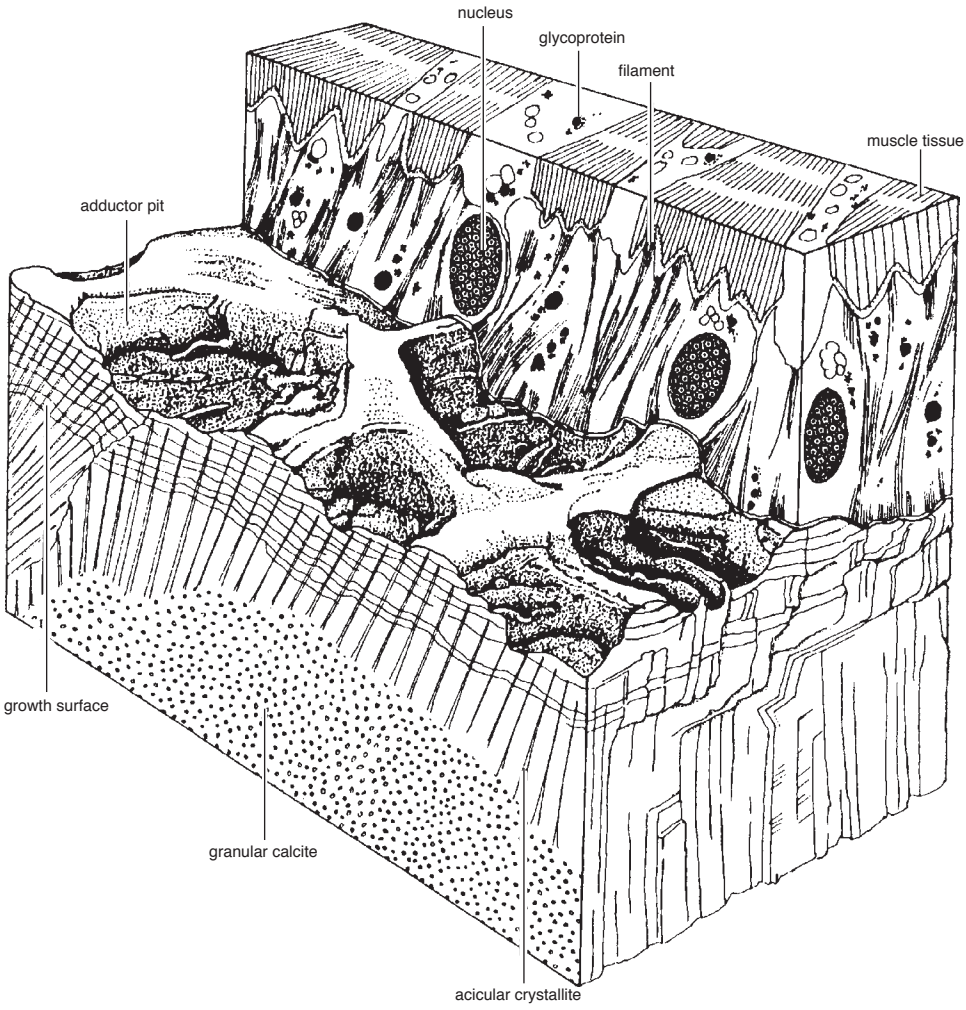

FIG. 27. Diagrammatic reconstruction of a pitted muscle scar in relation to the outer epithelium underlying the adductor muscle base of a typical thecideidine brachiopod, approximately ×3,000 (Williams, 1973).

by proteinaceous partitions sealing off the more distal part of the punctae.

The shell of *Neocrania* is also penetrated by punctae accommodating papillose outgrowths of the mantle, which are conveniently referred to as caeca to distinguish them from the contents of the fine lingulide canals (Fig. 36–37). They differ fundamentally from the terebratulide and thecideidine caeca in many respects, however (WILLIAMS & WRIGHT, 1970). The craniid caecum is typically highly branched, especially distally (Fig. 37.1) where fine, terminal tubules up to 150 nm in diameter and 2 μm long splay out radially within the primary layer and are connected to the periostracum, not through a well-organized brush but by filamentary trails. The trunk and main branches of a typical craniid caecum are lined by stretched, outer epithelial cells secreting the thickening secondary laminar layer. The axial lumen does not contain aggregated core cells but is normally charged (as are the finer branches and terminal tubules) with membrane-

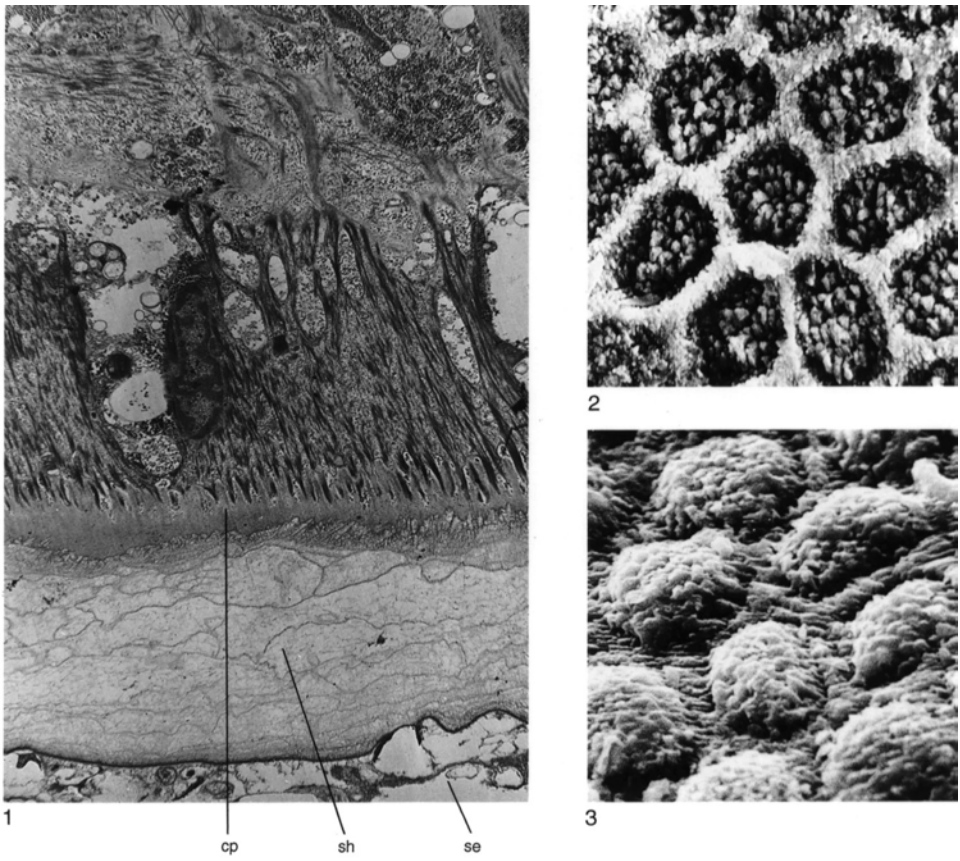

FIG. 28. Muscle attachment in *Neocrania anomala; 1,* TEM micrograph of a decalcified section of shell (*sh*), mantle, and adductor muscle base of a ventral valve, attached by folded periostracum to the substrate (*se*), showing densely distributed filaments permeating the outer epithelium and extending into a chitinous pad (*cp*), ×6,000; *2,* the raised (×1,500) and *3,* depressed (×1,400) hexagonally close-packed boundaries of calcitic pads that underlie regular cuboidal epithelium in the medial area of a posterior adductor muscle scar (Williams and Wright, 1970).

bound droplets of GAGs, glycoproteins, and some lipids as well as crystalline proteinaceous rods and stellate glycogen particles (Fig. 37.2–37.3).

The canals permeating organophosphatic shells are not so much extensions of the mantle as repositories of various extracellular secretions (see Fig. 25.1). In both lingulids and discinids, they are densely distributed with as many as three or four originating at the secretory plasmalemma of a single cuboidal epithelial cell (Fig. 38.1). They are normally up to 300 nm in diameter but may rapidly thicken into short, vertical chambers or horizontal galleries up to a micrometer or so across (Fig. 38.3–38.4). Many canals can be traced distally to slightly expanded terminal membranes situated subperiostracally. They usually have slightly undulatory axes and commonly branch dichotomously into subparallel sets so that impersistent segments of canals of variable length can be found within any section of the secondary shell. Canals may also be temporarily terminated and sealed off by transverse membranes well within laminar successions (Fig. 38.2). Arrays of them may even be displaced for a micrometer or so along interfaces within the shell succession, usually between organic and mineralized laminae.

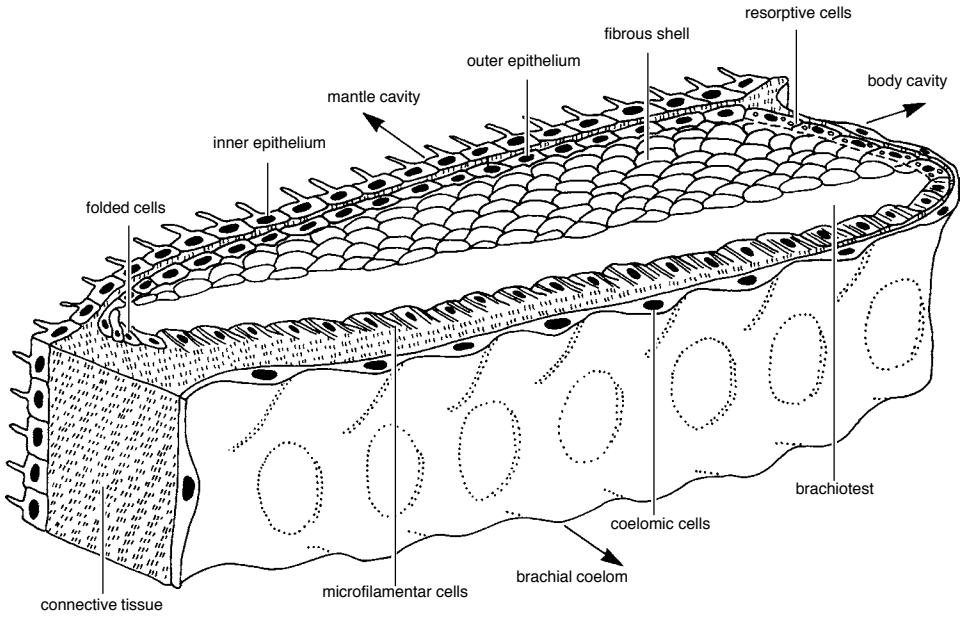

FIG. 29. Diagrammatic block section showing the differentiation of the outer epithelium enveloping a segment of the two-layered descending lamella of the loop of *Calloria inconspicua* (Mackay, MacKinnon, & Williams, 1994).

Accordingly, it is possible that some canals originate within the secondary shell. By far the most, however, must first appear beneath the periostracum and, although periodically interrupted during shell thickening, are probably perpetuated by the same patches of secretory plasmalemmas throughout growth.

The canals of *Lingula,* which are sporadically traversed by membranes and proteinaceous strands, are variably filled with

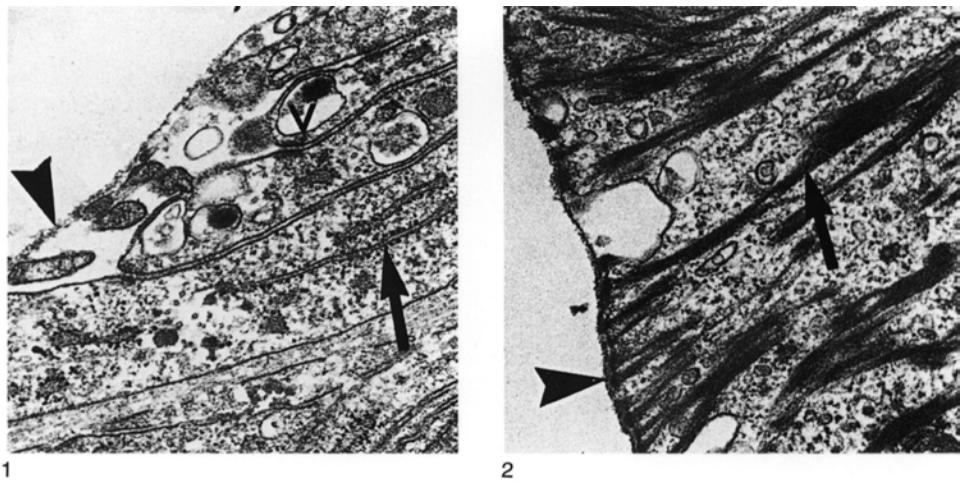

FIG. 30. TEM micrographs through tissue associated with the descending lamella of the loop of *Calloria inconspicua; 1,* zone of elongately folded outer epithelium with *arrow* pointing to rough endoplasmic reticulum, *arrowhead* to electron-dense apical membrane and vesicles (*V*) in cells responsible for the secretion of the growing edge of the lamella, ×30,000; *2,* outer epithelium, with apical granular membrane (*arrowhead*), permeated by bundles of filaments (*arrow*) and attaching connective tissue to the lamella, ×30,000 (Mackay, MacKinnon, & Williams, 1994).

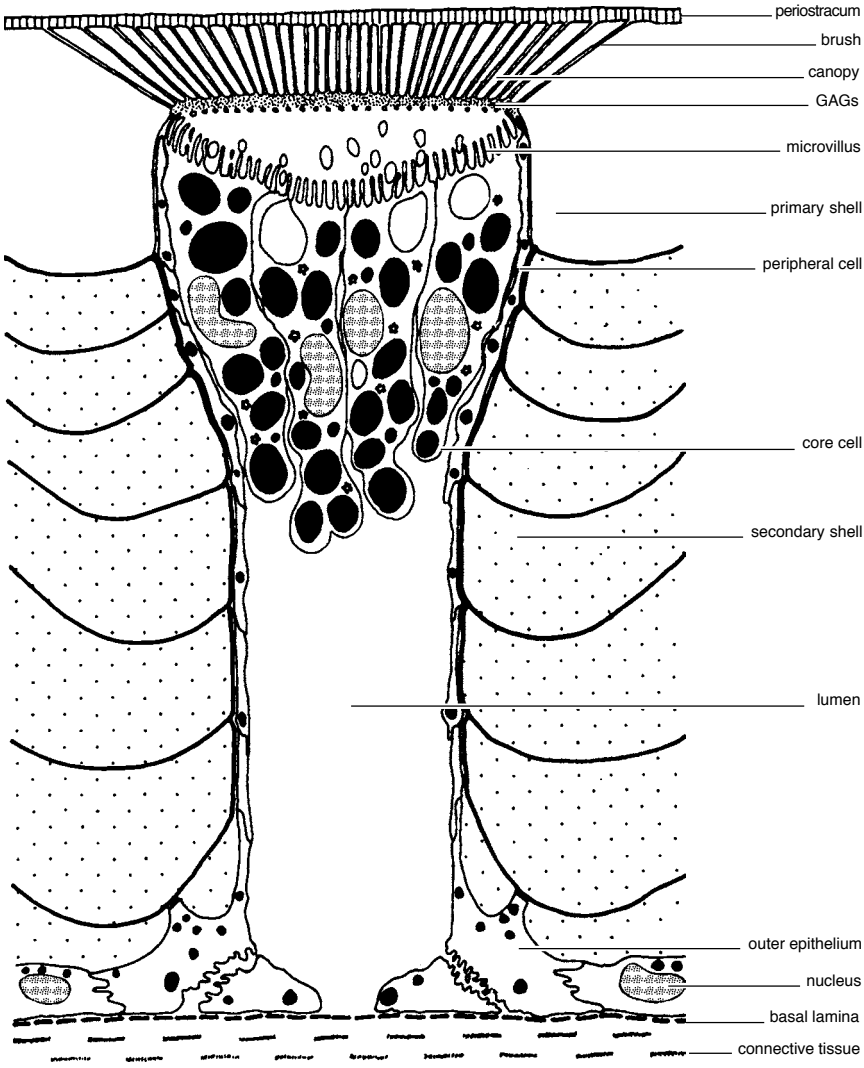

FIG. 31. Diagram of a medial longitudinal section of a terebratulide caecum showing its relation to shell and mantle (adapted from Owen & Williams, 1969).

electron-dense compounds, collapsed vesicle coats, and organically coated granules of apatite occasionally delineating ellipsoidal vacuoles. Sporadically occurring, enlarged chambers and galleries are formed around temporary, vertical and horizontal extensions of the tubular surface of the secretory plasmalemmas; but narrow canals can also be found contiguous with indentations in the plasmalemma surfaces, with which they may share a secreted infill of the same electron density. In effect, the organic constituents of the vertical canal system are assembled independently of those incorporated into the shell.

The *Discina* canal system is comparable with that of *Lingula* in disposition and content. A distinctive suite of organic components found in the *Discina* canals, however, has not yet been seen in the *Lingula* shell. These components are exocytosed deep within the interdigitating tubes of the plasmalemma surface as a bulbous assemblage of medium and lucent electron-dense particles.

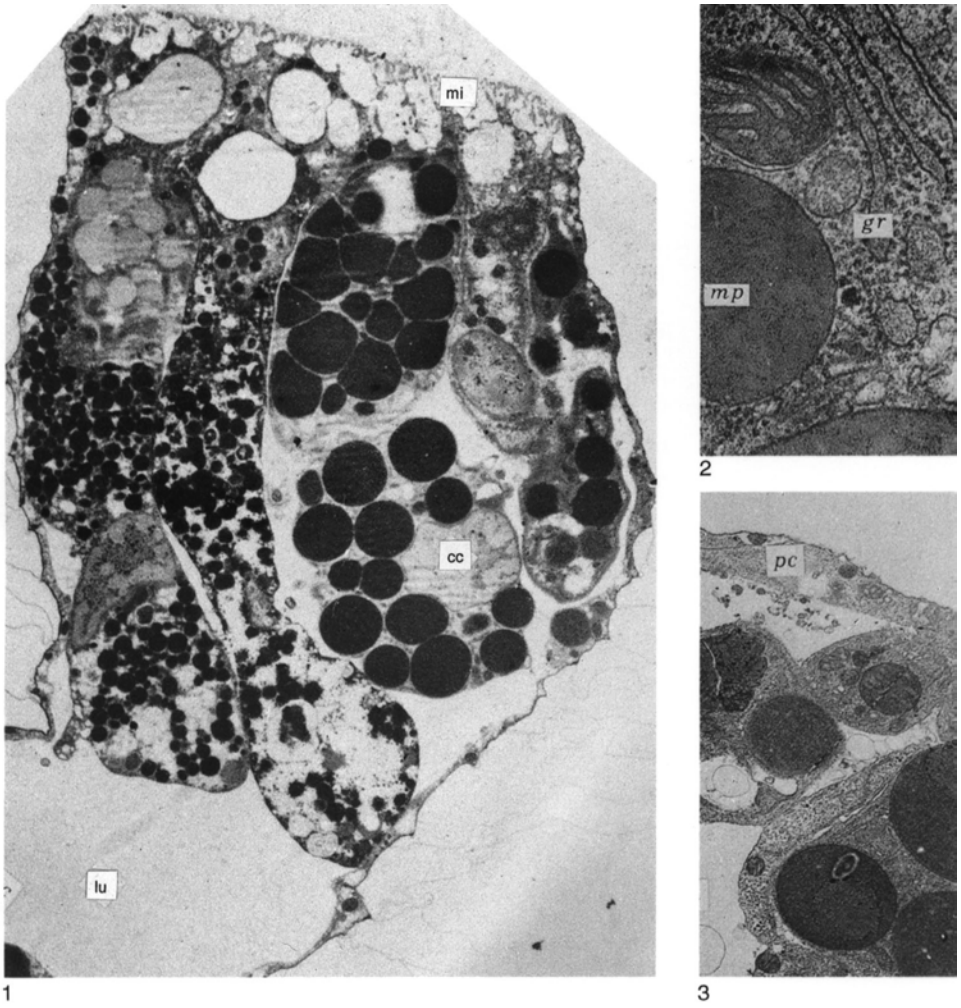

FIG. 32. TEM micrographs of decalcified sections of terebratulide caeca; *1,* caecum of *Macandrevia cranium* (MÜLLER) showing the core cells (*cc*) with their microvillous apical surfaces (*mi*) and lumen (*lu*), ×5,500; *2,* details of core cells (×55,000) and *3,* peripheral cells (*pc*) of *Calloria inconspicua* (×8,000) with conspicuous rough endoplasmic reticulum (*gr*) and glycosaminoglycans inclusions (*mp*) (Owen & Williams, 1969).

As these particles emerge from the apical surfaces of the secretory tubes, they polymerize into horizontally disposed alternating bands of electron-lucent and darker beaded lineations with a combined periodicity of 15 nm. This constituent appears to be a proteinaceous lining (with hydroxyproline) of at least part of the *Discina* canal system.

The concentric differentiation of cells at the mantle edge of living brachiopods, which can be correlated with the regular layering of the integument and especially the incorporation within the shell of caeca and canals arising at the mantle edge, raises the controversial issue on how precisely cells are added to an expanding brachiopod mantle. An incremental expansion of the mantle can be sustained by uniformly distributed mitosis keeping pace with the areal increase in the shell so that the same cells or their replacements always secrete the same skeletal components in the same relative position on the

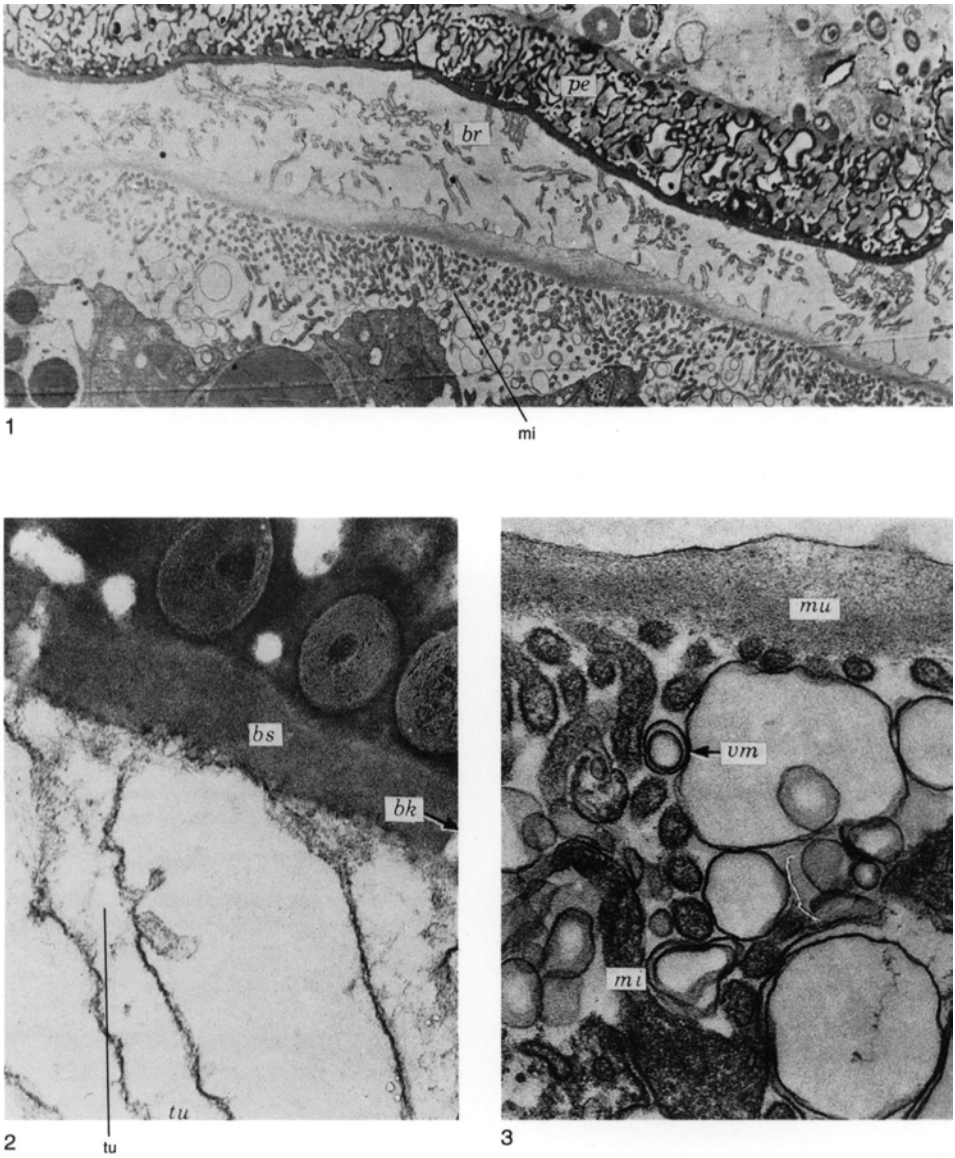

FIG. 33. TEM micrographs of decalcified sections of the caeca of *Calloria inconspicua; 1,* submedial section of the distal part of a caecum showing the composition of the caecal head with the microvillous surfaces (*mi*) of the core cells and their relationship to the brush (*br*) and periostracum (*pe*), ×6,000; *2,* detail of two tubules (*tu*) of the caecal brush showing their relationship to canal-like breaks (*bk*) in the basal layer (*bs*) of the periostracum, ×100,000; *3,* detail of the microvilli (*mi*) of the core cells showing their relationship to the GAGs layer (*mu*) and discarded vesicle membranes (*vm*), ×50,000 (Owen & Williams, 1969).

internal shell surface. (This is the process favored by KNIPRATH, 1975, to explain the growth of the shell and mantle of the gastropod *Lymnaea*.) Alternatively, the mantle can grow by peripheral addition of cells proliferated from a relatively narrow generative zone in the outer mantle lobe. As each cell migrates around the outer mantle lobe to become incorporated in the outer epithelial layer, it secretes a variety of exoskeletal

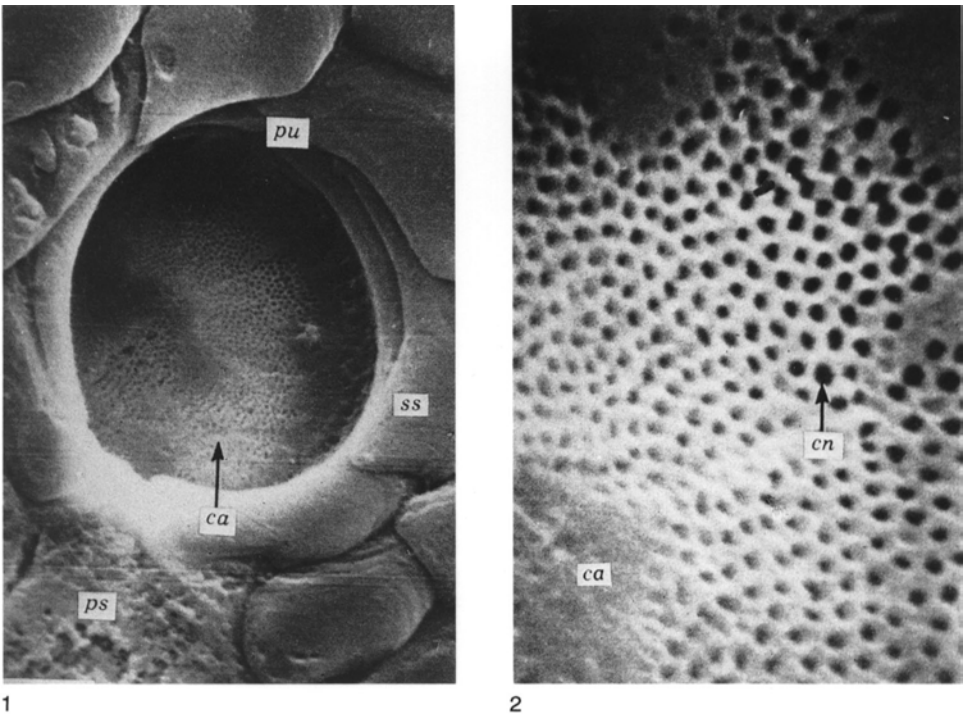

FIG. 34. SEM micrographs of a puncta (*pu*) of *Calloria inconspicua* at the internal junction between the primary (*ps*) and secondary (*ss*) shell; *1,* internal view of canopy (*ca*), ×2,600; *2,* detail of canopy (*ca*) showing a meandriform array of canals (*cn*), ×13,000 (Owen & Williams, 1969).

components in the same chronological order as their occurrence in the shell succession. In effect, except for adjustment during interphase (and minor, widely dispersed intramarginal mitosis), each cell of the mantle remains in proximity to that part of the shell it has secreted *ab initio.* The term conveyor-belt system has been applied to this mode of growth (WILLIAMS, 1968d).

The nature of the relationship between the outer epithelium and the shell succession of living brachiopods suggests that the growth of the mantle involves a continuous migration of cells from a mitotic zone at the outer mantle lobe. There is strong evidence for believing that the various constituents of organophosphatic shells are assembled intracellularly and, on exocytosis, become part of a thickening column of shell that has been secreted by the same patch of epithelium irrespective of structural and compositional changes within the layers. The study by PAN and WATABE (1989) of the regeneration of periostracum and shell in *Glottidia* showed that repair progressed in the same order of secretion of constituents as is followed consecutively by vesicular cells and cuboidal outer epithelium.

Calcareous-shelled brachiopods, on the other hand, appear to be separated from the secreting plasmalemma of the mantle by a space that could be the main site for assembling shell constituents. The occurrences of caeca, however, which can arise only at the outer mantle lobe, must involve conveyor-belt growth throughout the postprotegular shell of all punctate species (Fig. 35).

In accepting this mode of growth, account has to be taken of the secretory sequences of the cells making up the outer mantle lobe and the evidence for mitosis. Lobate cells, being responsible only for superstructural

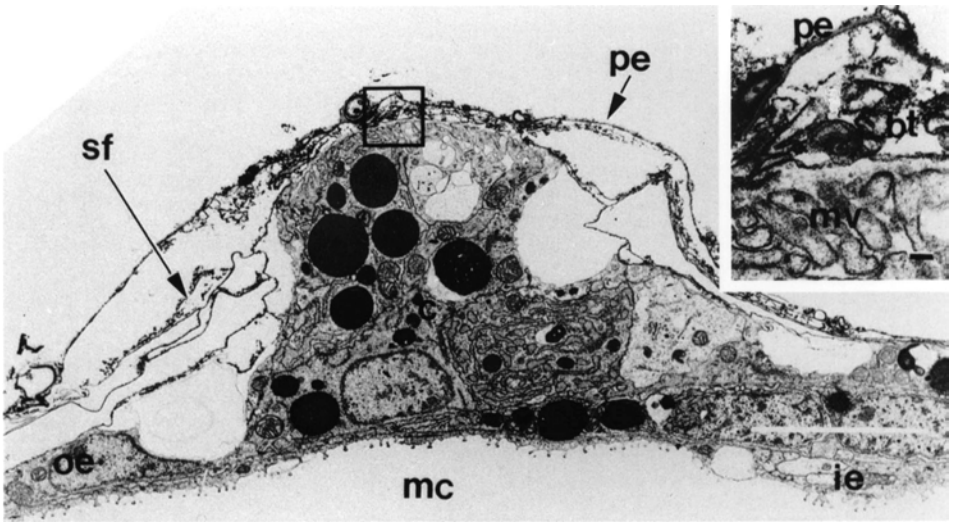

FIG. 35. TEM micrograph of a decalcified section of a juvenile caecum of *Terebratalia transversa* (SOWERBY) in relation to the periostracum (*pe*), membranes ensheathing secondary fibers (*sf*), and mantle consisting of outer (*oe*) and inner (*ie*) epithelium, ×5,000; the box as an enlarged inset shows microvilli (*mv*) of the core cells immediately below brush tubes (*bt*), ×32,800 (Stricker & Reed, 1985b).

embellishment of the periostracum, cannot be involved in migration into the position occupied by vesicular cells (WILLIAMS, 1973). Accordingly, any conveyor-belt movement would involve only the vesicular and cuboidal outer epithelial cells, in effect, the epithelial monolayer responsible for the secretion of the basal components of the periostracum and the succeeding shell succession. Moreover, the assumption that the mantle expands mainly by the addition of new cells at its margin prompts expectation that mitotic figures should be commonly found within that part of the outer mantle lobe delineated by the periostracal groove. Such evidence of active cell division has only been occasionally seen in margins of mature mantles (PAN & WATABE, 1989) and has not been found in the postlarval development of the mantle of *Terebratalia,* which has been subjected to an exhaustive scrutiny by STRICKER and REED (1985a, 1985b). Intercalation of new cells, however, must take place along the circumferential margin of an expanding epithelial monolayer, and the absence of evidence of significantly high mitotic activity does not preclude an incremental addition of new cells, which is more likely to be at an unexceptional rate.

MANTLE-PEDICLE RELATIONSHIP

In the umbonal areas of a brachiopod, the mantle is normally associated with a pedicle, and their relationship is variable and can be topologically complex.

In lingulids, the pedicle is differentiated as an outgrowth of the ventral part of the embryonic inner epithelium, which later becomes the posterior body wall (YATSU, 1902a). In maturity, the junction between the wall and pedicle occurs along the dorsal arc of the circular pedicle base (Fig. 39.1). It is marked by a sudden change from microvillous, nonciliated inner epithelium secreting a glycocalyx to a pedicle epithelium distinguishable as a band of cells charged with electron-dense vesicles and exuding an electron-dense outer bounding membrane of the **pedicle cuticle** through irregular, cylindroid prolongations of the plasmalemmas. The dorsal boundary of the **posterior body wall** is the inner lobe of the mantle margin

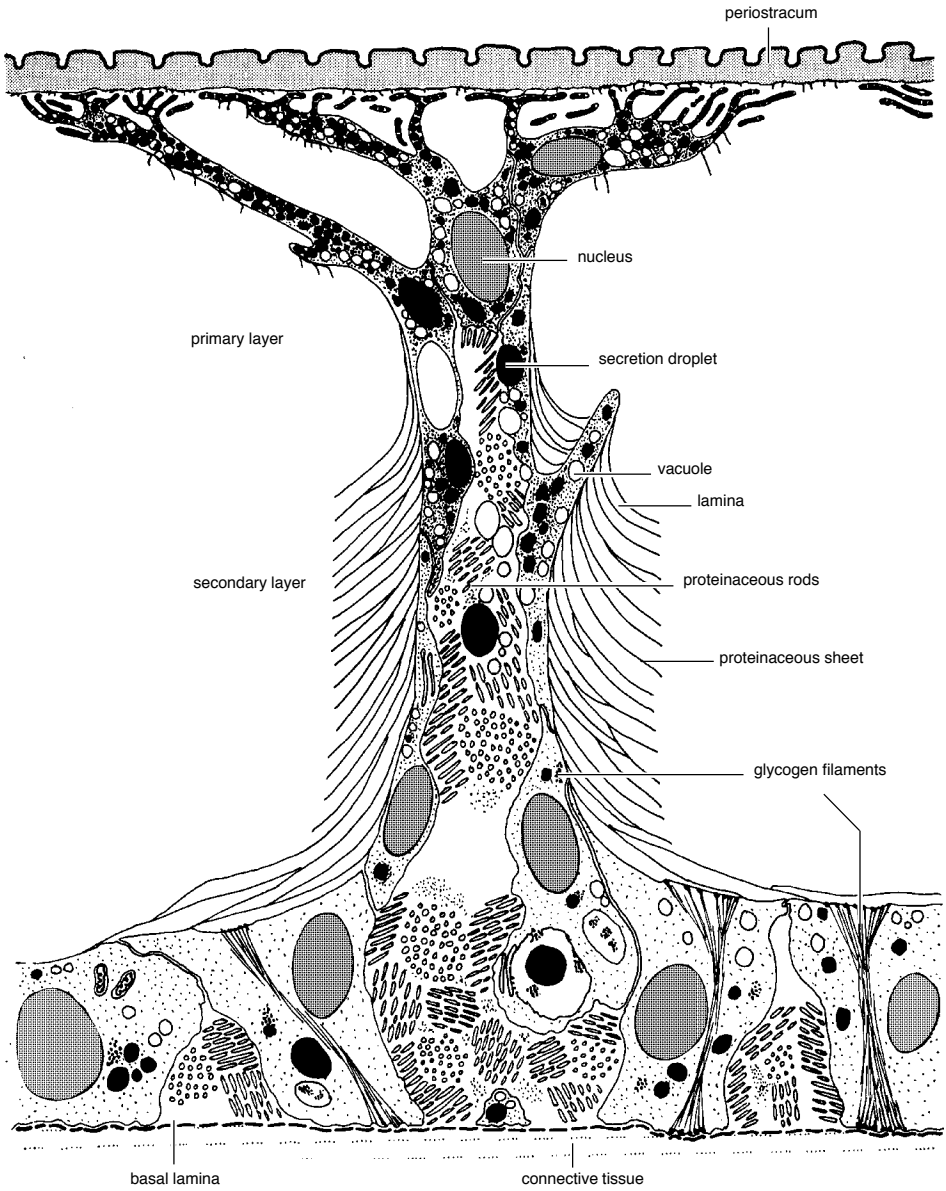

FIG. 36. Diagrammatic representation of a medial longitudinal section of a caecum showing its relationship to the periostracum and the dorsal mantle of *Neocrania anomala* (adapted from Williams & Wright, 1970).

underlying the posteromedian part of the dorsal valve. Here the junction between the inner and outer lobes is marked in the usual way by a marginal array of setae and their follicles (Fig. 39.1). The ventral sector of the pedicle base is also represented by a sharp junction, although between outer and pedicle epithelia. The junction is marked by a thick, electron-dense sheet (pedicle sheet), intervening between cuticle and shell and secreted by a narrow band of vesicular columnar cells, which are assumed to be homologous with the vesicular cells of the outer mantle (Fig. 40).

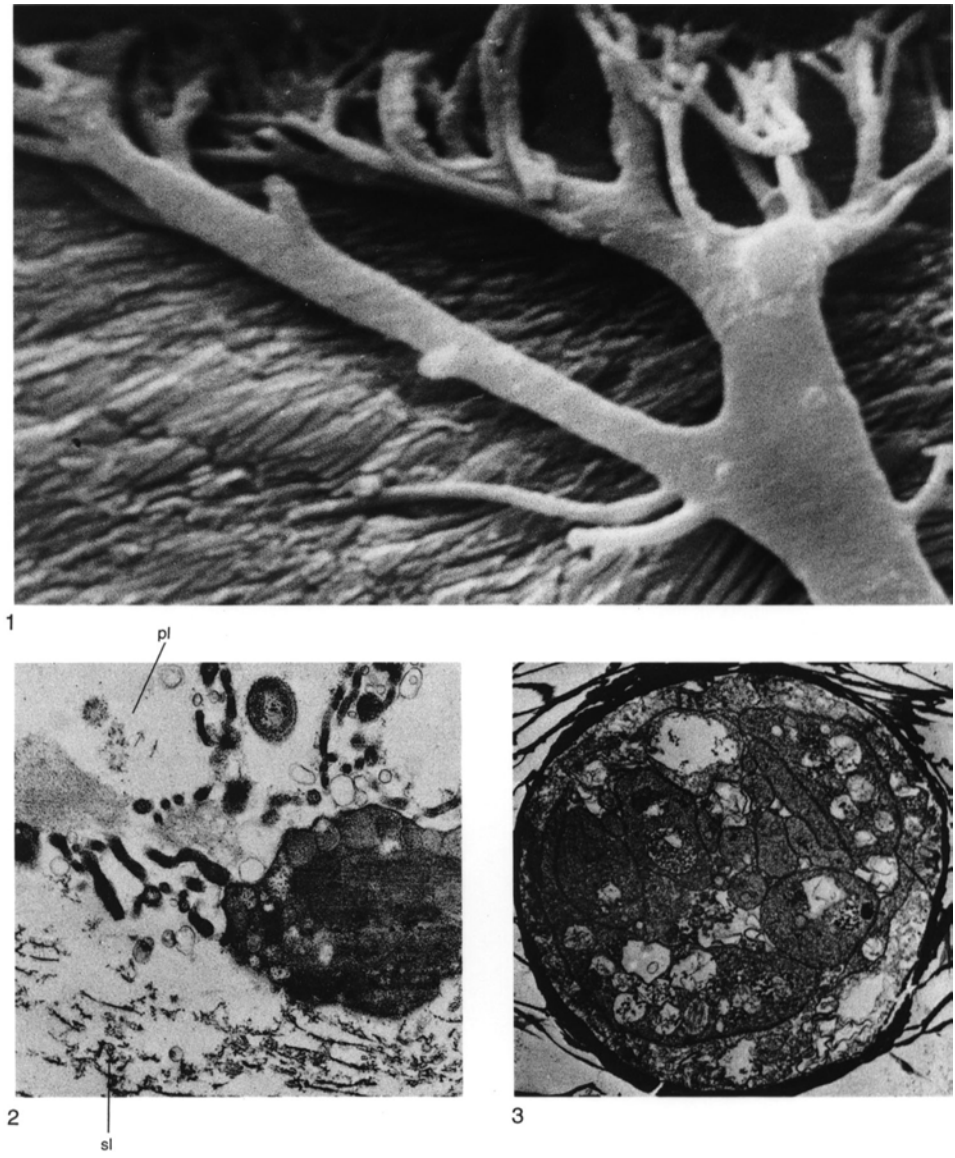

FIG. 37. Various aspects of the caeca and punctation of *Neocrania anomala; 1,* SEM micrograph of an etched section of the primary layer of the dorsal valve showing the branches and tubules of a puncta filled with resin, ×5,200; *2,* TEM micrograph of a terminal branch of a caecum with branching tubules seen in transverse to longitudinal sections in the primary layer (*pl*) with proteinaceous sheets of the secondary layer (*sl*) beginning to appear at the bottom of the micrograph, ×15,000; *3,* transverse section of a caecal branch, surrounded by the proteinaceous sheets of the secondary shell, showing the highly vesicular inclusions forming the core to stretched outer epithelium at the periphery, ×8,000 (Williams & Wright, 1970).

In lingulids the pedicle emerges between the umbones of both valves, but the pedicle of discinids is ventrally located relative to the commissural plane; and, although the early stages in discinid development are unknown, the disposition of epithelial junctions in mature shells clarifies the relationship between mantle and pedicle (Fig. 39.2). In

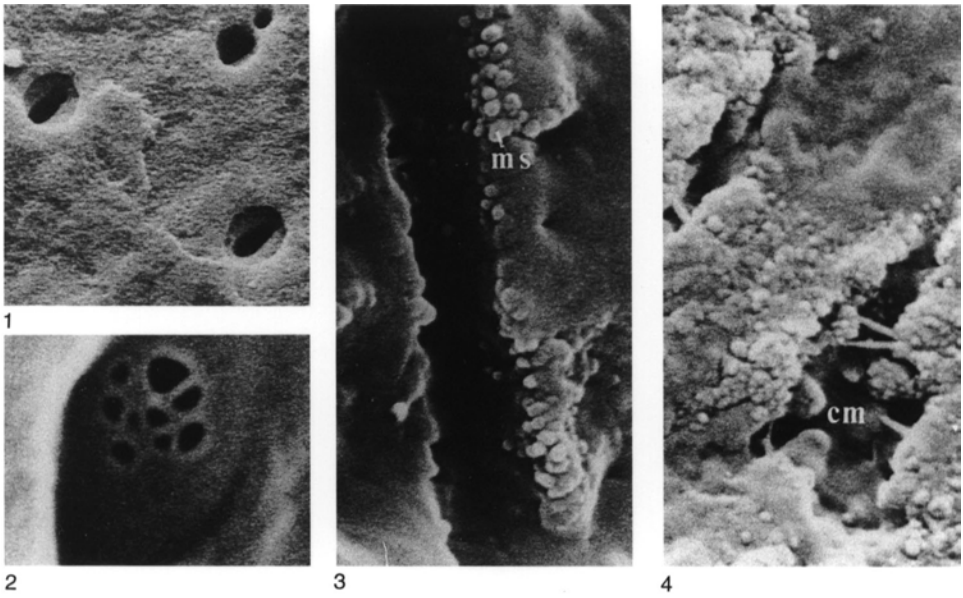

FIG. 38. Various SEM micrographs of canals and chambers in the shell of *Lingula anatina; 1,* canal apertures exposed on the internal surface of an apatitic lamina digested in chitinase, ×3,000; *2,* transverse membrane in a canal penetrating an apatitic lamina treated with Tris buffer, ×30,000; *3,* canal wall studded with apatitic mosaics (*ms*) penetrating a lamina of apatite and GAGs digested in endoproteinase Glu-C, ×14,000; *4,* vertical chamber (*cm*), intruded by apatitic mosaics, and branching canals all crossed by fibrous collagens in a lamina composed of botryoidal masses of apatitic mosaics and GAGs (especially in top right corner) treated with phosphate buffer, ×9,000 (Williams, Cusack, & Mackay, 1994).

mature *Discinisca,* the pedicle epithelium along the ventral sector of the pedicle base is also contiguous with the outer epithelium responsible for the secretion of the ventral valve. The only difference from the lingulid arrangement is that the pedicle base and its surrounding cuticular sheet encroach anteriorly over a much greater area of the external surface (BLOCHMANN, 1900). The junction between the posterior body wall and the outer epithelium of the dorsal valve is also the same. That junction between the posterior body wall and the dorsal arc of the pedicle base, however, is indented to accommodate another array of marginal setae. Consequently, the discinid posterior body wall is fringed by two arrays of setae so that the array between the pedicle and inner epithelia is likely to be the homologue of the array along the margin of the ventral mantle (Fig. 39.2).

This relationship suggests that the pedicle originated entirely within the embryonic precursor to the ventral outer epithelium and not as an outgrowth of inner epithelium as in *Lingula.* The assumption explains why the posteromedian margin of a maturing ventral valve appears to grow dorsally around the pedicle, which becomes enclosed in an oval slit bridged by periostracum and primary layer only in *Discinisca* but by some underlying apatitic shell as well in *Discina.*

The various junctions between mantle and pedicle are similarly differentiated in lingulids and discinids so that those studied ultrastructurally in selected species are typical of the organophosphatic group as a whole.

The inner-outer epithelial junction at the pseudointerarea forming the posteromedian margin of the dorsal valve of *Glottidia* is like that at the anterior margin of the shell except

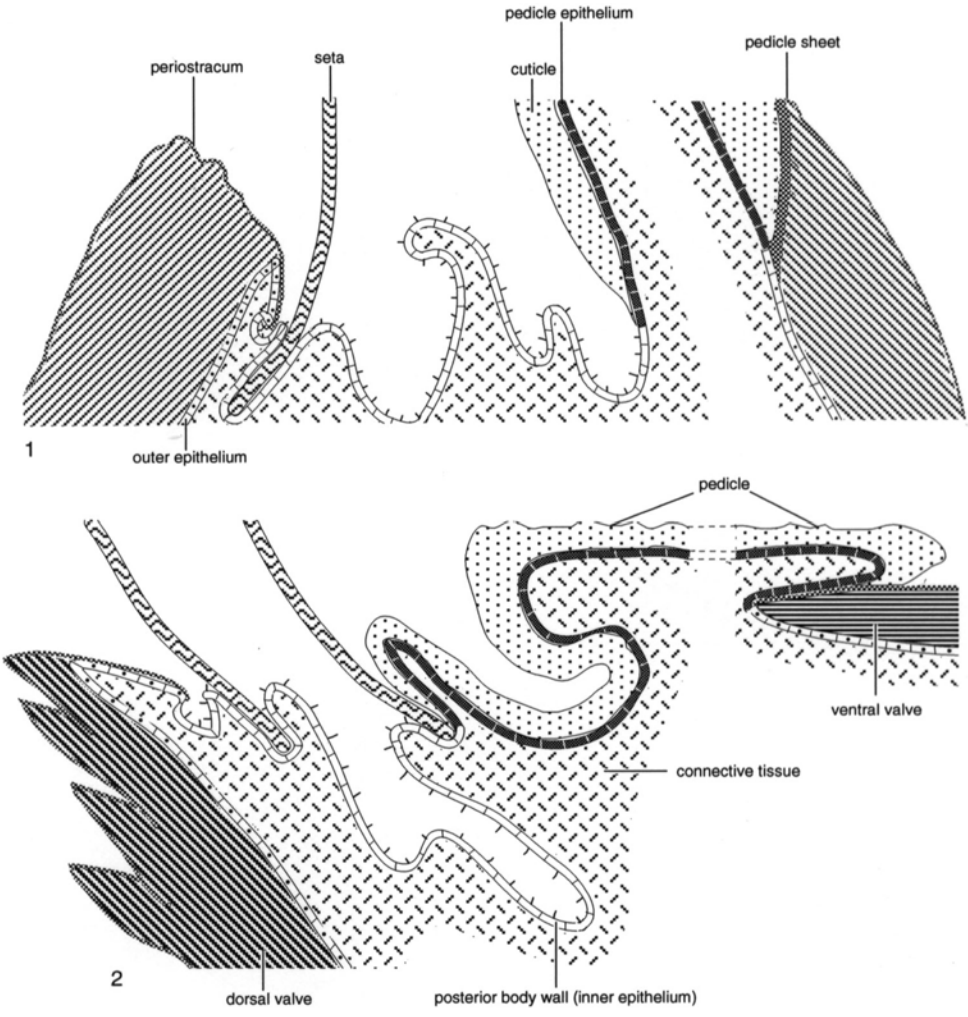

FIG. 39. Diagram of the inner, outer, and pedicle epithelia in relationship to the shell and pedicle of mature *1, Lingula* and *2, Discinisca* (new).

for the absence of the periostracal groove. Consequently, the microvillous, inner epithelium and periostracum-secreting outer epithelium, along the inner face of the outer lobe, are almost parallel to each other away from a deeply inserted, narrowly angled junction that is sharp (Fig. 41.1).

The junction between outer and pedicle epithelia in the posteromedian region of the ventral valve is also sharp with the short, microvillous apical plasmalemmas of the pedicle epithelium instantly distinguishable from the irregularly extended ones of the outer epithelium. Vesicles with electron-dense contents are common in both types of epithelia and, at the junction, contribute to the expansion of the electron-dense sheet separating the base of the pedicle from the inwardly sloping posterior surface of the ventral valve (Fig. 40).

The junction between inner and pedicle epithelia is as sharp as those involving the outer epithelium. The inner epithelium secretes a thick, speckled glycocalyx that is

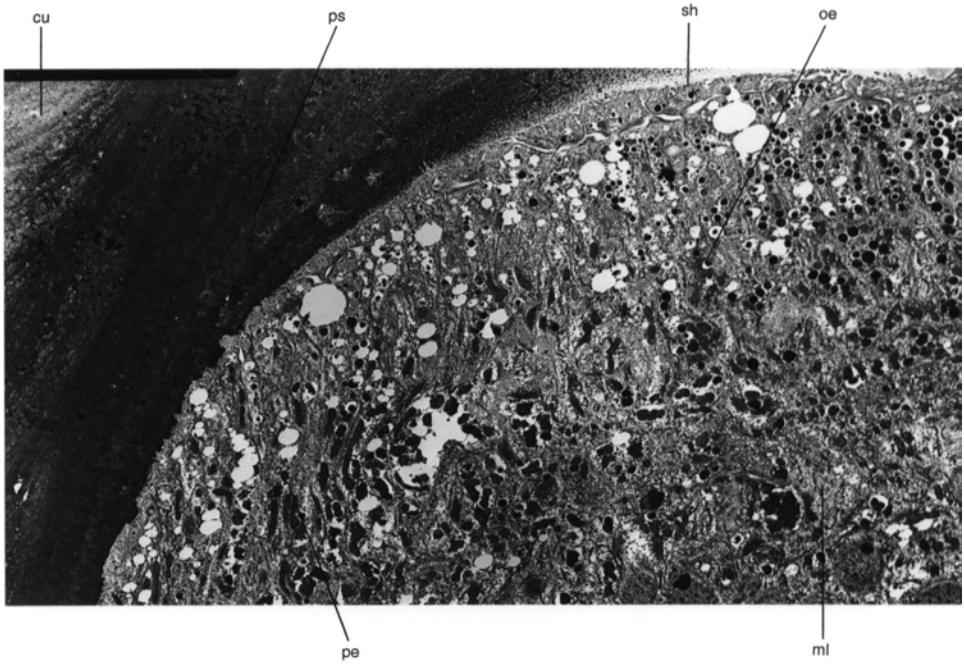

FIG. 40. TEM micrograph of a section of the posteromedian part of a decalcified ventral valve (with pedicle) of *Lingula anatina* showing the junction between outer (*oe*) and pedicle (*pe*) epithelium in relation to shell (*sh*), cuticle (*cu*), and pedicle sheet (*ps*) and the muscle layer (*ml*) lining the pedicle, ×3,000 (new).

propelled across the junction by microvilli up to half a micrometer long. At the junction the inner epithelium gives way to a narrow band, one or two cells wide, that secretes beneath the glycocalyx a continuous sheet of electron-dense nodules that, within a micrometer or so, polymerize into an electron-dense, sparsely fibrillar coat about 15 nm thick and discrete nodules up to 150 nm in size (Fig. 41.2). The coat and nodules form the cover to the pedicle cuticle, which consists for the most part of a fibrillar mesh of chitin in an electron-light matrix; the chitinous fibrils interconnect with the nodules. The cells secreting the cuticular cover are more like pedicle epithelium although their apical plasmalemmas are extended as irregular protuberances up to 50 nm thick and are thereby distinguishable from the microvillous pedicle and inner epithelia.

In living craniides no pedicle is developed, and the ventral valve is cemented to the substrate by a posterior attachment area in the larval stage (NIELSEN, 1991) and additionally by a film of adhesive mucin (Fig. 42), exuded as an external coat to the periostracum at the mantle edge in the mature shell (WILLIAMS & WRIGHT, 1970).

In articulated brachiopods, the relationship between the mantle lobes and between the pedicle and the mantle as a whole is fundamentally different from those of inarticulated species. In the former group, the pedicle is first differentiated, not as an outgrowth of the ventral mantle, but as a posterior pedicle rudiment continuous with a mantle rudiment that develops into both valves (see Fig. 63). Moreover, the mantle cavity contained by microvillous, inner epithelium is not continuous around the shell but restricted to the anterior part in the following way.

The mantle edges of both valves remain discrete around the gape of the shell as far as the cardinal extremities. Here at the lateral ends of the hinge line, the mantle edges join and simultaneously divide in another plane to accommodate the coelomic cavity. First,

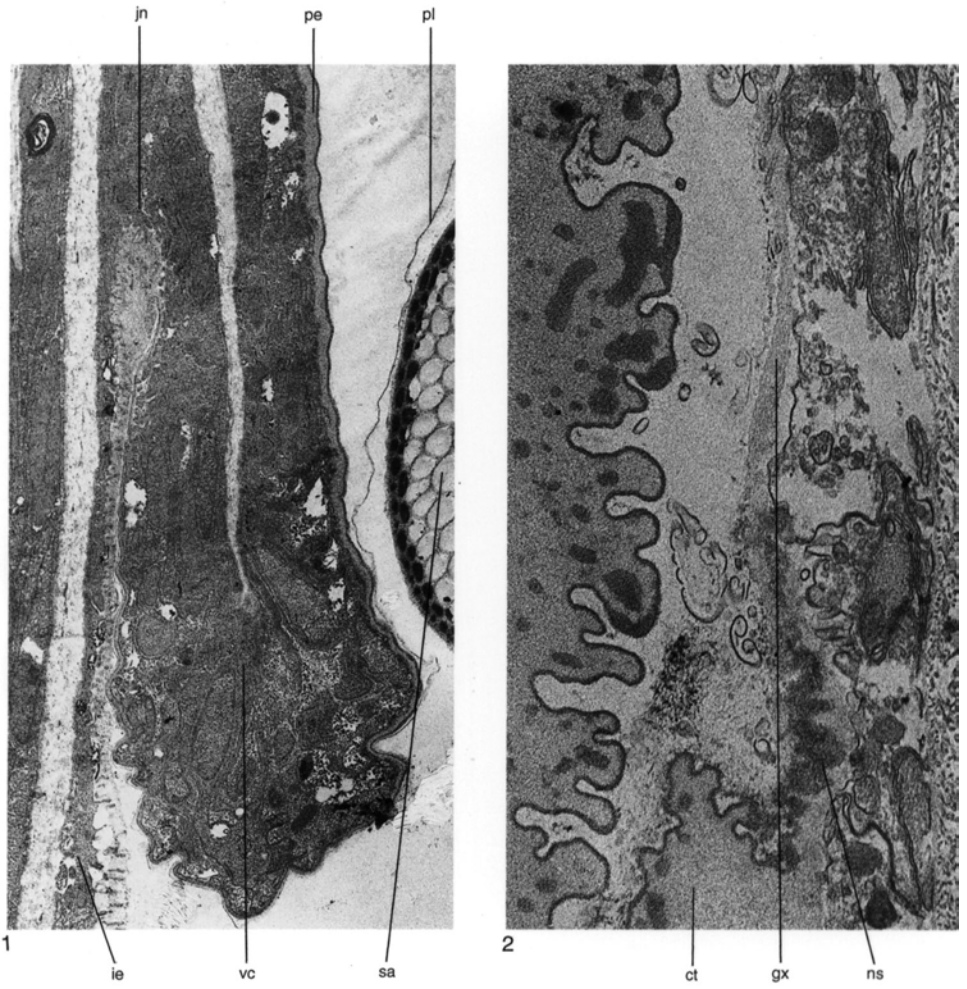

FIG. 41. TEM micrographs of sections of decalcified posteromedian regions of the shell of *Glottidia pyramidata; 1,* the junction (*jn*) between the vesicular cells (*vc*) of the outer mantle lobe secreting periostracum (*pe*) and the inner epithelium (*ie*) at the pseudointerarea of the dorsal valve with pellicle (*pl*) and seta (*sa*), ×5,250; *2,* the transition from cuticle-secreting (*ct*) pedicle epithelium to glycocalyx-exuding (*gx*) microvillous inner epithelium through cell(s) secreting electron-dense nodules (*ns*), ×17,750 (new).

the inner mantle lobes of inner epithelium fuse into one layer, which falls away to become the anterior body wall. Then the outer lobes of both edges come together to form a complex of cells (Fig. 43). These constitute two strips of outer epithelium that secrete the carbonate ventral and dorsal interareas and their periostracal covers (WILLIAMS, 1956; WILLIAMS & HEWITT, 1977).

The posterior outer epithelial zone is well developed in *Thecidellina* but differs fundamentally from that of other living articulated brachiopods by lacking a pedicle. In living thecideidines, no pedicle develops from the caudal rudiment of the embryo (KOWALEVSKY, 1874). Instead, the periostracum of the pedicle valve is directly attached to the substrate, probably by a film of mucin. Accordingly, the hinge line is unbreached by such medial openings as the delthyrium and notothyrium and is underlain by a continuous strip of posterior epithelium extending from

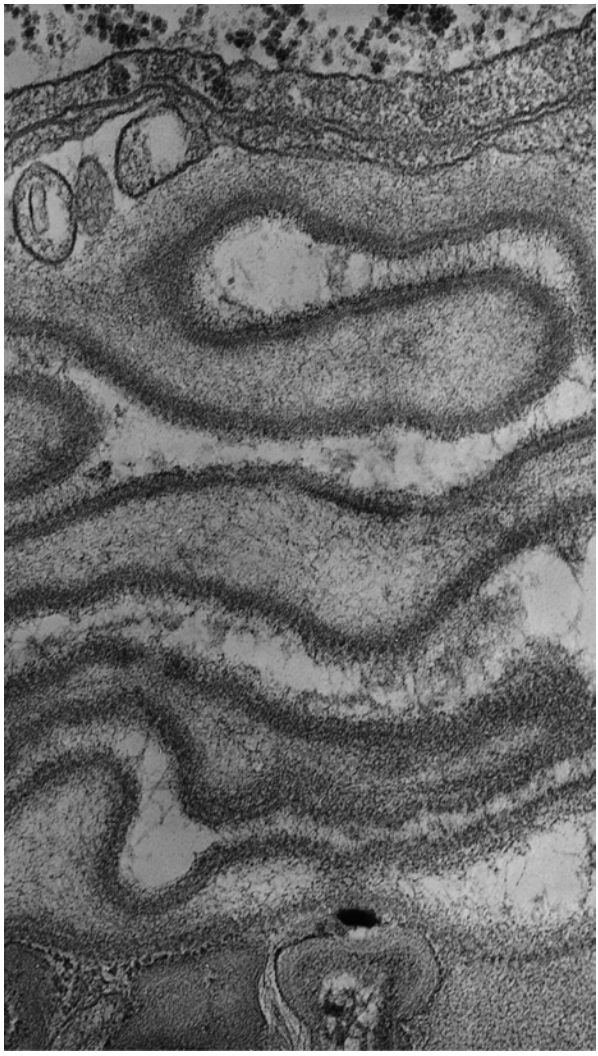

FIG. 42. TEM micrograph of a section of a decalcified ventral valve and mantle of *Neocrania anomala* showing a highly folded periostracum attached to the substrate (below) with tubular extensions of the plasmalemma of the secreting outer epithelium (above), ×40,000 (new).

one cardinal extremity to another (WILLIAMS, 1973).

This strip consists of an inner row of six to eight, highly vesicular, columnar cells grouped around an infold of periostracum and an outer row of larger cells, continuous with cuboidal outer epithelium and probably also concerned with secreting carbonate shell, especially along the slowly growing faces of each interarea (Fig. 44). Secretion of the periostracum begins in the anteromedian zone of the periostracal fold. Electron-dense granular material, probably comparable with the film of GAGs exuded at the outer mantle lobe, is secreted by two or three medially situated columnar cells along intercellular pathways as well as across the plasmalemmas. Within two micrometers of its deposition as a continuous mass, the exudation parts irregularly into two layers forming impersistent external coats of the ventral and dorsal interareas. The periostracum proper is

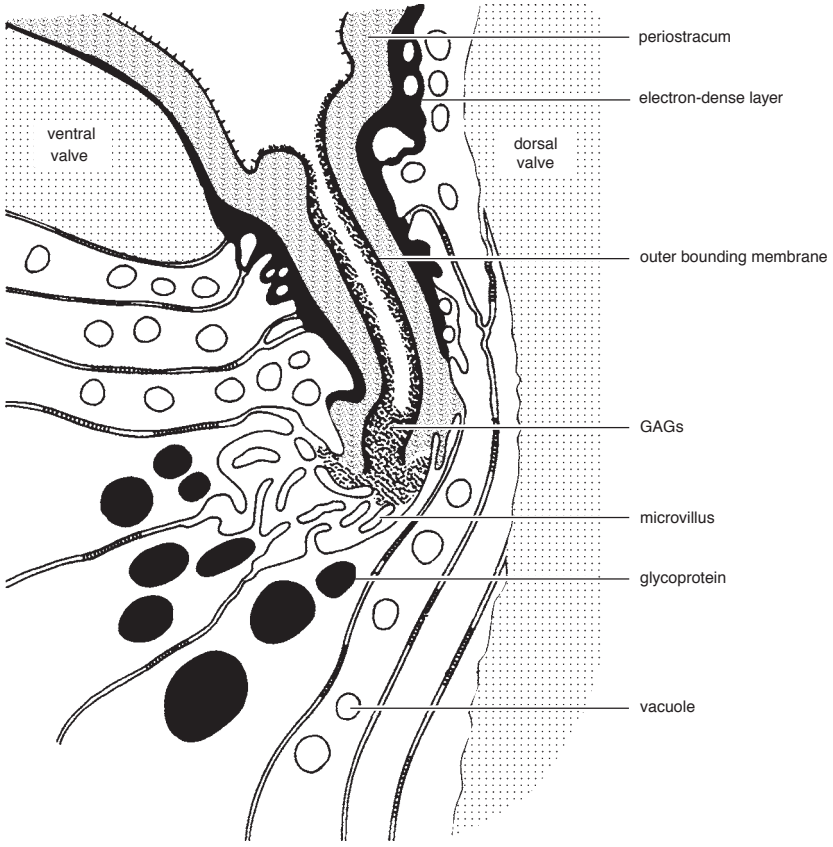

FIG. 43. Diagrammatic longitudinal section of the fused outer mantle lobes underlying the cardinal margins of a young *Notosaria,* approximately ×25,000 (Williams and Hewitt, 1977).

secreted even within the fold as two discrete layers separated by the medial mass of the external coat. Each periostracal layer is banded and is deposited as a series of acutely disposed, overlapping wedges that become progressively younger toward the fold. Secretion of periostracum terminates at the edge of the fold with the exudation of a sealing membrane a few nanometers thick. The membrane acts as a seeding sheet for calcite crystallites representing the beginnings of the carbonate layer of the interarea.

In rhynchonellides and terebratulides, a posterior rudiment or lobe, which is nonciliated (STRICKER & REED, 1985c), develops into a pedicle filling the larger, delthyrial and smaller, notothyrial openings in the ventral and dorsal interareas respectively of adult shells. The junction with the mantle, therefore, is shared with the outer epithelium responsible for the secretion of both valves and intersects the fused mantle lobes secreting the carbonate interareas and their periostracal covers. The junction between the microvillous epithelium secreting the pedicle cuticle and outer epithelium is sharp. It is marked by a narrow band of one or two cells that differ from pedicle epithelium in lacking microvilli and from outer epithelium in secreting granular calcite sealing off secondary fibers and their sheaths and a thin proteinaceous membrane, which acts as a bonding sheet for the folded cuticle (Fig. 45–46).

The ringlike junction can be distorted by differential growth of its biomineralized boundaries, but its circumference can only increase at its intersection with the fused mantle lobes underlying the hinge line. The

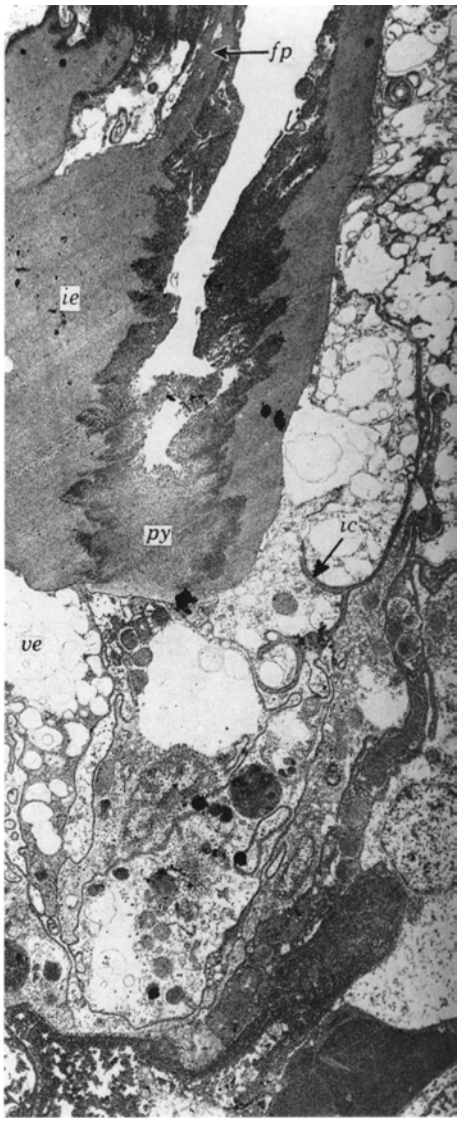

FIG. 44. TEM micrograph of a decalcified dorsoventral section of the periostracal fold and columnar cells at the hinge-line of *Thecidellina barretti* showing the periostracum consisting of an external flaplike layer (*fp*) and an internal layer (*ie*) of medium electron density, intercellular (*ic*) and medial (*py*) GAGs, and vesicular cell (*ve*), ×5,500 (Williams, 1973).

fused mantle lobes of such rhynchonellides as *Notosaria* and such terebratulides as *Terebratulina* have been studied (WILLIAMS & HEWITT, 1977) and are structurally comparable with those described for the thecideidines.

The most striking deformation of the ringlike junction occurs when the ventral, outer-mantle lobes grow dorsomedially from their intersection with the pedicle-outer epithelial junction and secrete a pair of tetrahedral structures, the **deltidial plates.** The plates can extend medially only because they grow posterodorsally of the umbo of the dorsal valve. Further growth leads to a median conjunction of deltidial plates to form a **deltidium** and, in such genera as *Liothyrella,* to a median fusion of the paired ventral lobes to form a common secretory unit exuding both periostracum and underlying carbonate shell as a continuous structure (**symphytium**) across the delthyrium (see Fig. 317). The symphytium is frequently identified in such other terebratulides as *Gryphus* and *Laqueus,* but usually there is a well-developed median suture; and even in *Liothyrella,* transverse sections near the posterior margin of the symphytium will always show that the structure originated by fusion of ventral mantle lobes.

MARGINAL SETAE

Fine, chitinous bristles (**setae** or chaetae) occur in clusters at the epithelial surface of all brachiopod larvae and in closely spaced sets emerging from the mantle grooves of all adult brachiopods except for craniids, thecideidines, and megathyrids. A typical, mature seta within the mantle groove occupies a cylindroid invagination (**follicle**) of a single layer of cells with many characteristics of the inner epithelium (Fig. 47). In particular, they are covered with regular arrays of microvilli up to 500 nm long and contain abundant mitochondria with arcuate cristae, densely distributed glycogen, and filamentar bundles connected with the microvilli. The base of the follicle is formed of a specialized cell(s) (Fig. 48–49), the setoblast (GUSTUS & CLONEY, 1972; STORCH & WELSCH, 1972), with erect, apical microvilli up to 6 μm long in *Lingula* and in the larva of *Terebratalia.*

A seta occupying such a follicle, which may be several millimeters long, consists of closely packed cylindrical or prismatic canals with diameters of 600 nm or so medially but dwindling to less than 100 nm at the circum-

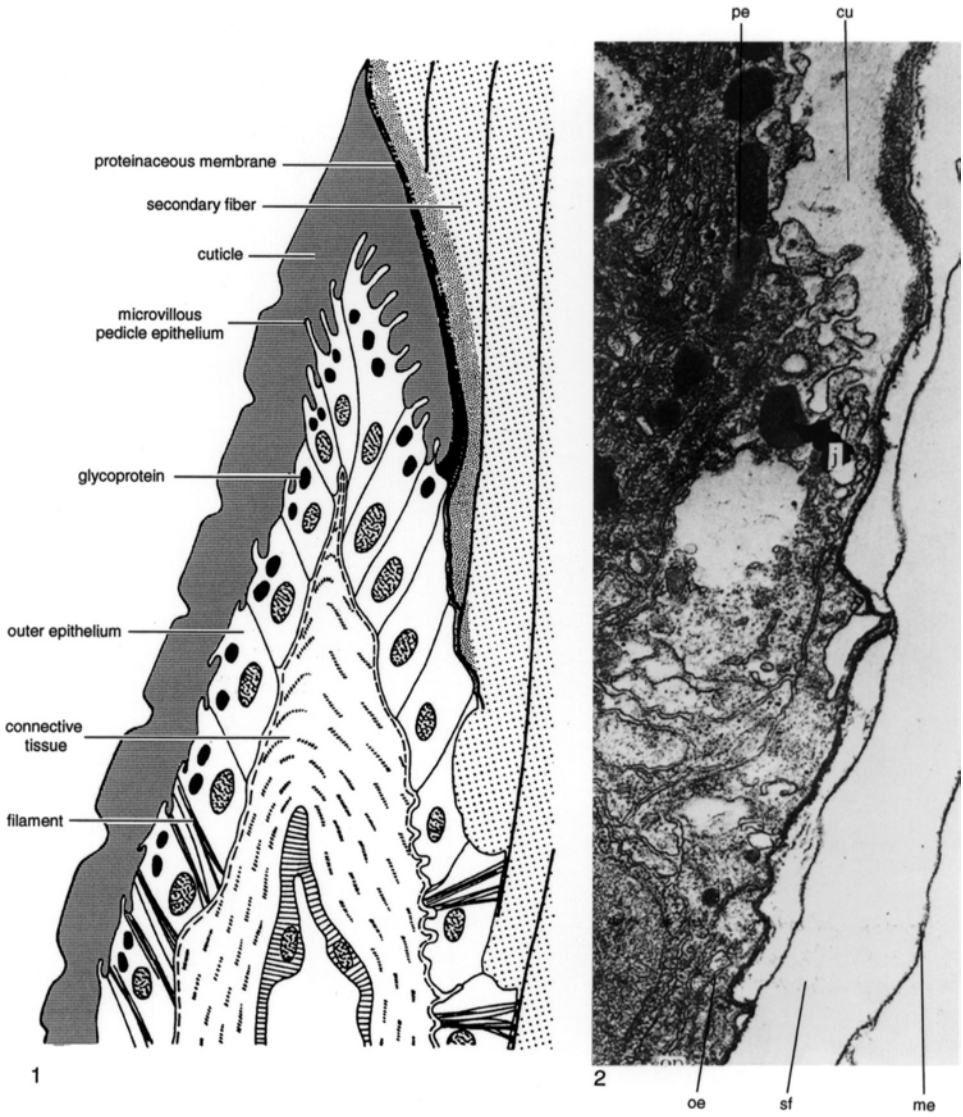

FIG. 45. Drawing and TEM micrograph of a decalcified longitudinal section of the ventral-pedicle mantle junction in young *Notosaria nigricans; 1,* relationship between the cuticular fold and the pedicle collar, approximately ×10,000; *2,* detail of junction (*j*) between pedicle epithelium (*pe*) secreting the cuticle (*cu*) and outer epithelium (*oe*) depositing secondary fibers (*sf*) with membranous sheaths (*me*), ×20,600 (Williams & Hewitt, 1977).

ference (Fig. 47.1; 50.1). The walls defining the larger, medial canals are secreted by the setoblast as chitinous casts around but not over the long microvilli. The walls polymerize and, as secretion proceeds, move distally to form a seta that can eventually be composed of several hundred such canals. Although most of a seta is secreted by the setoblast, the outer layers of smaller canals, which have thicker walls, are exuded by the cells lining the follicle (Fig. 50). In *Lingula,* electron-dense clots, composed of fibers and scattered throughout a loose mesh of branching chitinous fibers up to 300 nm long, migrate from the tips of the microvilli to become attached to and assimilated within the outer, cortical layer of the seta. Many such clots are emptied of their fibrous

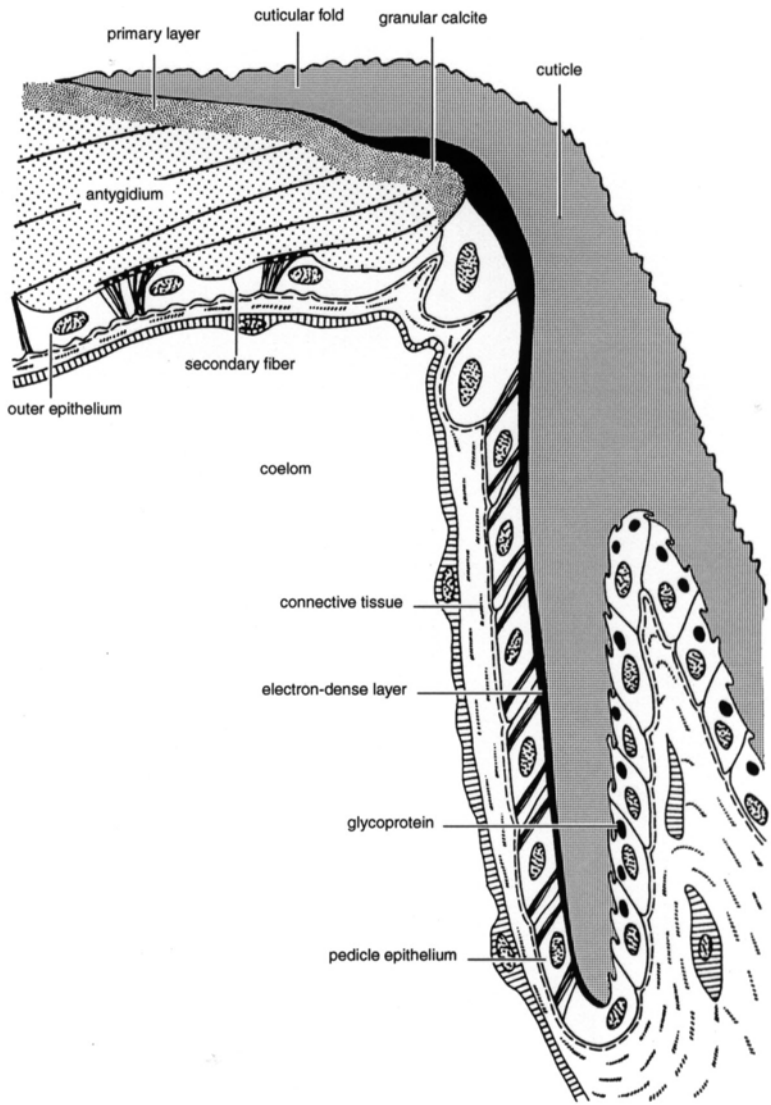

FIG. 46. Diagrammatic longitudinal section showing the relationship between the dorsal sector of the pedicle-outer epithelial junction and the antygidium of the dorsal valve of a young *Notosaria nigricans,* approximately ×10,000 (Williams & Hewitt, 1977).

constituents presumably through their incorporation within the matrix of the cortical layer. This bounding layer is further differentiated so that, by the time the seta emerges from the follicle, it consists of a triple-layered membrane of contrasted electron density, about 60 nm thick, with an array of very short, erect fibers on the outer surface.

The larval setae of *Terebratalia* (GUSTUS & CLONEY, 1972) and *Terebratulina* (STRICKER & REED, 1985a) are indistinguishable from those of adults except for diameter, as they are seldom composed of more than 50 canals. Setae of comparable delicacy are interspersed among more robust ones along the mantle edge of an adult valve and have evidently been secreted by newly formed follicles. Slender setae may also occupy the same follicles as mature ones; and this arrangement has been interpreted by RUDWICK

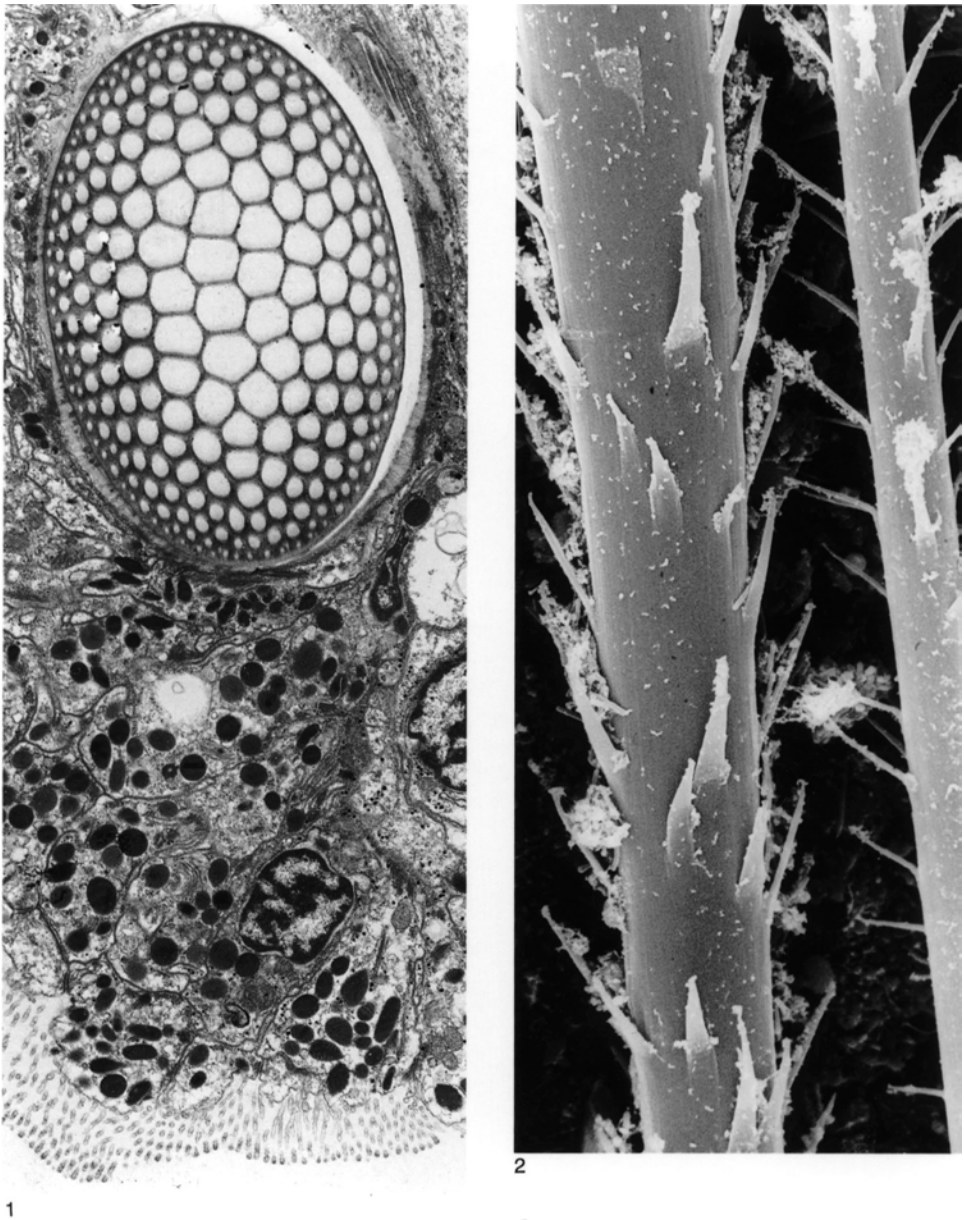

FIG. 47. TEM and SEM micrographs of a decalcified section and critical-point-dried mantle edges of *Discina striata; 1,* transverse section of a seta and its follicle with microvillous inner epithelium charged with glycoproteinaceous vesicles (below), ×3,990; *2,* setae with distally pointing barbs, ×1,900 (new).

(1970) as the formation of new follicles by a process of budding. In such brachiopods as *Discina,* however, the occurrence of pairs of slender and robust setae in the same follicle (Fig. 47.2) is so common as to suggest that their association is a normal condition related to their function or to a periodic shedding of the older set of setae.

Setae have not been comprehensively studied, but those that are known show some variation from one species to another. The canals of the setae of *Terebratalia* larvae and

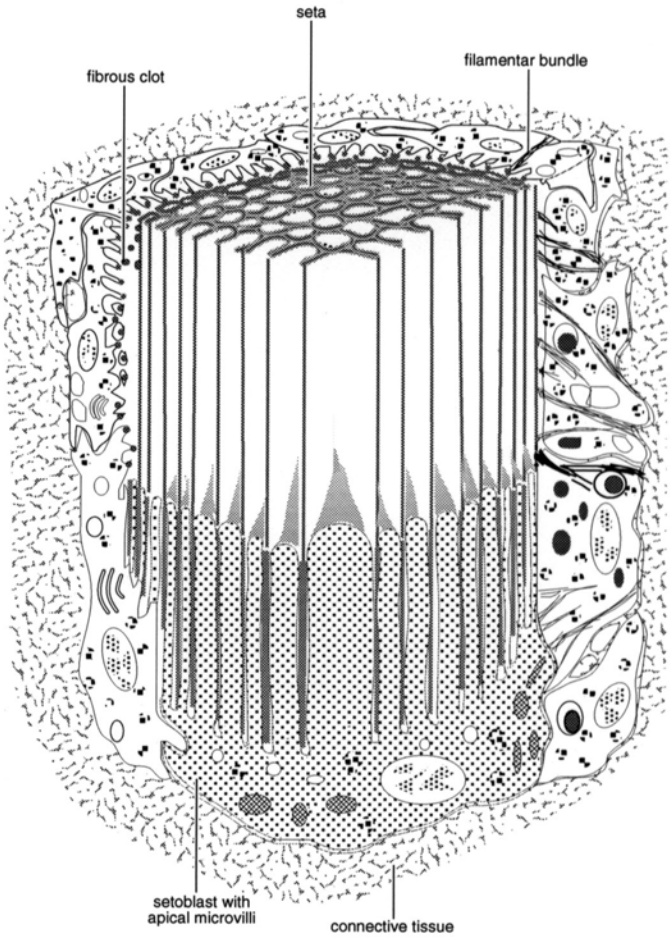

FIG. 48. Generalized diagram of the proximal part of a follicle of a lingulid showing the relationship of its seta to the apical microvilli arising from the setoblast (new).

of *Notosaria* adults (Fig. 51) have rounded transverse sections and relatively thick walls (up to 100 nm or so medially in *Notosaria*). The medial canals of the setae of the organophosphatic *Lingula* and *Discina* (Fig. 47.1) are normally hexagonal in cross section and thin-walled (about 30 nm). There are also differences in shape, with the setae of *Lingula* being more oval than those of *Notosaria* and *Discina.* The most distinctive variability, however, is in the external morphology. In many such genera as *Lingula* and *Notosaria,* setae are devoid of surface embellishments apart from some longitudinal striation and an occasional impersistent, thickened ring marking variations in the rate of secretion, which very rarely may be extended as slivers up to 2 or 3 μm long along the setal axis. In the discinids, however, the setal surfaces are usually strongly striated at intervals of about 300 nm, and especially they are festooned with narrow, lanceolate, barblike outgrowths that may be up to 30 μm or so long (Fig. 47.2). The barbs occur at intervals of up to 10 μm but are not distributed in any recognizable pattern along the surface although they tend to cluster at nodes between 30 and 50 μm apart. It is noteworthy that the larval setae of *Neocrania* are also embellished with short, acutely inclined barbs that

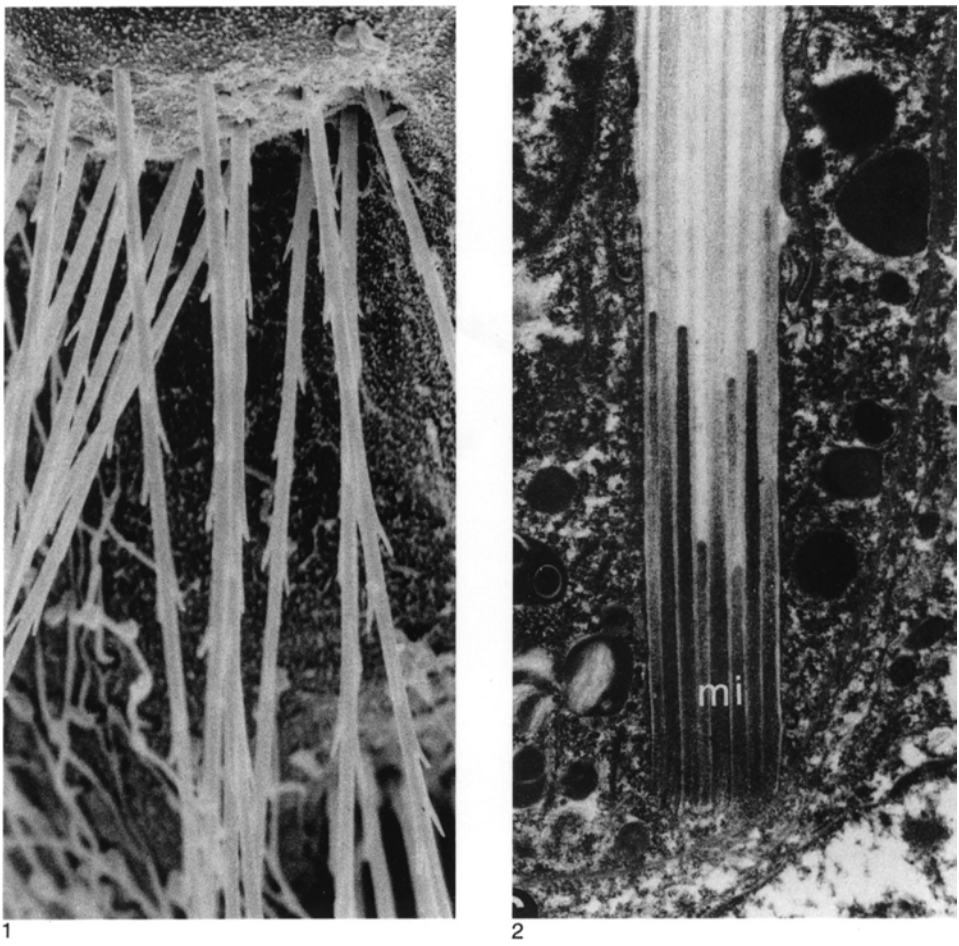

FIG. 49. SEM and TEM micrographs of larvae of *Neocrania anomala* showing *1,* the proximal part of the first bundle of setae with their distally pointing barbs, ×2,500, and *2,* a section of the proximal end of a seta with the microvilli (*mi*) of the setoblast extending into the setal channels, ×16,000 (Nielsen, 1991).

have been shown by NIELSEN (1991) to arise as terminations of peripheral canals (Fig. 49.1).

The close spacing and great length of most setae are related to their primary function as sensory grilles (RUDWICK, 1970). The setal fringe extending beyond the shell margin is normally longest anteromedially and posterolaterally and, in the planktonic genus *Pelagodiscus,* can exceed the length of a shell of several millimeters. In the related *Discina,* a fringe of some millimeters forms an effective sensory grille by supporting mucous curtains on the barbed outgrowths of the setae. The shorter, simple setae of terebratulides (*Neothyris*) and rhynchonellides (*Notosaria*) are also disposed to serve as a tactile safety sieve for the mantle cavity. The most extraordinary setal differentiation, however, occurs in *Lingula* (MORSE, 1902). The setae of this infaunal genus vary in size, attaining lengths of several millimeters posterolaterally and anteriorly where they are longest in a median and two lateral zones. The posterolateral and lateral setae, lubricated by mucus exuded by the inner mantle lobe, assist in the burrowing of *Lingula* into the substrate. The anterior fringe of setae cluster to form three

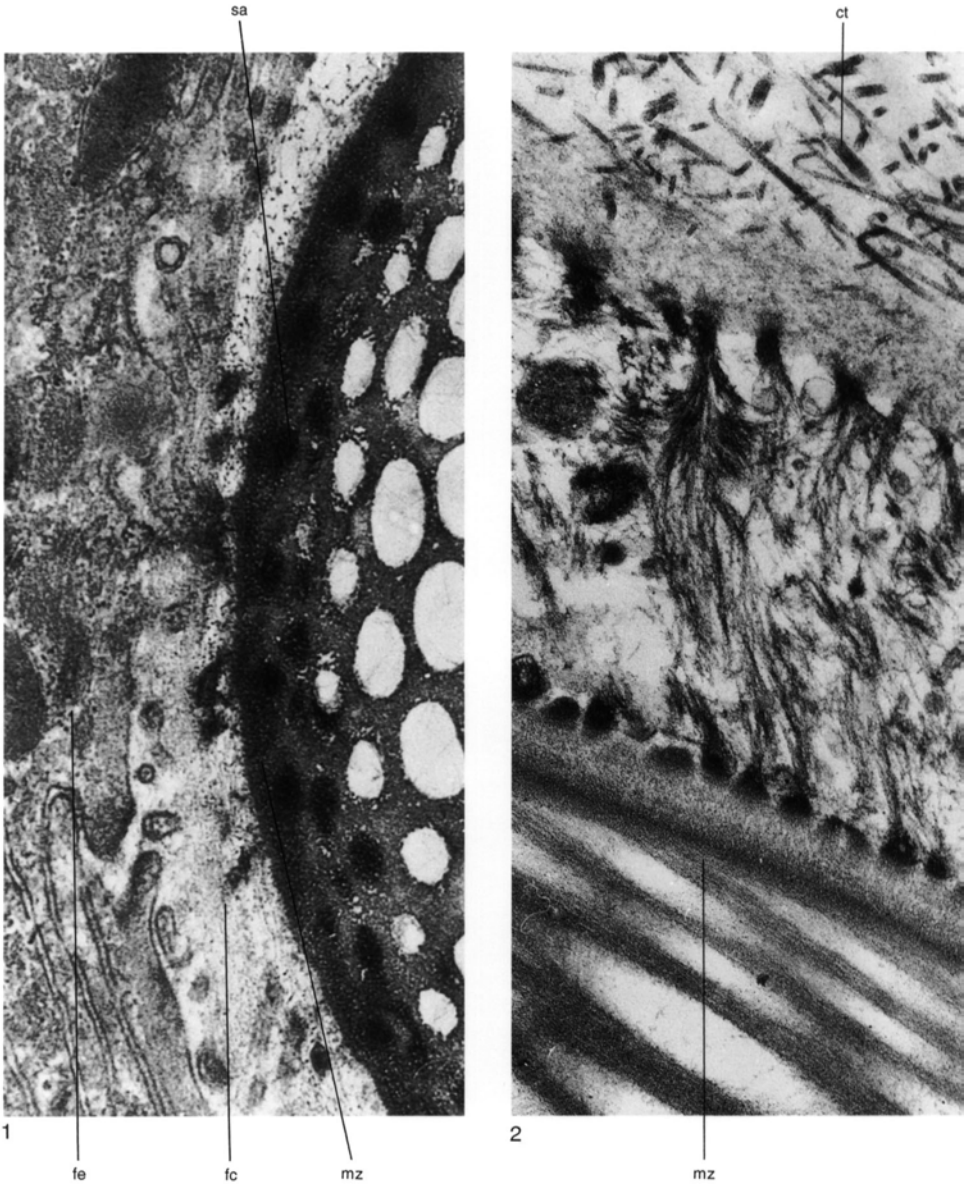

FIG. 50. TEM micrographs of sections of setal follicles in decalcified mantle edges; *1,* edge of seta (*sa*) of *Glottidia pyramidata* showing the migration of fibrous clots (*fc*) secreted by follicular epithelium (*fe*) and incorporated into the electron-dense marginal zone (*mz*) of the seta, ×55,000; *2,* detail of follicular epithelium of *Discina striata,* between connective tissue (*ct*) and setal margin (*mz*), showing the filamentar bundles attached to hemidesmosomal plaques in the basal lamina and apical plasmalemma, ×40,000 (new).

siphons through which the buried *Lingula* feeds by means of two lateral inhalant and one median exhalant currents.

All setae are mobile to a varying degree depending on the development of musculature controlling the follicles. In carbonate-shelled brachiopods, bundles of filaments within the connective tissue are attached to the follicles and are evidently responsible for some retraction of the setae as well as the

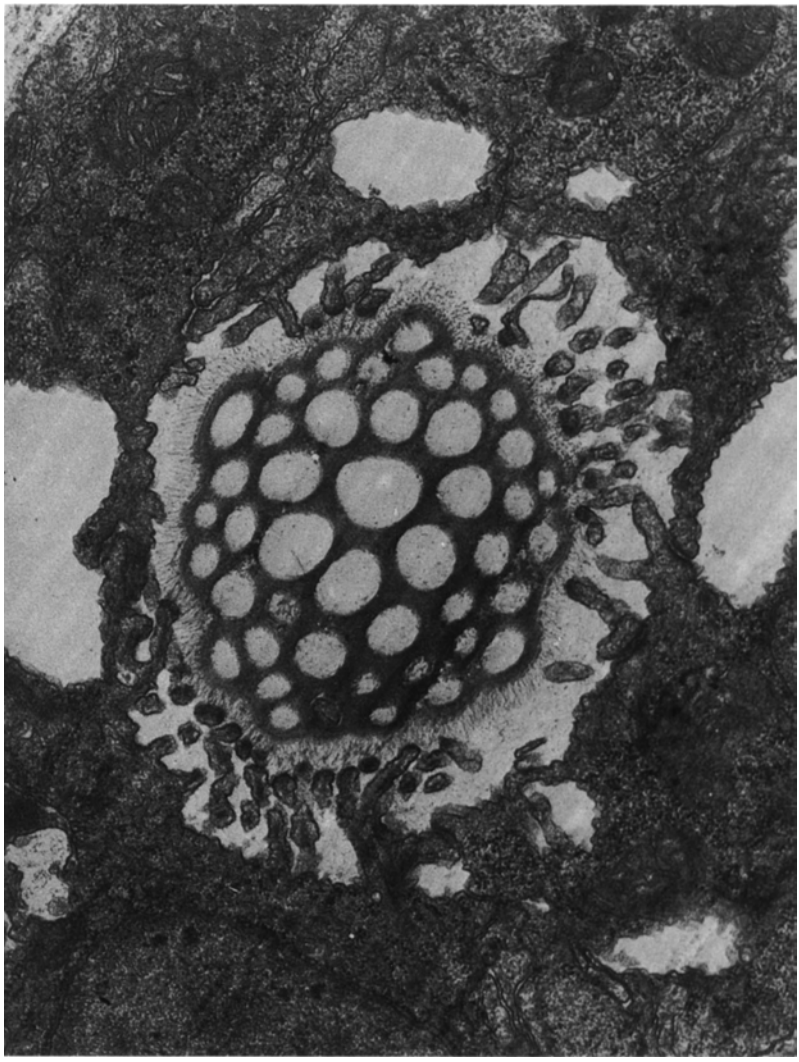

FIG. 51. TEM micrograph of the transverse section of a decalcified mantle edge of a young *Notosaria nigricans* showing the cylindroid nature of the canals and the microvillous apical plasmalemmas of the follicular epithelium, ×25,000 (new).

mantle margin as a whole. The setal follicles of organophosphatic brachiopods (Fig. 52), however, are controlled by a highly organized muscle system (BLOCHMANN, 1900). In *Lingula* the muscle sets are located in the marginal mantle sinus and are capable of retracting, protracting, flexing, and elevating the setae and have been appropriately named.

The connective tissue immediately proximal of the mantle lobes of organophosphatic brachiopods also contains two circumferential bands of circular fibers connected by diagonal bundles of filaments (BLOCHMANN, 1900). These are responsible for the retraction of the mantle edge, which occurs frequently and is indicated in shell successions by deep insertions of periostracal layers among the organophosphatic laminae. Despite the absence of comparable muscle sets in the mantles of articulated brachiopods,

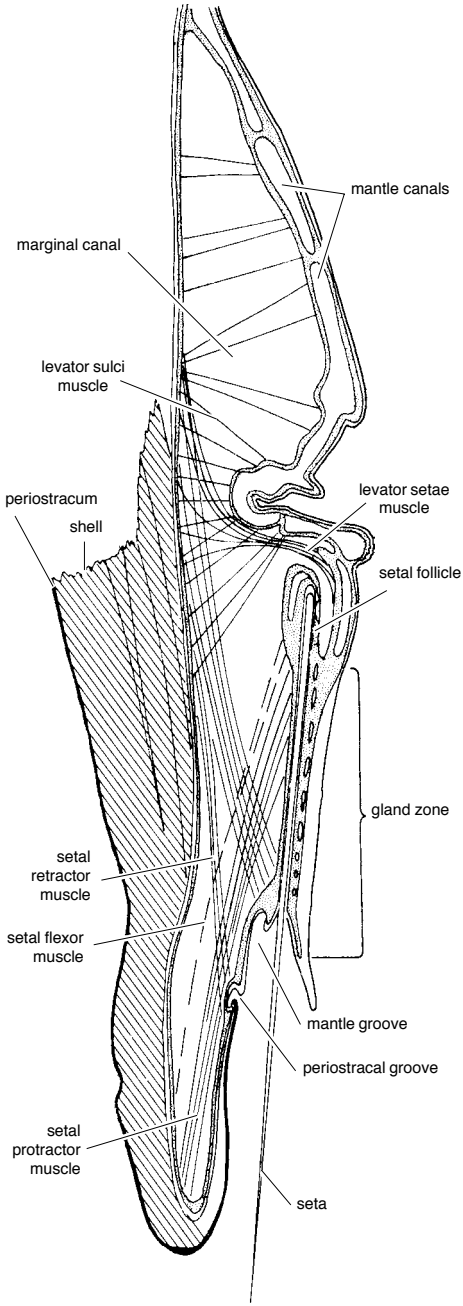

FIG. 52. Diagram of section through the mantle margin of *Lingula anatina* (Blochmann, 1900).

retraction of the mantle is commonly registered as variable regressions that are usually facilitated by the secretion of a proteinaceous membrane (see Fig. 279–280) between the outer epithelium and the carbonate successions (WILLIAMS, 1971a). Following a regression, all cells resume shell deposition at that phase in the secretory regime where they left off. This phenomenon has been noted in the impunctate *Notosaria* and in such terebratulides as *Magasella,* in which punctae that had contained caeca before retraction took place are sealed by the membrane of regression.

MANTLE SPICULES

Although a biomineralized exoskeleton, secreted by outer epithelium, is characteristic of all brachiopods, calcitic bodies (**spicules**) also occur within the connective tissue and inner epithelium of terebratulides and thecideidines and constitute an endoskeleton of variable solidity and continuity (see Fig. 339–340). In the heavily calcified mantle and lophophore of *Terebratulina,* the spicules are flattened to lie in the plane of the connective tissue (Fig. 53) so that segments of a spicule are lenticular in cross section and anastomose to form a sievelike, uniaxial structure with rounded perforations and curved peripheral horns. An outer, thin calcitic skin, which is patchily smooth, encloses highly inclined laminae (WILLIAMS, 1968d). SCHUMANN (1973) has shown that the laminae are composed of calcitic spherules about 200 nm in diameter.

Spicules are secreted as membrane-bound structures by mesenchymal cells (scleroblasts) that are attached to walls of cavities scattered throughout the connective tissue (JAMES & others, 1992). Accretionary growth of a spicule is indicated by the distension of the connective tissue so that collagen fibers in the vicinity of a well-developed scleroblast are streamlined parallel with the sides of the flattened scleroblasts (Fig. 54). Between adjacent scleroblasts, however, collagen fibers are aligned more or less normal to the connective tissue layer, while the immediately adjacent epithelia become folded inward toward each other within the rounded perforations of the spicular sieve. In other directions distension can be great enough to disrupt membranes and bring about an amalgamation of spicules to form a single struc-

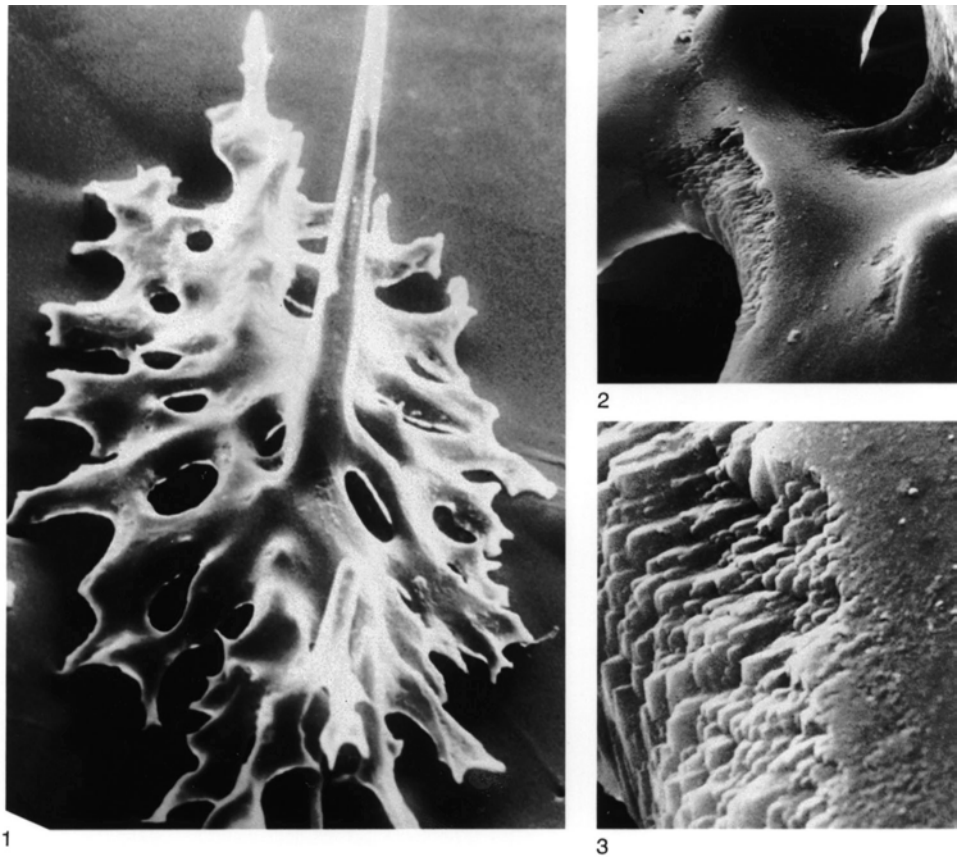

FIG. 53. SEM micrographs of a spicule in the mantle of *Terebratulina retusa; 1,* in general view, ×300, and in progressive detail, *2,* ×1,500, *3,* ×8,000 (Williams, 1968d).

ture that is still contained within a proteinaceous sac but is now sustained by an encircling group of scleroblasts.

Spicular endoskeletons are not invariably characteristic of living terebratulides, being feebly developed in some families (Dallinidae) and unknown in others (Terebratellidae). Endoskeletal meshes are, however, strongly developed in the Terebratulidae, Platidiidae, and Krausiidae and have been well documented by SCHUMANN (1973). Spicular meshes are particularly conspicuous: as canopies over the lophophore and filaments of *Terebratulina,* within the main mantle canals of *Megerlia* (Fig. 55.1) where they form roofs over the gonads, and in association with the dorsal adductor bases of *Gryphus.* Spicule morphology is so specifically differentiated as to form part of the diagnosis of various groups. It can vary from the dispersed hook of *Gryphus* to the solid shield of *Platidia* (Fig. 55.2). Morphology of spicules is known to vary during the ontogeny of *Terebratulina,* however, and could well be related, in this genus at least, to facilitating a mechanical stiffening of the connective tissue (FOUKE, 1986).

Thecideidine spicules, as typified by those of recent *Pajaudina* (LOGAN, 1988), are predominantly platelike structures. According to LACAZE-DUTHIERS (1861), spicules are absent from the lophophore of *Lacazella* but are densely packed into a vaultlike structure covering the gonads in the ventral mantle. Loose spicules have been recorded in fossil shells (THOMSON, 1927), and this is their

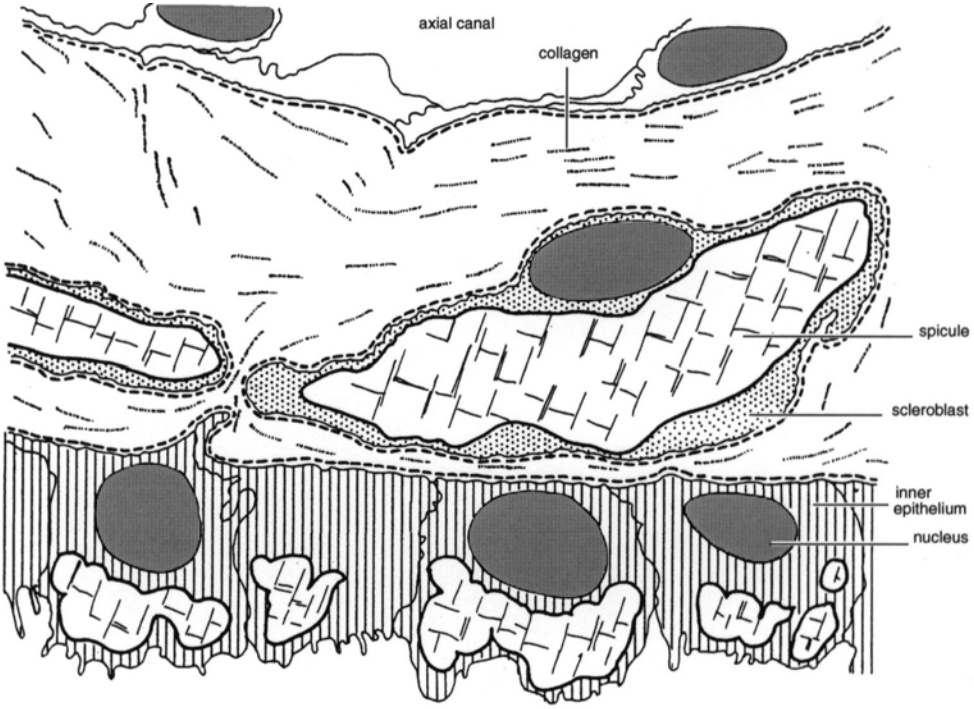

FIG. 54. Diagrammatic section of the lophophore filament of *Terebratulina retusa* showing the distribution of spicules in the inner epithelium and connective tissue (Williams, 1968d).

most common mode of occurrence in the shells of living species (Fig. 55.3).

PEDICLE

Most recent brachiopods are attached to their substratum by a pedicle. The pedicles of articulated and inarticulated brachiopods, however, are only analogous organs, being of different origin and morphology (Fig. 56). The pedicle of inarticulated brachiopods develops as an outgrowth of the posterior body wall and is associated with the ventral valve only. In contrast, the pedicle rudiment of articulated brachiopods is continuous

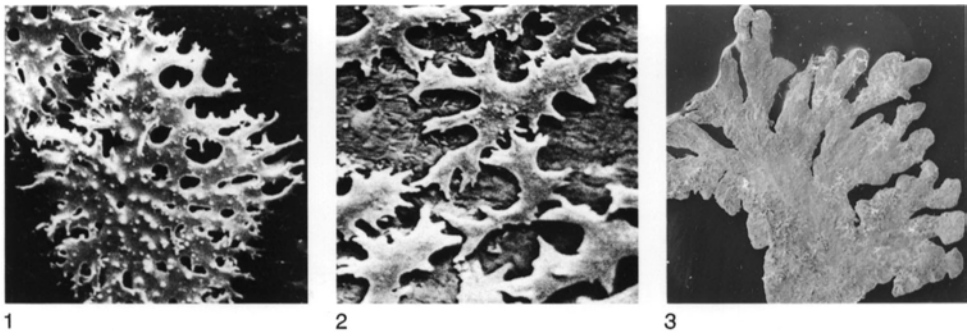

FIG. 55. SEM micrographs of various types of spicules; *1,* from the lophophore of *Megerlia truncata* (LINNÉ), ×65; *2,* from the mantle of *Platidia anomioides* (SCACCHI & PHILLIPI), ×140 (Schumann, 1973); *3,* from within the dead shell of *Pajaudina atlantica* LOGAN, ×50 (Alan Logan, new).

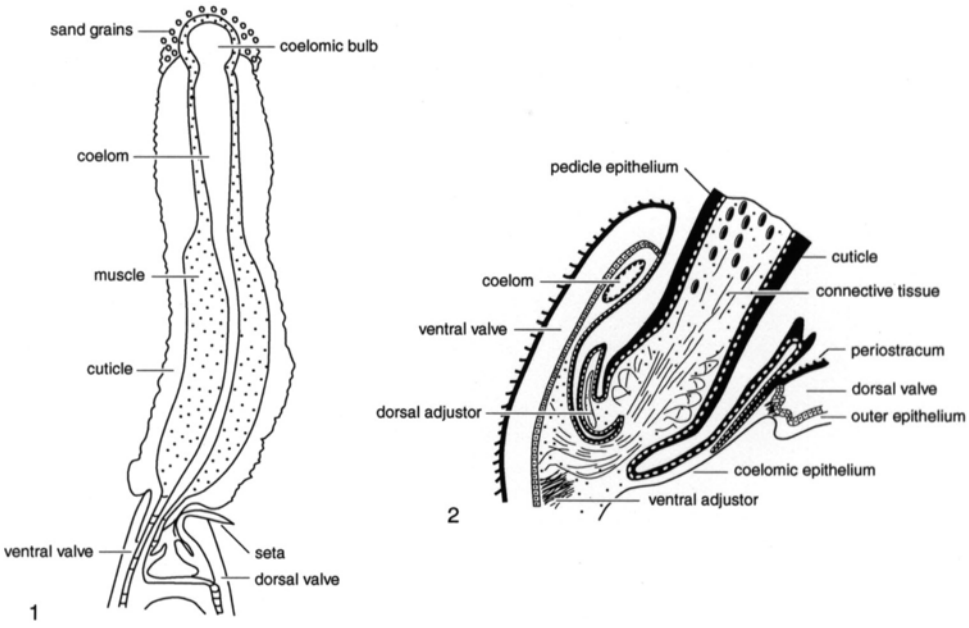

FIG. 56. Diagram showing generalized pedicle anatomy *1,* of the representative inarticulated brachiopod, *Lingula* (adapted from Mackay & Hewitt, 1978; Yatsu, 1902a) and *2,* articulated brachiopod, *Terebratulina* (Williams & Rowell, 1965a).

with the mantle rudiment, which produces both the ventral and dorsal valves; therefore the adult pedicle is continuous with the body wall of both valves.

An example of pedicle structure in inarticulated species is provided by a transverse section through that of *Glottidia pyramidata* (Fig. 57). There is a central coelomic cavity (pedicle cavity), an extension of the mantle canals present only in lingulids, which terminates distally in a small sac. The canal is filled with coelomic fluid containing erythrocytes and amoebocytes and is lined by coelomic epithelium about 5 μm tall with a microvillous border. The coelom is surrounded by a ring of muscle fibers running longitudinally along a spiral axis. Outside the muscle layer is a thin layer of connective tissue from 3 to 6 μm thick containing striated collagen fibers. This connective tissue layer supports the pedicle epithelium, which is found within the outer cuticle (MACKAY & HEWITT, 1978). The latter contains randomly oriented chitin fibrils arranged in concentric layers (RUDALL, 1955) and is continuous with the periostracum.

The pedicle of *Lingula anatina* has a similar structure (Fig. 58) with a central coelomic cavity and an outer cuticle that is transparent in life. Circumferential muscle fibers of the body wall are antagonized by adductors and oblique fibers by means of the fluid skeleton formed by the perivisceral coelom, in a similar manner to the action of circular and longitudinal muscles in a classical hydrostatic skeleton. The mantle and brachial canals are closed during muscular activity so that the coelomic fluid is maintained at constant volume in the body cavity, but the canal to the pedicle remains open and its longitudinal muscle is part of the system (TRUEMAN & WONG, 1987). The basic structure of the *Discinisca* (Fig. 59) pedicle is also similar to that of *Glottidia* although the muscle layer in the wall of the pedicle is not as well developed, and three paired, principal pedicle muscles are found occupying the pedicle coelom. These principal muscles appear to

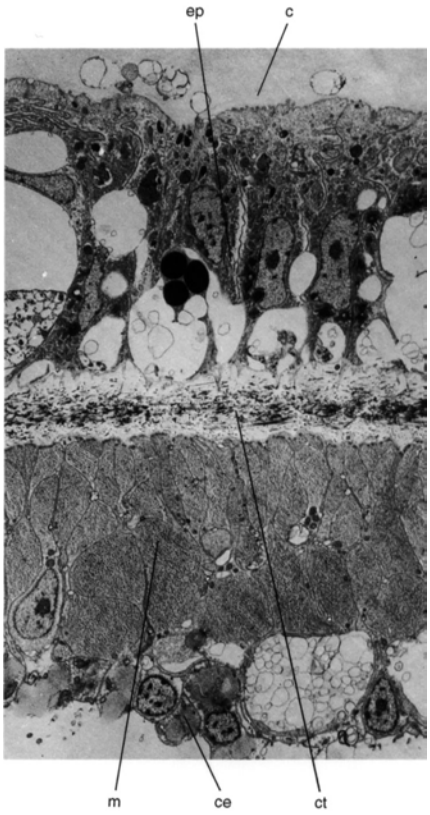

FIG. 57. TEM of a transverse section through the pedicle of a *Glottidia* showing the cuticle (*c*), pedicle epithelium (*ep*), connective tissue (*ct*), muscle layer (*m*), and coelomic epithelium (*ce*), ×2,300 (new).

have been a late development in the evolution of the discinoid pedicle. Specimens of *Orbiculoidea* with pyritized soft parts, collected by Dr. W. H. Südkamp from the Lower Devonian Hunsrück Slate, were equipped with pedicles protruding for at least 1.5 cm beyond the shell margin (Fig. 60). Such a slender, cylindroid pedicle probably had a coelom, like that of lingulids, although it would have functioned as a holdfast.

In structure, the pedicle of articulated species consists of a core of connective tissue, a pedicle epithelium, and an outer chitinous cuticle (Fig. 61). The pedicle trunk is enveloped by a thick cuticle, but this does not extend onto the surface in contact with the substrate (BROMLEY & SURLYK, 1973). Indeed, the structure of the pedicle rootlet changes with distance from the pedicle trunk (MACKAY & HEWITT, 1978). First, the chitinous cuticle is replaced by a layer of fibrous tissue, and the connective tissue core shows less densely packed collagen fibers. Next, in more distal sections of the rootlets, collagen fibers disappear from the central core, being replaced by cellular processes, presumably from the pedicle epithelium, and aggregations of electron-lucent material.

The pedicle epithelial cells of *Terebratulina retusa* are cuboidal to columnar, measuring between 10 and 20 μm in height. Apical, cytoplasmic protrusions extend into a web of

FIG. 58. TEM showing a transverse section through the pedicle of *Lingula;* the pedicle epithelium (*ep*) can be seen below the cuticle (*c*), which has a dense exterior edge; note also the connective tissue (*ct*) and muscle (*m*) layers, ×4,000 (new).

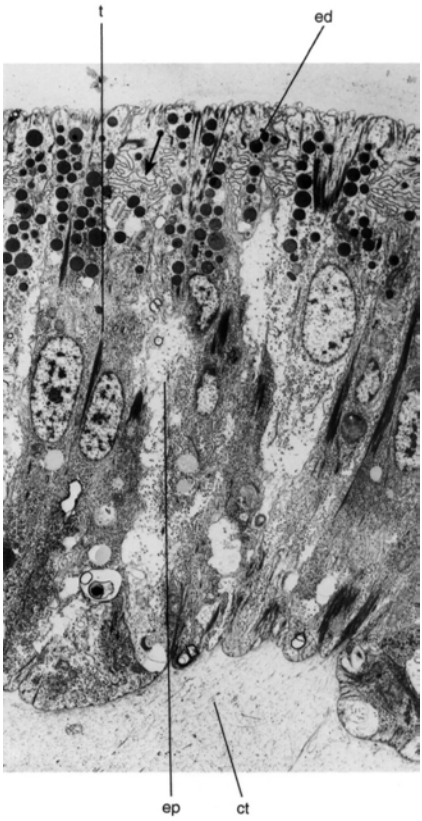

FIG. 59. Transverse section through the pedicle of *Discinisca* showing the pedicle epithelium (*ep*) supported by a layer of connective tissue (*ct*); note the characteristic features of the pedicle epithelium: folded lateral cell membranes (*arrow*), tonofibrils (*t*), and electron-dense droplets (*ed*), ×2,500 (new).

finely fibrillar material. The basal cell membrane is irregular, and lateral cell borders are tightly folded, perhaps to allow expansion during changes of shape of the pedicle.

Typical organelles and inclusions at the ultrastructural level include tonofibrils; electron-dense, membrane-bound droplets; and clear vesicles. Free ribosomes, rough endoplasmic reticulum, and mitochondria are also found; the Golgi apparatus is not well developed. The pedicle epithelium of *Glottidia* is similar in shape and height and shows similar ultrastructural features, although apical cytoplasmic protrusions are larger and cell membranes are not as folded as in *Terebratulina.* The common ultrastructural features of cytoplasmic protrusions, folded lateral cell membranes, tonofibrils, rough endoplasmic reticulum, electron-dense droplets, and clear vesicles are also present in the outer epithelial cells of the *Glottidia* mantle but not in those of *Terebratulina.* These common features may be related to the production of chitin.

In *Terebratulina,* pedicle epithelium, when followed into the pedicle rootlet, undergoes ultrastructural changes, with cell membranes becoming more regular in the absence of tonofibrils and rough endoplasmic reticulum. Electron-dense droplets are twice as large as those of the epithelium lining the pedicle trunk. Smaller, clear vesicles are found both apically and basally, the Golgi apparatus is more well developed, and glycogen is now present. As the epithelium is followed into the distal part of the rootlet, droplets of electron-dense material appear to be in the process of being extruded to the core of the rootlet, and fibrous material is

FIG. 60. External view of *Orbiculoidea mediorhenana* FUCHS with a pyritized, distal part of the pedicle protruding from beneath the left margin of the dorsal valve. Lower Devonian Hunsrück Slate, ×2.5 (photograph courtesy of W. H. Südkamp).

FIG. 61. Micrograph of a transverse section through the pedicle of *Terebratulina* showing connective tissue (*ct*), pedicle epithelium (*pe*), and cuticle (*c*), ×2,300 (new).

produced at the free surfaces. Modifications of the pedicle epithelium are also seen at the *Glottidia* pedicle ending (Fig. 62). Some groups of pedicle epithelial cells bear microvilli, and there is an impersistent film of glycosaminoglycans (GAGs) apically. Ultrastructural features are similar to those of the pedicle trunk epithelium, although rough endoplasmic reticulum is more plentiful and is found in the folds of the lateral cell membranes. The cells also contain glycogen and large mucous droplets; these differences may be related to the ability of the pedicle ending to collect sand grains.

In *Terebratulina,* the central connective tissue of the proximal pedicle consists largely of densely packed, longitudinal collagen fibers with fibroblasts and fat cells (MACKAY & HEWITT, 1978). It has been reported that brachiopod pedicles contain cartilage (HARO, 1963), but this has not been confirmed in more recent studies of *Terebratulina* and *Glottidia* (MACKAY & HEWITT, 1978), although a proximal mass of tissue resembling cartilage has been found in the pedicle of *Terebratalia transversa* (STRICKER & REED, 1985c). A study of pedicle development in the latter species (Fig. 63) showed that it is only the posterior half of the larval pedicle lobe that develops into the pedicle proper (from the distal part) and the pedicle capsule (from the proximal part). The connective tissue pedicle capsule lines the posterior end of the shell and forms a cuplike canopy around the pedicle. The anterior half of the pedicle lobe develops into the caudal end of the juvenile body. In young juveniles, the pedicle is continuous with and surrounded by the cuticle-covered epithelium and underlying pedicle capsule. Fibrils seen in the cuticle of adult specimens of *Terebratalia* may represent chitin. The pedicle epithelial cells show tonofibrils and hemidesmosomes as in *Terebratulina.* Although the pedicles of subadult and adult specimens are nonmuscular, at earlier stages fibers from pedicle adjustor muscles occur within the pedicle core. Furthermore, in subadult specimens, collagen fibers representing rudimentary tendons of the adjustor muscles extend into the pedicle (STRICKER & REED, 1985c). The adult pedicle bulb is attached to the posterior ends of the shell and body by sheets of dense connective tissue, the pedicle connectives (LABARBERA, 1978). Collagenous fibers, densely packed and oriented parallel to the long axis, are the most prevalent pedicle components.

Holdfast papillae of representatives of all major pedunculate groups (*Hemithiris psittacea, Terebratulina retusa, Macandrevia cranium,* and *Argyrotheca cistellula*) can dissolve carbonate substrates (EKMAN, 1896). The mechanism of boring remains unresolved except for a report that the pedicle rootlets of

Terebratulina contain vesicles similar to those associated with the resorption of bone by osteoclasts (MACKAY & HEWITT, 1978).

A study of borings made by both fossil and recent brachiopod pedicles showed pedicle form in articulated brachiopods to be much more variable than had previously been assumed (BROMLEY & SURLYK, 1973). Not only are different types of pedicle found among different higher taxonomic categories, but also, in many instances there is extreme variability in the pedicle of a single species. The pedicles of articulated brachiopods can be separated into a number of morphological groups (Fig. 64), depending on the size and length of the pedicle and adhesive processes sheathed with connective tissue (holdfast papillae):

i) massive pedicle of medium length with short, holdfast papillae that corresponds to a normal brachiopod pedicle of most textbooks;

ii) long, massive pedicle with long holdfast papillae;

iii) very long, massive pedicle with long, holdfast papillae that may be split distally into rootlets (processes with chitinous coverings);

iv) short massive pedicle with short holdfast papillae;

v) short massive pedicle divided distally into rootlets;

vi) very long pedicle with irregular lateral branches; and

vii) pedicle divided into rootlets immediately posterior to the pedicle opening.

Etched traces produced by pedicles of recent brachiopods vary with the nature of the substrate and the form of the pedicle. Furthermore, the pedicles of several recent brachiopods etch a very characteristic trace into hard calcareous substrates. A trace is a number of pits, closely spaced in brachiopods with solid unbranched pedicles, which correspond to holdfast papillae. The trace etched by brachiopods with divided pedicles consists of a series of more widely scattered pits corresponding to the rootlets of the pedicle. Here the scatter of pits can be recognized only as an individual entity where the substrate is extensive and flat. Similar traces can be found on fossilized substrates (BROMLEY & SURLYK, 1973).

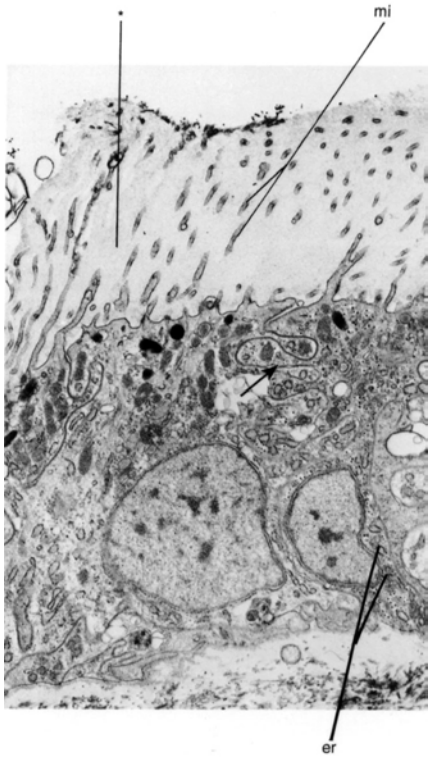

FIG. 62. Pedicle epithelium from the bulb of the pedicle of *Glottidia* in transverse section; note microvilli (*mi*), film of glycosaminoglycans (*), folds of lateral cell membranes (*arrow*), and rough endoplasmic reticulum (*er*), ×5,000 (new).

The gross morphology of the pedicle can vary even within a single species, for example, within a population of the recent brachiopod *Terebratulina septentrionalis* living where little hard substrate is available. Most *Terebratulina* specimens in this habitat attach to the shells of living or dead scaphopods; others lie on the sea floor, enmeshed within a bushlike network of pedicle rootlets. Some larvae then settle on adult pedicle rootlets. In this way, constant refurbishment

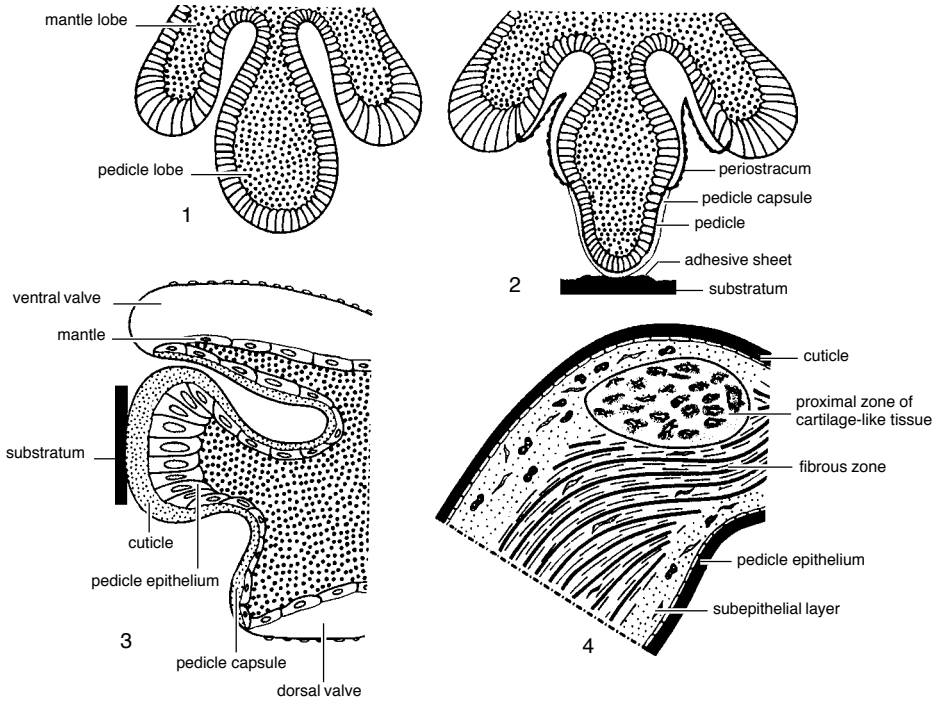

FIG. 63. Diagram showing longitudinal sections through the pedicle of *Terebratalia transversa* at different stages of development; *1,* free-swimming larval stage, posterior half; *2,* posterior half of a settled larva; *3,* newly metamorphosed juvenile, pedicle, and surrounding tissues; *4,* adult pedicle stalk; the distal end of the pedicle (below the *dotted line*) is not depicted (Stricker & Reed, 1985c).

of pedicle networks ensures survival; and, in effect, the brachiopods create their own substrate (CURRY, 1981).

The musculature of the pedicle of living articulated brachiopods varies greatly in size, position, and relation to the organ. Different pedicle types (immobile and rigid or muscular and flexible) can be related to differences in the disposition of pedicle muscles and in the form of the associated shell structures. The clearest guide to pedicle type in fossil forms is provided by the beak, since this houses the pedicle (RICHARDSON, 1979).

Paired ventral adjustor muscles pull the valves closer to the substrate in species with an inert pedicle (Fig. 65) but can also retract a muscular pedicle. Ventral, adjustor muscle fibers contribute to the shaft of the pedicle, and these may be contractile or tendinous. There is a greater muscle mass of ventral adjustors in species with muscular pedicles, for example, *Notosaria* (Fig. 66). Median pedicle muscles (paired or single) of attached species consist predominantly of tendinous fibers and stabilize the pedicle, preventing its displacement when dorsal and ventral adjustors contract. In *Anakinetica cumingi,* however, homologues of the median pedicle muscles lie within the pedicle capsule and control withdrawal and extrusion of the pedicle. The motile pedicle of this species is used to adjust the animal to varying levels within the sediment (RICHARDSON & WATSON, 1975). When compared to that of an attached species, *Magadina flavescens,* differences in the pedicle and its muscles could be correlated with dissimilarities in the beak and cardinalia of these forms.

Paired, dorsal, adjustor muscles are usually attached to the ventrolateral surfaces of the pedicle. These muscles enable the shell to rotate and move laterally. Unilateral contrac-

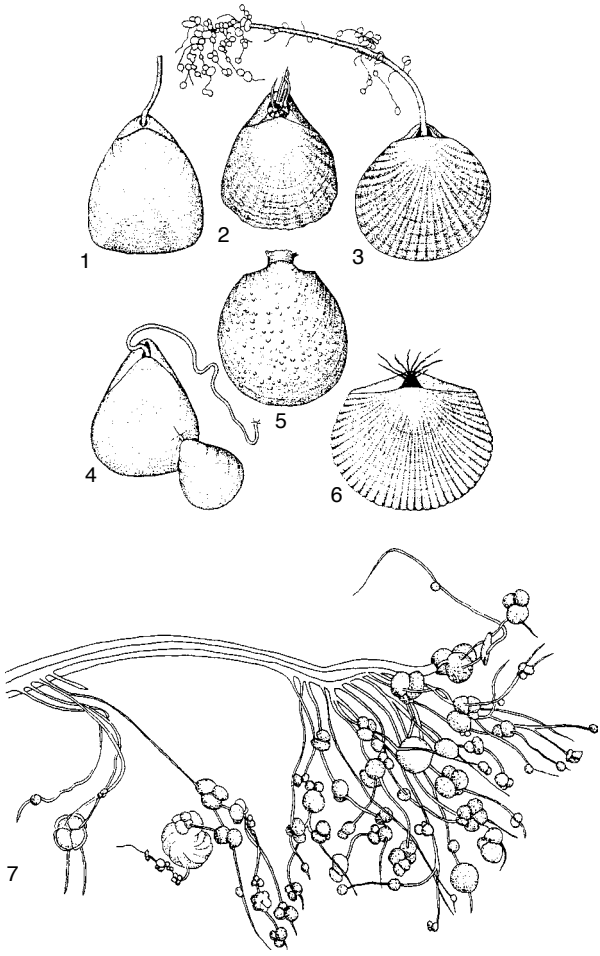

FIG. 64. Diagram showing different types of pedicle in articulated brachiopods: *1, Macandrevia cranium; 2, Eucalathis murrayi; 3, Chlidonophora chuni; 4, Cryptopora gnomon; 5, Gwynia capsula; 6, Chlidonophora incerta; 7,* detail of pedicle of *Chlidonophora chuni* with penetrated and attached foraminifera (Bromley & Surlyk, 1973).

tion pulls the shell to the same side, while contraction of muscles on both sides pulls the pedicle down anteriorly, elevating the posterior part of the shell.

There appear to be two extremes of pedicle function. At one extreme, the pedicle is a relatively rigid organ for permanent attachment, acting as a pivot around which the shell moves due to the contraction and relaxation of the attached muscles. In this case, the shell rather than the pedicle moves, the pedicle acting as an intermediary between the muscles and the substrate. At the other extreme, the pedicle is a contractile organ with muscle fibers continuous with those of the ventral adjustors and can adjust the position of the shell as a result of its own mobility. There is a graduation of intermediary types between these two extremes. All muscles (the median pedicle and the dorsal and ventral adjustor muscles) may contribute either tendinous or contractile fibers to the pedicle. Pedicles with few fibers (such as those of *Magadina, Cancellothyris,* and *Magellania*) are immobile and inflexible, while pedicles with a high, muscle-fiber

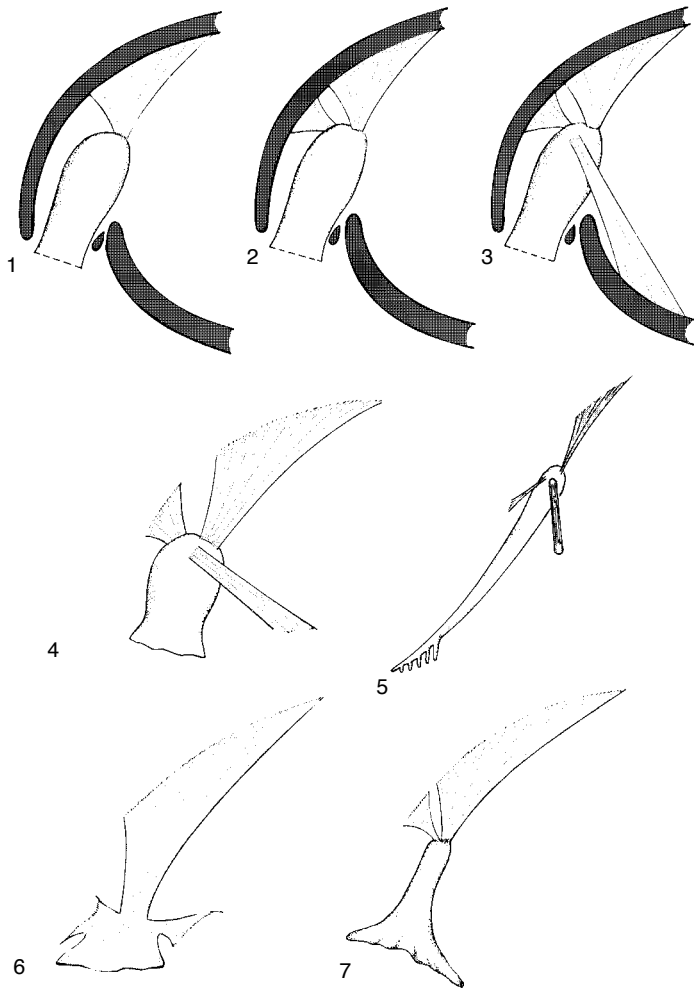

FIG. 65. Diagram showing the pedicle and muscles in articulated genera with different substrate relationships; *1–3,* muscle arrangement common to *Magellania, Cancellothyris, Liothyrella,* and *Campages; 1,* ventral adjustor that pulls the valves close to the substrate, *2,* adding the median muscle which acts as a stabilizer and *3,* also including the dorsal adjustor which, acting with its partner, controls lateral and rotatory movements of the valves; *4–7,* muscle arrangement in genera with a different substrate relationship than that seen in *Magellania; 4, Terebratella, 5, Anakinetica, 6, Megerlina,* and *7, Notosaria* (Richardson, 1979).

component, such as *Notosaria,* are contractile (RICHARDSON, 1979).

In *Terebratalia transversa,* the median pedicle muscles are absent, with only a ventral and a dorsal pair of pedicle adjustors present from the free-swimming larval stage to the adult form (STRICKER & REED, 1985c).

Little information is available on lingulid pedicle musculature. The principal pedicle muscles of *Discinisca* consist of three pairs that nearly fill the pedicle coelom (Fig. 67). A large pair of rectus muscles runs dorsoventrally and is attached to the distal end of the pedicle and to the shell at the sides of the pedicle opening. There are two pairs of oblique muscles, the pedicle oblique median muscles and oblique external muscles. A sphincter is present at the proximal end of

the pedicle and controls the opening to the body cavity. A thick muscle layer is present in the *Lingula* pedicle, deep to the coelomic epithelium. Fibers run longitudinally along a helical spiral, coiled both clockwise and counterclockwise (Williams & Rowell, 1965a). Similarly, a transverse section through the pedicle of *Glottidia* shows obliquely cut muscle fibers, some with a predominantly longitudinal and some with a predominantly transverse orientation (Fig. 68–69). Craniid inarticulated brachiopods lack a pedicle at all stages of development, being attached instead by cementation of the pedicle valve to the substratum, effected by adhesive properties of the mucus covering the periostracum.

The lingulid pedicle may be lost by breakdown and resorption, perhaps in response to stress (Rowley & Hayward, 1985; James & others, 1992). Regeneration of the pedicle bulb of *Lingula anatina* after damage has been reported (Trueman & Wong, 1987).

COELOMIC AND CIRCULATORY SYSTEM

As far as is known, all brachiopods possess an open circulatory system containing a colorless or faintly pigmented fluid that is coagulable and contains a variety of free cellular inclusions. The circulatory system is composed of a series of blood vessels that communicate with coelomic canals and sinuses (Hyman, 1959b; Williams & Rowell, 1965a; Rowley & Hayward, 1985).

COELOMIC SYSTEM

The coelom contains the main muscles, digestive tract, excretory organs, and reproductive structures. The part of the coelom that constitutes the main body (perivisceral) cavity occupies the posterior part of the shell. Coelomic canals and sinuses extend into the mantles, brachia, and tentacles and into the pedicle of inarticulated brachiopods. Parts of the coelom are subdivided by flat sheets or ribbons of connective tissue (mesenteries) or may be isolated during development. The coelom and the tissues and organs it contains are lined with a flat, ciliated epithelium.

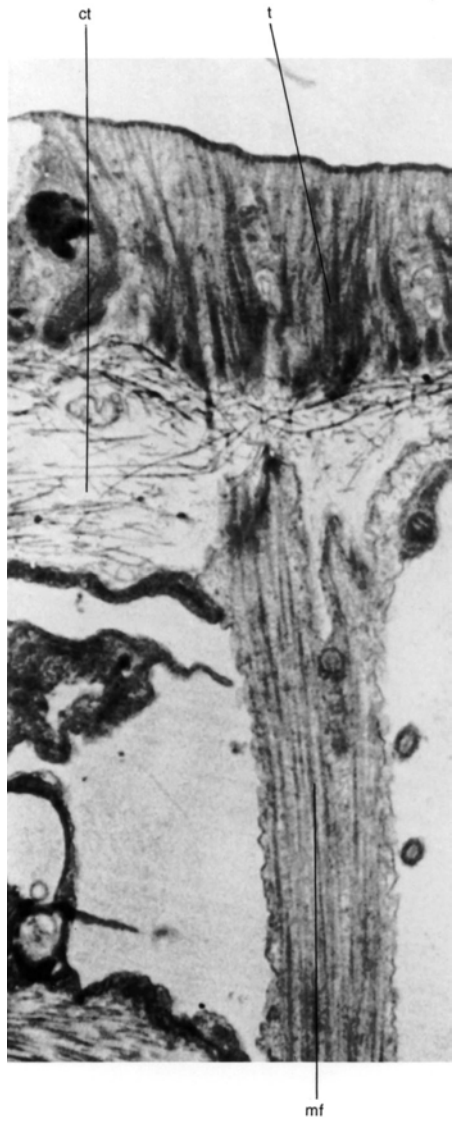

Fig. 66. TEM showing a ventral adjustor muscle fiber (*mf*) of *Notosaria* attaching to the ventral valve; note the extension of the muscle fiber through the connective tissue layer (*ct*) and the apparent continuity of myofibrils with the tonofibrils (*t*) of the outer epithelial cells providing a firm attachment point, ×26,500 (new).

Mesenteries traverse the body cavity and contain fine muscle fibers. Dorsal and ventral mesenteries support and anchor the

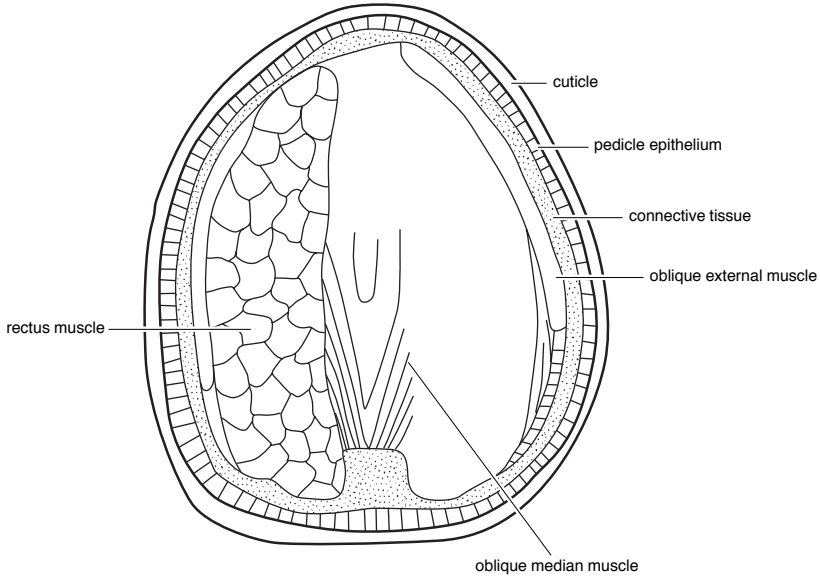

FIG. 67. Diagram showing the pedicle of *Discinisca* viewed ventrally after the ventral surface and left rectus muscle have been removed (Blochmann, 1900).

alimentary canal to the body wall. Only in *Neocrania* do the mesenteries completely divide the body cavity into two separate compartments (BLOCHMANN, 1892). Two lateral mesenteries, the gastro- and ileoparietal bands, also connect the alimentary tract and other organs in the body cavity to the body wall. Gastroparietal bands are absent in *Neocrania,* but in all other brachiopods they are relatively narrow, lie anteriorly to, and extend on both sides from the stomach, near the digestive diverticula, to the lateral body wall. The ileoparietal band is more complex, extending between the lateral body wall and the stomach, along which it may persist for some distance posterior to the gastroparietal band. The ileoparietal bands also support the posterior end of the excretory organs (metanephridia) extending anteriorly as a series of variably branched lamellae that carry the gonads (Fig. 70; see also Fig. 91).

Tubular extensions of the coelom penetrate the mantle to form a characteristic pattern of ciliated canals. In articulated brachiopods a thin layer of muscle underlies the coelomic epithelium of the inner mantle membrane. In inarticulated brachiopods, two main mantle canals (*vascula lateralia*) emerge from the main body cavity through muscular valves and bifurcate distally to produce an increasingly dense array of blindly ending branches near the periphery of the mantle (Fig. 71.1–71.2). *Discinisca* has two additional mantle canals emanating from the body cavity into the dorsal mantle (*vascula media*). *Neocrania* lacks the muscular valve at the junction of the body cavity with the mantle canals. Unlike other inarticulated taxa, the primary canal of *Neocrania* gives rise to secondary and, only exceptionally, tertiary branches. In addition, these canals may also contain part of the gonads (Fig. 71.3).

Recent rhynchonellides and terebratulides possess two pairs of principal canals in each mantle (WILLIAMS, 1956), but the pattern may be complicated because some contain part of the gonads (Fig. 72). In rhynchonellides, for example, each mantle contains a pair of submedian canals (*vascula media)* curving posterolaterally and branching repeatedly toward the mantle edge. In *Hemithiris* the *vascula media* are flanked by a pair

of short, broad canals (*vascula genitalia*), which are unbranched extensions of the body cavity containing the gonads (Fig. 72.1). In *Notosaria* the pattern is identical except that the *vascula genitalia,* although still saclike proximally, branch repeatedly toward the mantle margin, and the *vascula media* are correspondingly abbreviated (Fig. 72.3). In living terebratulides the pattern is similar to that of *Notosaria:* the *vascula genitalia* are branched, and the *vascula media* are restricted peripherally (Fig. 72.2). In such genera as *Macandrevia, Pumilus, Fallax* (Fig. 72.4), and *Magellania,* however, gonads are also found in the *vascula media.* The fine distal branches of all canals that terminate just within the shell margins connect with the setal follicles in articulated brachiopods.

Circulation of Coelomic Fluid

Ciliated epithelium lining the coelomic canals circulate the coelomic fluid. In lingulids a defined pattern of circulation is maintained by rhythmically beating cilia. Aided by a median ridge, the cilia create separate outgoing and return currents within each coelomic canal (Fig. 73).

Similar medial epithelial ridges occur in *Discinisca* and *Terebratalia* on the inner side of the outer mantle membrane. The mantle canals have a respiratory function, facilitating the circulation of coelomic fluid. Gill ampulae are an unusual adaptation found only in the lingulid *Glottidia.* Small, thinly walled, tubular, saclike extensions of the mantle canals occur in the periphery of the anterior part of the mantle cavity, thereby increasing the surface area of the mantle canal system (Morse, 1902).

VASCULAR SYSTEM

Comprehensive descriptions of the vascular system of inarticulated brachiopods are available (Blochmann, 1892, 1900; Schaeffer, 1926), but no complete account exists for articulated species. It is generally accepted, however, that the open circulatory system is composed of a series of coelomic canals and a communicating vascular system.

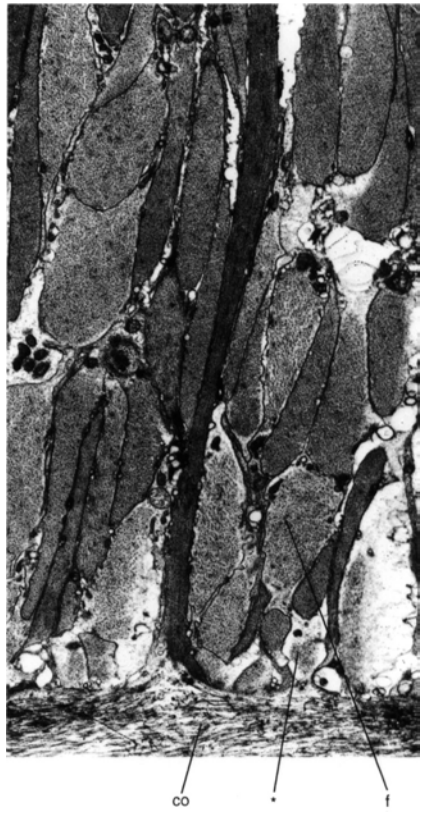

Fig. 68. TEM showing the muscle layer of the pedicle of *Glottidia* cut in transverse section; note muscle fibers (*f*) with connective tissue between (*) and a supporting layer of connective tissue with circularly running collagen fibers (*co*), ×3,500 (new).

The vascular system consists of a main dorsal vessel that contains one or more contractile appendages or hearts that are supported by a dorsal mesentery in the vicinity of the stomach (Hyman, 1959b). Blood vessels, formed within the connective tissue, branch from the main dorsal vessel and communicate with sinuses in the digestive tract and with the small brachial and tentacular canals of the lophophore.

Posterior to the heart, the main dorsal vessel gives rise to two mantle vessels that divide, forming a network of vessels beneath the coelomic epithelia of the mantle membrane of the mantle canals. The vessels serve an extensive system of anastomosing sinuses

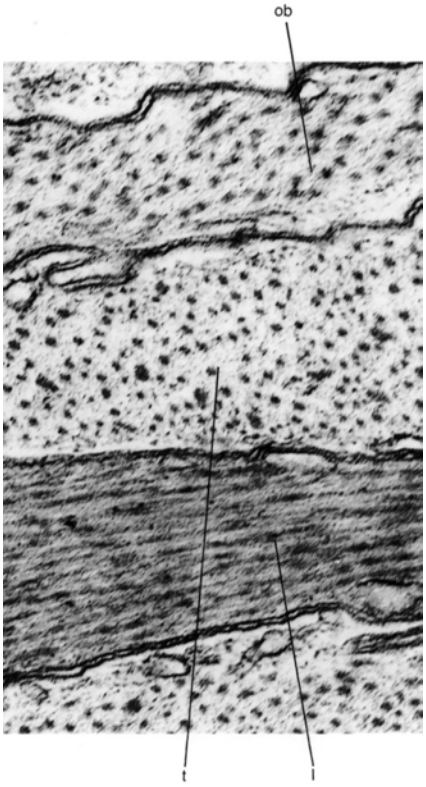

FIG. 69. Detail of a transverse section through the muscle layer of *Glottidia* showing adjacent muscle fibers; one fiber is cut obliquely (*ob*), while neighboring fibers are cut predominantly transversely (*t*) and longitudinally (*l*), ×35,000 (new).

within the ileoparietal band, metanephridia, and gonads (see Fig. 133, 136; HYMAN, 1959b; WILLIAMS & ROWELL, 1965a). Accessory hearts have also been observed in *Liothyrella* as distended portions of the ileoparietal bands (FOSTER, 1974).

The heart of *Lingula* is a muscular chamber consisting of an outer coelomic epithelium covering a thick layer of circularly disposed muscle fibers but lacking an inner endothelial lining. In the main dorsal vessel, the muscles are disposed helically, but all the main vessels continue within the connective tissue. Subordinate blood vessels within the tentacles of the lophophore of the articulated *Terebratalia* (REED & CLONEY, 1977), the inarticulated *Lingula* (STORCH & WELSCH, 1976), and probably all brachiopods are composed of a single layer of squamous myoepithelial cells, the basal lamina of which faces the blood space (Fig. 74). The course of the principal vessels is similar in *Neocrania* and *Lingula,* although in the former genus several contractile sacs fulfill the function of one or rarely more appendages in *Lingula* (Fig. 70). In front of the heart the main dorsal vessel runs forward dorsally of the esophagus and bifurcates to serve each brachidium of the lophophore. Inside the lophophore the branch runs ventrally and laterally in the central canals to the entrance of the brachial canal. At this point another branch arises and runs medially in the ventral part of the central canal to connect with the corresponding branch in the other brachium. In this way the circulatory systems of both the brachia are joined by a connective blood vessel ventral to the esophagus. The main branch in each brachium continues along the length of the small brachial canal. The lophophore circulatory system terminates as blind tentacular vessels arising from the small brachial or ventral connective vessels (see Fig. 110.1–110.2; BLOCHMANN, 1892, 1900).

Behind the heart, the main dorsal vessel splits into a left and right branch, each of which runs ventrally for a short distance before bifurcating into anterior and posterior branches; these two pairs of branches form the dorsal and ventral mantle vessels respectively. The two dorsal mantle vessels pass to the anterior body wall along the outer surface of the alimentary canal, on either side of the midline. They are then inserted into the dorsal mantle canal and send a branch that ends blindly in each branch of the mantle canal system. The ventral mantle vessels follow a more complex course before they reach the ventral mantle canals. The course of these vessels is different in *Neocrania* and *Lingula,* but they or their branches supply the ileoparietal bands and associated gonads in both genera and form a network of small vessels in

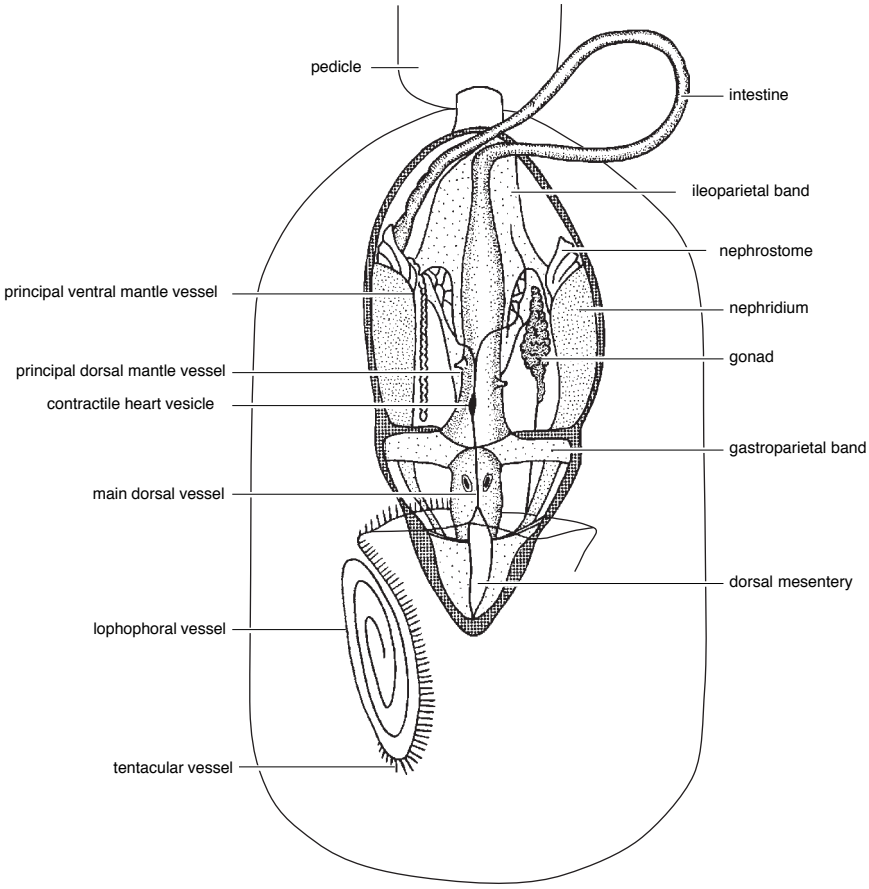

FIG. 70. Generalized diagram of the circulatory system of *Lingula* (adapted from Storch & Welsch, 1976).

this region. Both vessels then run anteriorly along their respective metanephridia and at the front turn laterally to be inserted in the ventral mantle canals, sending branches into the ramifications of the mantle canal system. *Discinisca* appears to have a poorly developed circulatory system (BLOCHMANN, 1892, 1900). The vessels in the lophophore are developed like those in *Neocrania* and in *Lingula,* but the remainder of the system appears to be absent.

FREE CELLULAR INCLUSIONS

Free cellular inclusions may be classified as blood cells (erythrocytes), coelomocytes, and, in *Lingula,* spindle bodies.

Erythrocytes, which may carry a respiratory protein, occur throughout the circulatory system. The erythrocytes of *Lingula* impart a pale purple or violet color to the coelomic and vascular fluid (blood) (Fig. 75; 76.2–76.3; YATSU, 1902a; OHUYE, 1937). Lingulid blood cells are cowrie-shaped and have a central nucleus with few mitochondria (STORCH & WELSCH, 1976; ROWLEY & HAYWARD, 1985). The pigments present consist of two hemerythrins (KAWAGUTI, 1941; JOSHI & SULLIVAN, 1973). Erythrocytes are present in both the vascular and coelomic fluids, suggesting considerable interchange between the two systems (ROWLEY & HAYWARD, 1985). It is assumed that some of the

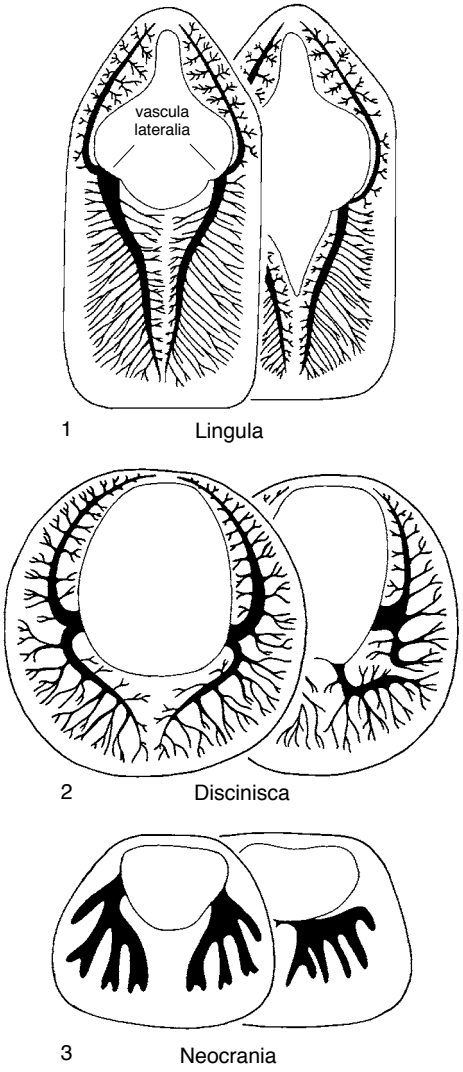

FIG. 71. Mantle canals; *1, Lingula anatina; 2, Discinisca lamellosa; 3, Neocrania anomala* (adapted from Blochmann, 1892).

disciform or spherical cells found in articulated brachiopods (OHUYE, 1937) are similar to the erythrocytes of inarticulated species.

Brachiopod coelomocytes have been frequently and variously described (JAMES & others, 1992). At least two forms of coelomocytes exist, performing many diverse functions including immune responses (STORCH & WELSCH, 1976; ROWLEY & HAYWARD, 1985); the breakdown, recycling, and translocation of useful compounds as evidenced by oosorption (CHUANG, 1983a); the initiation of shell and mantle repair (PAN & WATABE, 1989); and hemostasis (ROWLEY & HAYWARD, 1985).

In *Lingula* several amoebocytes have been described (OHUYE, 1937) including hyaline eosinophylic and basophylic forms. Recent evidence suggests that only one population of variably granular cells exists, which is believed to be formed from the hyaline amoebocyte (ROWLEY & HAYWARD, 1985). The amoebocytes of *Lingula* contain large numbers of homogeneous granules, few mitochondria, alpha glycogen granules, free ribosomes, and debris-laden vacuoles, which are probably lysosomes (Fig. 76.1, 76.4–76.5). In life, the granules may be colorless or red, orange, or brown spherules or globules (HYMAN, 1959b). The cell membrane forms pseudopodia and is capable of ingesting bacteria (STORCH & WELSCH, 1976; ROWLEY & HAYWARD, 1985). Amoebocytes in a number of articulated genera occur as red to purple clumps along the distal margin of the genital lamella (JAMES, ANSELL, & CURRY, 1991b; JAMES & others, 1992). These cells produce pseudopodia and contain clusters of mitochondria often enmeshed with profiles of granular and agranular endoplasmic reticulum interspersed with lipid granules and vacuoles, some of which may be lysosomes (Fig. 77; JAMES & others, 1992).

The testes of some male brachiopods contain clusters of lipid-charged cells (SAWADA, 1973; JAMES & others, 1992). The cells are often present during the early stages of development, forming a band around the proliferating mass of gametes, and are believed to be trophocytes that nourish the proliferating gametes.

Spindle bodies have been described in the coelomic fluid of *Lingula.* Recent evidence has shown that lingulid spindle bodies are fragments of muscle fiber that have been broken down, probably by some form of stress-induced autolysis and shed into the coelomic fluid (ROWLEY & HAYWARD, 1985).

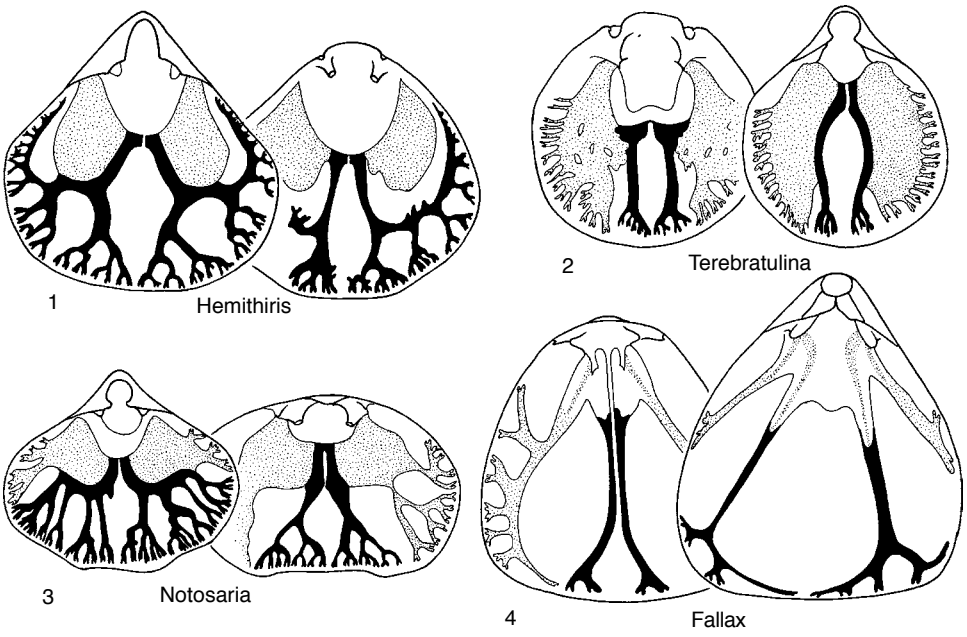

FIG. 72. Mantle canal systems; *1–2,* recent rhynchonellids; *3,* terebratulide (adapted from Williams, 1956); *4,* terebratulide (adapted from Atkins, 1960a); *vascula media,* black; *vascula genitalia* and gonadal sacs stippled.

MUSCULAR SYSTEM

The brachiopod muscular system contains two main forms of muscular tissue. These exist as either discrete bundles of muscle fibers that control the movement of the valves or as myoepithelia (musculoepithelia), which are found on the inner side of coelomic epithelia, in the parietal bands, in mantle lobes, and in the lophophore. In turn, the muscular tissue contains either smooth or striated myofilaments, which impart different physiological and contractile properties to the muscle.

The principal valve muscles open, close, and rotate the valves relative to one another and to the pedicle. The absence of a hinge mechanism in the shell of inarticulated brachiopods also permits rotation of the valves and creates fundamental mechanical differences in the way in which muscles are disposed and operate.

Where the principal valve muscles are attached to the shell, the intervening outer epithelium consists of a series of striated cells containing tonofibrils that penetrate the secondary layer (BLOCHMANN, 1892; YATSU, 1902a; PRENANT, 1928). These attachment areas are commonly seen on the inner side of the valve as muscle scars and result from the significantly slower rate of secondary shell secretion by the modified epithelium.

PRINCIPAL VALVE MUSCLES OF ARTICULATED BRACHIOPODS

The posterior hinge of articulated brachiopods permits valve opening (abduction) and closing (adduction) in a single plane. The adductor (occlusor) muscles close the valves, and the diductor (divaricator) muscles open the valves. Adjustor muscles, generally a dorsal and ventral pair, extend between the pedicle and the valves, moving the entire shell relative to the pedicle. A median, sometimes paired, pedicle (peduncular) muscle has been reported in some older works, but the presence, extent, and functional properties of pedicle muscle fibers remain controversial (EKMAN, 1896; RICHARDSON, 1979).

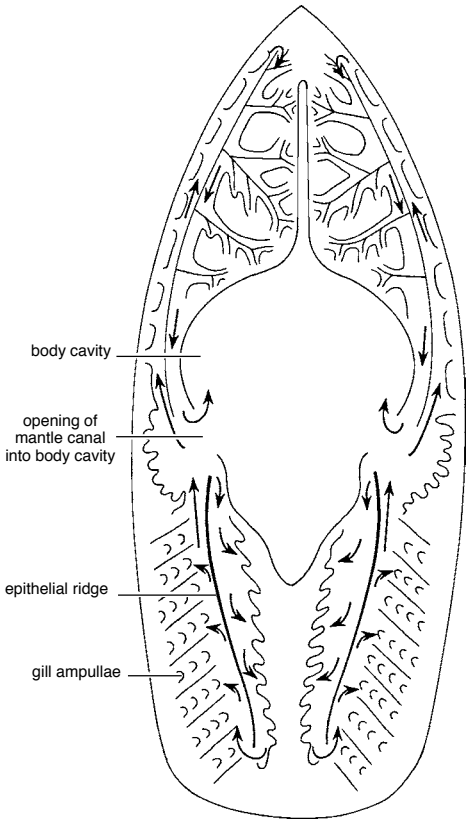

FIG. 73. Circulation in the dorsal mantle canals of *Glottidia* (adapted from Morse, 1902).

A set of adductor muscles extends from the dorsal to the ventral valve in front of the posterior margin, while a set of diductors is typically inserted into the dorsal valve posterior to the teeth and sockets that form the hinge axis or fulcrum about which the valves articulate (Fig. 78).

The adductor muscles are attached to the ventral valve posteromedially in two places. As the muscles pass between the valves, they bifurcate and attach anteromedially to the dorsal valve in four places (Fig. 79). In the thecideidines, the adductor muscles do not divide dorsally, but an extra set of adductor muscles occupies posterolateral positions in front of the hinge line. This arrangement, combined with highly developed teeth and sockets, presumably prevents lateral movement that might arise from an articulation that is sufficiently flexible to allow the dorsal valve to open at right angles to the cemented ventral valve (Fig. 80).

The diductor muscles are inserted immediately in front of the beak of the dorsal valve either in or at the side of the cardinal process. From this position, the diductor muscles splay out to occupy a pair of extensive attachment areas in the ventral valve, usually on either side of the adductor bases. The dorsal attachment of the diductor muscles is posterior to the hinge axis of the shell and thus provides the mechanical leverage about the fulcrum to open the shell (Fig. 78). The dorsal umbo of some terebratulids (e.g., *Platidia*) is resorbed to accommodate the pedicle (Fig. 81). In such a valve, the dorsal attachment areas are in front of the hinge axis and the ventral areas are posterior, thus reversing the normal arrangement but maintaining the necessary moment about the hinge axis to open the valves. Commonly a pair of slender accessory diductors is also present, passing from the cardinal processes to become inserted into a small pair of attachment areas situated posterior to the ventral adjustors.

PRINCIPAL VALVE MUSCLES OF INARTICULATED BRACHIOPODS

The valves of the inarticulated brachiopod lack a hinge but possess a complex arrangement of muscles that make them capable of a wider range of valve movements than those of articulated shells. Generally there are two pairs of conspicuous anterior and posterior adductors (except in the lingulids, which have only one laterally placed posterior adductor), two pairs of oblique muscles (three in *Lingula*), an elevator, and three pairs of minor muscles: the lophophore protractors, retractors, and elevators (Fig. 82). The adductors pass dorsoventrally through the body cavity and are the largest sets in brachiopods. They have been given different names in different stocks, but all are concerned with the closure of the shell. The oblique muscles

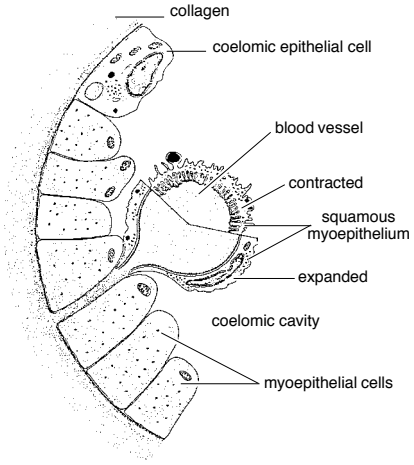

FIG. 74. Diagram of a transverse section through part of a tentacular canal, showing the coelomic epithelium and myoepithelial cells; the tentacular blood vessel is illustrated in both an expanded and contracted condition (adapted from Storch & Welsch, 1976).

control the rotation and sliding or longitudinal movements of the valves.

In *Lingula,* the shell is closed by a pair of medially located, central muscles and a third umbonal muscle, which is made up of two unequal bundles of muscle fibers (Fig. 82). The larger bundle of umbonal muscle fibers runs dorsoventrally. The smaller, flat bundle, which is inserted in front of the main bundle on the ventral valve, spirals around the main bundle, inserting posteriorly in the dorsal valve (BLOCHMANN, 1900). Both central muscles are double bundles of fibers passing dorsoventrally. Four pairs of oblique muscles are present, three of which (middle laterals, outside lateral, and transmedians) form a composite scar on the dorsal valve. The middle laterals arise between the central muscles in the ventral valve and pass obliquely backward to be inserted into the dorsal valve immediately in front of the scar outside the laterals. These outside lateral muscles converge slightly anteriorly from the dorsal valve and are inserted on the ventral valve lateral of the centrals. The third pair of muscles, the transmedians, are the largest of the oblique muscles and form the inner part of the composite scars. The right transmedian muscle runs ventrally from the dorsal valve to become attached to the left side of the ventral valve. The left transmedian muscle splits just below the insertion on the dorsal valve, and the two branches cross over the right transmedian to become fixed to the right side of the ventral valve. This is the usual condition of the transmedians, but the left transmedian of a few species may be undivided (BULMAN, 1939). The fourth pair of muscles with an oblique course is the anterior laterals. These are inserted in the ventral valve posterolateral of the outside muscles and rise anteriorly to become attached to both the dorsal valve and the anterior body wall near the midline of the valve.

The muscular system of *Glottidia* is similar to that of *Lingula* (MORSE, 1902), but those of other recent inarticulated genera are generally less complicated with fewer oblique muscles. In the discinids (Fig. 83) two pairs of adductor muscles, a small posterior pair and a larger anterior pair, run directly dorsoventrally between the valves. Each anterior adductor consists of a small median and a much larger lateral bundle of muscle fibers. Three pairs of oblique muscles occur, all of them relatively long and thin in comparison with the adductors. The internal obliques arise from near the center of the ventral valve

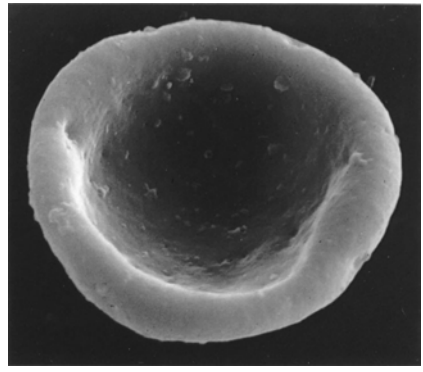

FIG. 75. SEM micrograph of a blood cell (erythrocyte) of *Lingula anatina,* ×2,700 (new).

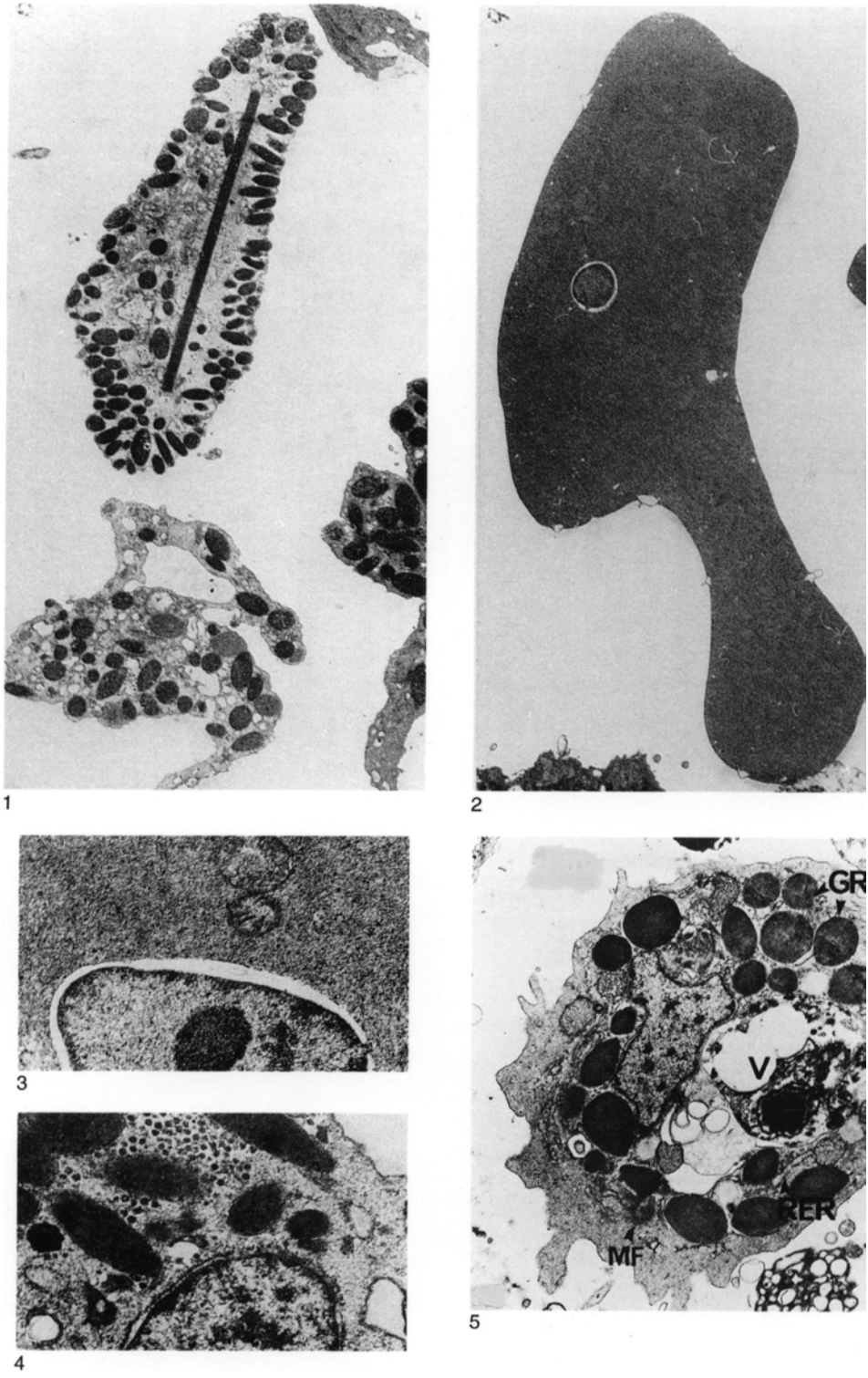

FIG. 76. *For explanation, see facing page.*

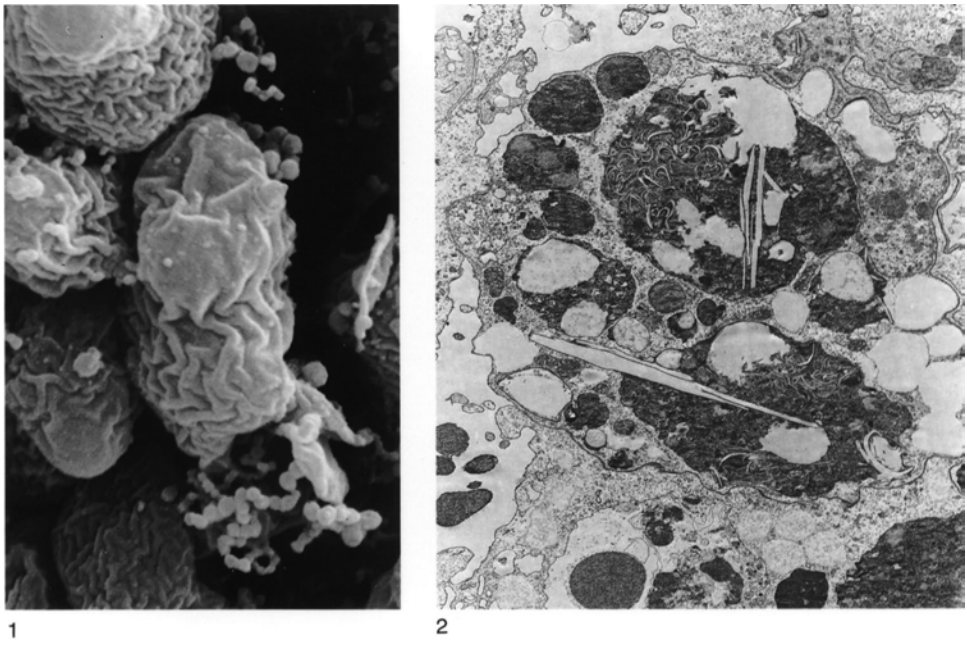

FIG. 77. *1,* SEM, ×9,000, and *2,* TEM micrographs of an amoebocyte in *Calloria inconspicua,* ×1,350; note vacuoles and heterogeneous granules in *2* with cytoplasm (new).

and diverge posteriorly to become inserted into the dorsal valve slightly anterolateral of the attachment of the posterior adductors. The third pair of oblique muscles, the posterior obliques, arise on the ventral valve slightly in front and median of the site of the attachment of the oblique laterals. They pass dorsally and converge posteriorly, becoming inserted into the dorsal valve close together near the midline, slightly in front of the posterior margin.

The principal muscles of *Neocrania* are similar to those of *Discinisca.* Two pairs of adductors occur, the anterior set consisting of two bundles of fibers. The oblique internals occupy a position similar to those of the discinids but follow a more S-shaped course. The oblique laterals originate on the ventral valve on the side of the posterior adductors and are attached not to the dorsal valve but to the anterior body wall (Fig. 84).

The correlation of the muscles of the lingulids, discinids, and craniids is based on form, assumed function, and, more fundamentally, innervation (BLOCHMANN, 1892, 1900). The posterior and anterior adductors of the craniids and the discinids are considered to be homologous to the lingulid umbonal and central muscles respectively. The transmedian, outside, and middle lateral oblique muscles of the lingulids, which are attached only to the shell, may be correlated with the discinid oblique posterior, and oblique internal muscles with the oblique internals of *Neocrania,* all of which are similarly attached.

FIG. 76. TEM micrographs of the coelomocytes of *Lingula anatina; 1,* amoebocytes with granules, ×9,400; *2,* an erythrocyte in cross section, ×1,316; *3,* nucleus and mitochondria of an erythrocyte, ×28,200; *4,* nucleus and cytoplasm with glycogen and granules of an amoebocyte, ×28,200 (Storch & Welsch, 1976); *5,* amoebocytes with granules (*GR*), rough endoplasmic reticulum (*RER*), vacuole containing debris (*V*), and microfilament bundles (*MF*), ×8,460 (Rowley & Hayward, 1985).

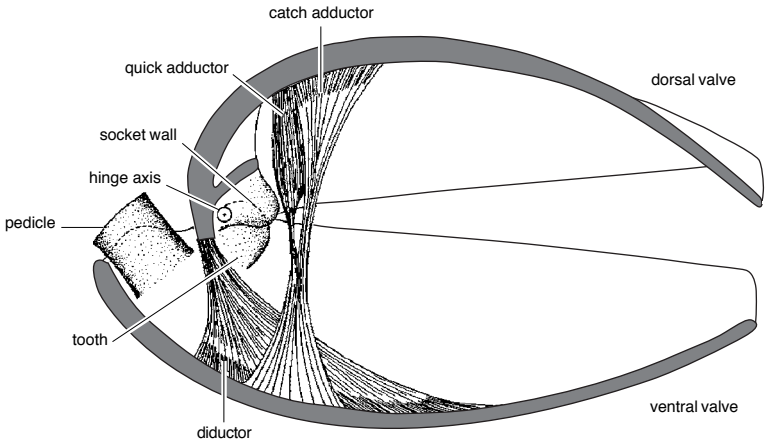

FIG. 78. Articulation and muscle system of the terebratulide *Calloria inconspicua* in median section showing the relationship of the muscles to the hinge axis (adapted from Rudwick, 1961).

STRUCTURE OF PRINCIPAL MUSCLES

Details of the ultrastructure of the adductor and diductor muscles of the articulated *Terebratalia* (ESHLEMAN, WILKENS, & CAVEY, 1982) and the adductor muscle of the inarticulated *Lingula* (KUGA & MATSUNO, 1988) are well documented, and both smooth and striated types are present (Fig. 85). Typically, articulated brachiopods possess one pair of striated and one pair of smooth adductors, originating as four separate muscles on the dorsal valve (the posterior is striated, while the anterior is smooth) and inserted by a common tendon (two tendons in some species) on the ventral valve (Fig. 79). In lingulids, each adductor muscle consists of smooth and obliquely striated components segregated into an anterior opaque and a posterior translucent portion that are constructed of smooth and obliquely striated muscles, respectively (Fig. 85.1–85.2; KUGA & MATSUNO, 1988). It is believed that the anterior adductor in the lingulid is responsible for the catch contraction. The smaller posterior adductors consist of quick, striated muscle fibers that snap the shell shut in response to various stimuli. The larger anterior adductors consist of unstriated catch fibers, which react more slowly and hold the shell closed for long periods. The posterior and anterior adductors form separate bundles of fibers on the dorsal side, but they share a single attachment on the ventral side (Fig. 79; WILLIAMS & ROWELL, 1965a; ESHLEMAN, WILKENS, & CAVEY, 1982).

The muscular tissue of articulated brachiopods has been described only as smooth or striated, but three cell types have been identified in the anterior adductor of *Lingula* (KUGA & MATSUNO, 1988). These consist of striated (translucent) muscle and two types of smooth (opaque) muscle. In the striated adductor muscles of lingulids, cell organelles such as the sarcoplasmic reticular system are located in peripheral regions of the cell (KUGA & MATSUNO, 1988). There is no information regarding the sarcomeric construction of the striated cells of the inarticulated species. In the articulated *Terebratalia,* the striated muscle apparatus consists of sarcomeres of interdigitating thin and thick myofilaments in the ratio of 6:1 (Fig. 86.5–86.6; ESHLEMAN, WILKENS, & CAVEY, 1982).

Thin and thick myofilaments in an unregistered array form the contractile apparatus of the smooth adductor muscle of *Terebratalia* and are indistinguishable from those of the diductor muscles (Fig. 86; ESHLEMAN, WILKENS, & CAVEY, 1982). In *Lingula,* two

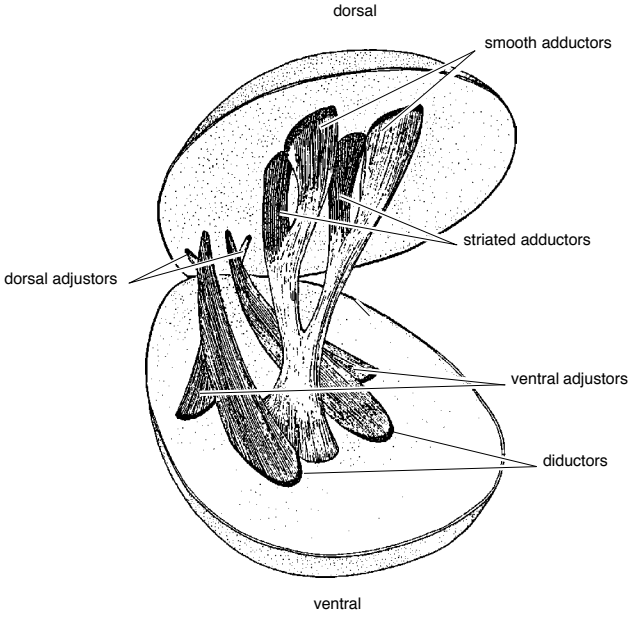

FIG. 79. Diagram of the musculature of *Terebratalia transversa,* with the anterior part of the shell cut away and the lophophore and viscera removed (adapted from Eshleman & Wilkens, 1979a).

populations of smooth muscle cells exist. Type A cells contain contractile fibers, which are relatively thin, thick myofilaments; type B cells contain thick myofilaments in addition to contractile fibers that are of similar size to those found in type A cells (Fig. 85.2–85.3; KUGA & MATSUNO, 1988).

Morphological and electrophoretic evidence suggests that, as in bivalve molluscs, paramyosin may be responsible for the catch contraction of the anterior adductor muscles in brachiopods (WILKENS, 1978a; ESHLEMAN, WILKENS, & CAVEY, 1982; KUGA & MATSUNO, 1988). In *Terebratalia* the presence of paramyosin has been demonstrated in both the smooth adductor and diductor muscles and to a lesser extent in the striated adductor muscle. The large fusiform myofilaments found within these muscles are morphologically characteristic of a paramyosin component and resemble molluscan smooth muscle and the very thick myoepithelial cells of brachiopod tentacles (REED & CLONEY, 1977). The structure of the smooth adductor of *Lingula* also suggests the presence of paramyosin (KUGA & MATSUNO, 1988).

MYOEPITHELIAL CELLS

Although the most conspicuous muscles within the brachiopods occur as well-defined bundles of muscular fibers or as muscular layers in contractile tissues, some specialized epithelial cells (myoepithelial cells) have been shown to contain contractile fibers. Myoepithelial cells have been described in tentacles of the lophophore of the *Lingula* (STORCH & WELSCH, 1974, 1976) and the articulated brachiopod *Terebratalia* (Fig. 87; REED & CLONEY, 1977). In the latter, striated and smooth myoepithelial cells occur in longitudinal rows that extend along each tentacle on opposite sides of the tentacular canal (see Fig. 106). A blind-ending blood vessel that penetrates each tentacle is formed from squamous, smooth myoepithelial cells (see Fig. 76). Myoepithelial cells have also been found in the mesentaria of *Lingula* (STORCH & WELSCH, 1974).

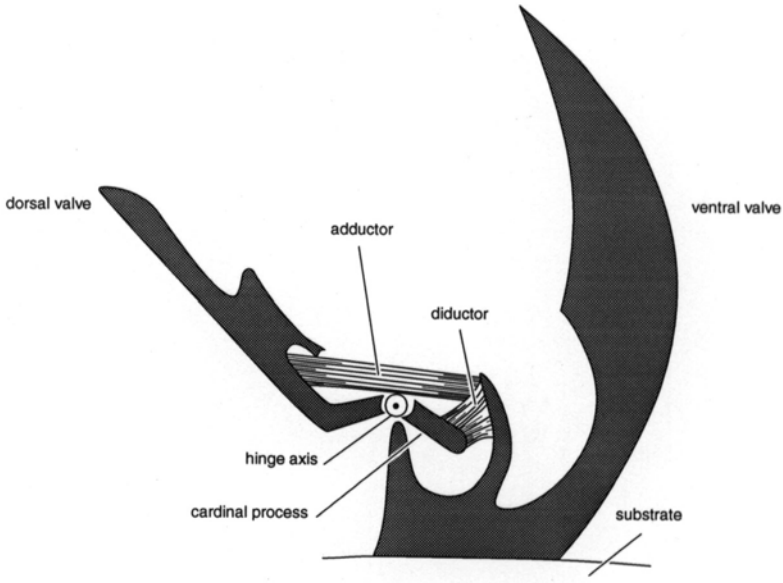

FIG. 80. Muscle system of the cemented thecideidine *Lacazella* showing the columnar muscles raised on a central platform (adapted from Lacaze-Duthiers, 1861; Rudwick, 1970).

The myoepithelial cells of both genera (STORCH & WELSCH, 1976; REED & CLONEY, 1977) appear to be similar. Occasionally ciliated, myoepithelial cells have a centroapical nucleus accompanying mitochondria and Golgi bodies. These organelles occur above a layer of thick and thin myofilaments, which are inserted into basal extensions of the cell. Glycogen occurs in abundance throughout the cells, as alpha particles in *Lingula* and beta particles or rosettes in *Terebratalia.* Lipid inclusions are present in *Lingula* (STORCH & WELSCH, 1974). Attached to a basal lamina with numerous hemides-

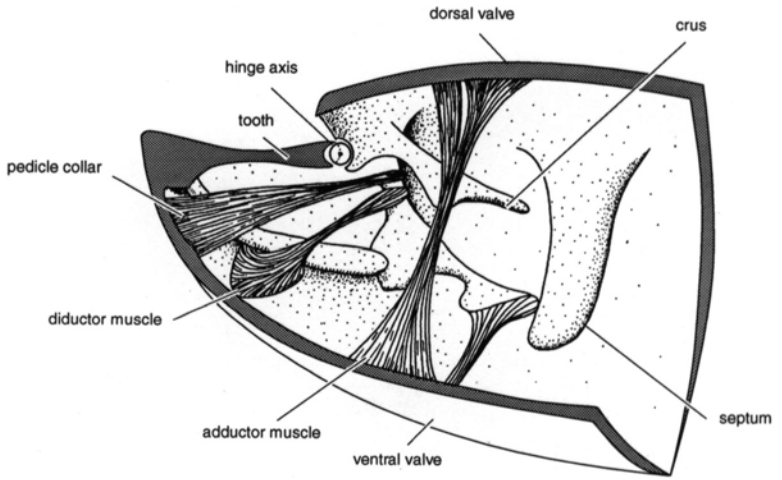

FIG. 81. Musculature of *Platidia annulata* (ATKINS) (adapted from Williams & Rowell, 1965a).

mosomes, the myoepithelia are joined to surrounding cells by *zonulae adhaerens* (Fig. 88; Reed & Cloney, 1977).

The fine structure of myoepithelial cells, myofilament fields, and sarcoplasmic reticula are known only for *Terebratalia* (Reed & Cloney, 1977). The striated myofilament field (Fig. 88.1) is composed of interdigitating, thin and thick myofilaments, which combine to produce the characteristic striation or banding rendered visible by light microscopy. Each thick myofilament is surrounded by 12 thin myofilaments giving a thin to thick ratio of 6:1. The sarcoplasmic reticulum, which is peripheral to the myofilament field, is a smooth, membranous system of tubules that frequently form subsarcolemmal cisternae that couple peripherally with the lateral sarcolemma.

Smooth myoepithelial cells (Fig. 88.2) also contain thick and thin myofilaments that are of indefinite length and staggered throughout the myofilament field. Thick filaments are fusiform, surrounded by thin myofilaments, and resemble the paramyosin filaments of bivalve mollusc adductor muscles. The sarcoplasmic reticulum is reduced, and peripheral couplings are rare in comparison to the striated myoepithelial cells.

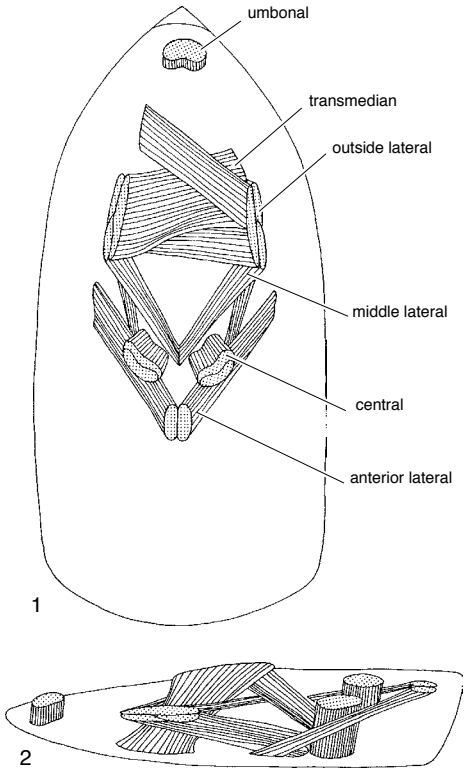

Fig. 82. Muscle system of *Lingula* viewed *1,* dorsally and *2,* laterally (adapted from Bulman, 1939).

Functional Morphology of the Principal Valve Muscles

In articulated brachiopods when the adductor muscles relax and the diductor muscles contract, the anterior margin of the valves separate (gape). The gape is maintained by tonic contraction in the smooth diductor muscles. Closure of the shell occurs in two modes depending upon the stimulus and reflecting the physiological properties of the striated (quick) and smooth (catch) components of the adductor muscles. In articulated brachiopods, the anterior adductors are quick; the posterior adductors catch. A combination of slip, the rapid loss of tetanus in the diductors, and contraction of the striated portion of the adductors assures rapid shell closure. Closure of the valves is completed and maintained by the smooth portion of the adductor contracting and achieving tetanus.

Pedicle muscles vary greatly in size, position, and relationship to the pedicle. The positions of these muscles are the most explicit guide to the pedicle type and function (Richardson, 1979, 1981a, 1981b). During closure of the shell, contraction of the adjustor muscles pulls the proximal end of the pedicle deep into the body cavity, but it is believed that, since the diductors are intimately associated with the connective tissue around the base of the pedicle, their contraction during the opening of the shell assists in ejecting the pedicle, thus moving the shell forward into an erect position (Williams & Rowell, 1965a).

It is thought that the contraction of the posterior adductors or the umbonal muscle

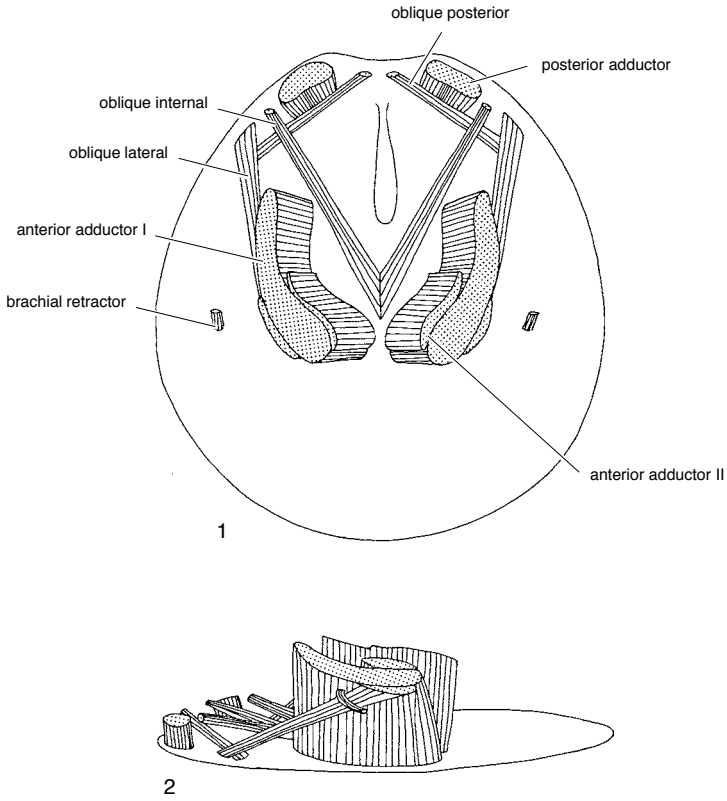

FIG. 83. Muscle system of *Discinisca* viewed *1,* dorsally and *2,* laterally (adapted from Bulman, 1939).

and relaxation of the anterior adductors or their homologues opens the valves of inarticulated genera. The action is probably assisted and partly controlled by the various oblique muscles and dermal muscles of the body wall.

DIGESTIVE SYSTEM

The brachiopod digestive system is composed of a continuous gut or alimentary tract, opening at the mouth and terminating with an anus or ending blindly in inarticulated and articulated species respectively. In both groups the digestive system consists of a mouth, pharynx, esophagus, stomach, digestive diverticula (liver), and a pylorus. In inarticulated brachiopods the gut continues beyond the pylorus through an intestine, terminating in an anus (Fig. 89).

ALIMENTARY CANAL

The mouth is a transverse slit that occurs medially in the brachial groove where the two arms of the lophophore (brachia) unite (see Fig. 103). The mouth opens to the pharynx, a short, dorsally curved, muscular tube embedded in the bases of the brachia. The gut continues as an esophagus, a relatively short tube leading to the stomach, which is a pouchlike distended portion of the digestive tract supported by mesentaries (the gastro- and ileoparietal bands). A number of ducts join the stomach to the digestive diverticula, which are formed from anastomosing clusters of blindly ending tubes (acini). A sphincter separates the stomach from the pylorus. In inarticulated brachiopods, the pylorus leads into an intestine that opens to the exterior (the mantle cavity) through the

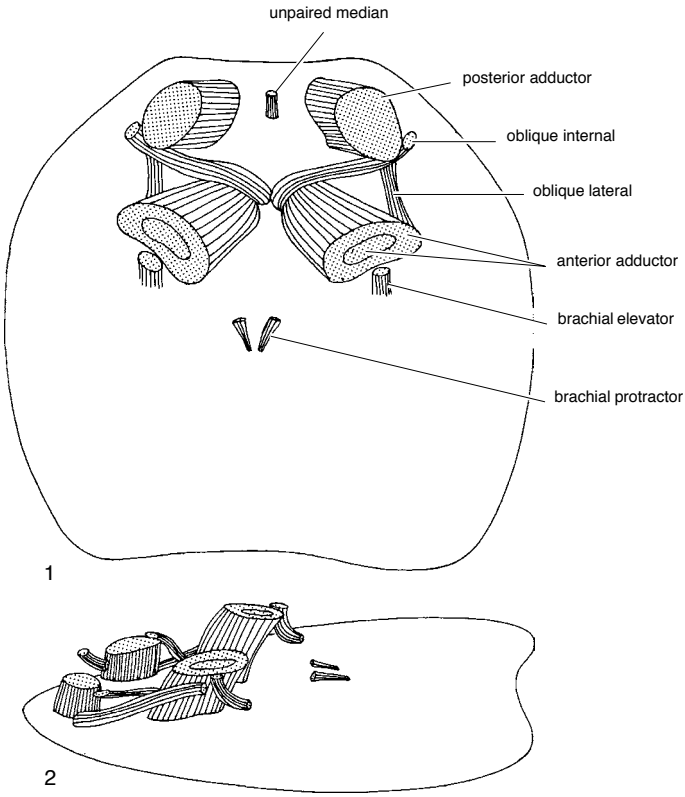

FIG. 84. Muscle system of *Neocrania* viewed *1,* dorsally and *2,* laterally (adapted from Bulman, 1939).

anus. The opening of the anus is also controlled by a sphincter (Fig. 90).

The esophagus of the inarticulated brachiopods is relatively short and leads to the stomach. In older literature, the stomach was described as being divided into posterior and anterior parts. These are now considered to be homologues of the stomach and pylorus respectively of articulated brachiopods (Fig. 89; CHUANG, 1960; STEELE-PETROVIC, 1976). The stomach extends posteriorly along the median line and in both lingulids and discinids is attached by part of the ileoparietal band to the posterior body wall. In *Neocrania* it curves ventrally forward toward the posterior end of the coelomic cavity. The stomach is separated from the pylorus by a sphincter, which is clearly visible in *Lingula* (BLOCHMANN, 1900) but less so in *Neocrania* (BLOCHMANN, 1892).

Digestive diverticula open through ducts into the stomach. There are four digestive diverticula in *Lingula* and *Discinisca* and two in *Neocrania* (JOUBIN, 1886; BLOCHMANN, 1892). They open separately into the stomach and are subdivided into lobes, each comprising several bunches of short acini in lingulids and *Neocrania* (JOUBIN, 1886; BLOCHMANN, 1892; MORSE, 1902; CHUANG, 1959b) but are long and tubular in *Discinisca* (JOUBIN, 1886). Each of the four diverticula present in *Lingula* (three dorsal and one ventral) opens through a separate duct into the stomach. The three dorsal diverticula consist of an anterior diverticulum situated on the midline of the stomach and a posteriorly placed pair of diverticula on the left and right of the midline, slightly behind the point of attachment of the gastroparietal band. Diverticula of adults vary in size, the

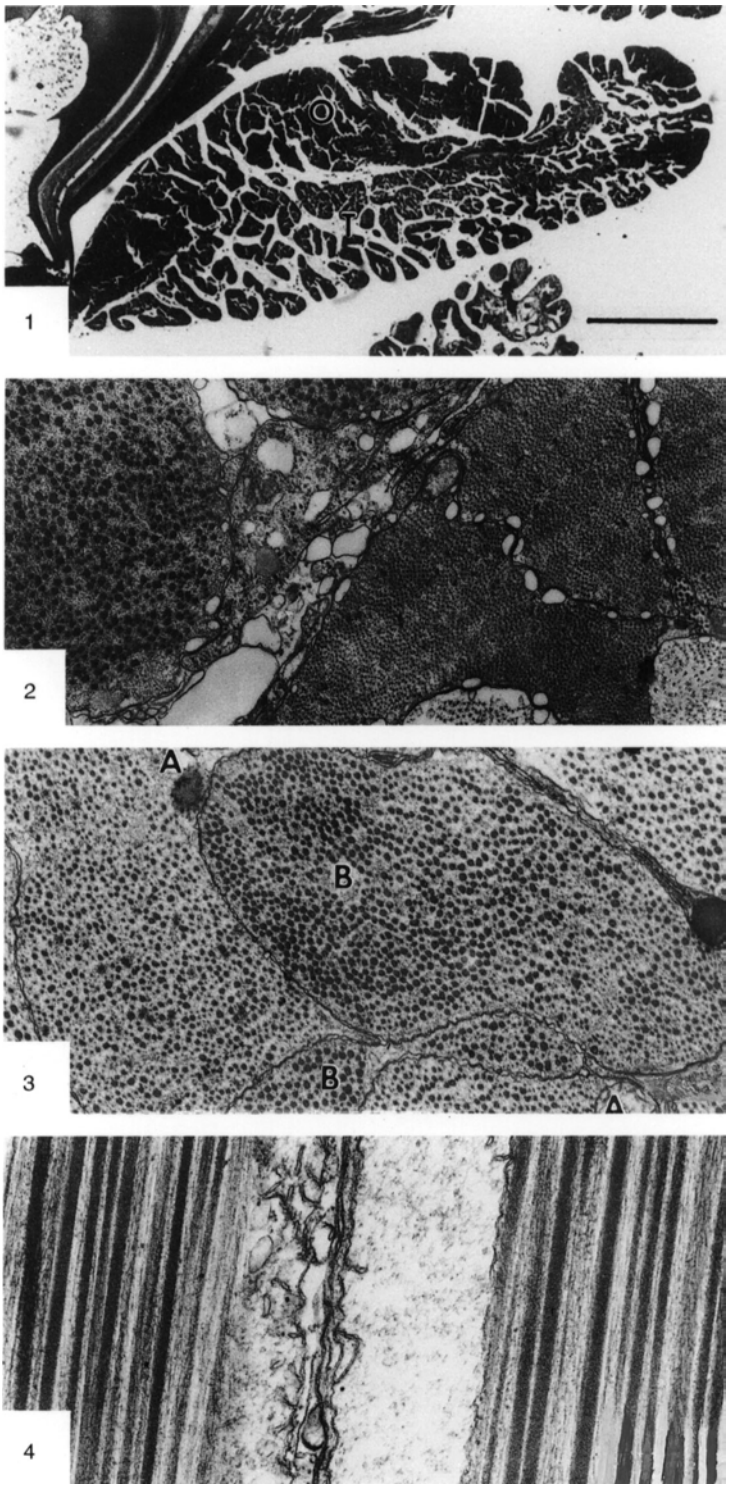

FIG. 85. *(For explanation, see facing page.)*

right posterior being the largest and the anterodorsal the smallest. All have a similar structure, with each diverticulum consisting of a fixed number of lobes, seven in the right posteroventral, two in the right posterodorsal, and four in the ventral and anterodorsal diverticula. The main duct of each diverticulum bifurcates shortly after leaving the stomach, and from the bifurcation a number of lobular ducts arise to serve the lobes. The lobes consist of repeatedly branching ducts terminating in bunches of acini (CHUANG, 1959b).

In *Neocrania* a pair of dorsal diverticula are separated by a mesentery. Each diverticulum is divided into four lobes, which have a similar construction to those of *Lingula* (JOUBIN, 1886; BLOCHMANN, 1892). *Discinisca* has three diverticula, all situated in front of the gastroparietal band as a dorsal pair and a single unpaired diverticulum. They open into the stomach by separate ducts but are apparently not divided into lobes, their terminal portions being long tubes (JOUBIN, 1886).

Both *Lingula* and *Neocrania* have a ciliated epithelial groove running along the stomach (CHUANG, 1959b, 1960). In *Lingula* it arises in the right posterodorsal diverticula, traverses all the lobes of this organ, and

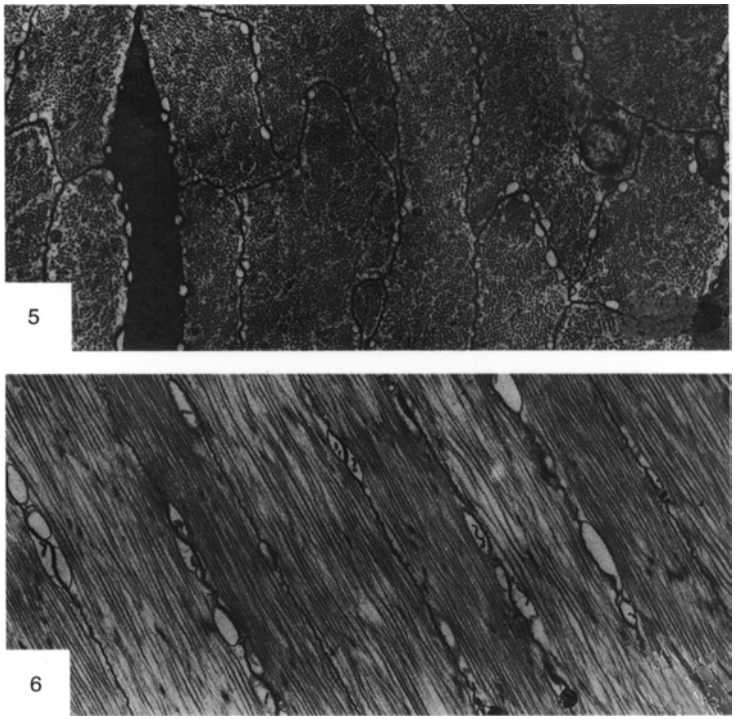

FIG. 85. The structure of muscles of *Lingula anatina; 1,* a light micrograph of a cross section of the anterior adductor of *Lingula anatina.* The dark area of the adductor (*O*) is the opaque (smooth) portion. The light area (*T*) is the translucent (striated) portion, ×15.75; *2,* TEM micrograph of a cross section of the opaque and translucent portions to the left and right respectively, ×7,290; *3,* TEM micrograph of a cross section of the opaque portion; cell organelles are located at the periphery of the cell, type A cells (*A*) have thinner-sized thick myofilaments. Type B cells (*B*) have two kinds of thick myofilaments, ×4,860; *4,* TEM micrograph of a longitudinal section of the opaque portion showing the differences in the size of the thick myofilaments in type A cell to left and type B cell to right, ×24,300; *5,* TEM micrograph of a cross section of the translucent portion with cell organelles located in the peripheral region of the cells; the thick myofilaments are gathered into units of 50 to 60, ×6,480; *6,* TEM micrograph of a longitudinal section of a translucent portion with thick myofilaments running parallel to the longitudinal axis of the cells, ×7,290 (Kuga & Matsuno, 1988).

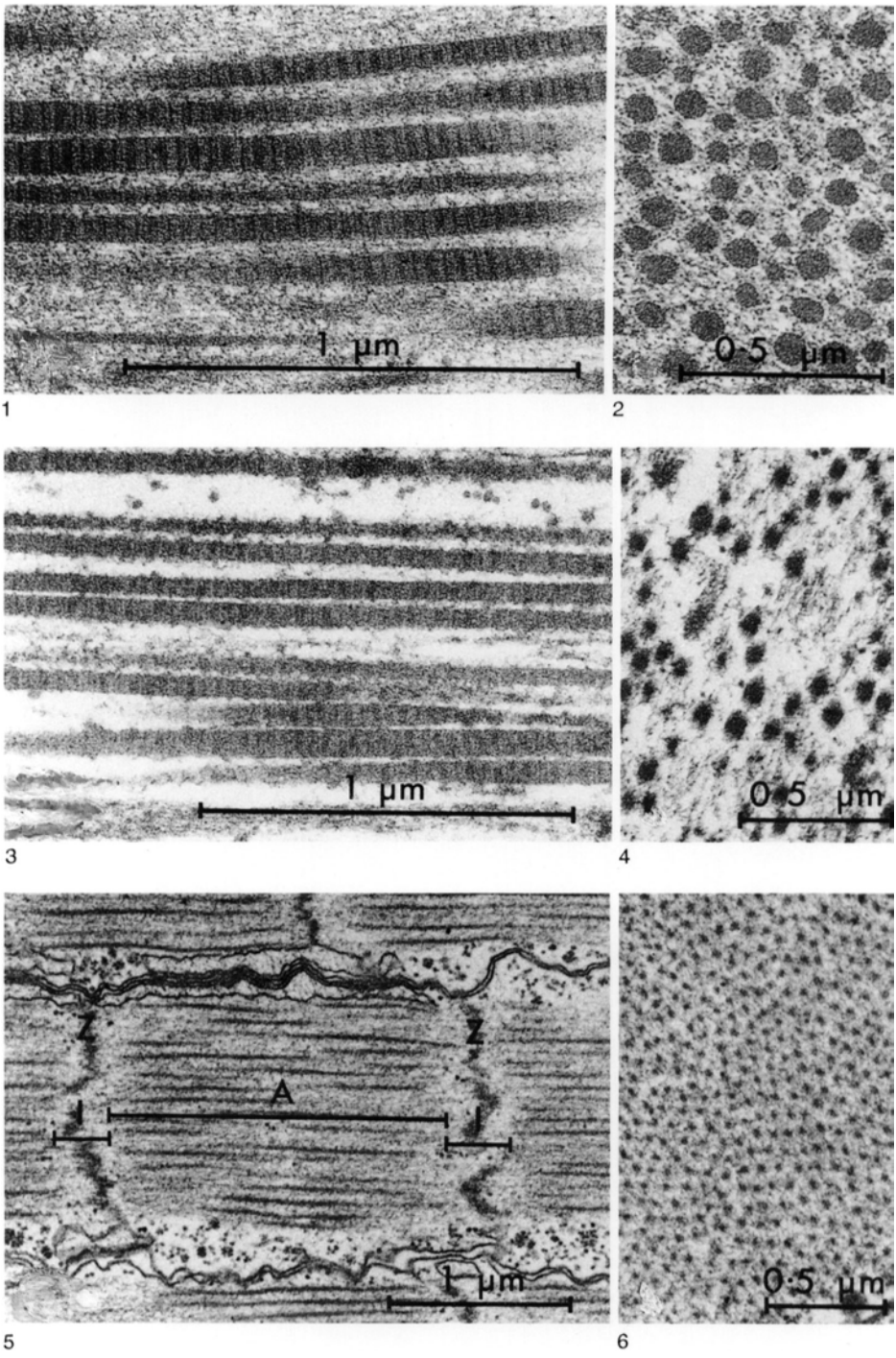

FIG. 86. TEM micrographs of myofilaments of *Terebratalia transversa; 1,* longitudinal section and *2,* transverse section of smooth adductor cell; myofilaments of the diductor cells in *3,* longitudinal section and *4,* transverse section; myofilaments of the striated adductor cells (*A,* A-band; *I,* I-band; *Z,* Z-line) in *5,* longitudinal section and *6,* transverse section (Eshleman, Wilkens, & Cavey, 1982).

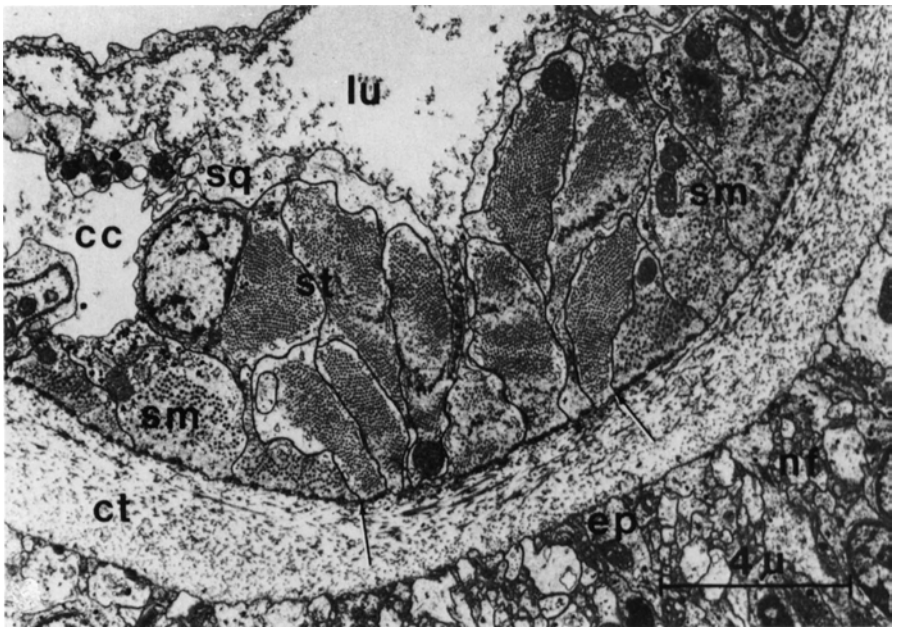

FIG. 87. TEM micrograph of a transverse section of the frontal contractile bundle near the distal end of the inner tentacle of *Terebratalia transversa;* about 10 striated myoepithelial cells (*st*) occupy the central part of the contractile bundle (betweeen the *arrows*) and are bordered on either side by a group of three smooth myoepithelial cells (*sm*) (outside the *arrows*); striated fibers adjoin the squamous peritoneal cells (*sq*) of the tentacular blood vessel; the acellular connective tissue cylinder (*ct*) separates the myoepithelial cells from the epidermis (*ep*) and the neuronal processes (*nf*) at the bottom of the picture; also identified, lumen of blood vessel (*lu*) and tentacular canal (*cc*) (Reed & Cloney, 1977).

emerges to run along the dorsal surface to the pylorus. The epithelial groove in *Neocrania* lies longitudinally along the floor of the stomach and continues into the pylorus, rising dorsally from the floor to the roof of the pylorus by the right lateral wall.

Formally known as the posterior stomach, the pylorus of inarticulated brachiopods is narrower, has thicker walls, and is separated from the stomach by a constriction. Another, posterior sphincter separates the pylorus from the start of the intestine. The intestine in lingulids and discinids (JOUBIN, 1886; BLOCHMANN, 1900; MORSE, 1902; CHUANG, 1960) is a slender tube, while in *Neocrania* (JOUBIN, 1886; BLOCHMANN, 1892) it is dilated posteriorly.

In the lingulids, the thin-walled, tubular intestine bends to the left and forms a free loop before returning to the end of the coelomic cavity. It then turns right and follows an oblique course anteriorly to open at the anus on the right body wall. The intestine of the discinids is shorter but similar to that of the lingulids, turning right from the stomach toward the lateral body wall and then obliquely forward in a dorsal direction, also opening on the right body wall at an anus. *Neocrania* differs considerably in possessing a V-shaped gut with the apex directed anteriorly. From the sphincter at the end of the stomach the intestine continues anteriorly and then bends back acutely to open at the anus, which is medially placed on the posterior margin. Although the anus is on the midline, it lies to the right of the attachment of the ventral and dorsal mesentaries to the intestine. As in other inarticulated brachiopods, the anus opens on the right side of the body but is posteriorly placed (CHUANG, 1960).

In most articulated genera, the esophagus is divided into a relatively long anterior and a short posterior section, separated by a

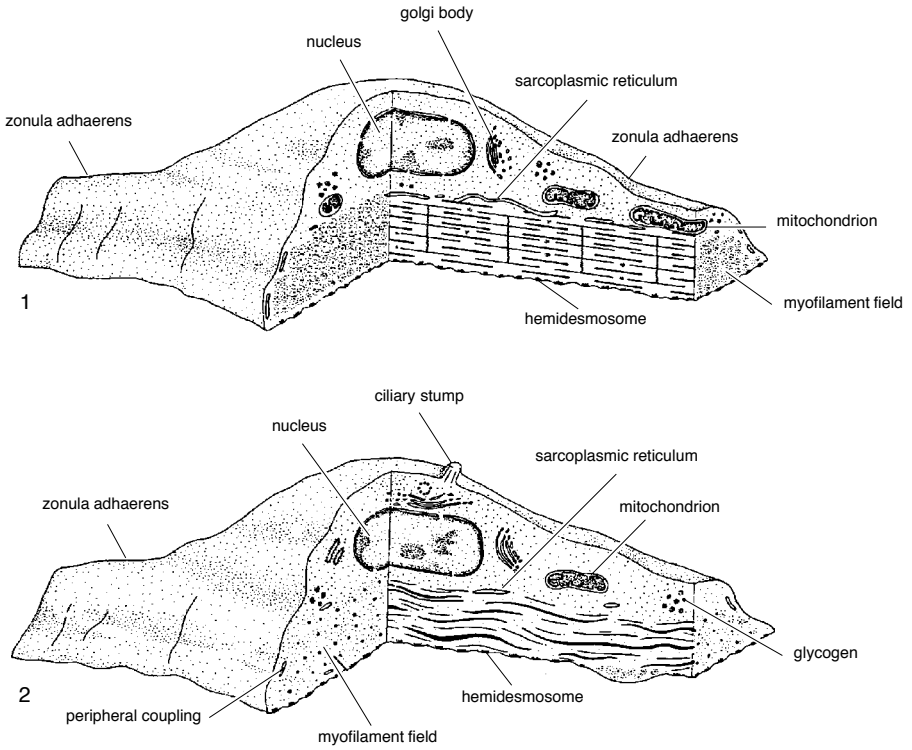

FIG. 88. Schematic diagrams of *1,* a striated myoepithelial cell and *2,* a smooth myoepithelial cell (adapted from Reed & Cloney, 1977).

valvelike thickening of the esophageal wall (MORTON, 1960). It is distinguished from that of inarticulated brachiopods in being strongly inclined anterodorsally before it bends abruptly to the relatively short stomach (Fig. 90).

The digestive diverticula of articulated species are not well known but commonly consist of a pair of posterior lobes that are symmetrically disposed around the dorsal mesentery and communicate with the stomach through 1 of 3 pairs of ducts. Different arrangements occur in *Argyrotheca* and *Lacazella,* where the diverticula consist of 6 to 8 pairs and 10 to 16 pairs of elongate tubules respectively.

The stomach passes middorsally into a tapering pylorus directed posteroventrally and terminating blindly as either a blunt end supported by a mesentery or exceptionally, as in *Hemithiris,* as a bulbous end twisted upon itself and hanging free (Fig. 91; HANCOCK, 1859).

HISTOLOGY OF THE GUT

The histology of the gut in all brachiopods appears to be similar. The gut is essentially a variably elastic, connective tissue (collagen) tube encompassed by two layers of muscle, an inner, circular layer and an outer, longitudinal layer. These muscles appear to be smooth in the intestine and stomach of all brachiopods, but the esophageal muscles in some rhynchonelloids and terebratuloids are known to be striated. The gut is sheathed by a thin, ciliated, coelomic epithelium. The lumen of the connective tissue tube is covered by a basal lamina and columnar epithelium, the cells of which are modified in different parts of the gut to perform different

functions. Most of the lumen of the gut is covered by ciliated columnar cells interspersed with mucous (glandular) cells and wandering phagocytes (CHUANG, 1959b). Neurons pass along the axis of the gut between the bases of the columnar epithelial cells above the basement membrane (D'HONDT & BOUCAUD-CAMOU, 1982).

Each digestive diverticulum consists of acini connected to the stomach by a series of ciliated, branching ducts (Fig. 92; BLOCHMANN, 1892; STORCH & WELSCH, 1975; STEELE-PETROVIC, 1976; D'HONDT & BOUCAUD-CAMOU, 1982). Acini range in structure from the globular or tubular sacs in *Lingula* (CHUANG, 1959b) to the long, unbranched, digitate forms of a number of articulated brachiopods (Fig. 93; STEELE-PETROVIC, 1976; PUNIN & FILATOV, 1980; D'HONDT & BOUCAUD-CAMOU, 1982). Acini are constructed from a tube of collagen covered externally by a ciliated coelomic epithelium and musculoepithelial cells. Internally the acini are lined with an epithelium containing ciliated, glandular, and phagocytic cells.

The fine structure of columnar cells lining the lumen of the pylorus and stomach is known only for *Terebratulina* (D'HONDT & BOUCAUD-CAMOU, 1982), while the digestive diverticula have been documented for *Terebratulina* (D'HONDT & BOUCAUD-CAMOU, 1982), *Hemithiris* (PUNIN & FILATOV, 1980), and *Lingula* (STORCH & WELSCH, 1975). The fine structure of the digestive diverticula appears to be similar in all brachiopods so far investigated (*Hemithiris,* PUNIN & FILATOV, 1980; *Terebratulina,* D'HONDT & BOUCAUD-CAMOU, 1982; and *Lingula,* STORCH & WELSCH, 1975). A number of different types of cells line the acini, reflecting its role as the main site of intracellular digestion in the brachiopod (CHUANG, 1959b; STORCH & WELSCH, 1975).

Two kinds of cells have been noted in the digestive diverticula of the articulated genera, *Magellania, Notosaria, Terebratella* (STEELE-PETROVIC, 1976), and *Terebratulina*

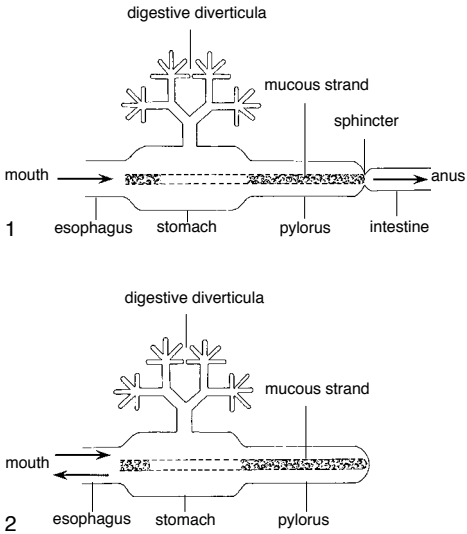

FIG. 89. Schematic diagrams of the guts of *1,* inarticulated and *2,* articulated brachiopods (adapted from Steele-Petrovic, 1976).

(D'HONDT & BOUCAUD-CAMOU, 1982); and, although three types of cells have been distinguished in *Lingula* (STORCH & WELSCH, 1975), at least two exhibit features common with those described in articulated brachiopods and probably function in the same way (Fig. 94; JAMES & others, 1992).

Although it is not presently possible to define unambiguously all the different types of cells forming the epithelial lining of the lumen of the gut and diverticula, broad categories can be recognized. They include ciliated cells, glandular cells, and digestive cells.

Monociliated columnar cells occur throughout most of the gut, and the available evidence suggests that they are similar in all living brachiopods (BOSI VANNI & SIMMONETTA, 1967; STORCH & WELSCH, 1975; D'HONDT & BOUCAUD-CAMOU, 1982). Most of the columnar epithelial cells lining the gut possess an apical cilium surrounded by long, distal microvilli. In *Terebratulina,* many of these cells, especially in the stomach, contain paracrystalline inclusions, of unknown origin or function (D'HONDT & BOUCAUD-CAMOU, 1982).

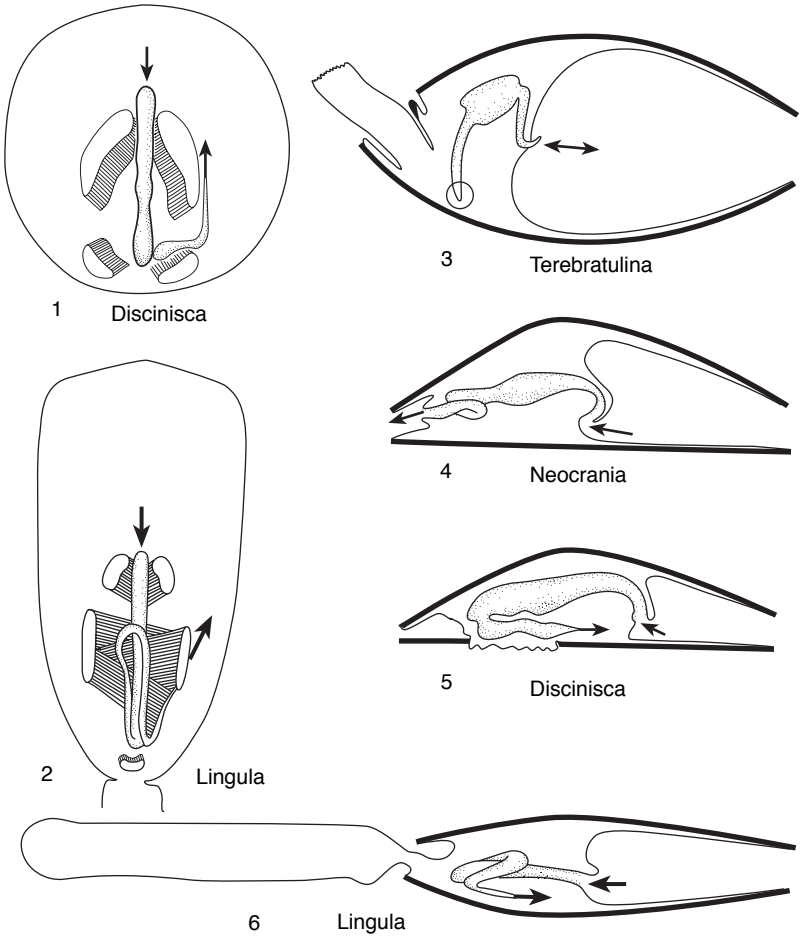

FIG. 90. *1–6,* The position of the gut in relation to the major muscles between the valves in *Lingula* and *Discinisca* and comparisons between lateral views of the four main types of brachiopod gut arrangement. The end of the intestine is indicated by an open circle in *Terebratulina* (*3*) where the gut ends blindly. The position of the mouth and anus and the direction of movement of material are indicated by *arrows* (adapted from Nielsen, 1991).

Glandular cells are associated with the ciliated cells and two cell types, A and B, have been identified in *Terebratulina.*

Type A glandular cells are unciliated and distributed throughout the pyloric epithelium. The apical part of the cell contains vacuoles and glycogen granules and has a narrow basal region containing abundant mitochondria and reticulated vacuoles. A similar cell type also occurs in the digestive diverticula. These ciliated cells (cell type 1 in *Lingula* (Fig. 94–95; STORCH & WELSCH, 1975), with dense microvilli, extend into the lumen of the acini and constitute the largest proportion of the parietal epithelium in *Terebratulina* and *Hemithiris,* where the cells are vacuolated and the vacuoles contain large numbers of glycogen granules. Some of these cells are packed with non-osmophilic globules with paracrystalline inclusions. Supranuclear Golgi give rise to secretory granules, which accumulate in the apices of the cells (D'HONDT & BOUCAUD-CAMOU, 1982).

Type B glandular cells differ from type A (D'HONDT & BOUCAUD-CAMOU, 1982) in possessing vacuoles with homogeneous con-

tents. They occur sporadically and do not seem to be present in the pylorus of *Terebratulina* (D'HONDT & BOUCAUD-CAMOU, 1982). A similar cell type (type 3 cell; Fig. 94, 96) occurs in *Lingula* (STORCH & WELSCH, 1975), which may be analogous to the type B cells of *Terebratulina.* The former occur mainly in the intestine and infrequently in the digestive diverticula; they are mucous-producing cells and contain electron-dense granules (STORCH & WELSCH, 1975).

Digestive cells (cell type 2 in *Lingula,* STORCH & WELSCH, 1975) occur in the acini of the digestive diverticula (Fig. 94, 97). These large, pleomorphic cells have been reported in various stages of growth and disintegration (CHUANG, 1959b, 1960; STORCH & WELSCH, 1975; STEELE-PETROVIC, 1976; PUNIN & FILATOV, 1980). During early stages of its development, the digestive cell of *Lingula* bears a cilium and is characterized by basally located lipid inclusions. As the cell matures, the apex of the cell bulges into the lumen of the acini. Digestive cells can absorb soluble material and ingest particulate material by both pino- and phagocytosis at the bulging plasmalemma of the cell (STORCH & WELSCH, 1975; STEELE-PETROVIC, 1976). These cells also contain a well-developed lysosomal system; and in *Lingula,* algal cells and starch granules have been observed in their vacuoles (STORCH & WELSCH, 1975). Digestive cells are probably subject to cyclical disintegration following the completion of intracellular digestion (CHUANG, 1959b, 1960).

Basophil-like cells have been recorded in *Notosaria* and *Terebratella.* This type of cell is well known in bivalve molluscs, but their function is unknown (STEELE-PETROVIC, 1976).

FUNCTIONAL MORPHOLOGY OF THE DIGESTIVE SYSTEM

Details of the passage of food particles through the alimentary canal are well known only for *Lingula* (CHUANG, 1959b). Food particles, gathered by the lophophore, are entrapped by mucus in the food (brachial)

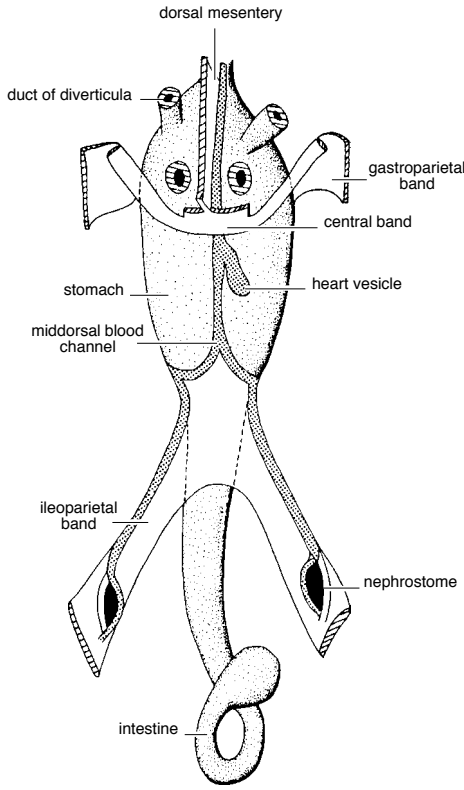

FIG. 91. View of part of the alimentary canal of *Hemithiris psittacea* (GMELIN) showing the distribution of the main mesentaries (adapted from Hancock, 1859).

groove and carried by ciliary currents into the mouth and pharynx, where the mucus becomes shredded. Posteriorly directed ciliary currents in the pharynx, esophagus, and intestine keep the food particles suspended. Movement of the particles through the gut is regulated and maintained by a combination of peristalsis, constriction, and pendular movements generated by the sequential contraction of the muscles surrounding the gut.

In *Lingula,* the stomach, pylorus, and digestive diverticula can be isolated from the rest of the digestive tract by the folded muscular pharynx, the esophagus, and the sphincter at the beginning of the intestine, thus creating a restricted area for the retention, agitation, and circulation of the ingested fluid and particles. Once food particles enter the stomach, ciliary action causes

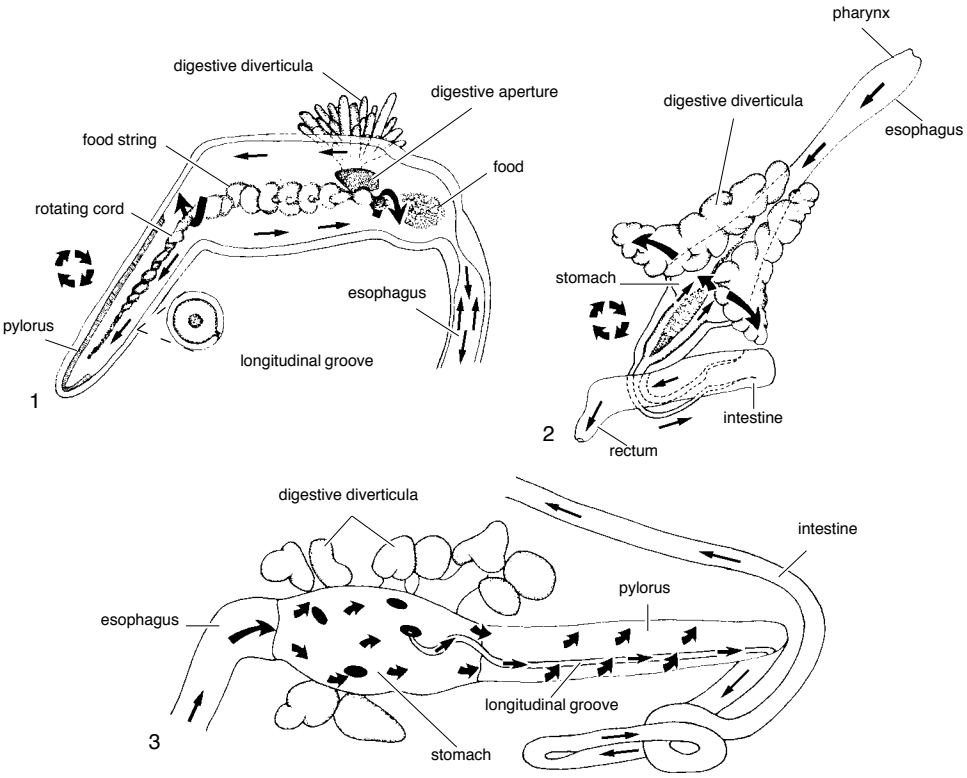

FIG. 92. Ciliary currents and direction of particle motion in brachiopod digestive tracts; *1, Macandrevia; 2, Neocrania* (adapted from Morton, 1960); and *3, Lingula* (adapted from Chuang, 1959b); note the clockwise rotation of mucus and food string; particles are passed back and forth between the stomach and the digestive diverticula in both articulated and inarticulated species during digestion; feces are expelled through the anus in *2* and *3* by peristalsis, constriction, and pendular motions; feces are disgorged through antiperistalsis in *1*.

the suspended food particles to rotate, usually in a clockwise direction in *Lingula* (CHUANG, 1959b).

The acini of the digestive diverticula have an elastic and muscular sheath (STORCH & WELSCH, 1975) and are able to perform vigorous pulsations (MORTON, 1960). This action causes food particles to be drawn into the acini from the stomach. Relaxation of the acini and peripherally directed ciliary currents returns particles to the stomach. The rotation of particulate material in the stomach ceases during diverticular pulsations.

Most digestion in brachiopods is considered to be intracellular, and the digestive diverticula are the main sites of intracellular digestion (CHUANG, 1959b; STORCH & WELSCH, 1975). Strong carbohydrase activity in the lumen of the digestive diverticula and the stomach of *Lingula* also indicates extracellular digestion (CHUANG, 1959b). Digestion is mainly the responsibility of the digestive cells in the acini of the digestive diverticula, which absorb soluble nutrients and phagocytose and pinocytose particulate food material. Wandering phagocytes are also found in the epithelium of the intestine, digestive diverticula, and esophagus. When intracellular digestion is complete, the digestive cells disintegrate into the lumen of the digestive diverticula. This appears to facilitate the elimination of undigested particulate material. The material discharged from the diverticula is gathered into a mucous rope that runs through the ventral, ciliated, epithelial groove from the duct of the right-posterior,

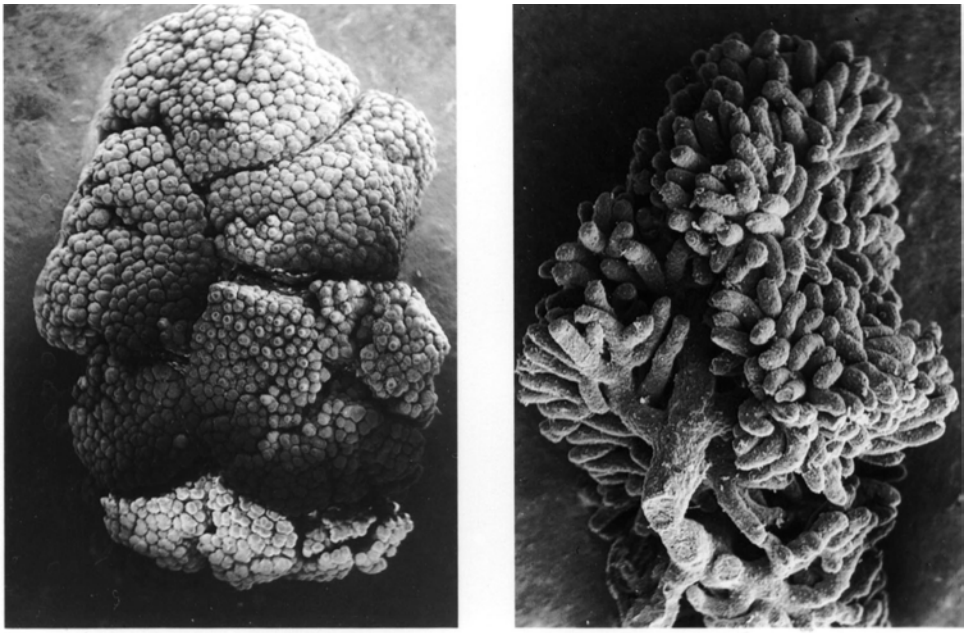

FIG. 93. SEM micrographs of the digestive diverticula of *1, Lingula anatina,* ×12, and *2, Calloria inconspicua,* ×30 (new).

digestive diverticula to the pylorus (Fig. 90). The residence time of food particles in the stomach and pylorus may be minutes; undigested material is retained and concentrated in the intestine for several hours. These processes are probably much the same for other inarticulated brachiopods (CHUANG, 1960).

The digestive process of articulated brachiopods appears to be similar, except that they have ventroanteriorly directed ciliary currents in the stomach (STORCH & WELSCH, 1975). Articulated brachiopods also have an epithelial groove running from the stomach to the pylorus, which generates a rotating mucous rope of particles (Fig. 92.1). It is suggested that the undigested remains are concentrated as fecal pellets and packed at the esophageal end of the stomach prior to elimination by antiperistalsis (MORTON, 1960; STORCH & WELSCH, 1975).

Possible digestive cycles of brachiopods are consistent with observations made on ventilating or feeding brachiopods in the laboratory (JAMES & others, 1992). Intermittent feeding and ventilation are known to occur in brachiopods, which are constantly gaping (ATKINS, 1959; PUNIN & FILATOV, 1980; LABARBERA, 1984; RHODES, 1990; RHODES & THAYER, 1991).

EXCRETORY SYSTEM

The brachiopod excretory system consists of one or exceptionally, as in the rhynchonelloids, two pairs of metanephridia, which, during spawning, act as gonoducts and allow the discharge of gametes from the coelom into the mantle cavity. Although some solid waste may be ejected through the nephridiopore enmeshed in mucus (RUDWICK, 1970), the main excretory product, ammonia (HAMMEN, 1968), is probably voided by diffusion through the tissues of the mantle and lophophore. The metanephridia of *Calloria* are closed until the onset of sexual maturity toward the second year of life (PERCIVAL, 1944), which may indicate that, in this species at least, metanephridia serve primarily as gonoducts.

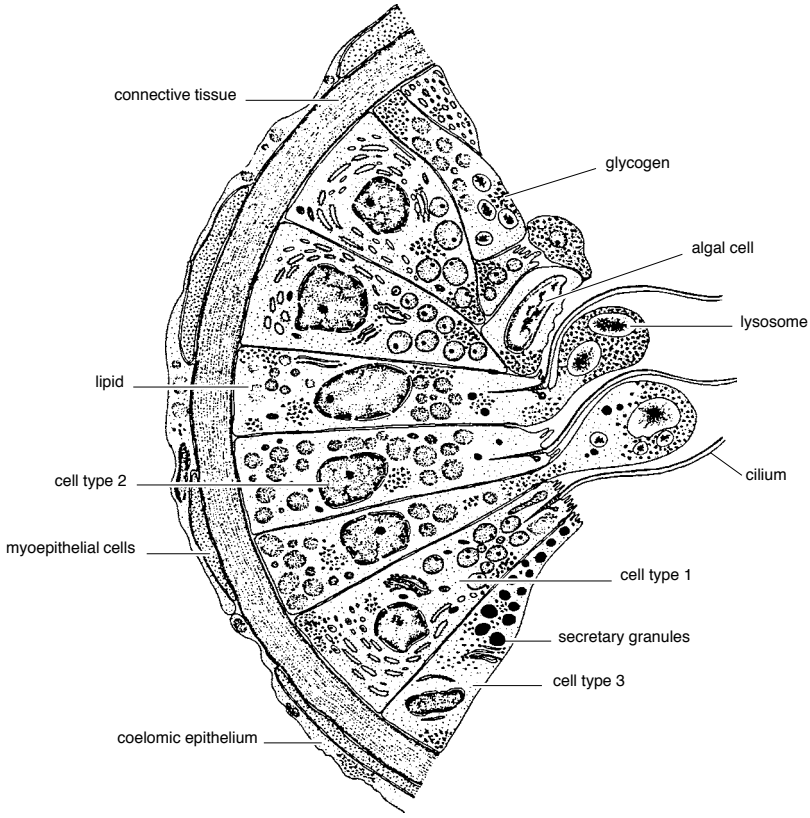

FIG. 94. Diagrammatic representation of a section through part of an acinus of the digestive diverticulum of *Lingula anatina* (adapted from Storch & Welsch, 1975).

Lingulid metanephridia are broad and relatively long, and the nephrostomes are turned laterally away from the midline to face the lateral body wall (Fig. 98). In the discinids and craniids, the metanephridia are relatively shorter, the nephrostomes facing dorsally and slightly medially in the discinids and medially in the latter. The nephrostomes of articulated brachiopods are generally oriented to face dorsally or dorsomedially.

The structure of the metanephridia is similar in all brachiopods. Each metanephridium is essentially a ciliated funnel with a ruffled and densely ciliated inner surface. The widest aperture within the coelomic cavity consists of a broad funnel-shaped nephrostome that continues anteriorly as a narrow tube, usually ventrally placed against the lateral body wall and opening into the mantle cavity through a small nephridiopore on the anterior body wall close to the midline and ventral to the mouth (Fig. 99–100). The ileoparietal bands support the nephrostomes of all brachiopods, including the posterior pair in the rhynchonellides. The anterior nephrostomes of rhynchonellides are supported by the gastroparietal bands.

The histology of the metanephridia is also similar in all brachiopods. The inner surface is covered by a highly microvillous, ciliated epithelium interspersed by secretory, probably mucous cells. The apices of these cells contain large vacuoles with coarse and variably granular contents. Beneath the vacuolated surface cells lies a much thicker layer consisting of a large number of nucleated cells with dense concentrations of glycogen and irregularly shaped, electron-opaque

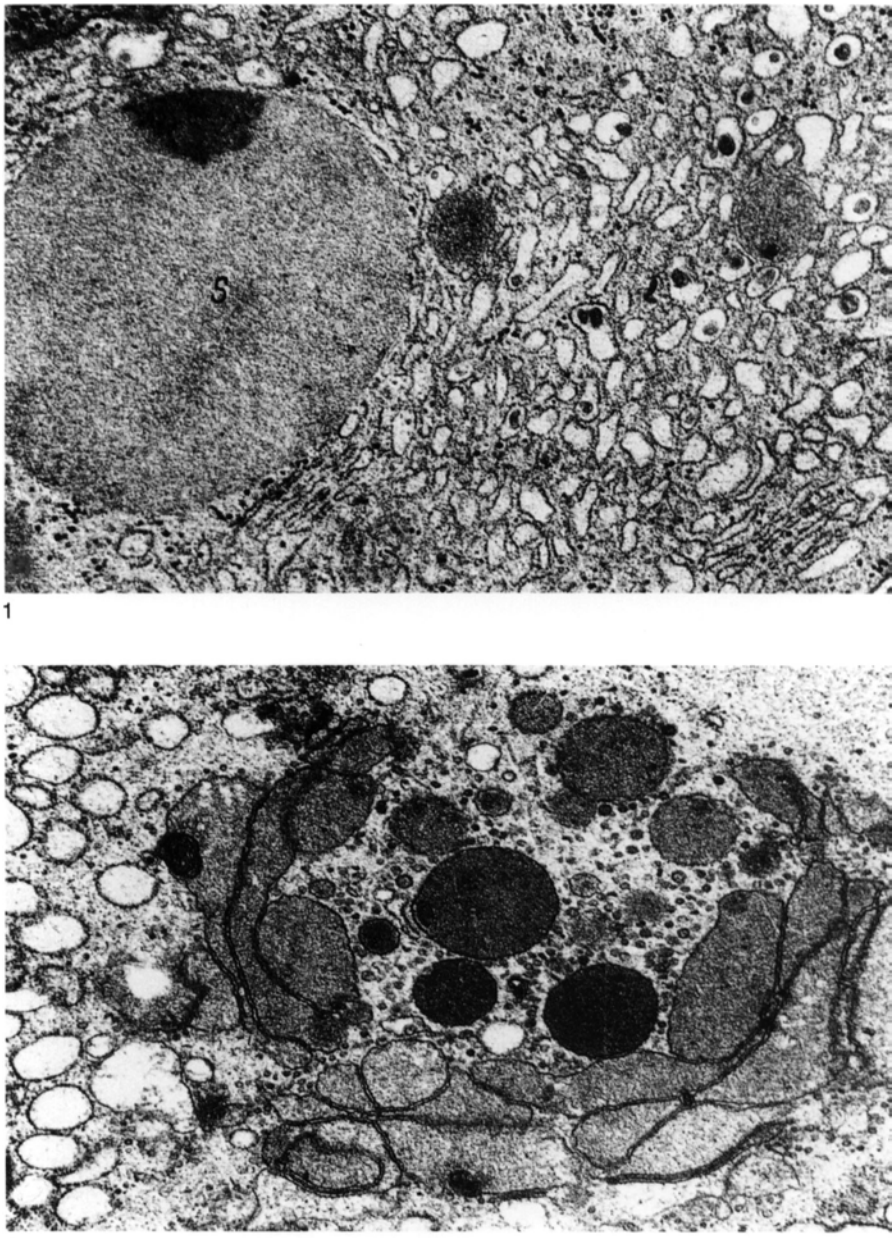

FIG. 95. TEM micrographs of cell type 1 in the digestive diverticula of *Lingula anatina; 1,* granular endoplasmic reticulum and secretory granules (*S*), ×20,000; *2,* Golgi apparatus and granules, ×20,000 (Storch & Welsch, 1975).

granules. The latter may be responsible for the pigmentation visible in the metanephridia of many species. The nature and function of the pigmentation is unknown, but it could be an accumulation of metabolic waste products (JAMES, unpublished, 1991). This stratified epithelium overlies a differentially thickened layer of connective tissue that

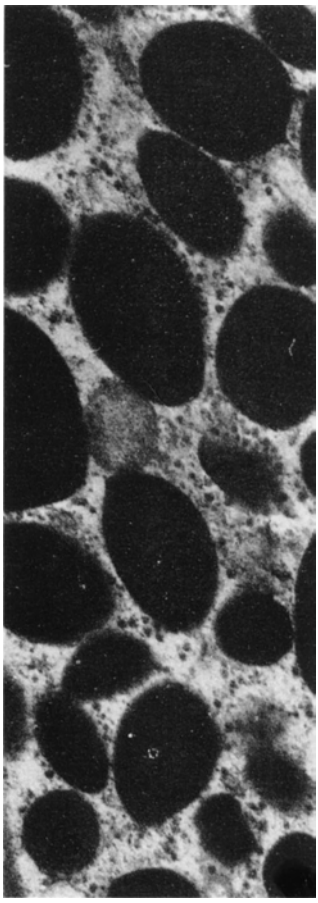

FIG. 96. TEM micrograph of the contents of a type 3 secretory cell in the digestive diverticula of *Lingula anatina,* ×20,000 (Storch & Welsch, 1975).

creates the ruffled surface of the nephrostome. Coelomic epithelium covers the outer surface (Fig. 99).

THE LOPHOPHORE

The lophophore has been described as a tentaculated extension of the mesosoma (and its cavity, the mesocoelom) that embraces the mouth but not the anus (HYMAN, 1959b; EMIG, 1976). The lophophore is ciliated and generates an inhalant and exhalant flow of water through the mantle (brachial) cavity, trapping particulate food material, allowing ventilation, and assisting in the removal of waste products.

GENERAL STRUCTURE

The lophophore is composed of two brachia (arms), disposed symmetrically about the mouth, attached to the anterior body wall, and extending into the mantle cavity. Brachia are fringed with one row of ciliated tentacles (filaments or cirri) in either a single or an alternating series. The brachial lip or fold runs perpendicular to the row of tentacles. The brachial (food) groove, created between the brachial lip and the base of the tentacles, is ciliated and runs along the entire length of the brachia, terminating at the slitlike mouth. Tentacles that are reflected toward the brachial groove are designated inner (adlabial), and those tentacles reflected away from the brachial groove are termed outer (ablabial) (Fig. 101–102; 103.2). Brachia are tubular with extensions of the coelom penetrating the main axes of the lophophore and giving off a branch into each tentacle. In inarticulated brachiopods, the form and position of the lophophore are maintained by a combination of muscles, connective tissue, and hydrostatic pressure created by muscle fibers in the brachial axis acting antagonistically against the incompressible fluid enclosed within the great brachial canal. In most articulated groups the support of the hydrostatic skeleton is commonly supplemented by the brachidium, a calcareous outgrowth of the secondary shell layer of the posterior part the dorsal valve. Calcareous spicules may also be secreted by scleroblasts within the connective tissue, thereby increasing the flexural stiffness of the brachia (FOUKE, 1986). The brachia may be partially fused to the dorsal mantle throughout and rest in brachial grooves in the inner surface of the dorsal valve, bounded on one or both sides by narrow ridges, as in the thecideidines (Fig. 104; LACAZE-DUTHIERS, 1861).

Coelomic Canals

Two, fluid-filled, coelomic canal systems, the great and small brachial canals, extend within the main axes of the brachia. The great brachial canal is closed off from the

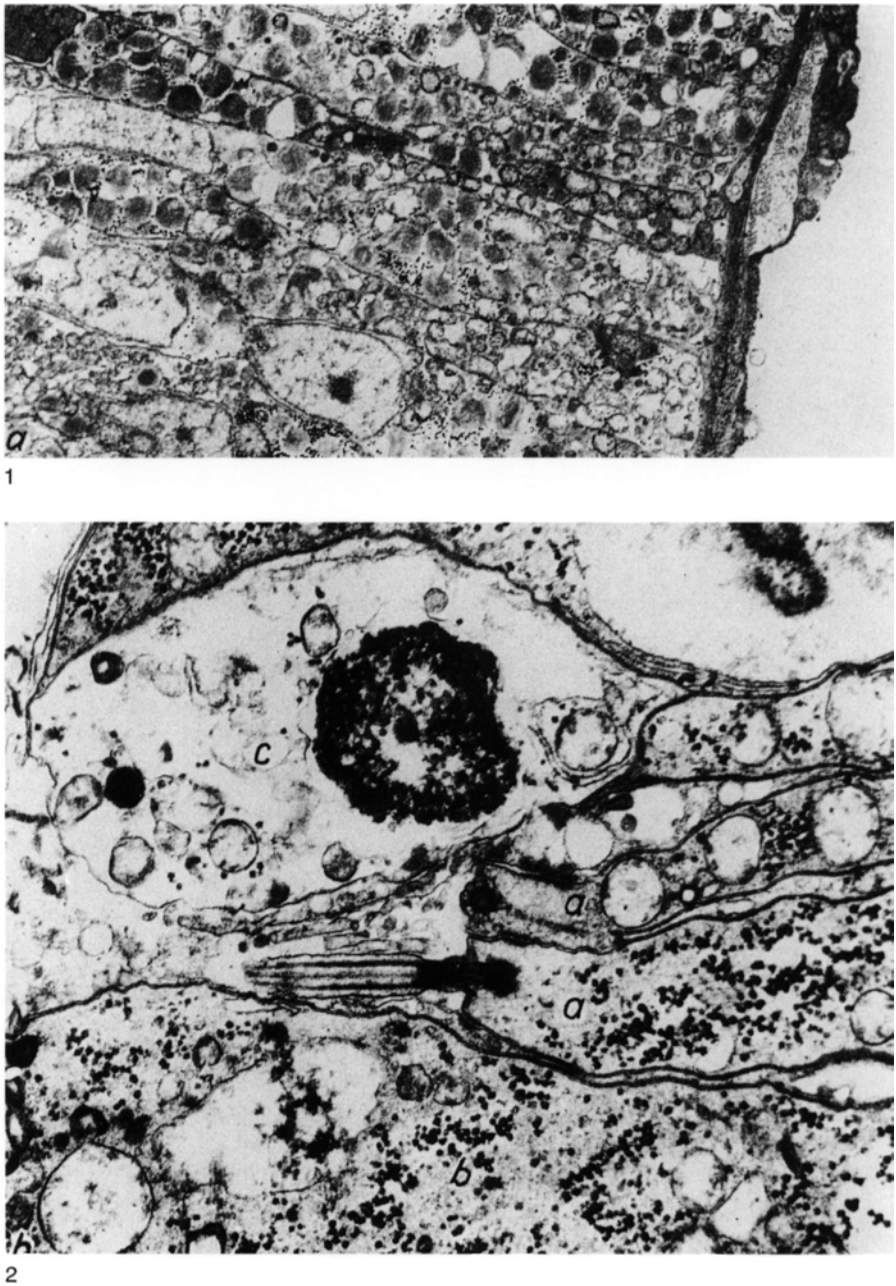

FIG. 97. TEM micrographs of type 2 cells in the digestive diverticula of *Lingula anatina; 1,* base of cells, ×5,500; *2,* apices of cells, ×20,000; *a,* ciliated cell; *b,* cell apex with glycogen and lysosomes; *c,* greatly enlarged cell apex (Storch & Welsch, 1975).

main body cavity, at least during the life of the adult, and in inarticulated brachiopods is divided into two separate cavities symmetrically disposed about the midline. The small brachial canal gives off a branch into each tentacle (tentacular canal) that, except for

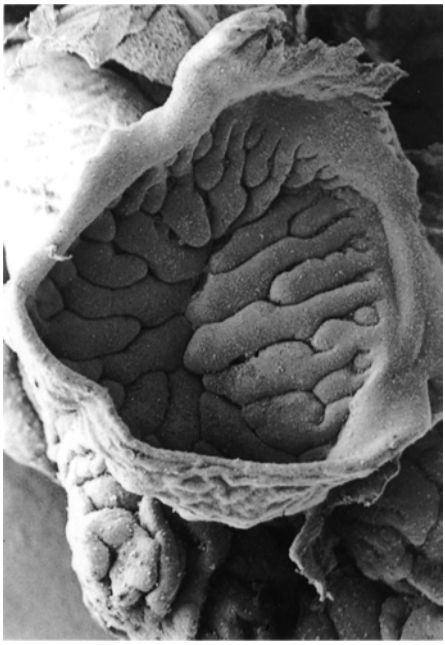

FIG. 98. SEM micrograph of the ruffled and densely ciliated nephrostome of *Lingula anatina,* ×30 (new).

craniids and discinids, opens into the body cavity around the esophagus. In *Lingula* and, to a lesser extent, *Discinisca* the proximal ends of the great brachial canals are divided into several lobes (BLOCHMANN, 1900). Near the esophagus, infolding of the main body cavity creates narrow pouches and, where the lophophore is attached to the main anterior body wall, all small brachial canals contract abruptly. The coelomic canals then continue medially as narrow tubes, which, in *Neocrania* and *Discinisca,* open into a large, median, central canal developed in the connective tissue of the lophophore on the ventral side of the pharynx (Fig. 105). In *Lingula,* the central canal is poorly developed although the two, small, brachial canals are connected medially. In all inarticulated genera, connective tissue surrounding the pharynx contains a number of small, interconnected chambers (the periesophagal spaces) that connect with small brachial canals (BLOCHMANN, 1892, 1900). In *Discinisca* and *Lingula* a further extension of the small brachial canal system is found in the coelomic spaces of the brachial lip (WILLIAMS & ROWELL, 1965a). The small, brachial canals of such articulated terebratellids as *Pumilus* are small, pouchlike extensions of the main body cavity and, although they have been called periesophagal sinuses (ATKINS, 1958), these canals are not infolded in the same way as in the inarticulated brachiopods. The body cavity is also prolonged as a pair of brachial pouches along the medially facing surfaces of the terebratulide side arms (Fig. 101). These pouches extend forward to more or less the same degree and are developed only incipiently in septate *Pumilus* but extend to the tip of the side arms in the long-looped *Macandrevia* (WILLIAMS & ROWELL, 1965a).

Musculature

Inarticulated brachiopods possess a pair of strongly developed brachial muscles that are attached to the connective tissue at the constricted proximal end of the small brachial canal and extend along the length of the canal in each brachium (Fig. 102). The discinids and the craniids also possess a pair of small brachial retractor muscles that appear to control the position of the lophophore relative to the dorsal valve and the anterior body wall. The retractor muscles are inserted in the dorsal valve lateral to the attachment of the anterior adductors. A further two pairs of muscles occur only in the craniids. A pair of stout, brachial elevator muscles, inserted on the dorsal valve anterolateral to the anterior adductors, are attached at their other extremity to the connective tissue at the base of the brachial muscle. A pair of small brachial protractor muscles placed anteromedially are also present (see Fig. 84). Calcified loops supplemented by calcareous spicules support the lophophore of terebratulide brachiopods. As a result, the muscles controlling the movement of the lophophore of articulated groups are less well developed than in inarticulated forms. Muscles are more numerous, however, in the spirally coiled, free brachia of the spirolophe of the rhynchonellides.

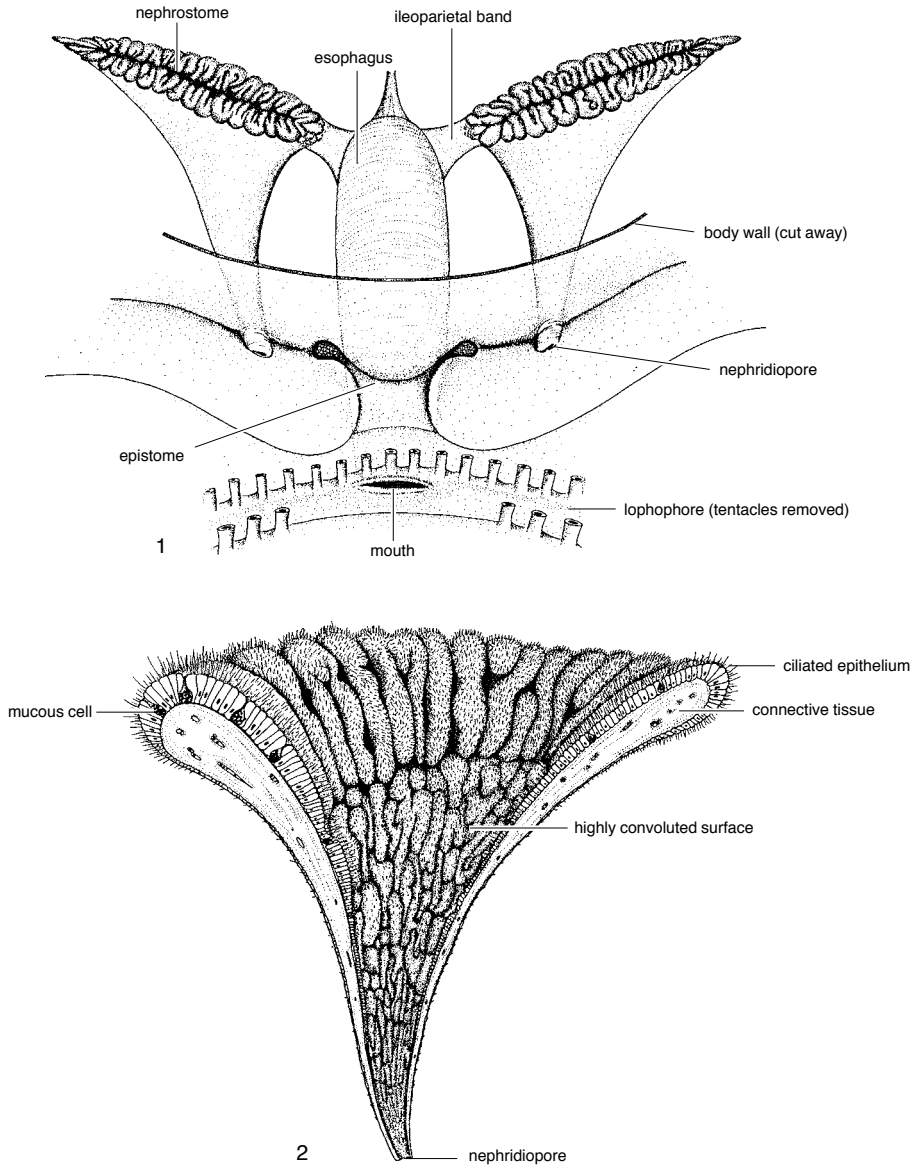

FIG. 99. Generalized diagrams of *1,* the attitude of the metanephridia of *Terebratulina retusa* relative to the anterior body wall, mouth, and esophagus; *2,* the structure of half a metanephridium in longitudinal cross section (new).

Tentacles

Rows of cilia on the tentacles are responsible for creating a flow of water past the tentacle and for diverting particulate material along the length of the tentacle to the brachial groove (see section on functional morphology of the lophophore, p. 116). There are two distinct types of tentacle in most adult lophophores. The first-formed tentacles of the trochophore stage occur on either side of the mouth. The number of these tentacles, which, except in lingulids and discinids, are arranged in a single row, varies between genera relative to the size of the fully

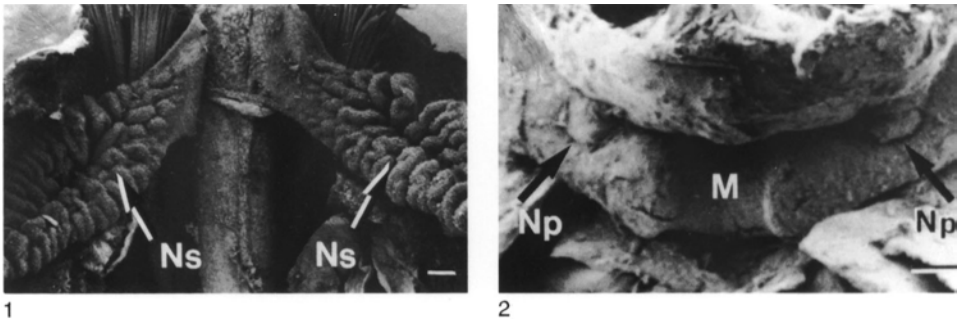

FIG. 100. SEM micrograph of *Terebratulina retusa,* showing *1,* the metanephridia with ciliated nephrostomes (*Ns*), ×35.5; *2,* view from within the mantle cavity of the mouth and the nephridiopores (*Np*) laterally displaced on either side of the mouth (*M*), ×14.2 (James, Ansell, & Curry, 1991b).

developed trocholophe (Fig. 103; WILLIAMS & WRIGHT, 1961). A few adult articulated brachiopods, such as *Argyrotheca* and *Dyscolia,* possess only this type of tentacle. The frontal surface (facing the brachial lip) of these outer tentacles forms two, rounded, laterofrontal epidermal ridges and a medial longitudinal groove, the latter bearing cilia that beat along the length of the tentacle. Two longitudinal tracts of longer cilia flank the frontal cilia and beat across the length of the tentacle from the frontal to the abfrontal surface. Modification of the trocholophe into more complex forms of lophophore, however, results in the addition of an alternating set of inner tentacles. Typically, inner tentacles have paired lateroabfrontal epidermal ridges that also develop long lateral cilia (Fig. 106). The abfrontal surface of both types of tentacle appears to be sparsely cili-

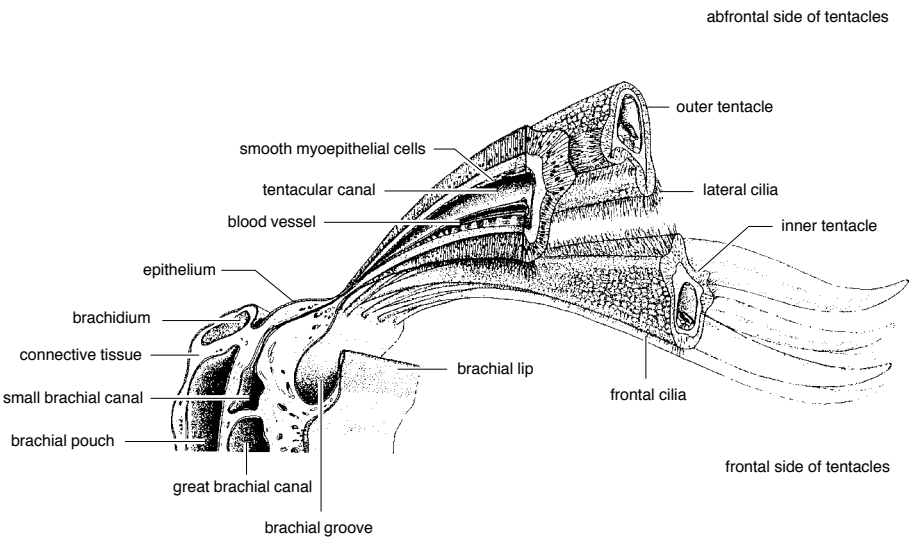

FIG. 101. Semidiagrammatic drawing of a cross section of part of the brachium and tentacles of an articulated brachiopod; the tentacles in the foreground are shown in transverse and longitudinal section (adapted from James & others, 1992).

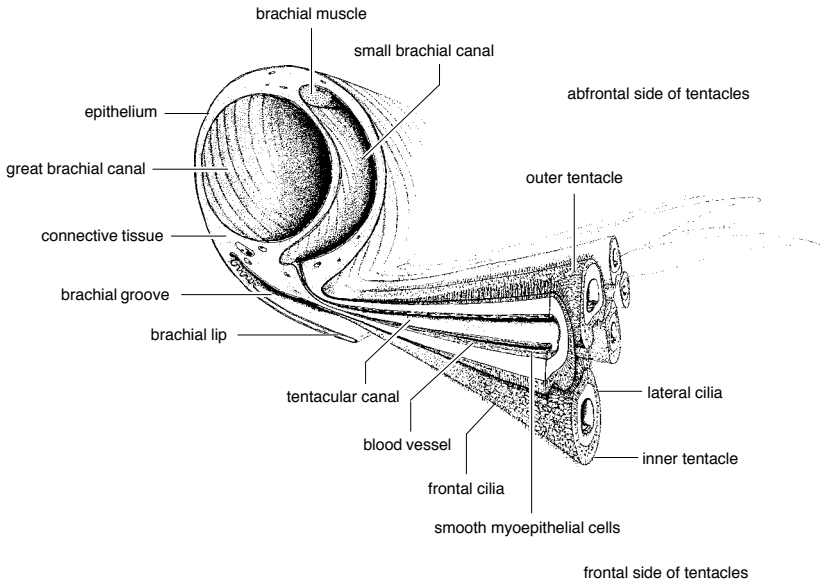

FIG. 102. Semidiagrammatic drawing of a cross section of the brachium and tentacles of the lophophore of *Lingula anatina;* the tentacles in the foreground are shown in transverse and longitudinal section (adapted from Pross, 1980).

ated in all brachiopods, with the exception of the lingulids, in which cilia are as densely distributed as on the frontal surface.

HISTOLOGY OF THE LOPHOPHORE

There are a number of accounts that feature the general histology of the brachiopod lophophore (HANCOCK, 1859; BLOCHMANN, 1892; RICHARDS, 1952; CHUANG, 1956; ATKINS, 1960a, 1960b, 1961a, 1961b, 1963). More recently, light microscopy and histochemistry have been used to study the lophophores of *Laqueus californicus, Terebratalia transversa, Hemithiris psittacea* (REYNOLDS & MCCAMMON, 1977), and *Notosaria nigricans* (HOVERD, 1985, 1986). Ultrastructural details of the tentacles of *Lingula anatina* (STORCH & WELSCH, 1976), *Glottidia pyramidata* (GILMOUR, 1981), and *Terebratalia* (REED & CLONEY, 1977) are also available. Histologically the lophophore consists of three main elements: an epidermal cover of a selectively ciliated epithelium with basiepithelial nerves, a variably complex connective tissue tube, and an inner coelomic epithelium underlain by either muscle fibers, or in the tentacles, myoepithelial cells. These tissues are modified to accommodate the different functional requirements of the main axes of the brachia and the tentacles.

EPIDERMIS

Descriptions of the epidermis of the brachia and tentacles of *Hemithiris, Laqueus, Terebratalia* (REYNOLDS & MCCAMMON, 1977), and *Lingula* (STORCH & WELSCH, 1976) generally agree with the most thorough description given by REED and CLONEY (1977) for *Terebratalia.* Only the tentacular epidermis, however, has been investigated in detail (STORCH & WELSCH, 1976; REED & CLONEY, 1977). The epidermis of the outer tentacles consists of an inner epithelium of columnar cells on the frontal side and cuboidal cells on the abfrontal side of the tentacle (Fig. 107). Inner tentacles are covered by a single layer of columnar epithelium. Ultrastructurally, four types of tentacular epidermal cell have been identified: microvillous

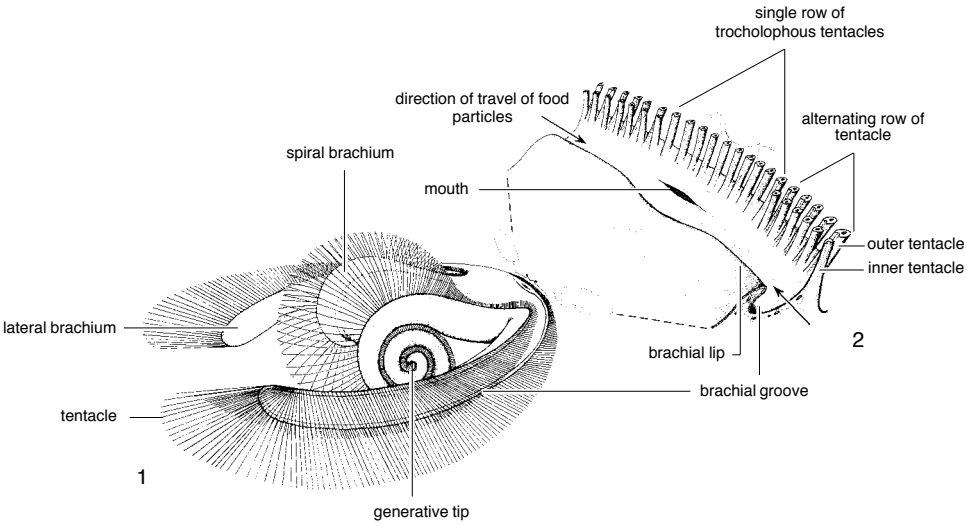

FIG. 103. Plectolophe of *Terebratulina retusa; 1,* general view and *2,* with an enlargement of the trocholophous tentacles behind the mouth (new).

epithelial cells, monociliated epithelial cells with distal microvilli, secretory cells, and intra-epithelial cells.

Microvillous Epithelial Cells

The distal margin of each microvillous epithelial cell has a dense, microvillous border, which is consistent with the view that the lophophore is the primary site for gaseous exchange in brachiopods (HYMAN, 1959b) and may be capable of direct absorption of nutrients (MCCAMMON & REYNOLDS, 1976; REYNOLDS & MCCAMMON, 1977) and calcium (PAN & WATABE, 1988a). The microvillous cells of *Terebratalia* contain putative secondary lysosomes (REED & CLONEY, 1977), and the epithelium at the base of the tentacles and in the brachial groove appears to be secretory and possibly involved in lysosomal activity (REYNOLDS & MCCAMMON, 1977), which may be suggestive of hetero- or autophagy (REED & CLONEY, 1977). HOVERD (1985) found unusally long microvilli in *Notosaria* and alluded to their possible chemosensory role.

Monociliated Cells

All ciliated tentacular epidermal cells are monociliated, and each cilium has an accessory centriole located on the downstream side of the ciliary root (ATKINS, 1958; STORCH & WELSCH, 1976; REED & CLONEY, 1977; NIELSEN, 1987). Reports of multiciliated cells in both *Laqueus* and *Glottidia* (GILMOUR, 1978, 1981) are considered to be erroneous (NIELSEN, 1987). The epithelium of *Terebratalia* is a simple, columnar structure (REED & CLONEY, 1977). Yet the frontal

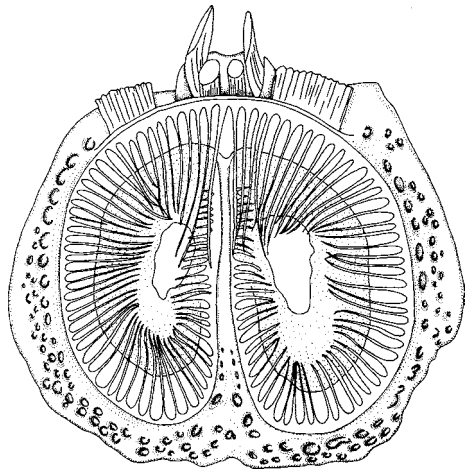

FIG. 104. Bilobed trocholophe of *Thecidellina* (adapted from Williams & Rowell, 1965a).

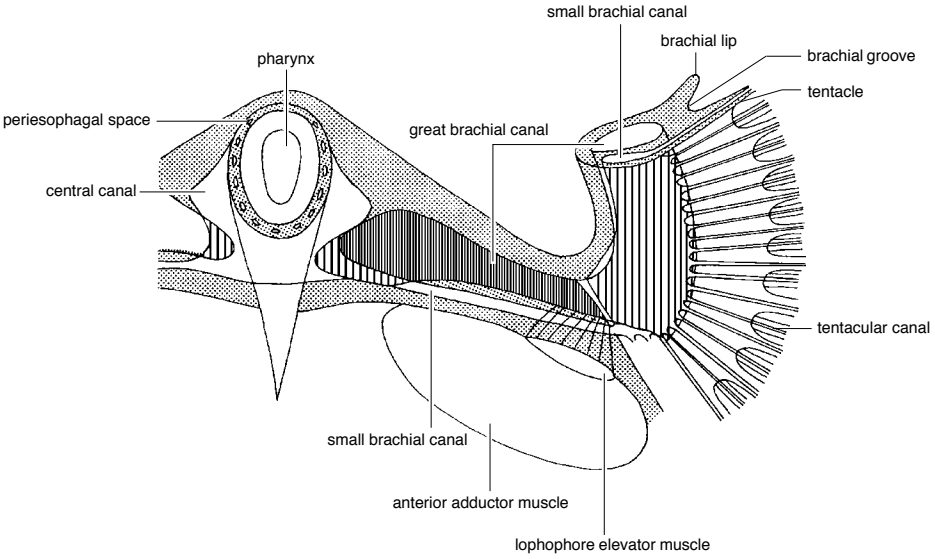

FIG. 105. Diagrammatic representation of canal systems in the lophophore of *Neocrania anomala* (adapted from Blochmann, 1892).

epidermis of the tentacles of *Laqueus* has been described as a stratified, columnar epithelium (REYNOLDS & MCCAMMON, 1977), while compound cilia have been described as forming part of a stratified, tentacular epithelium of *Lingula* (STORCH & WELSCH, 1976). Stratified epithelia are rare, however, in invertebrates (REED & CLONEY, 1977) and such observations may therefore be a misinterpretation of tangential sections. The knobbed, paddle, or disco cilia observed in *Notosaria* (HOVERD, 1985, 1986) are also considered to be artifacts (see SHORT & TAMM, 1991).

Secretory Cells

Mucous-secreting cells are commonly scattered throughout the epidermis and may be more numerous at the base of the tentacles (REED & CLONEY, 1977; REYNOLDS & MCCAMMON, 1977) particularly within the brachial groove. Some mucous cells are arranged in longitudinal rows along the tentacles of *Lingula* (Fig. 108; CHUANG, 1956). Ultrastructurally, two forms of secretory cell have been observed in *Lingula,* which contain large, electron-dense granules and may be ciliated during the early part of their development (STORCH & WELSCH, 1976). One of these cell types probably corresponds to the mucous cells seen in studies using lower resolution microscopy.

Intraepidermal Cells

Clusters of round cells occur at the base of the tentacles in the *Terebratalia* (REED & CLONEY, 1977). Believed to be amoebocytes or coelomocytes, these cells may correspond to either similar cells found in the tentacular epidermis of *Lingula* (CHUANG, 1956; STORCH & WELSCH, 1976) or dark-staining aggregates that occur in the epithelium and connective tissue of some articulated brachiopods (REYNOLDS & MCCAMMON, 1977; HOVERD, 1985).

NERVES

Two main nerves innervate the lophophore: the principal nerve branches from the subenteric ganglion and extends along each brachium near the brachial lip; a second nerve forms branches (accessory and lower brachial nerves) that serve the brachia and tentacles (BEMMELEN, 1883; WILLIAMS &

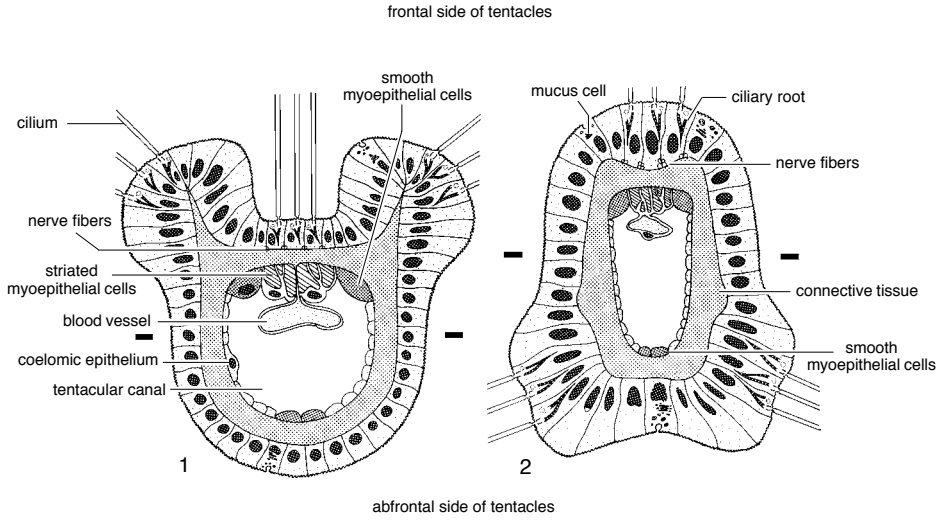

FIG. 106. Schematic diagrams of sections of tentacles of a brachiopod lophophore; *1,* section of an ablabial (outer) tentacle; the epidermis is ciliated in longitudinal tracts on the frontal surface and on the laterofrontal surface and on the laterofrontal epidermal ridges; nerves extend longitudinally between the bases of the frontal epidermal cells; a thick layer of acellular connective tissue separates the epidermis from the peritoneum, consisting of myoepithelial cells on the frontal and abfrontal sides of the tentacular coelomic canal; the frontal contractile bundle has both smooth (*stippled*) and striated (*slashed*) fibers, but the small abfrontal contractile bundle has only smooth fibers; a blood channel is formed by an involution of the frontal peritoneum; *2,* transverse section of an adlabial (inner) tentacle. The ciliary tracts arise from the frontal epidermis and the paired lateroabfrontal epidermal ridges; the rest of the histological organization is similar to that of the ablabial tentacle (adapted from Reed & Cloney, 1977).

ROWELL, 1965a). Bundles of nerve fibers lie between the bases of the epithelial cells (basiepithelial nerves) above the basal lamina (see Fig. 130; BLOCHMANN, 1892, 1900; STORCH & WELSCH, 1976; REED & CLONEY, 1977; HOVERD, 1985). Detailed studies of the tentacles of *Terebratalia* did not reveal any nerve fibers traversing the connective tissue to form myoneural junctions or evidence of peritoneal nerves (REED & CLONEY, 1977). Laterofrontal cells of the tentacles of *Glottidia* make synapses with the nervous system, suggesting that cilia may have a sensory role (GILMOUR, 1981) or that these nerves innervate the laterofrontal cells (see HAY-SCHMIDT, 1992).

CONNECTIVE TISSUE

The connective tissue of the lophophore has been variously described as a noncellular matrix resembling hyaline cartilage (HANCOCK, 1859; HYMAN, 1959b; STORCH & WELSCH, 1976; REYNOLDS & MCCAMMON, 1977; HOVERD, 1985) and as a structureless supporting substance (ATKINS, 1961a, 1961b, 1963). According to HOVERD (1985) the hyaline matrix contains cells and bears no resemblance to vertebrate cartilage. CHUANG (1956) and REYNOLDS and MCCAMMON (1977) stated that the cartilaginous framework continues into the base of the tentacles. REED and CLONEY (1977), however, are the only authors to distinguish between the connective tissue of the tentacles and the main axes of the lophophore. The brachial axes of *Terebratalia* are constructed from a cartilaginous framework, which is a metachromatic matrix; the tentacles are an acellular, densely fibrous connective material.

The connective tissue in the tentacles contains two types of collagen fibers: a thick, longitudinal subepidermal layer and an inner, circumferential layer, subadjacent to the coelomic epithelium. This orientation of fibers creates a relatively stiff, inextensible

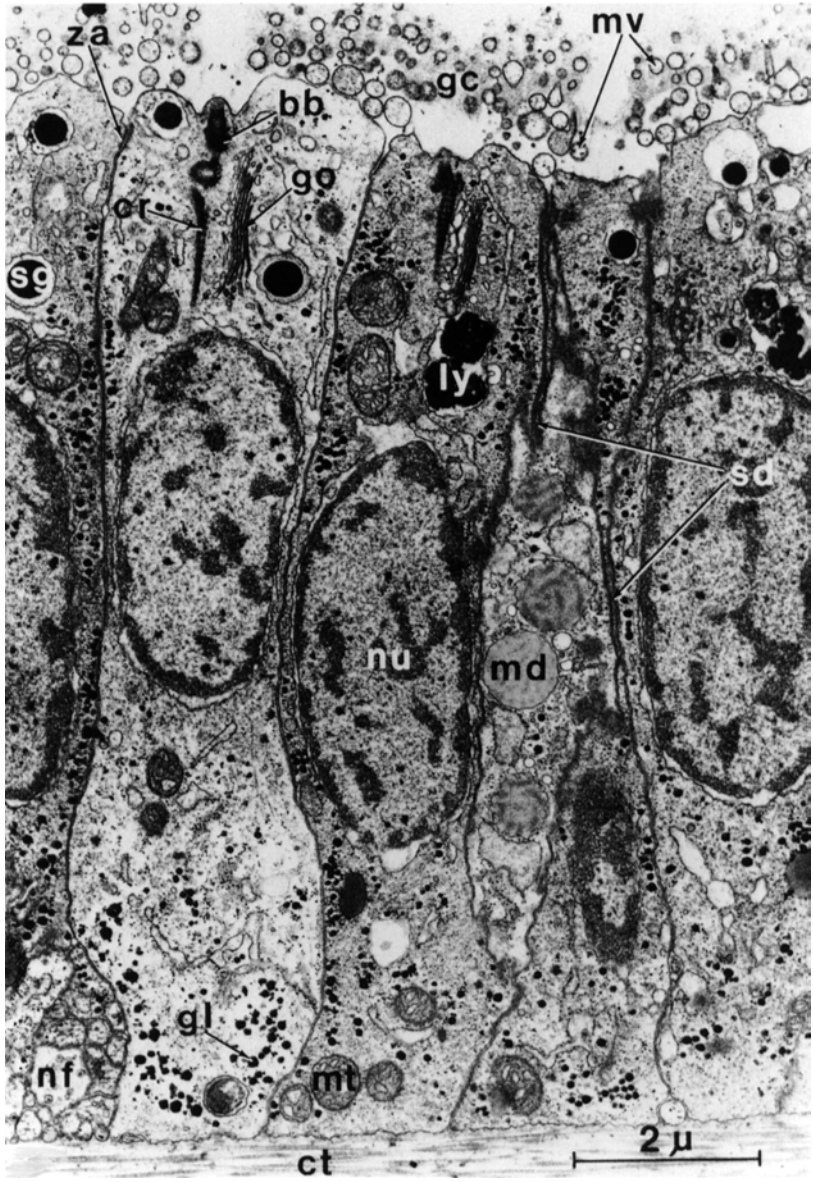

Fig. 107. TEM micrograph of a transverse thin section of the frontal epidermis near the base of an outer tentacle of *Terebratalia transversa;* columnar epidermal cells are joined apically by *zonulae adhaerens* and at the level of their nuclei by separate desmosomes; the apical plasmalemma of each cell bears a single cilium surrounded by sinuous microvilli perforating a faint glycocalyx; the apical cytoplasm in each cell is characterized by secretory granules, putative secondary lysosomes, and a supranuclear Golgi complex next to the basal body and the ciliary rootlet of the cilium; glycogen rosettes and occasional lipid droplets are also found dispersed throughout the cytoplasm; the section passes through part of a mucous cell containing large mucous droplets. A bundle of unsheathed nerve fibers is positioned between the bases of two epidermal cells in the lower left corner, scale bar: 2 µm; *bb,* basal body; *ct,* connective tissue; *cr,* ciliary root; *gc,* glycocalyx; *gl,* glycogen particles or rosettes; *go,* Golgi complex; *ly,* putative secondary lysosome; *md,* mucous droplet; *mt,* mitochondrion, *mv,* microvilli; *nf,* nerve fibers; *nu,* nucleus, *sd,* septate desmosome; *sg,* secretory granule; *za,* zonula adhaerens (Reed & Cloney, 1977).

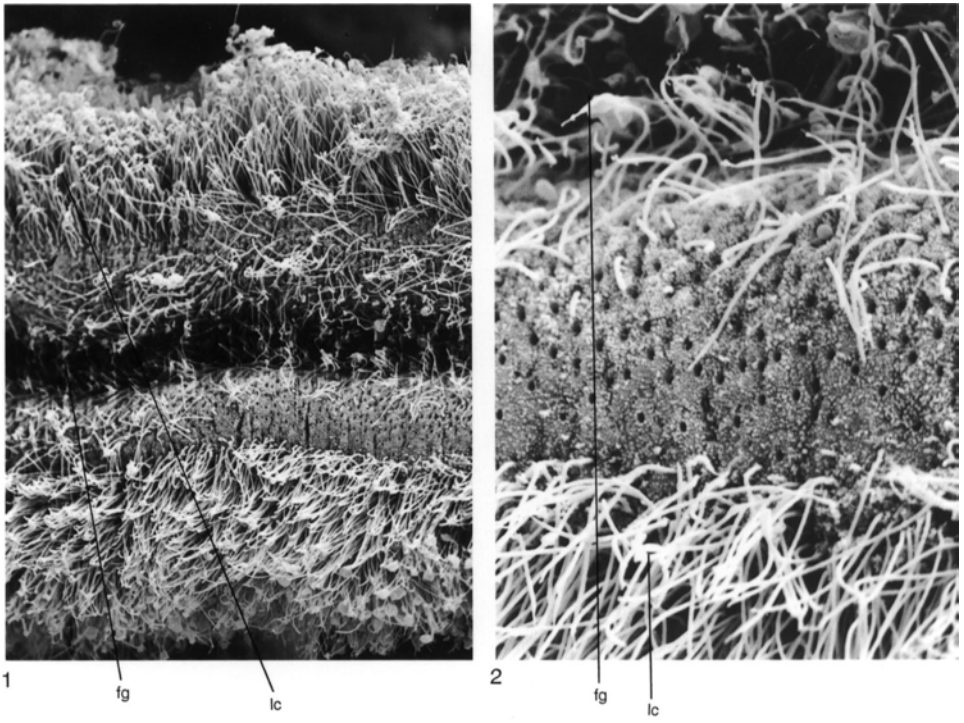

FIG. 108. SEM micrographs of the frontal surface of a tentacle of *Lingula anatina* showing *1,* dense lateral cilia (*lc*) separated from the ciliated food groove (*fg*) by a sparsely ciliated band, ×660; *2,* note microvillous surface and numerous pores of sparsely ciliated band (shown in *1*), ×2,500 (new).

tube with the longitudinal layer resisting elongation and the circumferential layer resisting changes in diameter (STORCH & WELSCH, 1976; REED & CLONEY, 1977). In regions where the connective tissue cylinder of the tentacle buckles during flexion, the longitudinal collagen fibers of *Terebratalia* contain baffles consisting of zonulae of parallel, crimped collagen fibers (Fig. 109; REED & CLONEY, 1977).The connective tissue may contain a variety of other inclusions in addition to the cells secreting the connective tissue matrix. The connective tissue matrix of *Lingula* contains single or paired, ovule-shaped, nucleated cells (STORCH & WELSCH, 1976). *Notosaria* (HOVERD, 1986), *Hemithiris, Laqueus,* and *Terebratalia* (REYNOLDS & MCCAMMON, 1977) have lacunae or nests of membrane-bound cells containing globular inclusion bodies, which occur throughout the connective tissue matrix. Globular inclusions present in the connective tissue of a number of species, including *Lingula, Hemithiris,* and *Terebratulina,* closely resemble those found predominantly in the outer mantle epithelium of these species, where they appear to be storage material (CURRY & others, 1989; JAMES & others, 1992). REED and CLONEY (1977) did not, however, find cells in the connective tissue of the tentacles

FIG. 109. TEM micrographs of the connective tissue associated with the lophophore of *Terebratalia transversa; 1,* longitudinal section of the frontal side of the connective tissue cylinder in an inner tentacle, which consists of a subepidermal longitudinal layer and a subperitoneal circumferential layer of fibrils embedded in an amorphous matrix; a zone of crimped and displaced fibrils corresponds to the baffles, scale bar: 2 μm; *ba,* baffles; *cct,* circumferential layer of connective tissue; *ep,* epidermis; *lct,* longitudinal layer of connective tissue; *sm,* smooth myoepithelial cells; *2,* longitudinal section of the subepidermal connective tissue on the frontal side of the cylinder, with the region
(Continued on facing page.)

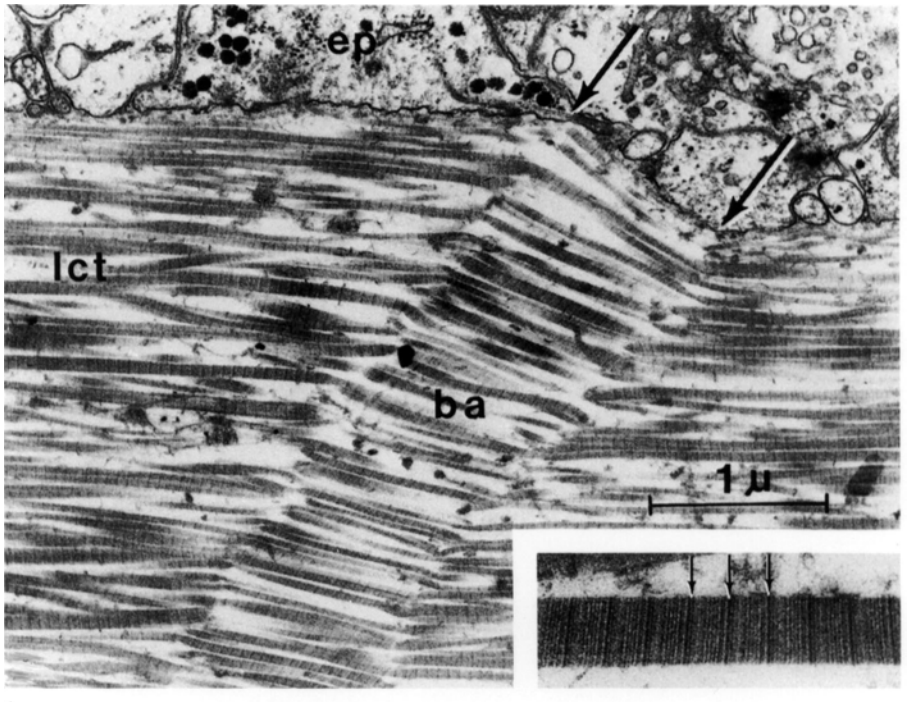

1

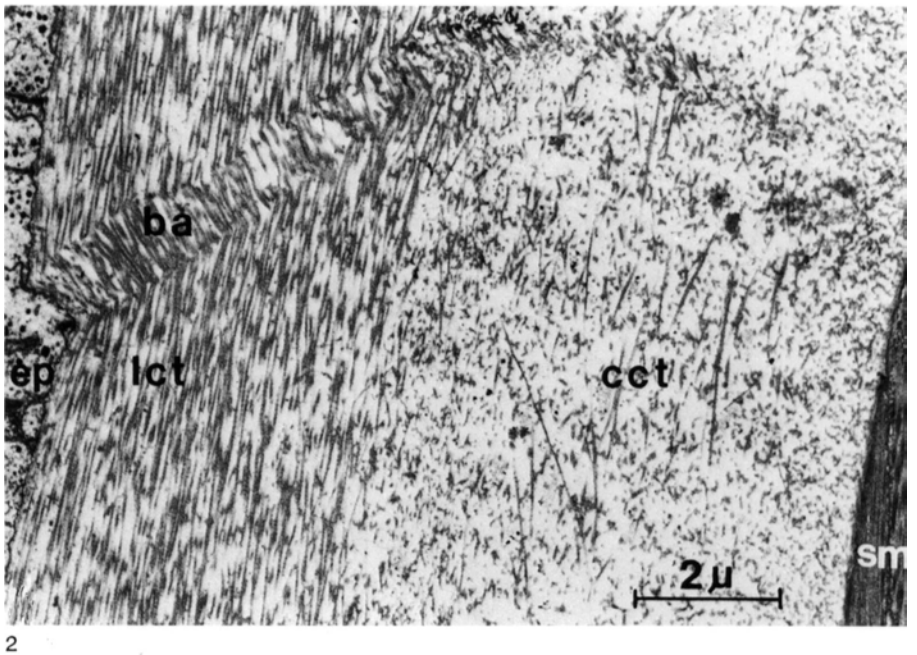

2

FIG. 109. *Continued from facing page.*
between the *arrows* corresponding to the part of one of the baffles where the parallel fibrils are crimped and oriented at a different angle from those in the rest of the cylinder; the fibers have a major axis periodicity of 63 nm (inset: distance between *arrows*) that is diagnostic of native vertebrate collagen fibrils, scale bar: 1 μm (Reed & Cloney, 1977).

of *Terebratalia.* The connective tissue of many terebratulide species contains a closely-knit array of interdigitating calcareous spicules that increases the flexural stiffness of the lophophore and, in *Terebratulina,* supply the rigidity necessary to support the lophophore in regions anterior to the short-looped brachidium (Fouke, 1986).

COELOMIC EPITHELIUM (PERITONEUM)

Brachial and tentacular canals are lined with ciliated coelomic epithelium (see, for example, Reynolds & McCammon, 1977; Hoverd, 1985, 1986), which, in the former site, is underlain by a layer of muscle and in the latter by myoepithelia. The subepidermal (peritoneal) muscle has been described as smooth in *Notosaria* (Hoverd, 1985) or as a single, prominent layer of longitudinal, striated muscle around the great brachial canal in *Hemithiris* (Reynolds & McCammon, 1977). The ultrastructure of the epithelial lining of the tentacular canal is known only for *Terebratalia.* The lining consists of four cell types: ciliated coelomic (peritoneal) cells, striated myoepithelial cells, smooth myoepithelial cells, and squamous smooth myoepithelial cells that form tentacular blood vessels (channels and capillaries) (see Fig. 76; Reed & Cloney, 1977). Both smooth and striated muscle fibers (myoepithelial cells) have been described in the tentacles of *Neocrania, Lingula,* and a number of articulated brachiopods (Chuang, 1956; Atkins, 1958, 1959, 1961a, 1961b; Williams & Rowell, 1965a). The fine structure of myoepithelial cells, however, is known only for *Terebratalia* (Reed & Cloney, 1977) and *Lingula* (Storch & Welsch, 1976). In *Terebratalia,* longitudinal rows of fusiform myoepithelial cells extend the length of each tentacle on the frontal and abfrontal sides of the coelomic canal. A bundle of myofilaments is confined to the basal cytoplasm of each cell (see section on muscular system, p. 75; Fig. 88). The frontal myoepithelial cells consist of a central group of striated fibers and two lateral groups of smooth fibers. The striated myoepithelial cells are continuous with the squamous myoepithelial cells of the blood vessel and are oriented parallel to the longitudinal axis of the tentacle. Smooth myoepithelial cells occur on the abfrontal surfaces. The smooth myoepithelial cells are oriented at an angle of about 12 degrees from the longitudinal axis of the tentacle. These fibers and the small group of abfrontal myoepithelial cells are contiguous with the ciliated, coelomic cells.

Based on the structure of the connective tissue cylinders of the tentacles and the physiological implications of the observed morphologies of the different myoepithelial cells in *Terebratalia,* Reed and Cloney (1977) postulated that striated myoepithelial cells are responsible for flicking motions and for initial flexion of the tentacle, while smooth, frontal, myoepithelial cells hold the tentacle down for extended periods against the resilience of the cylinder of connective tissue. Smooth, abfrontal, myoepithelial cells initiate the return of the tentacle to the extended position. In *Terebratalia* the tentacles of subtidal specimens possess striated myoepithelial cells, while intertidal specimens contain only smooth myoepithelia (Reed & Cloney, 1977). In *Lingula* only smooth, myoepithelial cells occur (Storch & Welsch, 1976).

A blind-ending blood vessel extends the length of each tentacular canal along the surface of the frontal coelomic epithelium. The vessel is composed of a single layer of squamous myoepithelial cells, with parallel myofilaments that are oriented circumferentially and a basal lamina that faces the lumen of the blood vessel (Fig. 110; see section on coelomic and circulatory system, p. 69; see also Fig. 74; Storch & Welsch, 1976; Reed & Cloney, 1977).

DEVELOPMENTAL PATTERNS OF THE LOPHOPHORE

The effective surface area of the adult lophophore is one of the main physiological

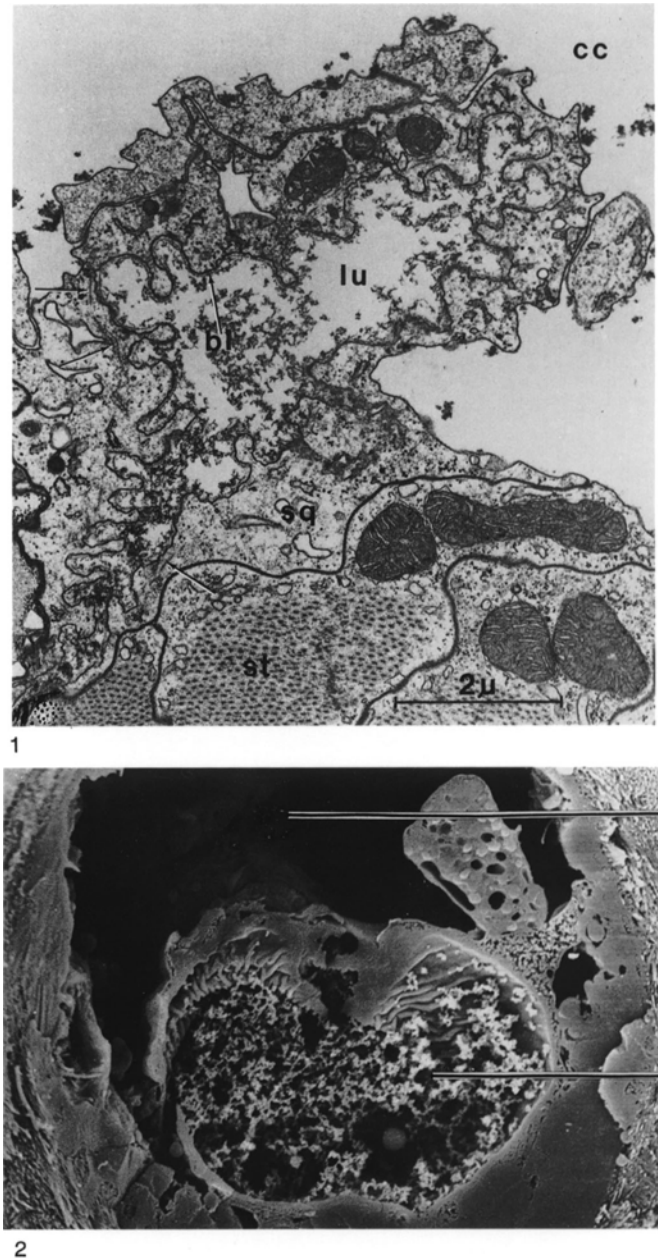

FIG. 110. Blood vessels in the tentacles of lophophores; *1,* TEM micrograph of transverse section of a tentacular blood (channel) vessel of *Terebratalia transversa;* squamous cells with myofilaments in their juxtaluminal cytoplasm (*arrows*) comprise the walls of the blood vessel with their basal (luminal) plasmalemmata thrown into folds, indicating that the cells have fixed in a contracted state; the blood vessel is laterally contiguous with the striated myoepithelial cells of the frontal contractile bundle; *cc*, tentacular coelomic canal, *lu,* lumen of blood vessel, *bl,* basal lamina, *sq,* squamous myoepithelial cell, *st,* striated myoepithelial cell, scale bar: 2.0 μm (Reed & Cloney, 1977); *2,* SEM micrograph of transverse section through the tentacular canal (*tc*) and blood vessel (*bv*) of *Lingula anatina* with the fibrogranular substance within a blood vessel, ×5,300 (new).

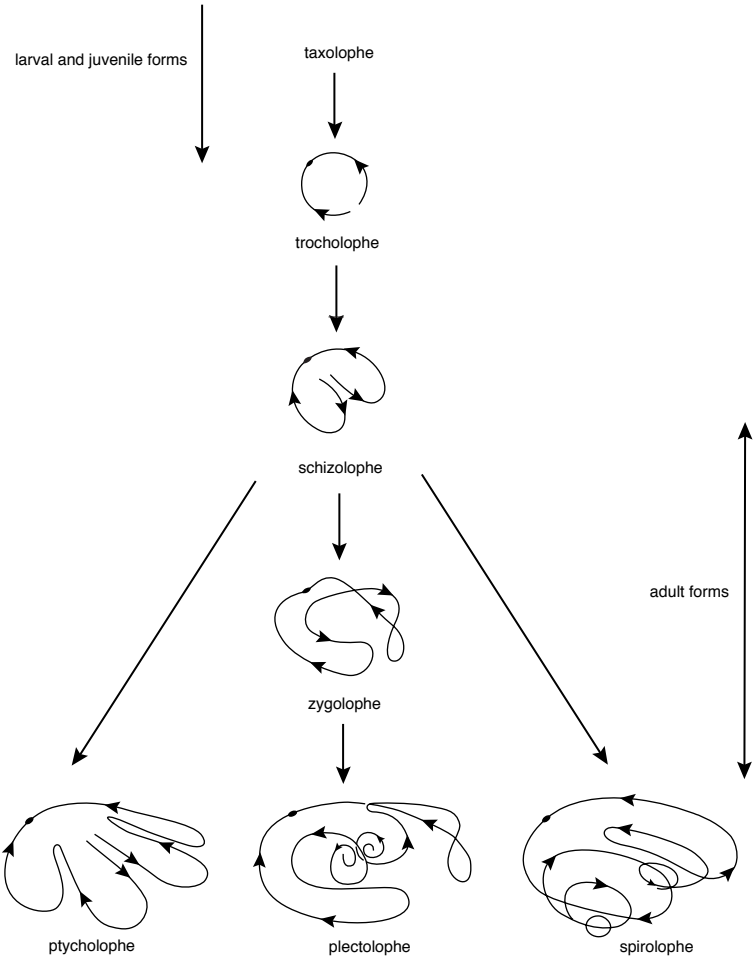

FIG. 111. Diagram showing three ontogenic pathways in the growth of the lophophore in living brachiopods; each drawing shows a perspective view of the course of the brachial axis (tentacles omitted), with *arrows* on the axis indicating the direction of transport of food particles toward the mouth (adapted from Rudwick, 1962a, 1970).

constraints governing the size of the brachiopod. As the brachiopod grows, the volume of body tissue increases. To supply the increase in metabolic requirements, the lophophore must undergo a commensurate increase in surface area. Given that the lophophore must also be arranged to create an efficient flow of water through the mantle cavity, evolution has provided several distinctive functional solutions to the problem of lophophore scaling, ranging from the simple crescent-shaped lophophore of larval or juvenile stages to the complex coils or spirals of some larger adults (Fig. 111; RUDWICK, 1962a; LABARBERA, 1986b; EMIG, 1992).

Trocholophe

The **trocholophe** is the simplest functional lophophore and is a stage shared by all larval and small, juvenile brachiopods. It also characterizes the adults of the genera *Gwynia* (CHUANG, 1990), *Dyscolia* (BEECHER, 1897), and *Goniobrochus* (EMIG, 1992). The lophophore first appears in the larval or early juvenile stages as a few pairs of ciliated tentacles arranged in a crescent around the preoral

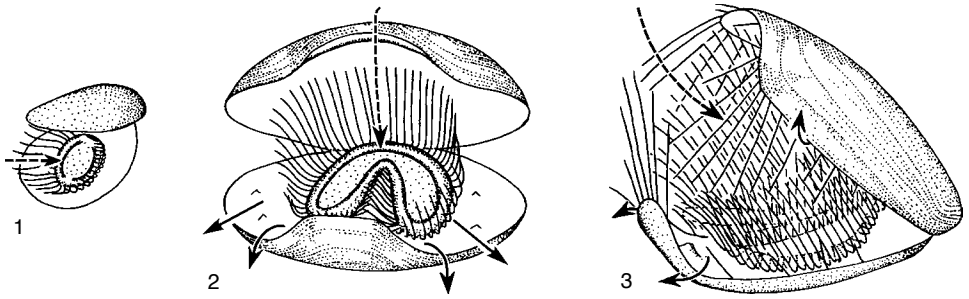

FIG. 112. Ontogeny of the lophophore and its current system in the small terebratulide *Pumilus antiquatus; 1,* the lophophore does not develop from the trocholophe, *2–3,* beyond the schizolophe condition; setae shown only in *3;* ventral valve above; *dashed arrows,* unfiltered (inhalant) water; *lined arrows,* filtered (exhalant) water (adapted from Rudwick, 1962a, 1970).

lobe and mouth on the anterior body wall or dorsal mantle surface. The crescent represents the first-formed brachia. Tentacles are added in pairs at the distal ends of the brachial axes on the dorsal or anterior side of the crescent. The frontal surface of all the tentacles faces inward. Although the number and length of the tentacles increase progressively, the spacing between tentacles remains constant (RUDWICK, 1970). The tentacles project forward, forming a bell-like aperture enclosed between two widely gaping valves. Water is drawn posteriorly through the mouth of the bell and is expelled laterally between the tentacles (Fig. 112.1; 113.1; 114.1).

Schizolophe

An involution of the brachial tips of the trocholophe forms the two lobes of the **schizolophe** and represents an increase in both structural complexity and surface area of the lophophore. Like the trocholophe, the schizolophe may be a transitional stage in the early growth of the lophophore, and for a few genera the schizolophe is the final form of the organ. Such genera include the discinid *Pelagodiscus,* such thecideidines as *Thecidellina,* and terebratulides including *Argyrotheca, Pumilus, Amphithyris, Thaumatosia,* and *Simplicithyris* (BEECHER, 1897; THOMSON, 1927; ATKINS, 1958; EMIG, 1992). As the lophophore increases in complexity, the brachia require additional support. In the schizolophe, the great brachial canal is sealed off from the coelom and becomes effective as a hydrostatic skeleton. In addition, calcareous outgrowths of varying complexity are developed to support the adult lophophore of articulated brachiopods.

Structurally the schizolophe differs little from the trocholophe except that the tentacles, which form the median indentation of the bilobed lophophore, create a tunnel that receives water pumped by these tentacles and directs it anteriorly (Fig. 112.3; 113.2; 114.2).

Ptycholophe

The bilobed schizolophe is enlarged by the addition of lateral indentations of the brachial axes creating the multilobed **ptycholophe.** In *Lacazella* and *Megathiris* the ptycholophe is four lobed (Fig. 115; RUDWICK, 1970). In *Pajaudina,* however, secondary indentations of the four-lobed ptycholophe produce up to eight lobes (LOGAN, 1988). Typically, the lophophore is supported by one median and two lateral septa. Each of the two anterolateral indentations acts as additional exhalant tunnels to the median tunnel; the current system is otherwise similar to the schizolophe of articulated brachiopods (ATKINS, 1960b).

Spirolophe

Both the schizolophe and the ptycholophe remain completely fused to the body wall

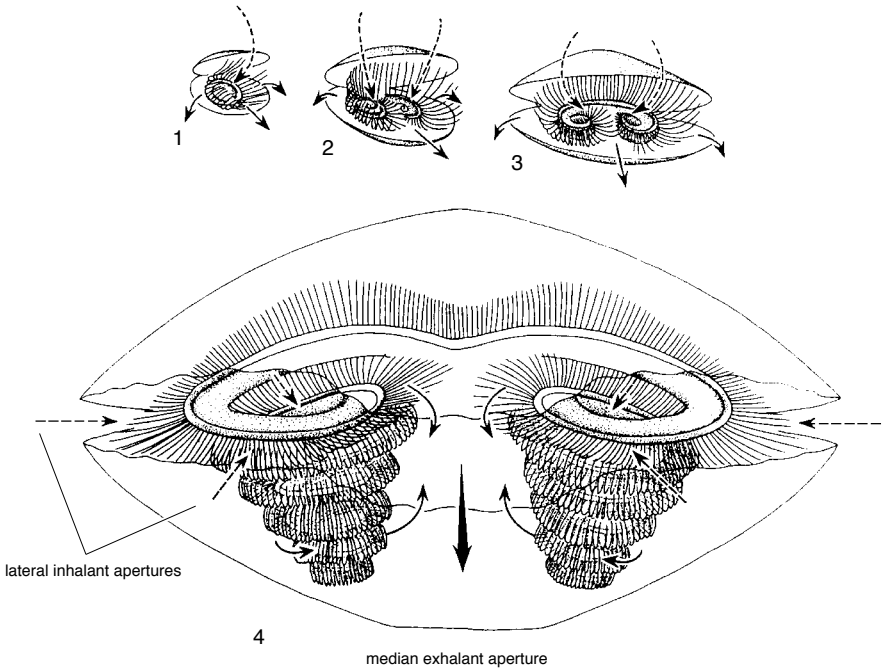

FIG. 113. Ontogeny of the lophophore and its current system in the rhynchonellide *Notosaria nigricans; 1,* trocholophe; *2,* schizolophe; *3–4,* spirolophes; valves in adult (*4*) are drawn as though transparent to show the full size of the spiral brachia; setae omitted; ventral valve above; *dashed arrows,* unfiltered (inhalant) water; *lined arrows,* filtered (exhalant) water (adapted from Rudwick, 1962a).

and the dorsal mantle so that any increase in the overall length of the lophophore lies in the same plane. In the **spirolophe,** the tips of the brachia diverge from each other and the mantle surface to form two, freely coiled spirals. The apices of the spirals converge toward one another and are generally oriented dorsally but point medially in the lingulids and ventrally in the discinids *Discina* and *Discinisca* (see EMIG, 1992). The spirolophe is characteristic of all inarticulated brachiopods (except the schizolophous *Pelagodiscus*) and rhynchonellides. *Leptothyrella* (possibly juvenile) is the only spirolophous terebratulide (MUIR-WOOD, 1965; MUIR-WOOD, ELLIOTT, & HATAI, 1965). The coiled brachia are supported principally by the hydrostatic skeleton of the brachial axes and, in the rhynchonellide spirolophe, by crura (Fig. 113).

In the spirolophe the tentacles of the proximal (first) whorl touch the mantle surface. The tips of the median tentacles touch each other, dividing the mantle cavity into two separate inhalant chambers and a single exhalant chamber. At the margin of the shell, the lateral inhalant apertures form the median exhalant. The tentacles of successive whorls are reflected upward toward the preceeding whorl, thus forming a cone that creates the main, exhalant current. Two posterolateral apertures exist in craniids and in the juvenile stages of rhynchonellides (ATKINS & RUDWICK, 1962; RUDWICK, 1962a; CHUANG, 1974) but not in discinids. *Crania californica* and *C. pourtelesi* have a median, incurrent flow (LABARBERA in EMIG, 1992). The discinid spirolophe is functionally similar to the schizolophe of *Pelagodiscus.* Discinids possess a large, median, inhalant compartment, which, at the shell margin, is delimited by long, anterior setae as an inhalant siphon, and two posterolateral exhalant gapes (PAINE, 1962a; LABARBERA, 1985). The

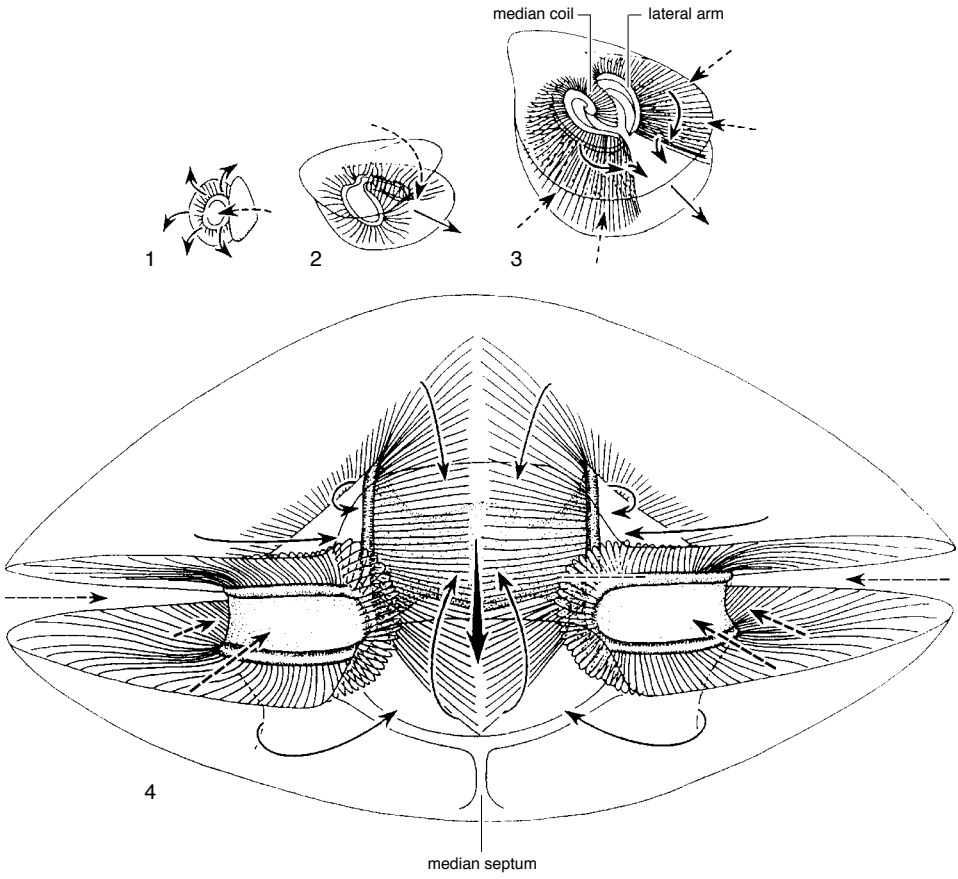

FIG. 114. Ontogeny of the plectolophe in the terebratulide *Calloria inconspicua; 1,* trocholophe; *2,* schizolophe; *3,* zygolophe; *4,* plectolophe; all except *1,* drawn as though the valves were transparent with ventral valve above; *dashed arrows,* unfiltered (inhalant) water; *lined arrows,* filtered (exhalant) water (adapted from Rudwick, 1962a).

reconstruction of *Discinisca* by ROWELL (1961) can therefore no longer be accepted (EMIG, 1992). In the sulcate rhynchonellides the exhalant aperture is shifted ventrally or dorsally, thus separating it from the lateral plane of the inhalant apertures (EMIG, 1992). Apertures are, however, never separated by fused or erected portions of the mantle edges except in the lingulids, where pseudosiphons are formed by the edges of the mantle and the arrangement of setae (EMIG, 1982).

Zygolophe and Plectolophe

Initially the lobes of the schizolophe twist laterally, away from the dorsal mantle surface and project freely into the mantle cavity. Fusion of the two great brachial canals forms a supporting tube that allows the brachial axes to remain united across the floor of each lobe. The brachia are connected by a membrane forming a brachial gutter between the dorsal and ventral rows of tentacles. Although a precursor of the plectolophe, this transitional stage is recognized as the **zygolophe.** The tips of the zygolophe brachia develop anteriorly between the lateral lobes and rotate forward together to form a plane-spiral, median coil. A diaphragm of connective tissue connects the parallel coils across the median plane. The **plectolophe** derives support from modifications of the zygolophe brachidium. The plectolophe is

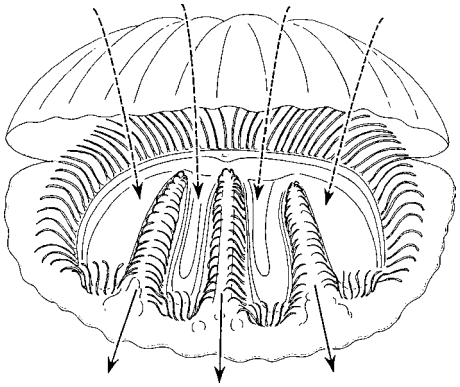

FIG. 115. Ptycholophe of *Megathiris detruncata; dashed arrows,* unfiltered (inhalant) water; *lined arrows,* filtered (exhalant) water (adapted from Atkins, 1960b).

characteristic of most adult terebratulides. The posterolateral inhalant apertures are defined by the tentacles of the lateral arms, which touch the mantle edges and, posteriorly, the mantle surface or body wall except anteriorly, where the tentacles separate these apertures from the median exhalant aperture (RUDWICK, 1962a). Water passes mainly through the tentacles of the lateral arms and partly through those of the median coil where the tentacles touch each other across the median plane. In many terebratulide genera, the exhalant aperture is deflected either dosally or ventrally by a median sulcus.

FUNCTIONAL MORPHOLOGY OF THE LOPHOPHORE

The brachiopod lophophore functions principally as a ciliary pump and feeding organ by creating water currents through the mantle cavity for the capture of food particles and the uptake of oxygen involved in respiration. These currents also assist in the elimination of metabolic waste products and undesirable particulate material from the mantle cavity. In a number of articulated species, the lophophore also functions as a brooding site for larvae (CHUANG, 1990).

The brachiopod lophophore is generally not capable of much extensive movement, even in the inarticulated brachiopods, where it has the best developed musculature. Some apparent extensive motion has been reported, however, in the rhynchonellid *Notosaria,* and the extension can even result in self-amputation of portions of the coils. The reasons for this activity are unclear and may be the result of oxygen deprivation. Damaged lophophores of *Notosaria* appear capable of at least partial regeneration (HOVERD, 1985, 1986).

Currents

The lophophore creates water flow into and out of the mantle cavity, which is divided into inhalant and exhalant regions by the extension of the tentacles and their contact with the mantle. This flow facilitates metabolic exchanges with the environment, such as oxygen uptake, feeding, nitrogen excretion, and elimination of feces or undesirable particles. This water flow is generally continuous, although some individuals may stop pumping for short periods of time either due to disturbance or for no obvious reasons (LABARBERA, 1977, 1985; RHODES & THOMPSON, 1992, 1993).

Water movement through the mantle cavity of articulated brachiopods is generally slow and laminar, thus minimizing the energy dissipation involved in turbulent flow regimes (LABARBERA, 1977, 1981). The lateral cilia on the tentacles generate the currents passing through the lophophore, and their activity is complemented by ciliary activity on the mantle (WESTBROEK, YANAGIDA, & ISA, 1980; THAYER, 1986a). Laminar flow has been observed directly by mapping the pathways of fluorescein dye through the lophophore in the plectolophous species *Laqueus californianus, Terebratalia transversa,* and *Terebratulina unguicula* (LABARBERA, 1981). The flow lines do not cross, even when the dye makes a right-angle bend while entering the median coil from the lateral arms. A number of other plectolophous and spirolophous species have exhibited laminar flow (JAMES & others, 1992).

Although brachiopods must use metabolic energy to produce currents for ventilation and feeding, some species including those of

Laqueus, Terebratulina, Hemithiris, Megathiris, Argyrotheca, and *Gryphus* orient themselves to external water currents such that their ciliary pumping activity is augmented by the hydrodynamics of the ambient flow regime (SCHULGIN, 1885; ATKINS, 1960a, 1960b; LABARBERA, 1977, 1981; EMIG, 1992). They use the pressure differences from favorable orientations to external water currents to assist their ciliary pumps. Species that are capable of rotating about their pedicles in the adult stage tend to orient themselves with their anterior-posterior axes perpendicular to the prevailing flow or the substratum in their environments. The ptycholophous thecideids orient themselves with their anterior-posterior axis facing the current; the ventral valve is cemented to the substrate while the dorsal valve opens to a 90-degree angle relative to the substrate during feeding (LACAZE-DUTHIERS, 1861; NEKVASILOVA & PAJAUD, 1969; EMIG, 1992). Species such as *Terebratalia transversa,* which cannot reorient themselves in the adult stage, are often found in field observations to occur in favorable orientations due to preferential settlement by the larvae (LABARBERA, 1977).

Zygoplectolophous and spirolophous articulated groups may not assume a preferential position if the velocities of the ambient bottom currents are lower than the velocities of the excurrents of the brachiopods. As the speed of the bottom current increases, however, the incidence of preferential orientation also increases (data from MCCAMMON, 1965, 1973; LABARBERA, 1977, 1978, 1981; RICHARDSON, 1981d, 1986; EMIG, 1987, 1992).

Orientation relative to the bottom currents maximizes the effects from Bernoulli's principle and viscous entrainment. When brachiopods orient themselves with their anterior-posterior axes perpendicular to the external flow, a low-pressure region is created near the anterior portion of the gape where the exhalant current exits, and relatively higher pressure is present on either side of the gape in proximity to the inhalant currents (Fig. 116). Thus brachiopods minimize the energy needed for creation of feeding and respiratory currents and avoid recirculation of previously filtered water (LABARBERA, 1977, 1981).

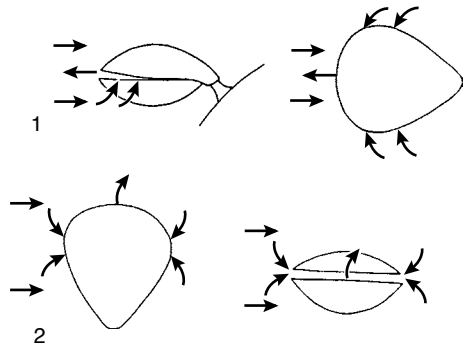

FIG. 116. Use of ambient external currents to assist in pumping water through the lophophore; *straight arrows* represent the current direction, with the velocity of the current proportional to the length of the *arrows; smaller curved arrows* indicate the inhalant and exhalant currents of the brachiopod; *1,* most unfavorable orientation as a brachiopod must work against high pressure in order to produce an exhalant current. Since the flow is moving parallel to the incurrent region, low pressure regions will occur because of viscous entrainment and will increase the effort required by the brachiopod to draw water into its shell; *2,* most favorable orientation as the excurrent region will be a low pressure zone because of viscous entrainment and the Bernoulli effect; the incurrent regions will be relatively higher pressure zones because the current decelerates on the upstream side as it approaches the brachiopod. The downstream side will have ambient hydrostatic pressure. This orientation enhances the pumping activity of the brachiopod (adapted from LaBarbera, 1977).

Some species, however, such as *Liothyrella neozelanica, Calloria inconspicua,* and *Notosaria nigricans,* live in dense, conspecific clusters, where the water pumped by one individual may include water already filtered by other individuals or epibionts, resulting in a decrease in food intake relative to the total energy needed for pumping water to obtain food.

The hydrodynamics of water flow through epifaunal inarticulated brachiopods has yet to be studied intensively (LABARBERA, 1985), but the similarities of configurations and areas of the lophophore and pumping velocities to those of articulated species suggest that flow through epifaunal inarticulated

species is also slow and laminar (see Fig. 411.1, section on ecology of inarticulated brachiopods).

Discinids orient the lophophore relative to the current so that it functions as a basket facing the current (see Fig. 411.1, section on ecology of inarticulated brachiopods; EMIG, 1992). In craniids that have cemented shells, orientation to external currents may occur only upon larval settlement and metamorphosis. Thus the anterior region faces the ambient flow regime, while the excurrent region is perpendicular. This orientation is functionally equivalent to that seen in articulated species that orient themselves to ambient flow, but it is anatomically perpendicular to orientation of articulated forms (M. LABARBERA, personal communication to C. EMIG, 1992).

Due to the experimental difficulties involved in studying infaunal animals, there are no published studies on the fluid mechanics of currents through infaunal, inarticulated brachiopods, although current pathways have been described in general qualitative terms (CHUANG, 1956; EMIG, 1976, 1982, 1992; WESTBROEK, YANAGIDA, & ISA, 1980; GILMOUR, 1981). The infaunal lingulides create separate inhalant and exhalant tubes within their mucous-lined burrows by the arrangement of their marginal setae and edges of the mantle (see Fig. 411.1, section on ecology of inarticulated brachiopods). As in articulated, spirolophous species, the mantle cavity of the lingulides is separated into inhalant and exhalant regions by the fully extended lophophore. Water currents drawn into the anterolateral inhalant setal tubes, however, may not remain laminar; they appear to diverge as they enter the inhalant region of the mantle cavity (CHUANG, 1956). Lingulides do not orient themselves toward ambient currents because they live in burrows (EMIG, 1982, 1992).

Respiration

The lophophore is the main respiratory organ in both articulated and inarticulated brachiopods (PECK, MORRIS, & CLARKE, 1986a). Due to its large surface area, it is ideally suited for gaseous exchange. Weight-corrected respiration rates of brachiopods are generally much lower than those of other marine invertebrates (JAMES & others, 1992).

Feeding

All living brachiopods are suspension feeders, and, although brachiopod lophophores occur in a number of configurations, species possessing different types of lophophores feed in essentially the same manner. When the tentacles of the lophophore are fully extended for feeding and respiration, the mantle cavity is separated into inhalant and exhalant chambers. Weak, throughgoing currents are created by the lateral cilia of the tentacles, while the frontal cilia transport food particles along the length of the grooved, outer tentacles toward the brachial groove for transportation to the mouth (Fig. 117).

Particle Capture

The mechanisms brachiopods use in capturing particles have been a subject of much debate since recent aerosol models have demonstrated the improbability of the cilia acting as sieves (RUBENSTEIN & KOEHL, 1977; LABARBERA, 1984). Additionally, there is no evidence that brachiopods use mucus to capture particles and move them down the tentacles toward the brachial groove, although once the particles enter the groove they are transported in mucus toward the mouth. One set of observations of *Laqueus* suggests that particles passing close to or within one particle radius of the cilia exert a drag force that induces a local reversal of the ciliary beat. This local reversal of lateral cilia captures the particles and their surrounding parcels of water and prevents them from wandering off the frontal cilia of the tentacle as they are moved toward the food groove (STRATHMANN, 1973; LABARBERA, 1984).

A second hypothesis to explain the capture of particles emphasizes possible adhesive properties of both cilia and particles due to electrostatic charge and suggests that par-

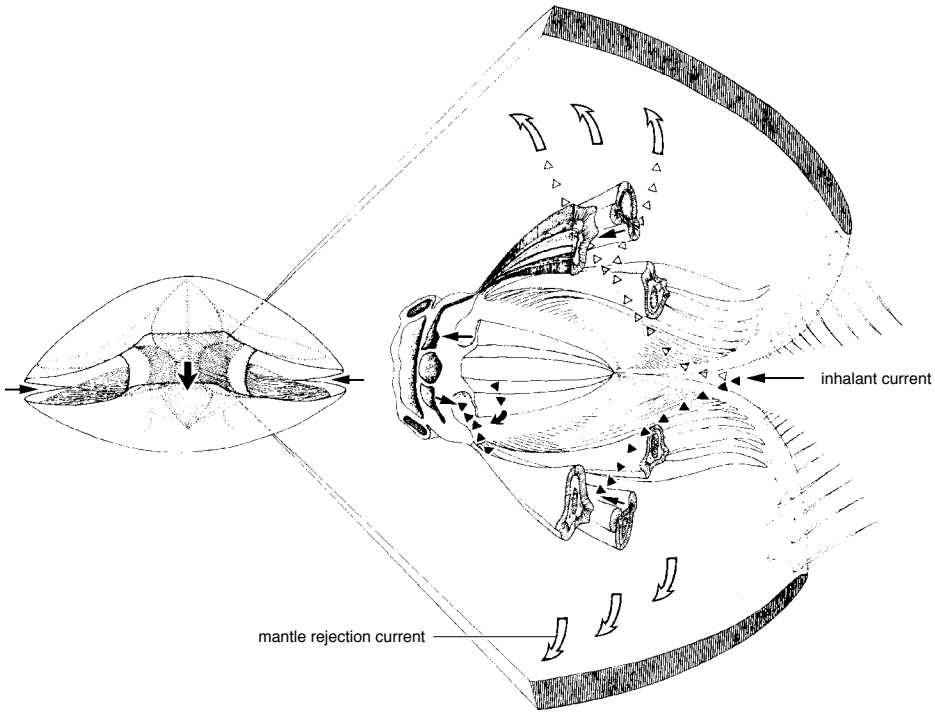

FIG. 117. Particle acceptance and transport down the frontal grooves of the outer (ablabial) tentacles to the food groove in a plectolophous brachiopod; *black triangles* represent the particles that are captured; *white triangles* represent the particles that pass through the tentacles and into the exhalant chamber; particles not intercepted are swept away in the exhalant current or by rejection currents on the mantle (adapted from James & others, 1992).

ticles approaching the cilia will be attracted by short-range, London-van der Waals forces and subjected to hydrodynamic retardation due to the viscosity of the fluid being squeezed out between the particles and the cilia (LABARBERA, 1984). A third hypothesis suggests that particles are extracted from suspension by steep velocity gradients created when the through-going currents meet currents perpendicular to them (JØRGENSEN, 1981), such as those potentially occurring when the through-going currents created by the lateral cilia on the tentacles encounter currents moving down the frontal ciliary tracts.

Finally, observations on the inarticulated species *Glottidia* and the articulated species *Laqueus,* using stroboscopic-interference-contrast optics, suggest that heavier and thus biologically undesirable particles impinge directly upon the frontal surfaces of the lophophore tentacles for rejection (BULLIVANT, 1968), while lower density, potential food particles are filtered through the lateral cilia of the tentacles without the use of ciliary reversals for acceptance (GILMOUR, 1978, 1981). The fluid mechanics of such an impingement mechanism operating in a flow regime where viscous forces predominate over inertial forces have yet to be understood (JAMES & others, 1992).

Particle Sorting and Rejection

Undesirable or excess particles are generally bound in mucus and eliminated by a variety of mechanisms (RUDWICK, 1970; THAYER, 1986a; JAMES & others, 1992; THOMPSON, WARD, & RHODES, 1992). Mantle cilia commonly assist the lophophore in rejection and the exchange of water

through the mantle cavity, as noted in *Neocrania anomala, Lingula anatina, Coptothyris grayii,* and *Terebratalia transversa* (CHUANG, 1974; WESTBROEK, YANAGIDA, & ISA, 1980; THAYER, 1986a).

Articulated species use several mechanisms to reject particles. In the presence of unwanted particles or particles in dense concentrations, many species reverse the beat of the frontal cilia to transport mucous-bound particles away from the food groove toward the tips of the tentacles (ATKINS, 1956, 1959, 1960a, 1960b; RUDWICK, 1962a, 1970). Particles to be rejected may become concentrated on the inner (adlabial) tentacle series (where present), while particles to be accepted become concentrated on the outer (ablabial) tentacle series, thus allowing simultaneous feeding and rejection (GILMOUR, 1978). Additional rejection mechanisms noted in studies on the species *Terebratalia transversa* include lifting of a single tentacle to permit removal of particles by mantle currents, a spiralling motion between two adjacent tentacles that rolls particles into a mucous string and moves it distally, wholesale rejection where the lophophore coils tightly to allow the mantle to remove excess matter (RUDWICK, 1970; THAYER, 1986a), and a wiping motion where one, outer tentacle passes its abfrontal surface over the frontal surfaces of a whole series of neighboring tentacles, thus transferring strings of mucous-bound particles directly into the rejection current (Fig. 118; THOMPSON, WARD, & RHODES, 1992). Occasionally, *Terebratalia* reverses its entire current system, with water and mucous-bound particles exiting the normally inhalant regions (RHODES & THAYER, 1991; THOMPSON, WARD, & RHODES, 1992). These rejection mechanisms are likely to be used by many species, especially those living in areas with high loads of suspended particles.

Lingula is capable of simultaneous feeding and rejection of particles due to the action of adjacent tracts of frontal cilia on the same tentacles. The individuals accept or reject particles by suppressing the action of one set of tracts while amplifying the opposite set. Reversals of frontal cilia have not been observed in this genus (CHUANG, 1956). Simultaneous feeding and rejection are particularly advantageous for the infaunal inarticulated groups because of the proximity of their anterolateral incurrents to the interface between water and unstable sediments. *Neocrania* is capable of reversing its frontal cilia to reject unwanted particles (ATKINS & RUDWICK, 1962; CHUANG, 1974).

Brooding in the Lophophore

Brooding of larvae in the lophophore appears to be quite common among articulated brachiopods, although it has not been found to occur in inarticulated groups (CHUANG, 1990). *Pumilus* broods its embryos using its schizolophous lophophore as a natural basket (RICKWOOD, 1968). The spirolophous species *Notosaria* and *Hemithiris* brood larvae using the coils and tentacles of their lophophores as baskets (Fig. 119; PERCIVAL, 1960; LONG, 1964, in CHUANG, 1990; HOVERD, 1985). The plectolophous species *Terebratulina unguicula* broods larvae between the tentacles on its lateral arms (LONG, 1964, in CHUANG, 1990), while the Antarctic species *Liothyrella,* which is also plectolophous, broods them within the median coil (PECK & HOLMES, 1989a; PECK & ROBINSON, 1994). The ptycholophous *Lacazella* species provides an attachment site behind the mouth by inserting modified lophophore tentacles with collars and swollen tips into a single median pouch (see Fig. 173; RUDWICK, 1970; CHUANG, 1990). The small trocholophous *Gwynia capsula* broods in a similar manner (SWEDMARK, 1967). Brooding in the lophophore protects the larvae, while allowing them maximum exposure to fresh seawater.

NERVOUS AND SENSORY SYSTEM

All brachiopods possess a central nervous system, but there are few detailed anatomical studies and little new neurophysiological data. *Gryphus vitreus* is the best documented

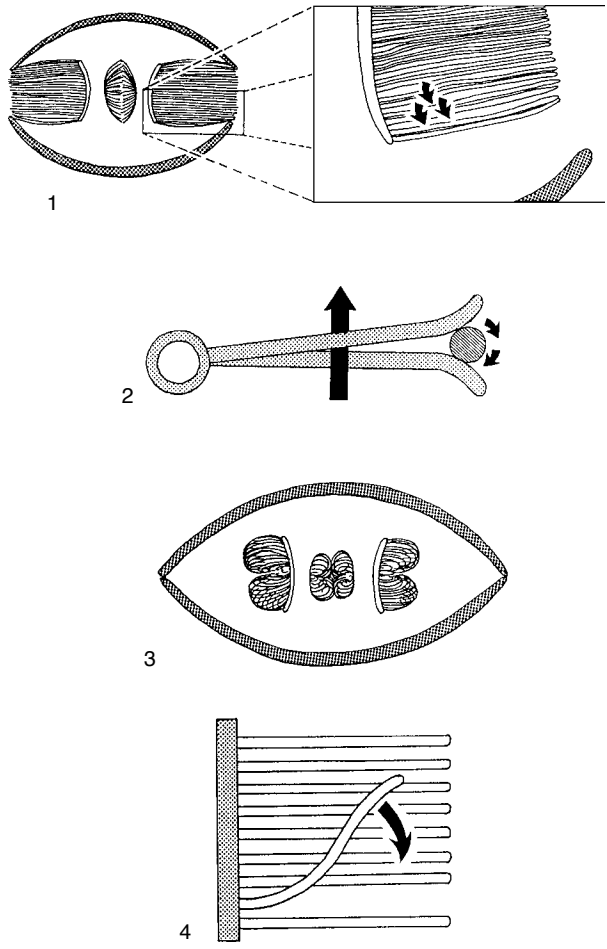

FIG. 118. Particle rejection mechanisms in brachiopods; *1,* rejection of a particle by the lifting of a single tentacle; the enlarged region shows particle rejection by spiralling activity around pairs of tentacles; *2,* construction of a mucous string by two tentacles to bind undesirable particles for rejection; *3,* wholesale rejection of high particle loads by the lophophore tentacles remaining coiled until the mantle currents sweep away excess particles (adapted from Thayer, 1986a); *4,* wiping motion of a single tentacle sweeping its ablabial surface across a region of neighboring tentacles and transferring mucous-bound particles directly into the excurrent region (new).

of the articulated brachiopods (BEMMELEN, 1883), while *Lingula anatina, Discinisca lamellosa,* and *Neocrania anomala* are the most widely cited examples among the inarticulated species (BLOCHMANN, 1892, 1900). The ultrastructure and immunocytochemistry of the nervous systems of the larvae of *L. anatina* and *Glottidia* sp. have also been studied (HAY-SCHMIDT, 1992).

The nervous system of articulated brachiopods is considered to be typified by *Gryphus* (Fig. 120). The main body of nervous tissue is found around the esophagus near its junction with the anterior body wall. Nerves emanate laterally from two ganglia, a larger subenteric ganglion and a smaller supraenteric ganglion, which lie above and below the esophagus respectively. One or more circumenteric nerves innervate the lophophore. The brachial lip is activated by a pair of nerves arising laterally from the subenteric ganglion. Branches of the

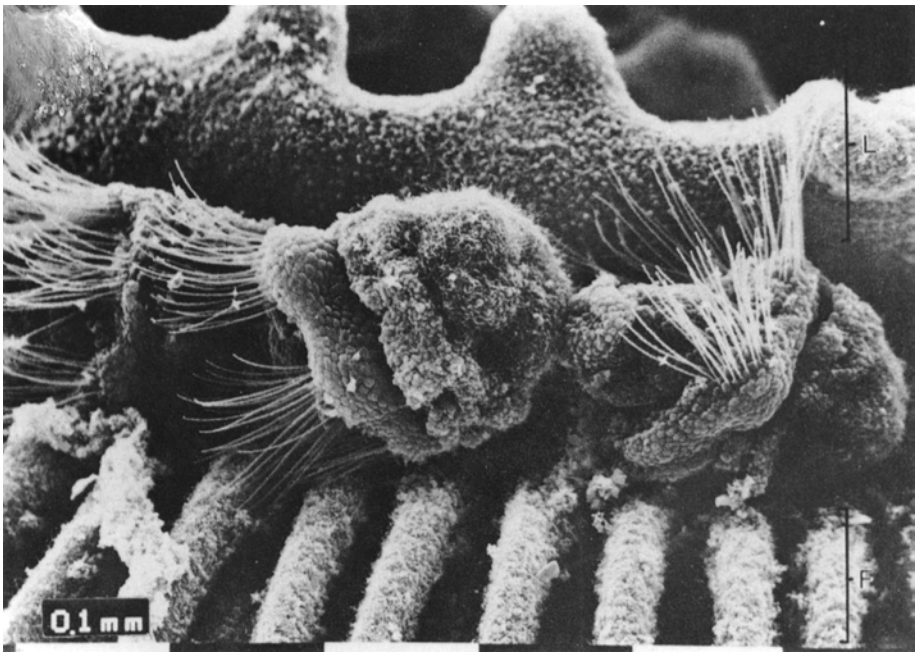

FIG. 119. SEM micrograph of the larvae brooded in the spirolophous lophophore of *Notosaria nigricans,* scale bar: 0.1 mm; *L,* lip of food groove; *F,* tentacle (Hoverd, 1985).

circumenteric nerves, accessory and lower brachial nerves, serve the brachia and tentacles. The dorsal mantle is innervated by two main nerves and a number of ancillary branches, which also arise from the subenteric ganglion. Similarly a pair of thick, subparallel branches, arising from the subenteric ganglion, serve the ventral mantle, adductor muscles, and pedicle. Mantle nerves radiate, splitting distally into ever finer branches that terminate close to the mantle margin at relatively regular intervals (Fig. 121; RUDWICK, 1970).

In the planktotrophic larvae of *L. anatina* and *Glottidia* sp., the nervous system appears to be divided into dorsal and ventral parts. The primary dorsal system consists of part of an apical ganglion, dorsal lophophore nerves, and a ventral ganglion. The second system is essentially ventral and includes part of an apical ganglion and ventral lophophore nerves. The dorsal lophophore nerves are believed to innervate the muscles (*musculus lophophoralis* and *m. brachialis*), and the ventral lophophore nerves and lateral processes innervate the ciliary band. The known physiological function of detected neurotransmitters supports this pattern of innervation (Fig. 122; HAY-SCHMIDT, 1992). As with many other invertebrates, the planktotrophic larvae of *Glottidia* contain serotonin-like (5-HT), catecholamines (CA), and neuropeptide FMR-like neurotransmitters (Fig. 123–125; HAY-SCHMIDT, 1992).

The nervous system of adult inarticulated brachiopods lacks a supraenteric ganglion. In *Discinisca* and *Neocrania* the circumenteric nerves emanate laterally from the subenteric ganglion and from a ring around the esophagus. In *Neocrania,* however, the subenteric ganglion is also divided into two parts that occur in the epidermis of the lateral body wall lateral to the anterior adductor muscles. Brachial nerves serving the lophophore and tentacles arise from the branches of the circumenteric nerves (Fig. 126–128).

A network of finely divided nerves originating from the subenteric ganglion ramifies

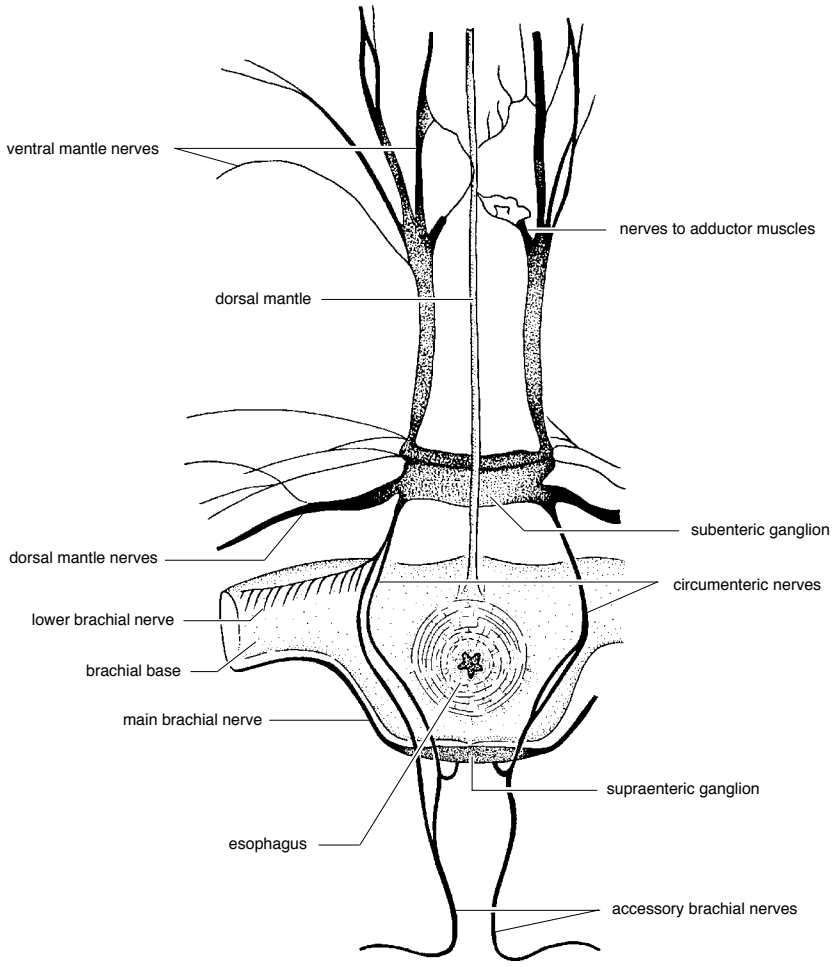

FIG. 120. Nervous system of *Gryphus vitreus* (adapted from Bemmelen, 1883).

throughout the dorsal and ventral mantles. In both *Discinisca* and *Lingula* the branches of the mantle nerves are joined distally to form dorsal and ventral marginal nerves. These peripheral nerves are found on the inner side of the setal follicles that occur around the edge of the mantle. Both follicles and marginal nerves are absent from *Neocrania.*

The pedicles of *Discinisca* and *Lingula* are each provided with a pair of nerves that branch from the subenteric ganglion or form ring-shaped, lateral nerves located in the body wall. The diagrams (Fig. 126–128) illustrate the course of the nerves that serve the more complex inarticulate musculature. A nerve plexus in the base of the epithelium lining the alimentary canal has also been identified (BLOCHMANN, 1900).

Although there may be differences within the phylum, current evidence suggests that bundles of unsheathed nerve fibers are generally located between the bases of the inner mantle epithelium covering the lophophore and lining the alimentary canal above the basement membrane (Fig. 129–130; PERCIVAL, 1944; GILMOUR, 1981; SAVAZZI, 1991). Bundles of neurons have also been found in the connective tissue of the pharynx of *Calloria* (Fig. 131). The neurological gap

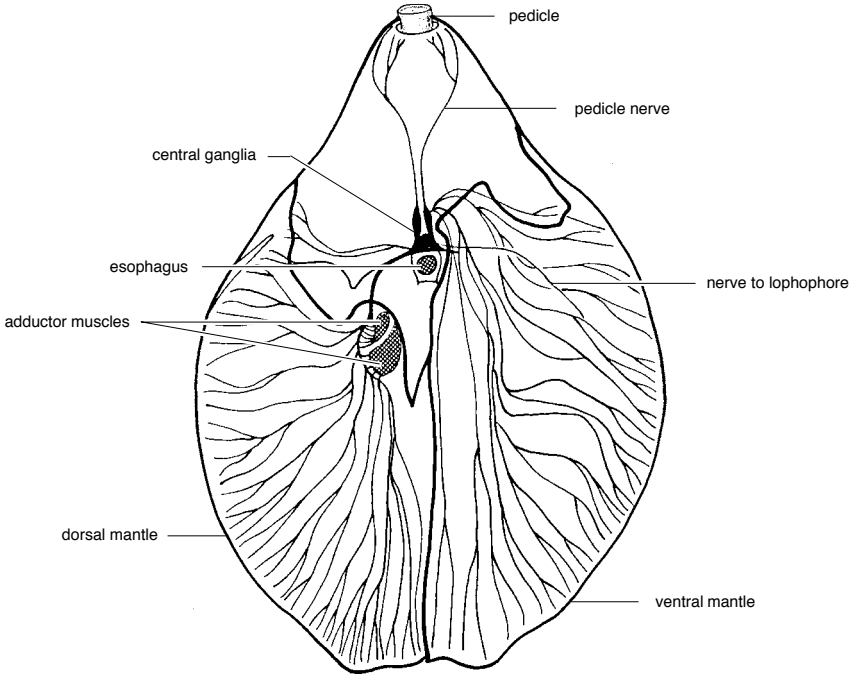

FIG. 121. Nervous system of *Magellania australis* QUOY & GAIMARD; dorsal view of decalcified specimen, with the dorsal mantle removed on one side; the sensory nerves terminate around the mantle edges and motor nerves are connected to the adductor muscles (adapted from Hancock, 1859).

junctions found between the nerves of the terebratulides *Calloria* and *Terebratella* have now been characterized as P-type junctions, which are also known to exist in the molluscs and bryozoans. The type of septate junction present, however, is identical to that found in many other lower invertebrate phyla and differs from the molluscan septate junction (FLOWER & GREEN, 1982).

FUNCTIONAL MORPHOLOGY OF THE NERVOUS AND SENSORY SYSTEM

Brachiopods show little evidence of differentiated sense organs. Although no rigorous experimental data exist, it is generally accepted that their responses to light and a range of chemical and physical stimuli indicate sensitivity.

The behavioral repertoire of the brachiopod, although limited, provides clues to their sensory capabilities. The most obvious sensory mechanisms appear to be confined to the edge of the mantle lobes and possibly the pedicle. No special receptor organs have been found, but the mantles are richly supplied with nerves leading to the central ganglia, through which there is a simple reflex circuit to the adductor muscles.

A dramatic response to unfavorable conditions is the rapid and tight closure of the valves by contraction of the adductor muscles. Closure may be accompanied by movement of the whole shell on the pedicle, drawing the shell nearer to the substratum or, in lingulids, into its burrow or merely rotating the shell into a different orientation.

A sudden decrease in light intensity initiates a shadow reflex resulting in rapid closure of the shell. The mantle seems to be capable also of detecting water that is highly turbid, brackish, or poorly oxygenated (RHODES & THAYER, 1991).

The behavior of some brachiopod larvae may change during ontogeny with respect to light, gravity, and possibly the physical or

chemical nature of the substratum (JAMES & others, 1992). Immediately prior to settlement, the behavior of such brachiopods as *Terebratulina* and *Neocrania* suggests selection of the substrate, emphasized by patchy distribution and apparently gregarious settlement. Such behavior suggests mediation by some sort of sensory capability.

Setae

With few exceptions, notably craniids, thecideidines, and megathyrids, living brachiopods possess chitinous setae that develop in follicles along the margin of the mantle, project beyond the edges of the valves, and extend tactile sensitivity beyond the mantle (see section on mantles and body walls, p. 9). As no direct neurological connection with the setae has been reported, it is assumed that their tactile properties are transmitted mechanically to the mantle (RUDWICK, 1970).

Statocysts

A pair of statocysts occur in larval or juvenile inarticulated brachiopods. According to YATSU (1902a) and MORSE (1902) these persist in adult *Lingula.* MORSE (1902) did not find them in *Glottidia.* Statocysts occur in the gastroparietal bands near the anterior adductor muscles and consist of a sac of tall epithelial cells containing about 30 statoliths (SAVAZZI, 1991). They are assumed to allow the sensation of orientation and enable the animal to maintain an optimal position in the soft sediments it inhabits, which would accord with the ability of lingulids to burrow (WORCESTER, 1969; THAYER & STEELE-PETROVIC, 1975; SAVAZZI, 1991).

Particle Selection

The lophophore appears to be capable of particle selection based on size, specific gravity, charge, and other chemical properties (RHODES & THAYER, 1991). The ciliated laterofrontal cells of the tentacles of *Glottidia* make synapses with the nervous system, and it has been suggested that the cilia serve as detectors of high densities of heavy waste particles in the feeding current (GILMOUR, 1981). In contrast, ultrastructural studies of *Terebratalia* did not reveal any nerve fibers traversing the connective tissue to form myoneural junctions or any evidence of peritoneal nerves (REED & CLONEY, 1977). The tentacles of the lophophore often react to adverse conditions by curling toward the brachial groove, presumably by contraction of their frontal group of myoepithelial cells.

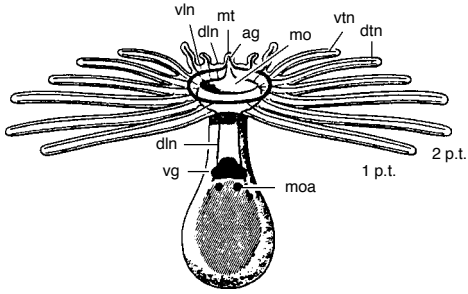

FIG. 122. Drawing of a planktotrophic brachiopod larva showing the course of the major nerves with the shell removed but the connection to the body wall (*oblique lines*) and *musculus occludens anterior* (*moa*) indicated; the median tentacle (*mt*) represents the prosoma and contains the apical ganglion (*ag*); the lophophore represents the mesosoma and consists of a ring of tentacles numbered according to their appearance during development (1 p.t., 2 p.t.; see section on embryology and development, p. 154); the major nerves are the ventral and dorsal lophophore nerves (*vln* and *dln*), and the ventral and dorsal tentacle nerves (*vtn* and *dtn*); the dorsal lophophore nerve is connected to the ventral ganglion (*vg*); *mo,* mouth (Hay-Schmidt, 1992).

Eyespots

There are numerous reports of the existence of eyespots (ocelli) and pigment granules in various larvae (see section on embryology and development, p. 151), but the anatomy and sensory potential of these structures is largely unknown (JAMES & others, 1992). *Argyrotheca* larvae possess eyespots that consist of cuplike invaginations of the ectoderm with underlying nerve fibers and vitreous humor (PLENK, 1913). The structure suggests photosensitivity.

REPRODUCTION

Most brachiopods occur as separate sexes (gonochoristic), although some are

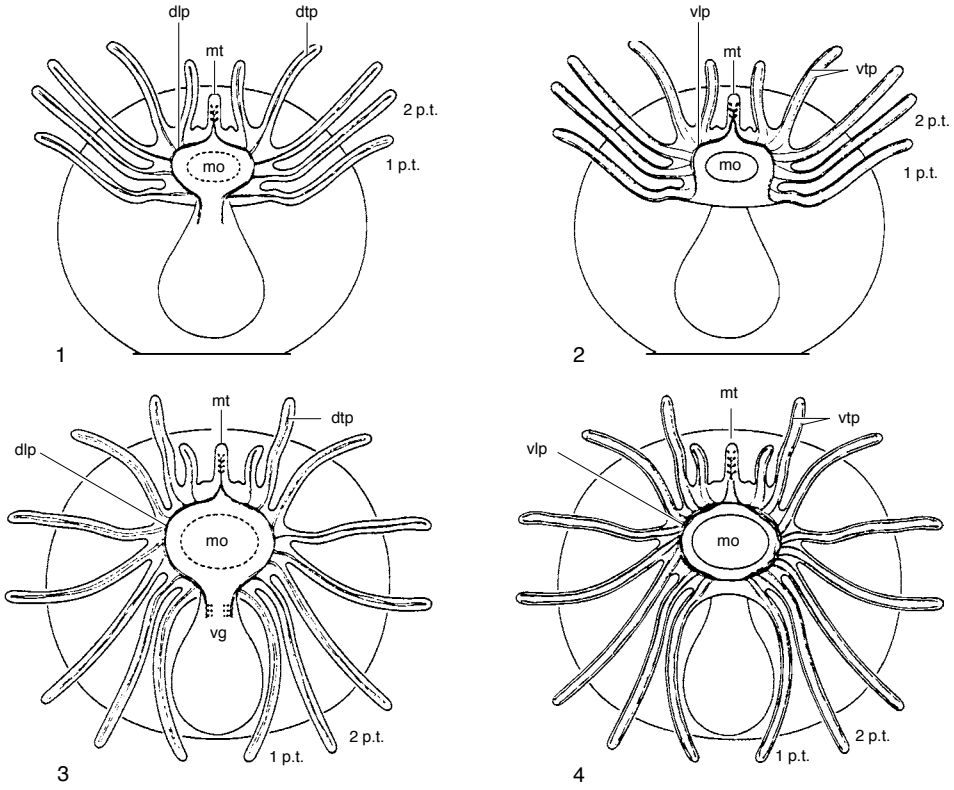

FIG. 123. Diagram of serotonin (5-HT) containing cells in a brachopod larva; *1,* dorsal and *2,* ventral view of a 6 p.t. larva showing the dorsal lophophore processes continuing along the esophagus before the formation of the ventral ganglion; *3,* dorsal and *4,* ventral view of a 9 p.t. larva with the dorsal lophophore processes (*dlp*) connected to the ventral ganglion (*vg*) and the ventral lophophore processes (*vlp*) continuous between the 1 p.t.; *dtp,* dorsal tentacle process; *mo,* mouth; *mt,* median tentacle; *vtp,* ventral tentacle process (Hay-Schmidt, 1992).

hermaphroditic. Those factors influencing sex determination in brachiopods are unknown (LONG & STRICKER, 1991), but body size and the degree of isolation of the population may exercise some influence over the mode of reproduction. Micromorphic brachiopods tend to be hermaphroditic and brood their larvae. All gonochoristic nonbrooding brachiopods are relatively large. For the few species that have been studied, an approximately 1:1 sex ratio exists (PERCIVAL, 1944; PAINE, 1963; DOHERTY, 1979; CURRY, 1982), although greater variation has been reported in *Notosaria nigricans* (PERCIVAL, 1960). Sexual dimorphism has been reported only in *Lacazella mediterranea* (LACAZE-DUTHIERS, 1861), in which the ventral valve of the female is distended to incorporate a brood pouch. The sex of mature gonochoristic brachiopods can sometimes be determined externally by the color of the gonads, observed either through the valve (ROKOP, 1977) or more reliably through the translucent, inner mantle membrane. Testes are usually white, cream, pink, or blue, while ovaries tend to be yellow to orange-brown. Hermaphroditic species such as three species of *Argyrotheca* (SENN, 1934), *Pumilus antiquatus, Platidia davidsoni* (ATKINS, 1958), *Lacazella* sp., and *Thecidellina barretti* (JAMES, unpublished, 1987) contain both ovary and testes simultaneously. *Fallax dalliniformis* possibly alternates between sexes (WILLIAMS & ROWELL, 1965a), and *Calloria inconspicua* may be predominantly male or predominantly female (JAMES & others, 1992). Some specimens of

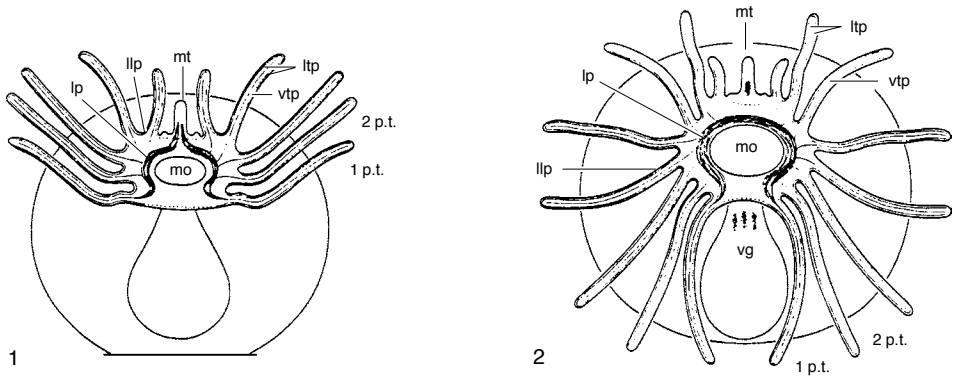

FIG. 124. Diagram of CA (catecholamine) containing processes in a brachiopod larva; *1,* 6 p.t. larva ventral view; from the median tentacle (*mt*) extend the lophophore processes (*lp*), from which project the ventral tentacle processes (*vtp*), with the lateral lophophore processes (*llp*) extending into the tentacles as the lateral tentacle processes (*ltp*); *2,* as for *1,* but at the 9 p.t. larval stage, the neurophil of the apical ganglion seems to be separated from the lophophore processes (*lp*), while the ventral ganglion (*vg*) consists of three separate neurophils; *mo,* mouth (Hay-Schmidt, 1992).

Lingula anatina and *Glottidia pyramidata* (GRATIOLET, 1860; BEYER, 1886; CULTER, 1980; CULTER & SIMON, 1987) have also been recorded as containing both male and female reproductive tissue in the same gonad.

GONAD MORPHOLOGY

Brachiopods have one or, more usually, two pairs of gonads with the largest gonads developing ventrally in articulated groups (Fig. 132). Some species of *Argyrotheca* possess only a dorsal pair of gonads (SENN, 1934), while only a ventral pair of gonads develops in *Lacazella mediterranea* (LACAZE-DUTHIERS, 1861). The gonads of inarticulated brachiopods are usually confined to the relatively large visceral cavity. The gonads of articulated brachiopods are only partially housed in the relatively smaller visceral cavity, with most of the gonad extending anteriorly into extensive mantle canals, the

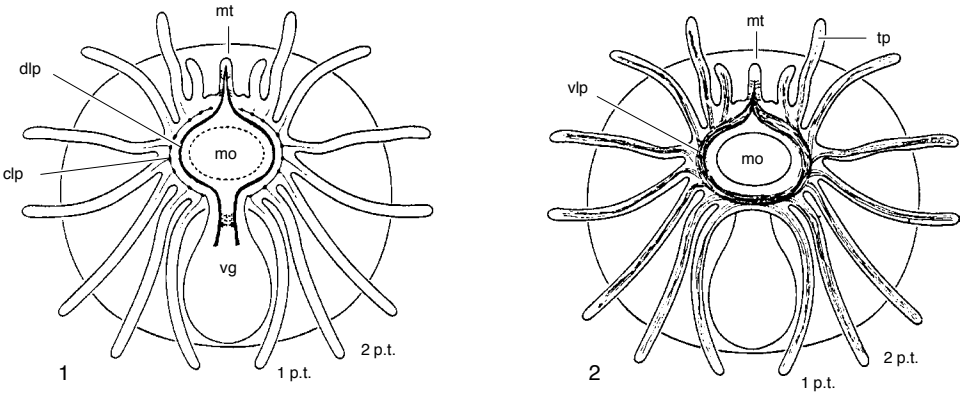

FIG. 125. Diagram of the distribution of FMRFamide containing cells and processes in a 9 p.t. brachiopod larva; *1,* dorsal view with the apical ganglion in the median tentacle (*mt*) consisting of two cell groups; the dorsal lophophore processes (*dlp*) continue to the ventral ganglion (*vg*), the central lophophore processes (*clp*) give rise to processes into the tentacles; *2,* as for *1,* but in ventral view, the ventral lophophore processes (*vlp*) give rise to processes into the tentacles as the tentacle processes (*tp*); *mo,* mouth (Hay-Schmidt, 1992).

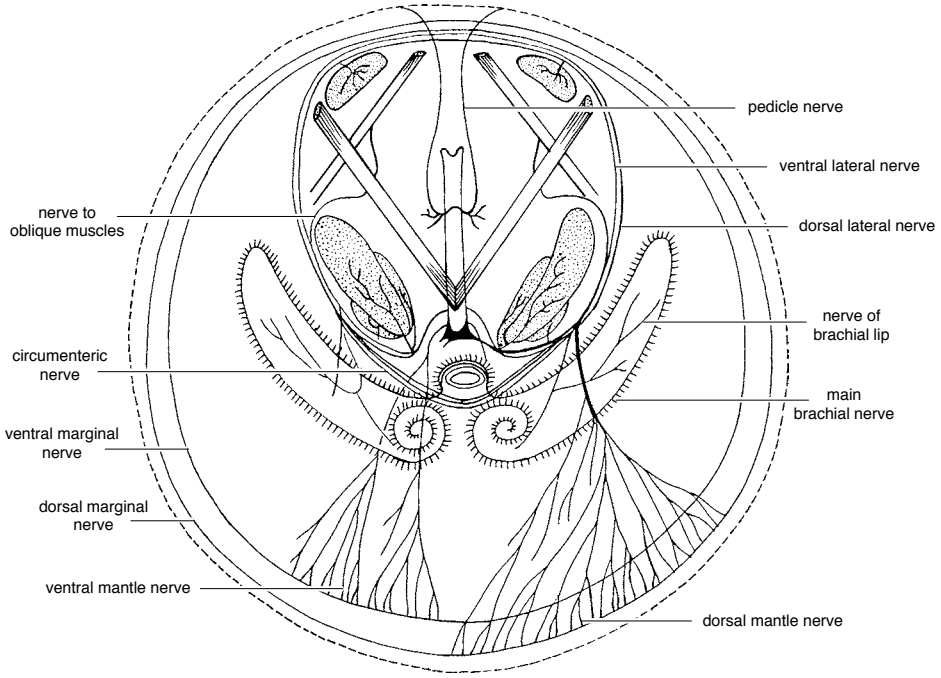

FIG. 126. Diagram of the nervous system of *Discinisca lamellosa* (mantle nerves shown only anteriorly) (adapted from Blochmann, 1900).

vascula genitalia, and in some species with arborescent gonads, the *vascula media* (Table 1, p. 134; see also Fig. 71). The craniids are the only inarticulated brachiopods with gonads partially inserted into the mantle canals (HANCOCK, 1859; MORSE, 1873; SCHAEFFER, 1926; SENN, 1934). The disposition of the gonads may be influenced by the flow of water through the mantle cavity (EMIG, 1992) as determined by the architecture of the shell and mantle and the type of lophophore.

The construction of the gonads appears to be similar in all brachiopods and consists of a folded ribbon of connective tissue, the genital lamella, which develops from the membranes supporting the stomach (gastroparietal bands) and the intestine (ileoparietal bands). Each fold is covered by a germinal epithelium from which the sex cells develop (Fig. 133–134).

The inarticulated *Discinisca lamellosa* possesses two portions of gonad that lie on the lower surface of the two gastroparietal bands, two more on the triangular ileoparietal bands, and a fifth free in the posterior region of the visceral cavity (JOUBIN, 1886). In

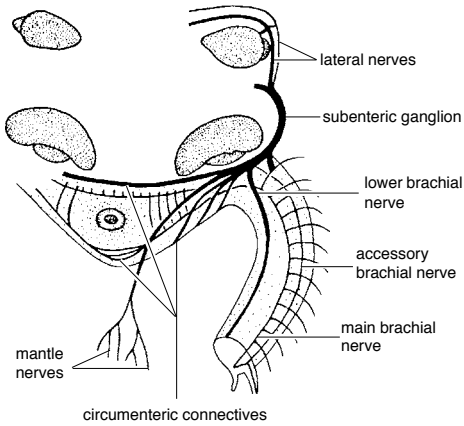

FIG. 127. Diagram of the nervous system of *Neocrania anomala* (mantle nerves shown only anteriorly) (adapted from Blochmann, 1892).

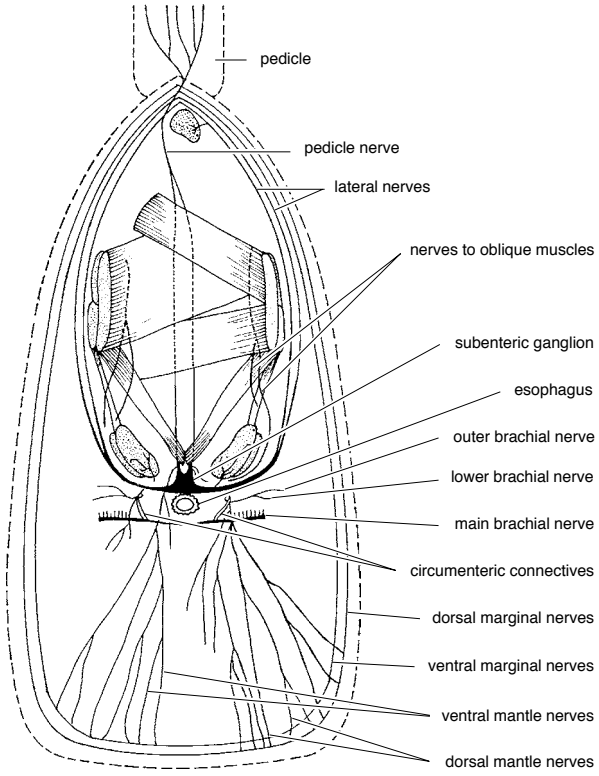

FIG. 128. Diagram of the nervous system of *Lingula anatina* (mantle nerves shown only anteriorly) (adapted from Blochmann, 1900).

young males of *D. laevis,* however, besides the two gonad portions on the lower surface of the gastroparietal bands, a single U-shaped portion of gonad lies on the ventral surface of the ileoparietal bands (CHUANG, 1983b). In adult *Lingula,* in which the germinal epithelium has developed into tufted lobes and lobules, the muscles crossing the body cavity partly separate each gonad into a dorsal mass of lobes in the ileoparietal band anchored to the sides of the stomach, while ventral masses on the same side of the visceral cavity remain connected by a small strand of apparently sterile ileoparietal band (CHUANG, 1983a, 1983b). Consequently *Lingula* has been reported as having four gonads (JOUBIN, 1886) or gonads in four groups (SCHAEFFER, 1926; SENN, 1934). Because of the physical continuity of the connective tissue band, all of the folds of the genital lamella on one side of the body are regarded as constituting a single gonad (CHUANG, 1983a, 1983b). In *Lingula* the posterior part of the gastroparietal band is a flat ribbon of connective tissue attached along its medial edge to the lateral wall of the stomach, its lateral edge hanging freely in the dorsal region of the visceral cavity. Posteriorly the band of connective tissue bifurcates into medial and lateral bands. The medial band fuses with its counterpart from the other side of the stomach to form a single horizontal membrane that proceeds posteriorly from the ventral body wall of the posterior end of the stomach and becomes attached to the posterior body wall. The lateral band on each side curves ventrally and continues anteriorly and has its lateral edge fused to the medial wall of the metanephridium. The medial edge of this band lies free in the

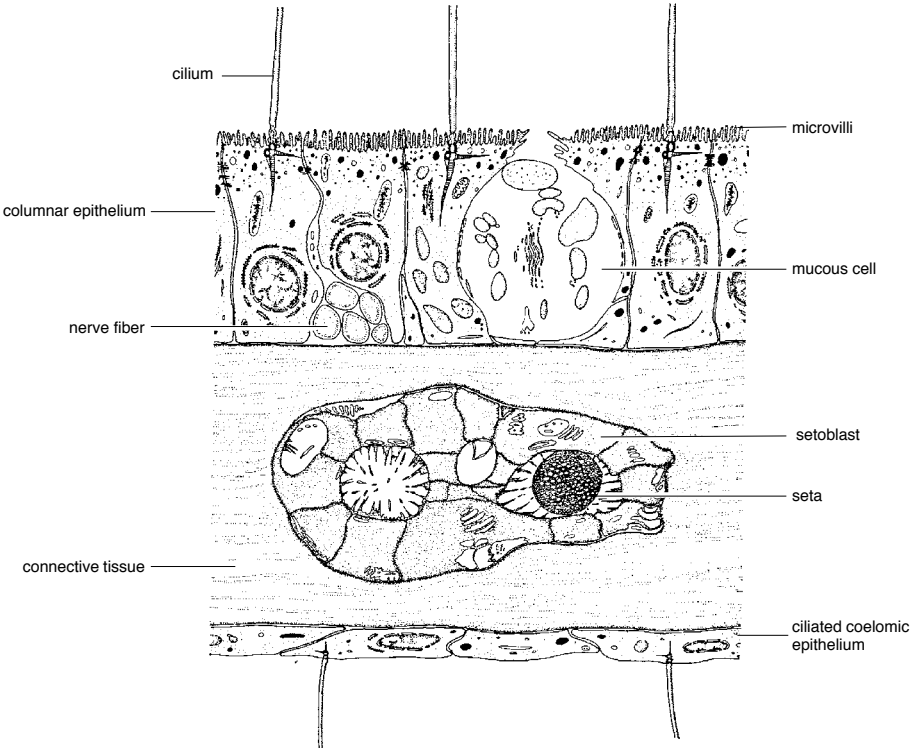

FIG. 129. Diagrammatic cross section through the periphery of the inner mantle membrane of *Terebratulina* (adapted from James & others, 1992).

ventral region of the visceral cavity (CHUANG, 1983a, 1983b). *Glottidia albida* and *G. pyramidata* also have right and left gonads, which occur along the continuous ileoparietal bands (CHUANG, 1983a, 1983b).

In *Neocrania anomala* the gonads occur in six portions, two in the visceral cavity and a pair in each mantle (JOUBIN, 1886). Genital lamellae develop only on the inner mantle membrane of the mantle canals of articulated brachiopods and the inarticulated *Neocrania*. The connective tissue fold of the parietal band is fused throughout its length along one margin to the inner mantle membrane, with the remainder of the tissue fold projecting into the mantle canal or *vascula genitalia* (Fig. 135).

In articulated brachiopods and *Neocrania* the genital lamella is sacciform proximal to the point of fusion with the inner mantle membrane, but in more distal regions adjacent folds are knit together with strands of connective tissue. The distended portions of the genital lamellae (Fig. 133, 136) form an anastomosing network that is traceable to the heart above the stomach and is believed to form part of the vascular (circulatory) system (CHUANG, 1983a; see section on coelomic and circulatory system, p. 69).

The morphology of the gonads ranges from the lobes of pleated ribbons of genital tissue found in *Lingula* (Fig. 137.4) to the complex reticular patterns that occur in some articulated brachiopods (Table 1, p. 134; Fig. 137.1–137.2). In those articulated species where the *vascula genitalia* are extensive and the genital lamellae form palmate reticulate lattices, the inner and outer mantle

membranes are periodically joined by pillars of connective tissue (Fig. 133; JAMES, ANSELL, & CURRY, 1991b). The genital lamellae of less complex genital morphologies may simply be separated by bands of connective tissue that unite the inner and outer membranes (JAMES & others, 1992). In *Neocrania* each extension of the genital lamella is contained in a separate canal within the mantle (Fig. 137.3).

The construction of the genital lamella is relatively uniform throughout the phylum, but the distribution of the germinal epithelium differs between the sexes. Male genital lamellae tend to be ruffled along the distal margin, increasing the surface area for production of gametes. Proliferating clusters of spermatogonia occur at the base of the genital lamella (JAMES, ANSELL, & CURRY, 1991b; JAMES & others, 1992). Subsequent stages in the development of spermatozoa occur more distally and are ultimately displaced by the proliferation of underlying cells, thus forming bands of cells at different developmental stages. Mature spermatozoa occur around the periphery of masses of spermatogenic and spermiogenic cells (Fig. 135.1–135.2; 138; JAMES & others, 1992).

The female genital lamella tends to be columnar with oogonia proliferating at the base of the genital lamella. As vitellogenic oocytes differentiate and enlarge through the accumulation of yolk, they occur on progressively distal regions of the lamella (JAMES, ANSELL, & CURRY, 1991c; LONG & STRICKER, 1991). The apparent migration of these cells is probably caused by elongation of the genital lamella. Eventually the oocytes become detached from the genital lamella and float freely in the coelomic fluid of the *vascula genitalia* where they complete their development prior to spawning. Once the ooctyes have been released, it is assumed that the extended lamellar region is phagocytosed, along with any other necrotic material remaining in the gonad after spawning (JAMES, ANSELL, & CURRY, 1991c).

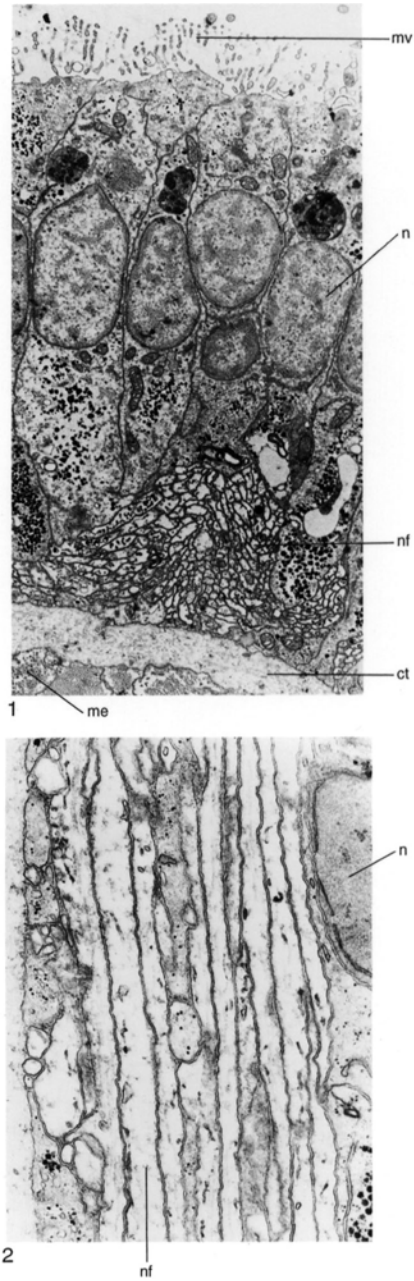

FIG. 130. TEM micrographs of unsheathed bundles of nerve fibers in the tentacles of *Calloria; 1,* transverse section showing the nerve fiber (*nf*) at the base of the epidermal cells with microvilli (*mv*); *n,* nucleus; *ct,* connective tissue; *me,* myoepithelium; *2,* longitudinal section of nerve fibers (*nf*); *n,* nucleus, ×16,600 (new).

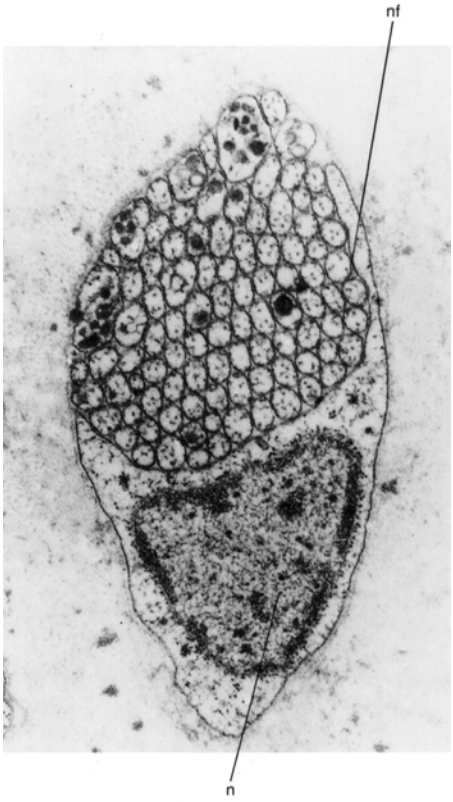

FIG. 131. TEM micrograph of a transverse section of a bundle of unsheathed nerve fibers (*nf*) and nucleated accessory cell in the connective tissue of the pharynx of *Calloria; n,* nucleus, ×20,000 (new).

Development of hermaphroditic gonads in brachiopods is well known only for *Calloria* (JAMES, unpublished, 1992). This species generates sperm and eggs on the same genital lamella although the lineage of the germ cells remains unclear. As in gonochoristic species, the germinal cells tend to occur at the base of the genital lamella, with more advanced stages occurring distally. *Calloria* shows considerable reproductive plasticity and appears to be male or female or to display a predominance of male or female reproductive tissue in gonads that are clearly hermaphroditic (Fig. 139; JAMES, unpublished, 1992).

SPERMATOGENESIS

Spermatogenesis in brachiopods is poorly documented, but accounts of the inarticulated *Lingula* (SAWADA, 1973; CHUANG, 1983b) and the articulated *Terebratulina* (JAMES & others, 1992), together with observations of *Calloria* and *Notosaria* (JAMES, unpublished, 1993), suggest that spermatogenesis is similar in these brachiopods.

Spermatogonia generally contain a large, distinct nucleus with condensed chromatin and proliferate from the germinal epithelium at the base of the genital lamella. Spermatogonia give rise to primary spermatocytes that are conspicuously larger than neighboring somatic cells and are attached to the genital lamella. The nucleus of each primary spermatocyte lacks nucleopores and contains sparsely granular chromatin, much of which is condensed against the inner side of the nuclear envelope. The cytoplasm contains clusters of mitochondria, granular and agranular endoplasmic reticulum, and ribosomes. Primary spermatocytes undergo meiosis to produce secondary spermatocytes that have extremely condensed cytoplasmic and nuclear material (Fig. 140).

Secondary spermatocytes undergo a second meiotic division to form spermatids. In the two spermatocyte divisions the various cytoplasmic inclusions are usually distributed equally to the four spermatids, which seems to result from the tendency of such inclusions to be grouped so that cytokinesis separates them equally. Spermatids have less electron-dense cytoplasm than the preceding stage, a spherical nucleus, two centrioles, a Golgi complex, and, posteriorly, one or more pyriform mitochondria, depending on the species.

SPERMIOGENESIS

Spermatids undergo a series of morphological changes as they develop into spermatozoa. Spermatozoa have a head consisting of

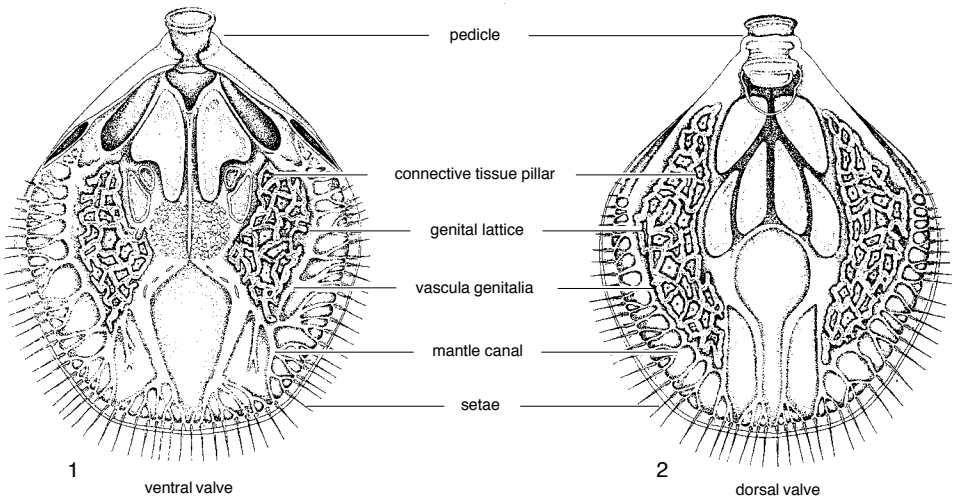

FIG. 132. Diagrammatic surface view of the mantle of the ventral (pedicle) and dorsal (brachial) valves of *Terebratulina retusa,* illustrating the mantle canals and the position and extent of the genital lattice (James, Ansell, & Curry, 1991b).

an acrosome and nucleus, a middle piece containing one or more mitochondria and two centrioles, and a tail (flagellum) (Fig. 141–142).

In *Lingula* (SAWADA, 1973) and probably *Terebratulina* (JAMES, unpublished, 1989), the Golgi complex or smooth endoplasmic reticulum gives rise to the acrosome. In *Lingula,* electron-dense granules are produced by the Golgi complex or smooth endoplasmic reticulum. These granules fuse to form the acrosomal vesicle, which migrates to the definitive pole of the spermatid (SAWADA, 1973). The acrosomal vesicle of *Terebratulina* contains a sparse, finely granular material (JAMES, unpublished, 1989), while in *Lingula* the acrosome contains dense, granular bands (SAWADA, 1973; CHUANG, 1983a). Acrosomes range in size and shape from the subapical, buttonlike acrosome found in *Terebratulina* (AFZELIUS & FERRAGUTI, 1978; JAMES & others, 1992) to the extremely elongate and conical acrosome of *Notosaria* (Fig. 141–142; JAMES, unpublished, 1992).

As spermatozoa mature, the nucleus is transformed from a spherical shape, normal in spermatocytes and young spermatids, to a more compact body (AFZELIUS & FERRAGUTI, 1978; JAMES & others, 1992). During the later stages of spermiogenesis the nuclear material undergoes condensation accompanied by a reduction in nuclear volume, and residual cytoplasm is discharged (SAWADA, 1973; CHUANG, 1983b; JAMES & others, 1992). The chromatin of spermatozoa is generally homogeneous but finely granular in later stages and may include a small but distinct empty space (Fig. 142.4; FRANZEN, 1987). The nuclear envelope also appears to be differentially thickened wherever it is modified to accommodate other organelles within the head of the sperm.

The mitochondrion of *Terebratulina, Calloria, Notosaria,* and *Terebratella sanguinea* enlarges to form an asymmetrical, doughnut shape. *Lingula* and *Neocrania* usually possess six and four spherical mitochondria, respectively, which develop around the base of the nucleus. Both of the centrioles come to lie to the posterior of the cell in the center of the mitochondrial ring. Most invertebrate spermatozoa have two centrioles, the

TABLE 1. Summary of the shapes of gonads of articulated brachiopods (adapted from Chuang, 1983b).

Gonad shape	Family	Species
Unbranched L-shaped	Megathyridae	*Argyrotheca johnsoni*
		A. baretti
Arborescent U-shaped	Terebratellidae	*Terebratella sanguinea*
		Magellania australis
		M. macquariensis
		Terebratella dorsata
		Calloria inconspicua
		Gyrothyris mawsoni
		Neothyris lenticularis
	Dallinidae	*Frenulina sanguinolenta*
		Macandrevia cranium
		Terebratalia transversa
	Laqueidae	*Laqueus californianus*
	Cranidae	*Neocrania anomala*[1]
Reticulate	Hemithyridae	*Hemithiris psittacea*
		Notosaria nigricans[1]
	Frieleidae	*Frieleia halli*
	Terebratulidae	*Liothyrella blochmanni*
		L. notocardensis
		L. neozelanica[1]
		Abyssothyris elongata
		Terebratulina retusa[1]
Ovoid	Basiliolidae	*Neorhynchia profunda*

[1]adapted from James & others, 1992

proximal or anterior and the distal or posterior (FRANZEN, 1987). In *Terebratulina* the proximal centriole is in approximately the same longitudinal axis as the distal one, whereas in *Neocrania* and *Lingula* it is transverse (CHUANG, 1983b). The nucleus may be modified posteriorly by invagination of the nuclear membrane to accommodate the proximal centriole. The distal centriole is oriented longitudinally and associated with the tail (Fig. 143).

The distal centriole of *Terebratulina* is suspended in a complex, fiber-anchoring apparatus with nine primary branches that bifurcate and fuse with their neighbors to form a stellate, satellite-like figure (AFZELIUS & FERRAGUTI, 1978). *Lingula* and *Neocrania* appear to have similar but less complex structures that consist of a series of tubules radiating from the distal centriole (SAWADA, 1973; CHUANG, 1983b). The fiber-anchoring complex is generally thought to be an anchor for the basal body of the tail. It enables the centrioles to resist the torque generated by the movement of the tail. The satellite complex may also transport ATP from the mitochondria to the tail (SUMMERS, 1970). The sperm of *Lingula* contain deposits of glycogen (SAWADA, 1973; JAMES, unpublished, 1993), whereas in *Terebratulina* this storage compound is absent (JAMES & others, 1992). It has been suggested that the energy necessary to drive the swimming activity of sperm that lack glycogen is derived from the oxida-

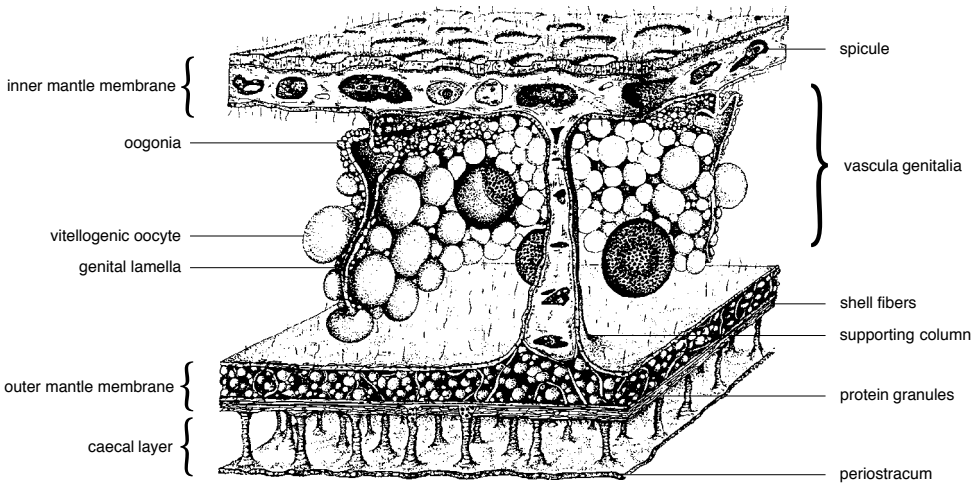

FIG. 133. Diagrammatic representation of a vertical section through the mantle of *Terebratulina retusa* showing part of an ovary and the mantle membranes (James, Ansell, & Curry, 1991b).

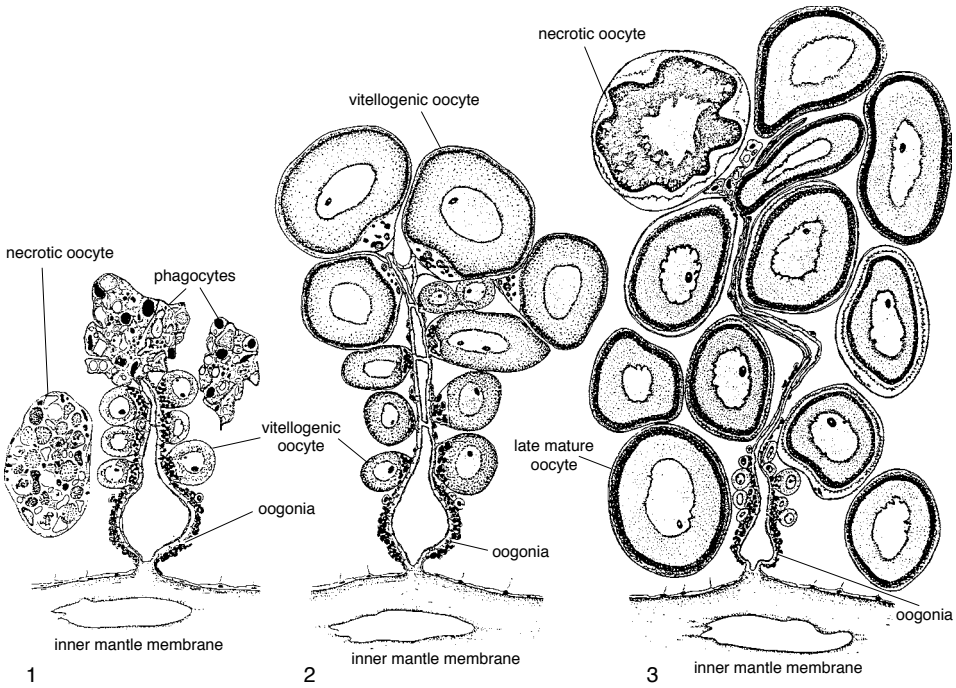

FIG. 134. Diagrammatic series illustrating the changes that occur during the development of the genital lamella and associated oocytes of *Terebratulina retusa; 1,* recently spawned individual; unspawned oocytes and necrotic genital tissues are phagocytosed, while the next generation of vitellogenic oocytes develop beneath; *2,* the genital lamella extends as the vitellogenic oocytes increase in size; *3,* a mature genital lamella; late stage vitellogenic oocytes have separated from the genital lamella and float freely in the *vascula genitalia* where they complete their development prior to spawning (James, Ansell, & Curry, 1991b).

tion of mitochondrial phospholipids (AFZELIUS & MOHRI, 1966).

The tail of the sperm issues from this anchoring complex, initially as peripheral microtubules, the central doublet appearing to originate from a more distal region. Tails of brachiopod sperm contain the familiar 9+2 arrangement of axonemes, but in *Neocrania* the tapering distal portion of the tail contains 9+2 single microtubules (AFZELIUS & FERRAGUTI, 1978).

Spermatozoan structure is generally related to the physiological demands of the fertilization environment (FRANZEN, 1956; AFZELIUS, 1979). Brachiopods have sperm of the ectoaquasperm type (ROUSE & JAMIESON, 1987), which is typical of animals that engage in external fertilization (FRANZEN, 1982). The shape and size of the head of brachiopod sperm, however, vary considerably (Fig. 143; Table 2, p. 144).

OOGENESIS

Precocious germ-cell determination due to the localization of a morphologically distinct germ plasm has been reported in the eggs of a number of invertebrates including brachiopods (see WOURMS, 1987). Primary germ cells are distinguishable by their large size from the coelomic epithelium of the ileoparietal band in *Lingula* larvae at the stage of eight pairs of tentacles (abbreviated p.t. hereinafter) (YATSU, 1902a, used the term: pairs of cirri—p.c.). In *Terebratulina, Calloria, Notosaria* (JAMES, unpublished, 1993), *Lingula* (SCHAEFFER, 1926), *Frenulina,* and other brachiopods studied by CHUANG (1983a), no transitional forms between germ cells and coelomic epithelium have been found, which suggests that primordial germ cells are differentiated early in ontogeny (Fig. 144; YATSU, 1902a; SCHAEFFER, 1926; CHUANG, 1983b; JAMES, ANSELL,

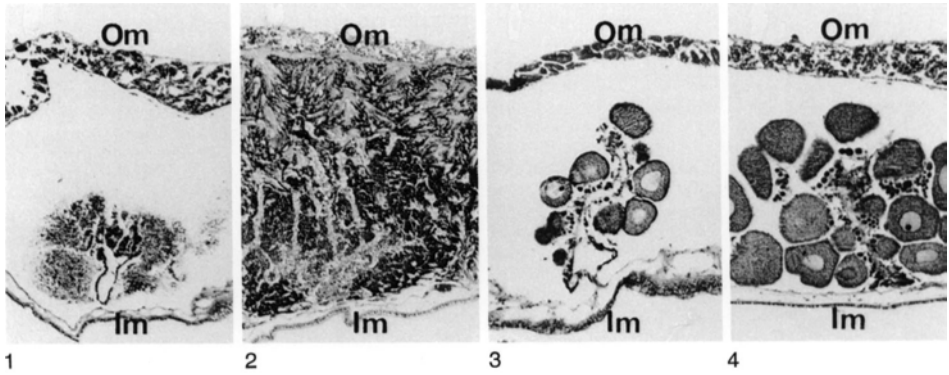

FIG. 135. Light micrographs of transverse sections of *Terebratulina retusa; 1,* immature testis; *2,* mature testis; *3,* immature ovary; *4,* mature ovary, scale bar: 50 μm; *Im,* inner mantle; *Om,* outer mantle (James, Ansell, & Curry, 1991b).

& CURRY, 1991c). A number of earlier reports, however, are contradictory and suggest that germ cells are derived from coelomic epithelium (BEMMELEN, 1883; JOUBIN, 1886; BLOCHMANN, 1892; LONG, 1964).

Primary oogonia occur at the base of the genital lamella proximal to the inner mantle membrane and contain cytoplasm and a nucleus of homogeneous electron density and relatively indistinct organelles (Fig. 145.1; JAMES, ANSELL, & CURRY, 1991c; JAMES, unpublished, 1993). Each cell is separated from its neighbor by the fine cytoplasmic processes of the coelomic epithelial cells. Primary oogonia undergo mitotic division to produce secondary oogonia that in turn divide meiotically to become primary oocytes (JAMES, ANSELL, & CURRY, 1991c). The early prophase changes of meiosis in brachiopod oocytes have not been observed, but all of the oocytes so far studied have been at the diplotene stage, an arrested stage of development, during which the oocyte undergoes vitellogenesis (the accumulation of yolk) (LONG, 1964; JAMES, ANSELL, & CURRY, 1991c; LONG & STRICKER, 1991).

The processes of vitellogenesis have been interpreted for the articulated *Terebratalia transversa* (LONG, 1964), *Frenulina* (CHUANG, 1983a), *Terebratulina* (JAMES, ANSELL, & CURRY, 1991c), *Calloria,* and *Notosaria* (JAMES, unpublished, 1993) and for the inarticulated *Lingula* (SAWADA, 1973; CHUANG, 1983a), *Discinisca,* and *Neocrania* (CHUANG, 1983a). Vitellogenesis has been divided into a series of stages, which have been defined according to the occurrence and distribution of yolk granules (Fig. 146; LONG, 1964; CHUANG, 1983a; JAMES, ANSELL, & CURRY, 1991c) and ultrastructural development of the vitellogenic oocyte and associated cells (Fig. 145; JAMES, ANSELL, & CURRY, 1991c; see summary by JAMES & others, 1992).

Vitellogenic oocytes are usually enveloped by a single layer of several extremely thin follicular cells (JAMES, unpublished, 1993) that are assumed to be modified coelomic epithelial cells (CHUANG, 1983a) and, in some species, may be highly modified (JAMES, unpublished, 1993). CHUANG (1983a) reported the occurrence of several layers of follicular cells in some species. The vitellogenic oocyte is identifiable from an early stage and possesses a nucleus containing condensed chromatin and a conspicuous nucleolus. The ooplasm of early vitellogenic oocytes contains discrete and evenly distributed ribosomes with organelles such as mitochondria and endoplasmic reticulum proliferating in what appear to be defined areas (CHUANG, 1983a; JAMES, ANSELL, & CURRY, 1991c). Small numbers of lipid and membrane-bound, electron-dense (proteina-

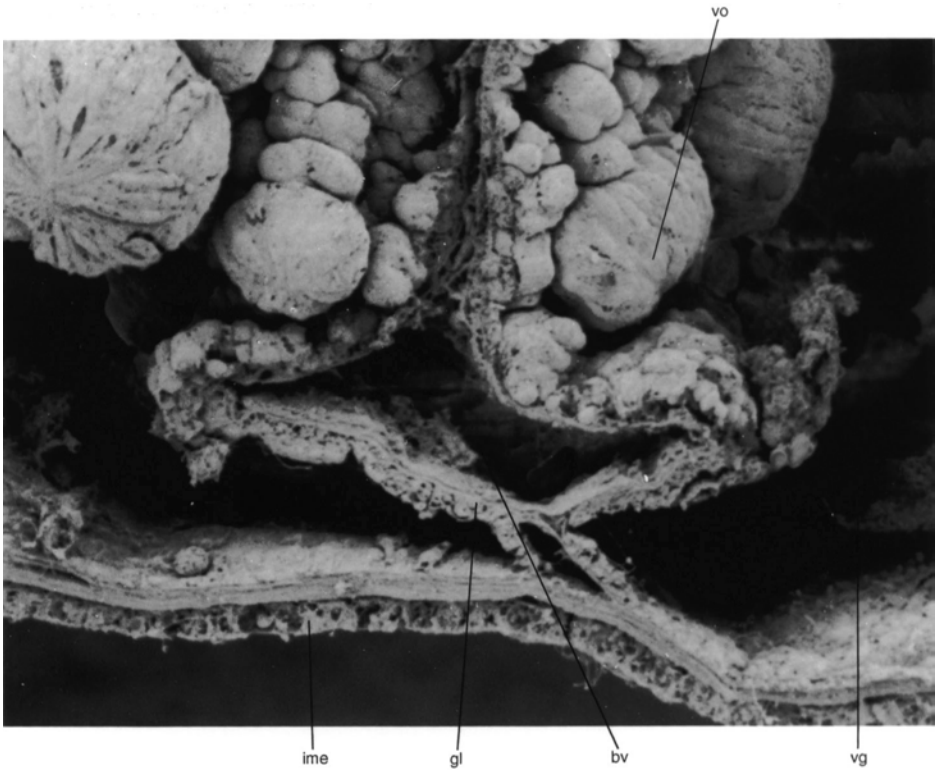

FIG. 136. SEM micrograph of a transverse section through the base of the genital lamella of the ovary of *Dallina septigera,* ×480; *bv,* blood vessel; *gl,* genital lamella; *ime,* inner mantle epithelium; *vg,* vascula genitalia; *vo,* vitellogenic oocyte (new).

ceous) granules may also be present. In regions where the follicle cells are not in close apposition to the surface of the oocyte, sections of the oocyte plasmalemma (oolemma) form simple digitate microvilli. While the order in which these events occur may vary, this pattern of early vitellogenesis has been observed at the ultrastructural level in a number of species, including *Terebratulina, Calloria, Notosaria* (JAMES, unpublished, 1993), and *Frenulina* (CHUANG, 1983a).

Currently available evidence, however, suggests that brachiopods have at least three distinct modes of vitellogenesis, follicular, nutritive, and mixed, which broadly define the mechanisms used to accumulate yolk (SENN, 1934; JAMES, unpublished, 1993) in the following way.

(1) Follicular vitellogenesis has been reported in *Neocrania, Lacazella, Macandrevia cranium, Argyrotheca cuneata, Terebratalia,* and numerous other brachiopods (SENN, 1934; LONG, 1964; LONG & STRICKER, 1991). The ultrastructure of follicular vitellogenic oocytes is unknown, but light microscopy indicates that the follicular cells are unmodified, and the oocyte develops a microvillous surface. Follicular vitellogenic oocytes are not directly associated with nurse or accessory cells (see below).

(2) Nutritive vitellogenesis occurs in *Lingula* (SENN, 1934), *Calloria, Notosaria* (JAMES, unpublished, 1993), and *Frenulina* (Fig. 147.1; CHUANG, 1983a). Vitellogenic oocytes are surrounded by a variably complex follicular envelope that is closely associated with large somatic cells, particularly during the early stages of development. The somatic cells contain a diminutive nucleus and few organelles but are packed with

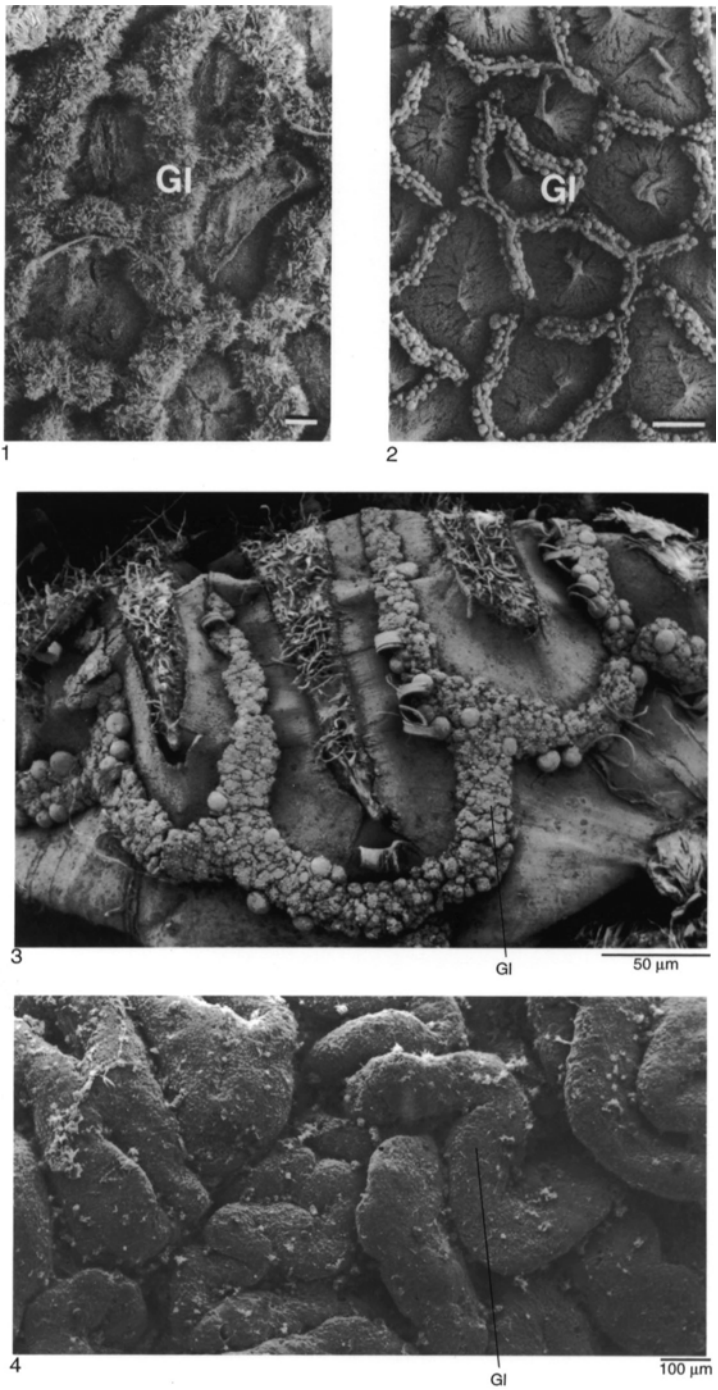

FIG. 137. SEM micrographs of surface views of the genital lamellae (*Gl*) of *1, Terebratulina retusa,* testis, scale bar: 200 µm, *2,* ovary, scale bar: 200 µm (James, Ansell, & Curry, 1991b); *3, Neocrania anomala,* ovary, scale bar: 50 µm; *4, Lingula anatina,* ovary, scale bar: 100 µm (new).

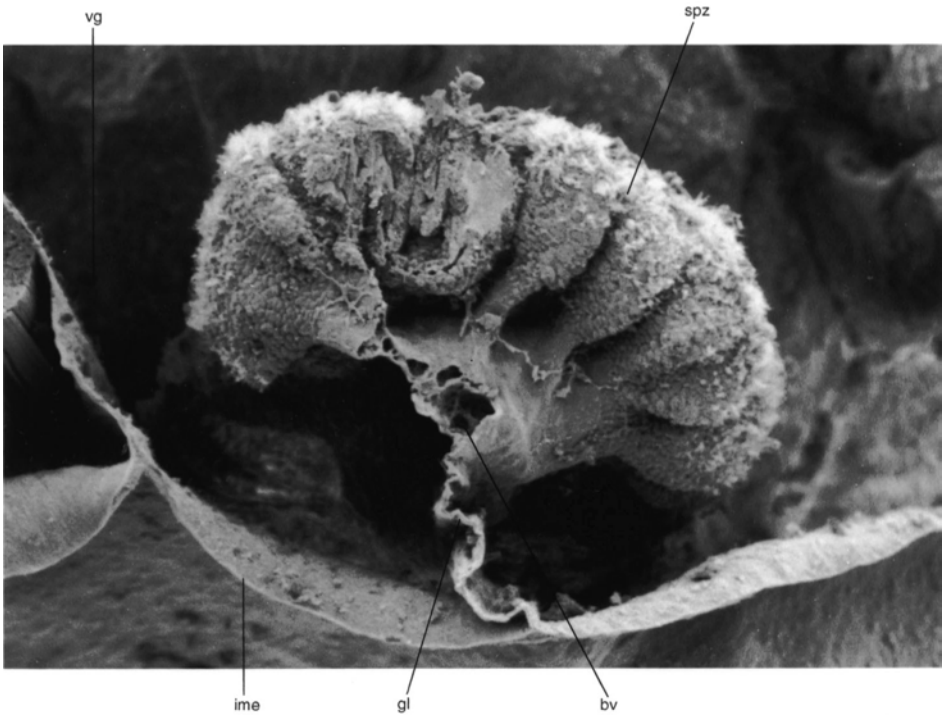

FIG. 138. SEM micrograph of a transverse section through the genital lamella of a male *Dallina septigera,* ×130; *bv,* blood vessel; *gl,* genital lamella; *ime,* inner mantle epithelium; *spz,* spermatozoa; *vg,* vascula genitalia (new).

profuse quantities of glycogen and large, electron-dense granules. These nurse or nutritive cells can be seen most prominently in *Lingula* and *Calloria* where they form a distinctive palisade covering the surface of the genital lamella (Fig. 148).

The oocytes produce dense but simple branched or digitate microvilli of uniform length (Fig. 149). The follicular cells, however, may be modified. In *Calloria, Notosaria, Terebratella* (JAMES, unpublished, 1993), and *Lingula* (SAWADA, 1973), the follicular cells produce papillose extensions of their inner plasmalemma, which attach to the surface of the oocyte with desmosome-like gap junctions (Fig. 147.1; 149.1). Dense concentrations of glycogen may occur both within the follicular cells and between the microvilli of the oocyte and the follicular cells. Oocytes of this type, however, have not been observed to engage in pino- or endocytosis (CHUANG, 1983a). In addition to papillose connections between the follicular cells and the vitellogenic oocyte, *Lingula* has serially banded strands that pass between the microvilli of the oocyte and the surrounding follicular cells (SAWADA, 1973). These strands form a fibrous matrix around the oocyte, but their function is unknown (Fig. 150).

Based on morphological evidence, the complex follicular cells are presumed to play a role in the synthesis of heterosynthetic yolk precursors or to regulate the transfer of these materials to the vitellogenic cell.

(3) Mixed vitellogenesis has been observed only in the terebratulids *Terebratulina* (JAMES, ANSELL, & CURRY, 1991c) and *Gryphus vitreus* (Fig. 147.2; BOZZO & others, 1983). Vitellogenic oocytes of *Terebratulina* develop in association with a series of accessory cells within an envelope of follicular cells, the follicular capsule (Fig. 145, 151).

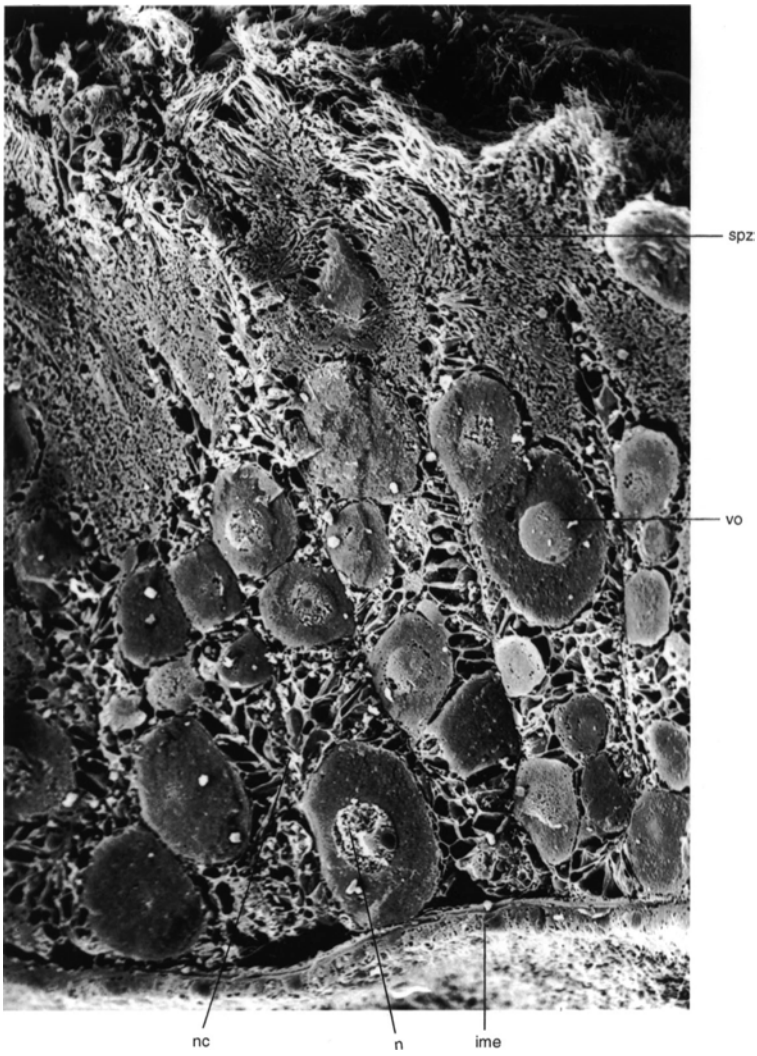

FIG. 139. SEM micrograph of a transverse section through the hermaphroditic gonad of *Calloria inconspicua,* ×300; *ime,* inner mantle epithelium; *n,* nucleus; *nc,* nutritive cells; *vo,* vitellogenic oocyte (new).

The origin of accessory cells is unclear, but they are capable of proliferation and resemble small, vitellogenic oocytes. Accessory cells communicate with other accessory cells and the vitellogenic oocyte via desmosome-like gap junctions. Cytoplasmic bridges may also occur between accessory cells (JAMES, ANSELL, & CURRY, 1991c).

The function of accessory cells appears to be to supply the vitellogenic oocyte with nutrients, probably low-molecular-weight yolk precursors, which are first synthesized in the accessory cell. In contrast to the less complex microvillous surface of oocytes engaged in follicular or nutritive vitellogenesis, the surface of the mixed vitellogenic oocyte is elaborated into a series of troughs and crests covered in highly modified microvilli (Fig. 152). Beneath the modified microvilli, the oolemma endocytoses yolk precursors. The enveloping follicular capsule consists of simple, follicular cells that make no connection with the vitellogenic oocyte. During the initial stages of vitellogenesis, accessory cells

proliferate and begin to accumulate small numbers of yolk granules, while the surface of the vitellogenic oocyte becomes sparsely microvillous. As vitellogenesis proceeds, the density and complexity of the microvilli increase until the microvilli effectively dissociate from the surface of the cell to form a characteristic pattern of crests and troughs (Fig. 152.2–152.3). The accessory cells gradually diminish in both size and number. Eventually the follicular capsule containing the vitellogenic oocyte and the remaining accessory cells is released from the genital lamella (JAMES, ANSELL, & CURRY, 1991c).

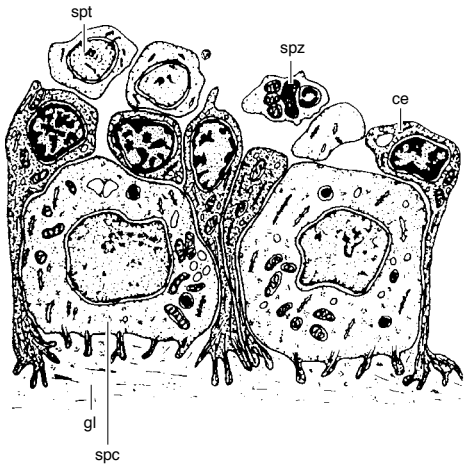

FIG. 140. Drawing of the genital lamella (*gl*) with coelomic epithelium (*ce*), spermatocyte (*spc*), spermatid (*spt*), and spermatozoon (*spz*). Note the pedal processes of cells attached to the genital lamella (adapted from Chuang, 1983b).

YOLK

Invertebrate carbohydrate yolk reserves include glycogen, galactogen, and various polysaccharide-protein complexes. Lipid reserves include fatty yolk globules, phospholipids, and triglycerides. Protein accumulations occur in the form of membrane-bound inclusions or platelets, lipoproteins, phosphoproteins (e.g., vitellogenins), and protein polysaccharide complexes (WOURMS, 1987). The biochemical nature and synthesis of brachiopod yolk is not well known.

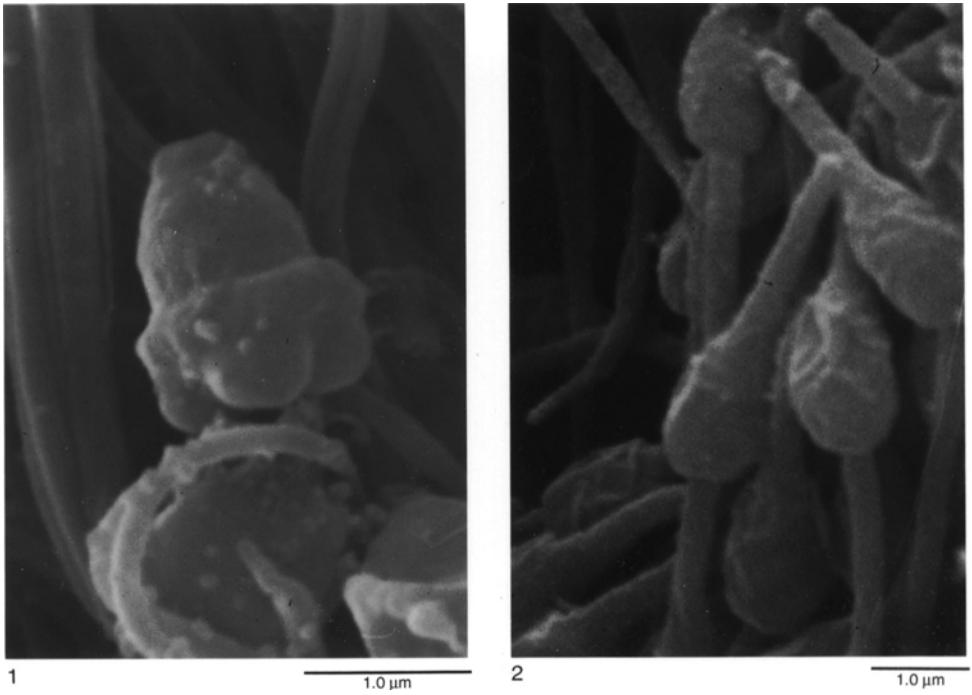

FIG. 141. SEM micrograph of sperm heads of *1, Lingula anatina,* scale bar: 1.0 µm; *2, Notosaria nigricans,* scale bar: 1.0 µm (new).

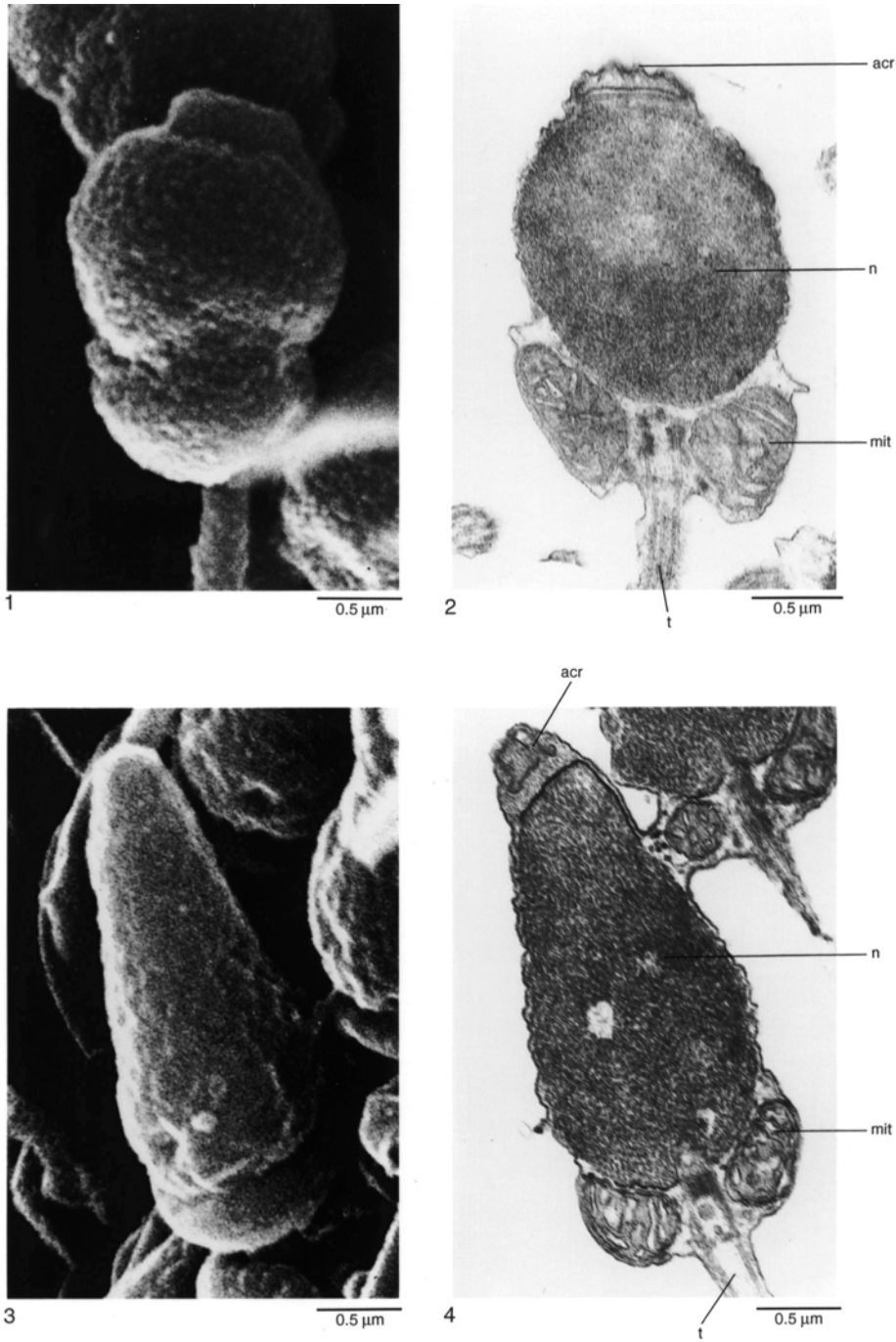

FIG. 142. SEM and TEM micrographs of sperm heads of *1–2, Terebratulina retusa,* scale bar: 0.5 µm; *3–4, Calloria inconspicua,* scale bar: 0.5 µm; *acr,* acrosome; *mit,* mitochondrion; *n,* nucleus; *t,* tail (new).

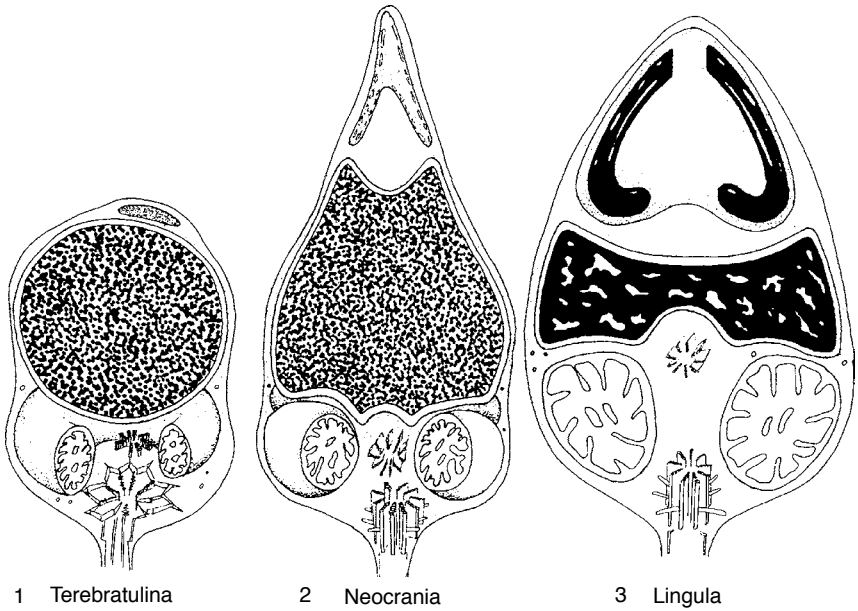

FIG. 143. Drawings of the spermatozoa of *1, Terebratulina retusa, 2, Neocrania anomala,* and *3, Lingula anatina* (adapted from Afzelius & Ferraguti, 1978; Chuang, 1983b).

Typically, yolk contains lipid droplets or granules, proteinaceous membrane-bound granules, cortical granules, glycogen, and a suite of cellular organelles that, if not involved directly in yolk synthesis, are stored for use after the egg has been fertilized. Glycogen is a prominent constituent of the ooplasm of *Terebratulina* (JAMES, ANSELL, & CURRY, 1991c), *Calloria, Notosaria,* and *Lingula* (JAMES, unpublished, 1993).

Lipid droplets or granules form a significant proportion of the volume of the yolk of brachiopods (LONG, 1964; CHUANG, 1983a; JAMES & others, 1992). In *Terebratalia* this lipid is believed to be neutral and not phosphorylated (LONG, 1964). Lipid granules or droplets lack a limiting membrane and are often enveloped by profiles of endoplasmic reticulum (Fig. 153; JAMES, ANSELL, & CURRY, 1991c).

As brachiopod oocytes mature, cortical granules form a distinctive band at the periphery of the oocyte. Cortical granules are membrane bound with either uniformly electron-dense contents, as in *Terebratulina,* or a structured, internal matrix, as seen in *Terebratella* and *Gryphus* (Fig. 154; BOZZO & others, 1983). The cortical granules of *Terebratalia* contain tyrosine, basic amino acids, and sulphydryl groups (Chevremont method) but do not stain for nucleic acids or with Periodic Acid Schiffs (PAS) (LONG, 1964). In *Terebratulina,* cortical granules have a proteinaceous component and give a positive reaction with PAS. Other proteinaceous yolk granules, which are distributed throughout the ooplasm, are also bounded by a continuous membrane. It has been suggested that some of these proteinaceous granules undergo a process of maturation and migration to become cortical granules (JAMES & others, 1992). Cortical granules are usually involved in the formation of a fertilization membrane at the time of penetration by the sperm. The function of cortical granules in brachiopods, however, is unclear. The cortical granules of *Terebratalia* (LONG & STRICKER, 1991), for example, are

TABLE 2. Summary of data of spermatozoan morphology (new).

Species	Head shape	Head length (μm)	Tail length (μm)	Number of mitochondria	Type of mitochondria	Authority
Terebratulina retusa	bullet	2.3	50	1	doughnut	Afzelius & Ferraguti, 1978
T. unguicula		1.9	30			Long, 1964
Notosaria nigricans	elongate	3.8		1	doughnut	James, unpublished
Hemithiris psittacea	elongate	4.3[1]	30			Long, 1964
Calloria inconspicua	conical	3.0		1	doughnut	James, unpublished
Terebratella sanguinea	bullet	2.0		1	doughnut	James, unpublished
Terebratalia transversa		2.1	30			Long, 1964
Neocrania anomala	conical	3.0		4–5	spherical	Chuang, 1983
Lingula anatina	conical	2.0	40	5–7	spherical	Senn, 1934

[1]4.3 μm long using light microscopy; noted a 2.2 μm acrosomal so-called filament in addition to the 2.1 μm head.

not discharged during fertilization but are retained near the surface of the ectodermal cells until late in the life of the larva. The origin, biochemical composition, and function of these nonsecretory, cortical granules are unknown (SCHEUL, 1978).

Ribosomes are also conspicuous components of the ooplasm, particularly during the

FIG. 144. TEM micrograph of the base of the genital lamella of *Notosaria nigricans* showing the discontinuity between the coelomic epithelium and the mass of proliferating gametes, ×2,184; *bv,* blood vessel; *fc,* follicular cell; *gl,* genital lamella; *n,* nucleus; *oog*, oogonia; *vo,* vitellogenic oocyte (new).

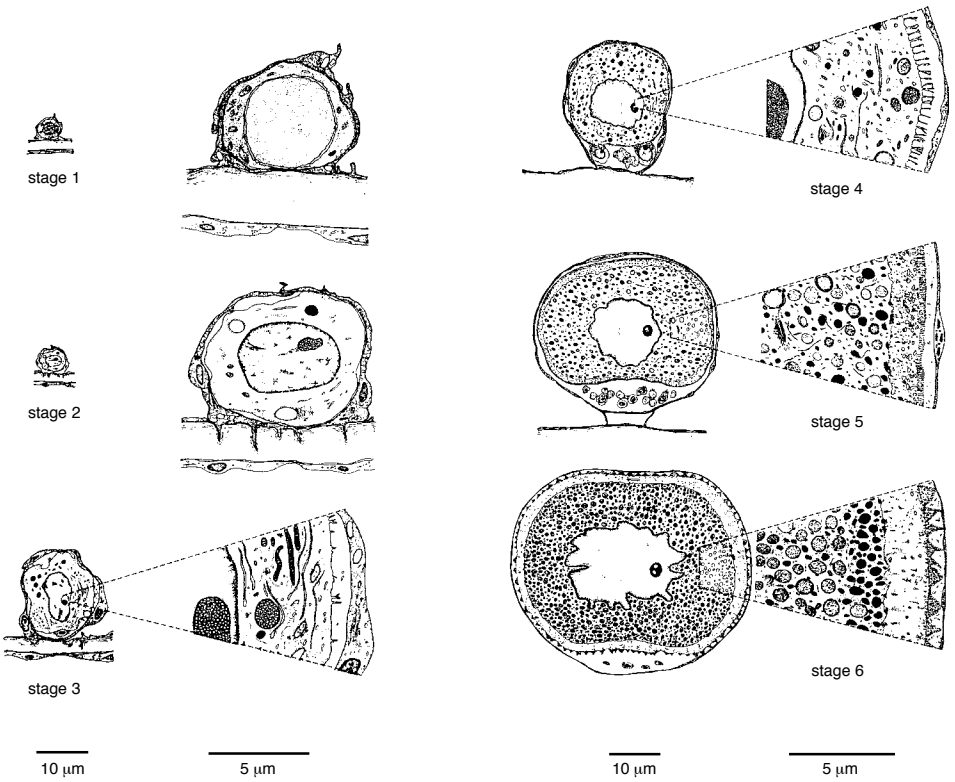

FIG. 145. Diagrammatic representation of stages 1 to 6 of vitellogenesis in *Terebratulina retusa* with all or a portion of each stage on the right enlarged to show features of the ooplasm and the microvillous fringe. Stages 1 to 5 are attached to the genital lamellae; stage 6 oocytes float freely in the *vascula genitalia,* and continue to increase in size; all stages are enveloped by follicular cells and each stage is marked by increasing complexity of the microvillous border of the vitellogenic oocyte; at stages 3 and 4, accessory cells appear and begin to proliferate; *darker granules* in the ooplasm represent proteinaceous and ultimately cortical granules in stage 6 oocytes; *lightly shaded granules* represent lipid granules (adapted from James, Ansell, & Curry, 1991c).

early stages of vitellogenesis (LONG, 1964; CHUANG, 1983a; JAMES, ANSELL, & CURRY, 1991c).

COELOMOCYTES

In addition to the complement of nurse and accessory cells found in the gonads of many brachiopods, coelomocytes also occur. Coelomocytes, in the form of phagocytes and trophocytes, play an integral role in the process of gametogenesis, resorbing necrotic tissue and supplying the gametes, particularly developing sperm, with nutrients (SAWADA, 1973; CHUANG, 1983b; JAMES & others, 1992). Dense concentrations of coelomocytes periodically occur along the distal edge of the genital lamella of articulated brachiopods (JAMES, ANSELL, & CURRY, 1991b; JAMES & others, 1992) or may become invested among developing gametes (Fig. 155). Coelomocytes appear to be most abundant in the gonads immediately after spawning and during the early stages of gametogenesis (SAWADA, 1973; CHUANG, 1983a; JAMES, ANSELL, & CURRY, 1991c) but are often present throughout gametogenesis (CHUANG, 1983a). The distal margins of the genital lamella of *Terebratulina* and a number of other species can be traced by the presence of a concentration of droplets or granules, often pigmented red to orange in *Terebratulina*. These cells are highly pleomorphic and often contain conspicuous, probably digestive vacuoles, suggesting their ability to

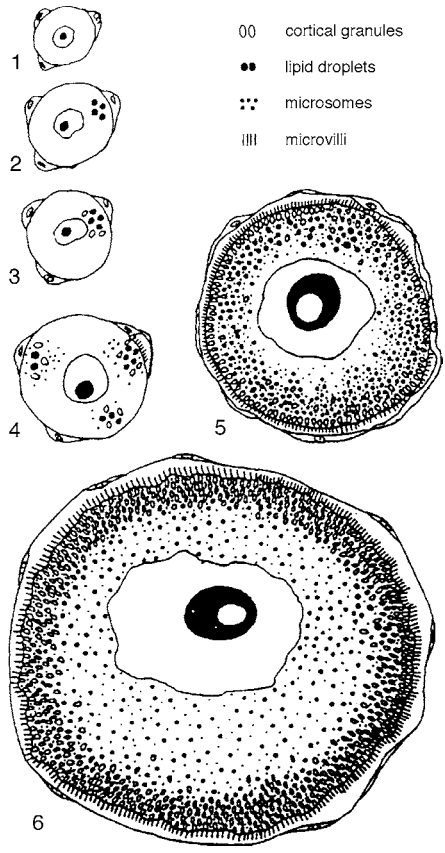

FIG. 146. Six stages of oogenesis in *Frenulina sanguinolenta; 1,* stage 1, oocytes without any lipid droplets or cortical granules; *2,* stage 2, oocyte with a few lipid droplets; *3,* stage 3, oocyte with a few lipid droplets and cortical granules; *4,* stage 4, oocyte with several groups of lipid droplets, cortical granules, and microsomes; *5,* stage 5, oocytes with random distribution of lipid droplets, cortical granules, and microsomes; *6,* stage 6, mature oocyte (adapted from Chuang, 1983a).

phagocytose necrotic tissue and perhaps act as part of an immune system (Fig. 155). Mature ova that are not spawned become necrotic and are resorbed in the ovary. Absorption of oocytes in *Frenulina* has been observed to occur in flattened cells that engulf small spheres of fragmented oocyte and large subspherical cells (CHUANG, 1983a). In *Terebratulina,* degradation of oocytes occurs while the oocyte is contained within the follicular capsule. The first sign of necrosis in the mature oocyte is that the nuclear envelope becomes highly convoluted and breaks down. Necrosis proceeds, producing an uneven distribution of ooplasm with regions devoid of inclusions. Finally the ovum breaks down into a number of unaltered but condensed fragments of ooplasm, and the follicular envelope degrades (JAMES, ANSELL, & CURRY, 1991c).

Trophocytes (nutritive cells) are common in the testes of many species of brachiopods and appear to supply the masses of spermiogenic and spermatogenic cells with nutrients (SAWADA, 1973; JAMES, ANSELL, & CURRY, 1991c; JAMES & others, 1992). In *Lingula,* nutritive cells are distinguished by the presence of lipid droplets of low electron density and granules of greater electron density (SAWADA, 1973). The nutritive cells of *Terebratulina* and *Calloria* contain glycogen and aggregations of lipid granules. Spermatids and spermatozoa can often be found with their heads touching the trophocyte or are oriented with their heads pointing toward the trophocyte (Fig. 156).

Spawning and Reproductive Strategies

Mature gametes are no longer attached to the genital lamella, having completed their development within the coelomic fluid of the *vascula genitalia* or body cavity. During spawning mature gametes are transported in coelomic fluid by strong ciliary currents generated by the metanephridia into the nephridial funnel where they leave the body cavity via the nephridiopores (HANCOCK, 1859; MORSE, 1873; CHUANG, 1983a, 1983b; JAMES, ANSELL, & CURRY, 1991b). The release of gametes is presumed to be assisted by increased pressure of the visceral fluid caused by muscular contractions (CHUANG, 1983a, 1983b).

Free-spawning brachiopods discharge their mature gametes via the densely ciliated metanephridia into the mantle cavity from which the gametes are expelled into the sur-

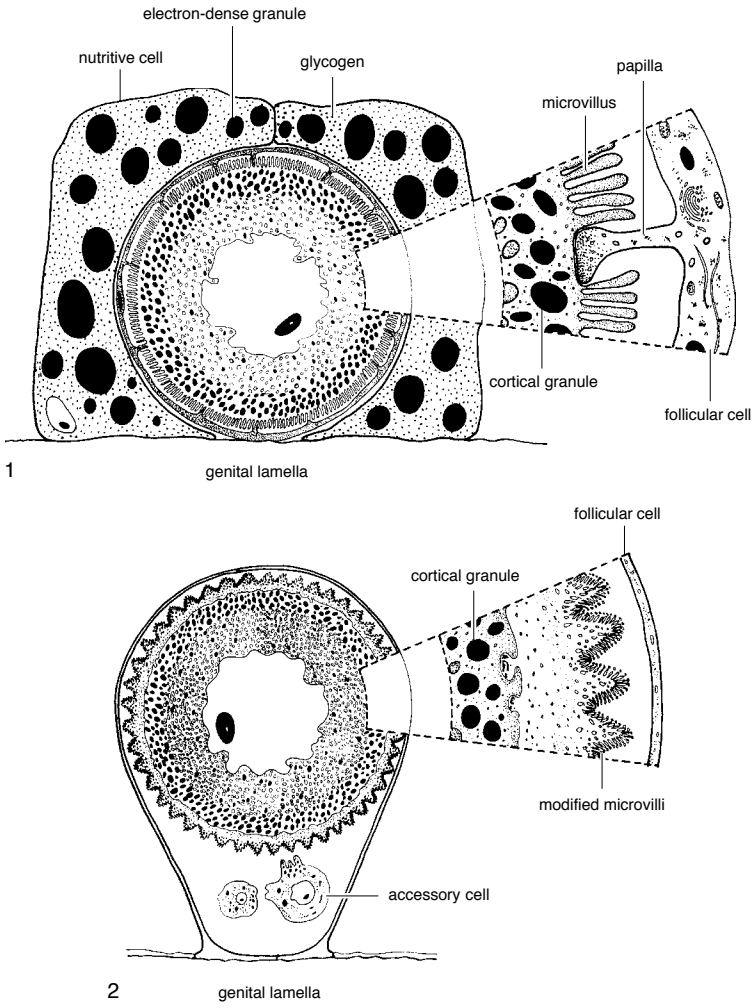

FIG. 147. Diagrammatic representation of oocytes undergoing *1,* nutritive vitellogenesis, and *2,* mixed vitellogenesis; to the right of each diagram is an enlarged portion to show the relationship between the follicular cell and the surface of the vitellogenic oocyte (new).

rounding water in the exhalant current generated by the lophophore. In *Lingula* (CHUANG, 1959a) and *Glottidia* (PAINE, 1963), spawning occurs in bursts, and females may release several thousand eggs per day. In *Terebratulina retusa,* spawned eggs are more dense than seawater and are deposited close to the female (JAMES & others, 1992). CHUANG (1959a) reports that *Lingula* will spawn in isolation, but *T. retusa* spawn synchronously (JAMES & others, 1992). Little is known of those factors that intitiate spawning in brachiopods, but spawning could be mediated by such environmental time cues as spring tides (PAINE, 1963), day length (KUME, 1956; PAINE, 1963), or temperature (CURRY, 1982). Ripe specimens of *T. retusa* can be induced to spawn *in vitro* by the introduction of sperm (CURRY, 1982; JAMES & others, 1992).

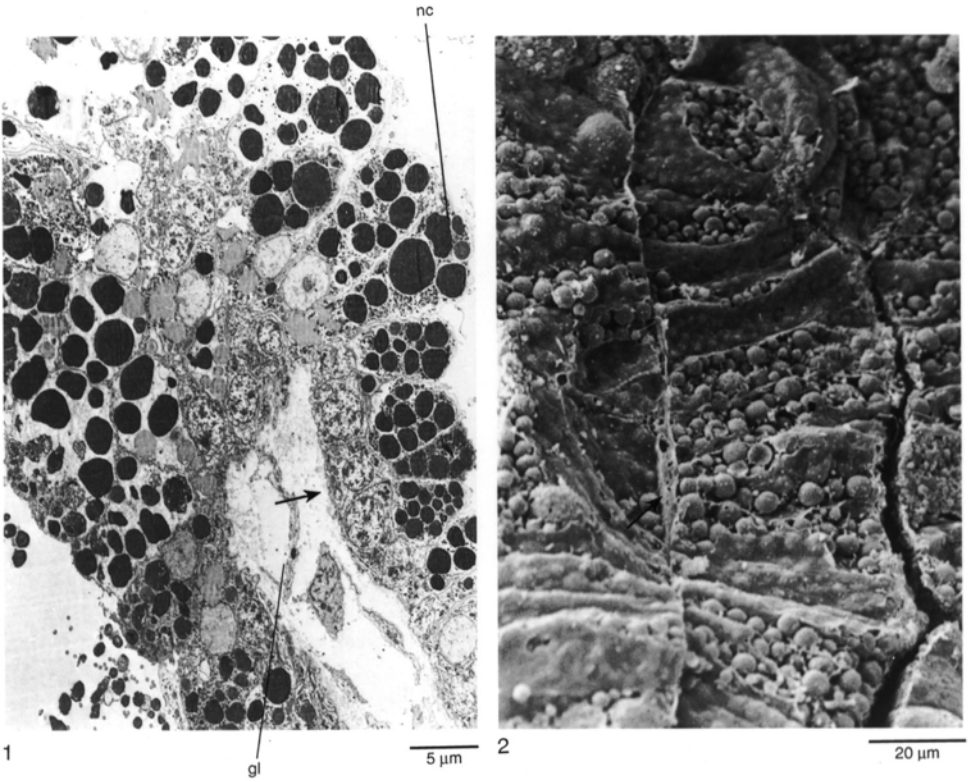

FIG. 148. TEM and SEM micrographs of the genital lamella (*gl*) and nurse cells (*nc*) in *1, Calloria inconspicua; arrow* indicating an early stage vitellogenic oocyte, scale bar: 5.0 µm; *2, Lingula anatina; arrow* indicating genital lamella, scale bar: 20 µm (new).

Liothyrella uva antarctica (BLOCHMANN, 1906), *Pumilus* (RICKWOOD, 1968), *Calloria* (PERCIVAL, 1944), *Notosaria* (PERCIVAL, 1960), *Hemithiris psittacea, Terebratulina unguicula* (LONG, 1964), and *T. septentrionalis* (WEBB, LOGAN, & NOBLE, 1976) retain their eggs within the mantle cavity where larval development takes place within the confines of the lophophore (see section on embryology and development, p. 151). Other brooding species deliver their eggs into specialized brood chambers. *Lacazella* possesses a single median pouch behind the mouth where modified tentacles with collars of large cells at the base of the swollen tip are inserted, thus providing an attachment site for the larvae (Fig. 173; LACAZE-DUTHIERS, 1861). Similar brooding occurs in *Gwynia capsula* (SWEDMARK, 1967). Some *Argyrotheca* have brood pouches formed from modified metanephridia (SHIPLEY, 1883; SCHULGIN, 1885; ATKINS, 1960b; KOWALEVSKY, 1974).

Few accurate accounts of brachiopod reproductive cycles exist. Most reports rely upon superficial analysis of the gonads or the detection of planktonic larva or juveniles. A summary of brachiopod reproductive cycles together with relevant corroborative information is provided in Table 3, p. 158–159.

FIG. 149. SEM and TEM micrographs of transverse sections *1–2,* of the margin and *3,* surface view of a vitellogenic oocyte of *Calloria inconspicua,* scale bars: 2.0 µm; *cg,* cortical granule; *fc,* follicular cell; *mv,* microvilli; *pa,* point of attachment of follicular cell papilla; *pp,* papilla (new).

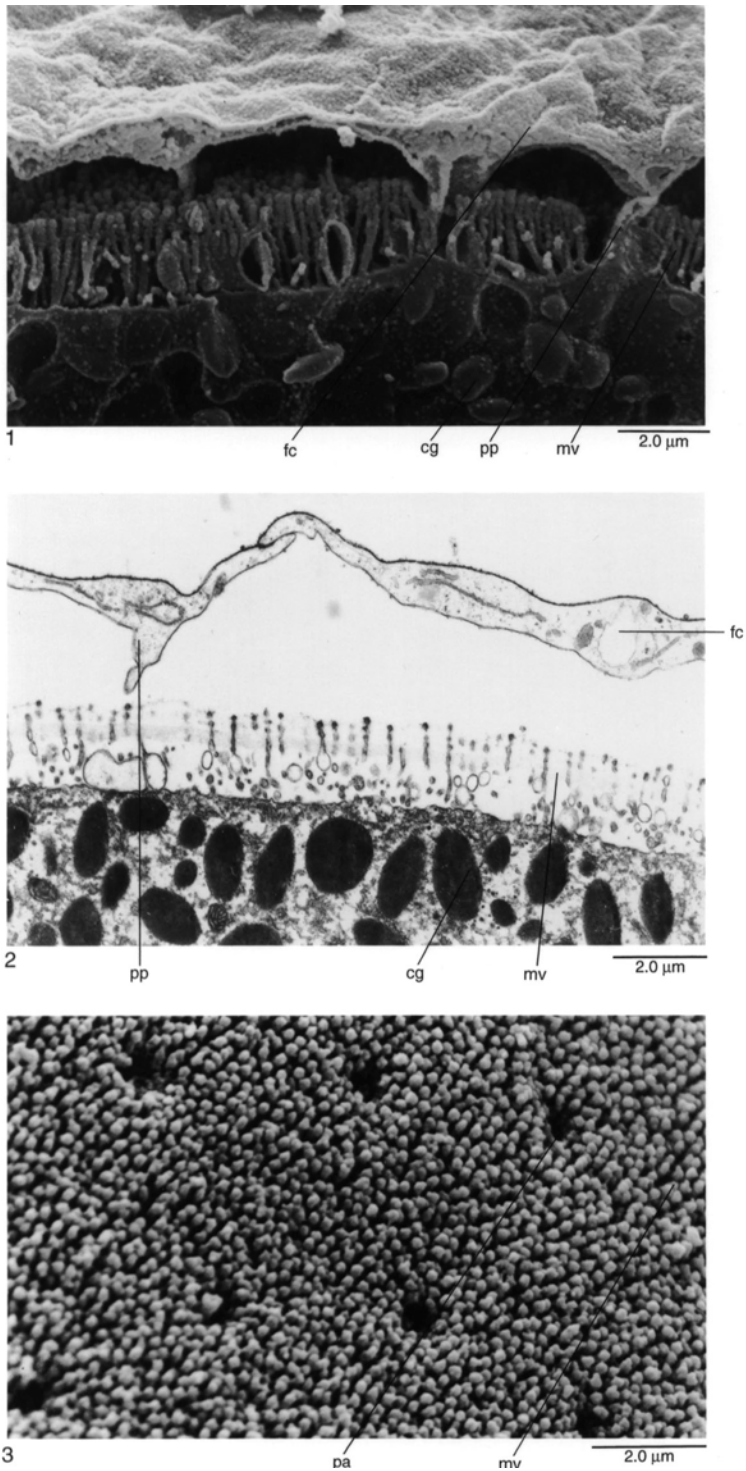

FIG. 149. *For explanation, see facing page.*

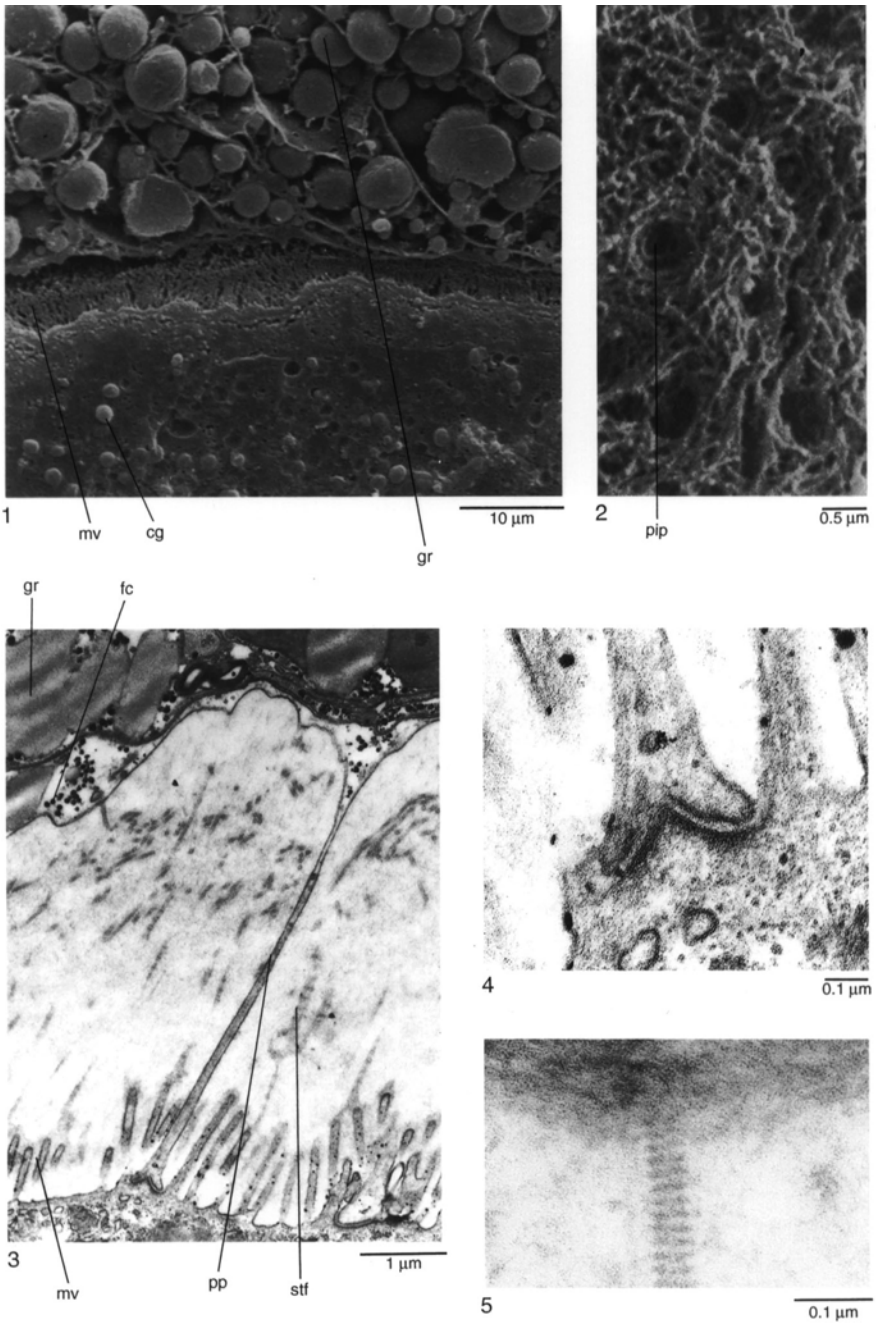

FIG. 150. SEM and TEM micrographs of *1, 3–5,* transverse sections of the margin and *2,* surface view of a vitellogenic oocyte of *Lingula anatina; 1,* the oocyte is surrounded by nutritive cells containing electron-dense granules, scale bar: 10 µm; *2,* the surface of the oocyte is covered with a dense fibrous matrix, scale bar: 0.5 µm; *3,* the follicular cell produces papillae that attach to the surface of the oocyte, scale bar: 1 µm; *4,* desmosome-like junctions form between the follicular cell papillae and the oocyte, scale bar: 0.1 µm; *5,* striated fibers appear to form a matrix around the vitellogenic oocyte (shown in *2*), scale bar: 0.1 µm; *cg,* cortical granules; *fc,* follicular cell; *gr,* electron-dense granules; *mv,* microvilli; *pip,* point of insertion of papilla; *pp,* papilla; *stf,* striated fibers (new).

The size of mature oocytes is relatively conservative within species (Table 4, p. 160), but fecundity may vary (see JAMES, ANSELL, & CURRY, 1991a), possibly because of disparity in the size of the individuals censused, genetic variation, or perhaps differences in availability of food. *Neocrania* and articulated brachiopods produce eggs that give rise to lecithotrophic larvae and, in this respect, have adopted a conservative reproductive strategy. Compared to other sessile marine invertebrates, they produce relatively small numbers of well-provisioned, lecithotrophic eggs, with the duration of the free-swimming larval phase ranging from hours to a few days (Fig. 157; see also section on embryology and development below). Micromorphic brachiopods produce very few eggs, which are retained within the adult and brooded; and well-developed motile larvae are released, which probably settle close to the adult. Larger species of brachiopods are more fecund, and both free-spawning and brooding strategies may occur even within genera: *Terebratulina retusa* is free spawning (CURRY, 1982; JAMES, ANSELL, & CURRY, 1991a, 1991b, 1991c), but *T. septentrionalis* (WEBB, LOGAN, & NOBLE, 1976) and *T. unguicula* (LONG, 1964) brood. Hermaphroditism tends to be a reproductive strategy that results from the isolation of a population or a size constraint on fecundity (GIESE, PEARSE, & PEARSE, 1987). All those brachiopods known to be hermaphrodites also brood their larvae (Table 4, p. 160; Fig. 157). *Calloria* displays a remarkable degree of reproductive plasticity, with individuals having apparently separate sexes or containing a predominance of either male or female reproductive tissue. Similar flexibility in the mode of reproduction can also be found within genera: *Lacazella* sp. and *Thecidellina* from Jamaica are hermaphroditic (JAMES, unpublished, 1987), while *L. mediterranea* from Naples is gonochoristic (LACAZE-DUTHIERS, 1861). *Argyrotheca jacksoni* from Jamaica is gonochoristic (JAMES, unpublished, 1987), but *A. cuneata* and *A. cordata* from Naples are hermaphroditic (SENN, 1934). *Lingula* and *Glottidia* in particular produce relatively large numbers of eggs. Lingulids and discinids produce eggs that develop into planktotrophic larvae, which may persist in the plankton for prolonged periods and travel over considerable distances (see section on embryology and development below).

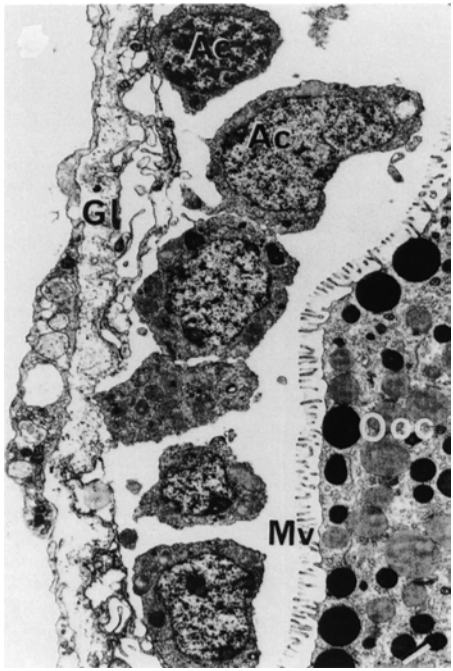

FIG. 151. SEM and TEM micrographs of accessory cells within the follicular capsule of a vitellogenic oocyte in *Terebratulina retusa;* accessory cells (*Ac*) proliferate during the early stages of vitellogenesis between the oocyte (*Ooc*) and genital lamella (*Gl*); early vitellogenic oocytes produce simple digitate microvilli (*Mv*), scale bar: 1.0 μm (James, Ansell, & Curry, 1991c).

EMBRYOLOGY AND DEVELOPMENT

The embryology of the Brachiopoda is pivotal to understanding their phylogeny. Apart from resolving basic questions of affinity, embryological studies should clarify many misconceptions including the view that the brachiopods represent the dichotomy between two fundamental lineages of animal development, the Protostomia and the Deuterostomia. The embryological development of a number of inarticulated and articulated brachiopods has now been

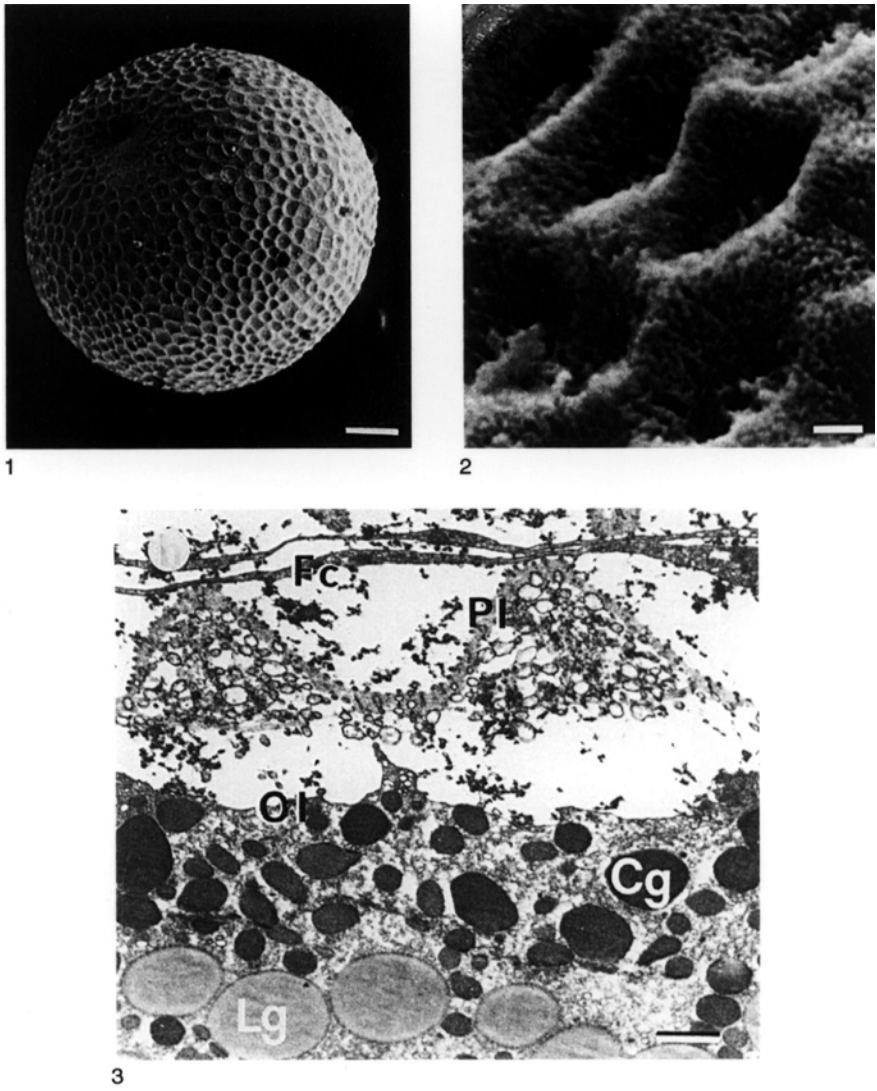

FIG. 152. SEM and TEM micrographs of a late-stage vitellogenic oocyte of *Terebratulina retusa; 1,* entire oocyte covered in follicular cells, scale bar: 20 μm; *2,* surface view of the mature oocyte without follicular cells, scale bar: 10 μm; *3,* periphery of late mature vitellogenic oocyte with convoluted microvillous fringe and containing membrane-bound microdroplets, scale bar: 1.0 μm; *Cg,* cortical granules; *Fc,* follicular cell; *Lg,* lipid inclusions; *Ol,* oolemma; *Pl,* glycocalyx (James, Ansell, & Curry, 1991c).

studied in varying detail, producing conflicting reports and introducing somewhat confusing and inconsistent terminology. In the following sections an attempt will be made to rationalize this terminology, and the salient developmental features will be reviewed.

Among inarticulated brachiopods, the embryology and development of *Lingula anatina* (YATSU, 1902a), early stages of *Glottidia pyramidata* (PAINE, 1963), and the craniid *Neocrania anomala* (NIELSEN, 1991) have been studied in detail, although a number of descriptions of planktonic larvae also

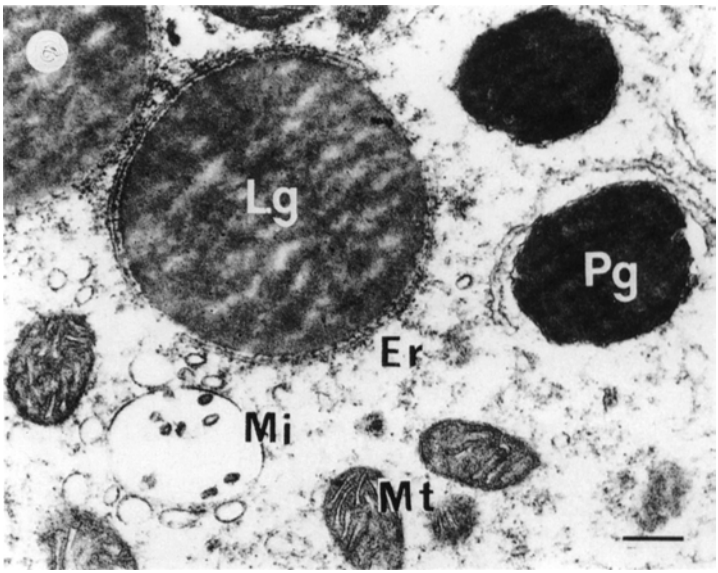

FIG. 153. TEM micrograph of yolk in a vitellogenic oocyte of *Terebratulina retusa* with mitochondria (*Mt*) and agranular endoplasmic reticulum (*Er*) in close association with lipid inclusions (*Lg*) and protein granules (*Pg*); coalescent microsomes (*Mi*) also occur, scale bar: 0.25 μm (James, Ansell, & Curry, 1991c).

exist (see Table 3, p. 158–159). Among the articulated groups, the embryology of *Terebratulina septentrionalis* (CONKLIN, 1902), *Calloria inconspicua* (PERCIVAL, 1944), *Notosaria nigricans* (PERCIVAL, 1960), *Terebratulina retusa* (FRANZEN, 1969), and *Terebratalia transversa* are best known (LONG, 1964; LONG & STRICKER, 1991).

MAIN FEATURES

Prior to fertilization, a number of structural and chromosomal changes of the gametes must take place in order for fertilization to be successful. The union of a mature ovum and a spermatozoon results in the formation of a zygote, which develops a fertilization (vitelline) membrane.

The zygote subsequently undergoes cleavage. Repeated cell divisions create a hollow ball of cells, the blastula (coeloblastula), which by a process of gastrulation by invagination (emboly) forms the gastrula. At this stage, the invaginated cells become the endoderm and the outer cells the ectoderm. The endoderm of the gastrula forms a chamber or archenteron, which gives rise to a third cell line, the mesoderm, within which a cavity or coelom is created. The archenteron opens to the exterior through the blastopore, which eventually closes.

In articulated brachiopods, closure of the blastopore has been used to define the transition from embryo to larva and, for lingulids, the escape of the embryo from the fertilization membrane (hatching or eclosion) (Fig. 158; CHUANG, 1990). In the free-swimming planktonic phases of the lingulids, the widely accepted term larva has also been replaced by juvenile (LONG & STRICKER, 1991). For comparative and practical purposes, however, it is desirable to standardize the terminology for both articulated and inarticulated developmental stages. Although the free-swimming stages of lingulids and discinids can quite legitimately be defined as precocious juveniles (LONG & STRICKER, 1991), the free-swimming stages of *Neocrania* and articulated brachiopods have also been described as embryos. Herein, all stages of development that occur within

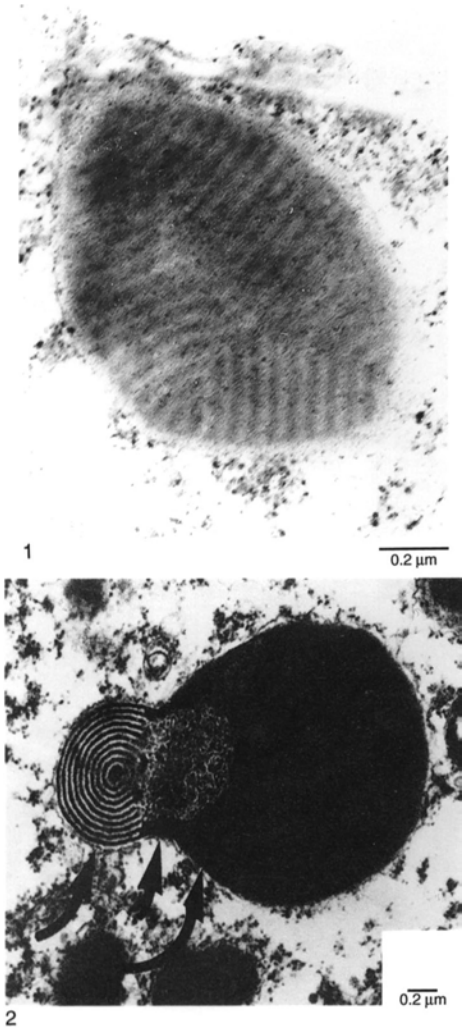

FIG. 154. TEM micrograph of cortical granules of *1, Terebratella sanguinea,* scale bar: 0.2 µm (new); *2, Gryphus vitreus,* scale bar: 0.2 µm; *arrows* indicate three distinct regions of cortical granule (Bozzo & others, 1983).

the fertilization membrane prior to hatching will be referred to as embryos, and subsequent presettlement stages will be regarded as larvae, which may include free-swimming or brooded stages. Early settled stages are referred to as postlarvae or juveniles (Fig. 158).

Size alone is an unreliable measure of development (YATSU, 1902a; CHUANG, 1990), and larval stages are defined in inarticulated species and to some extent in articulated species by the number of pairs of lophophoral tentacles.

Larval stages of articulated groups are less well defined. The lophophore is a postlarval development in articulated groups, and the formation of anterior, mantle, and pedicle lobes, the closure of the blastopore, and the occurrence of setal bundles are all used to define the stage of larval development. The larval stage terminates at settlement (CHUANG, 1990), when the postlarval or juvenile stage begins, involving growth and ultimately the attainment of sexual maturity.

The manner in which the cells or blastomeres cleave during early embryonic development, the origins of the mesoderm, formation of the coelomic cavities, and the position of the definitive mouth relative to the position of the closed blastopore determine embryological classification for protostomes and deuterostomes. Reports of brachiopod embryology refer to both enterocoelic and schizocoelic development (NIELSEN, 1991), and until more information is available no review can resolve this ambiguity.

GAMETE MATURATION

In studied articulated species, the oocyte is spawned as a primary oocyte at the prophase I stage of maturation with an intact germinal vesicle (nucleus) (CHUANG, 1990; LONG & STRICKER, 1991). Formation of the first polar body occurs soon after spawning, and fertilization takes place when the oocyte reaches metaphase of the second meiotic division. The germinal vesicle breaks down prior to the addition of sperm in *Hemithiris psittacea* (LONG, 1964), *Terebratalia coreanica,* and *Coptothyris grayii* (HIRAI & FUKUSHI, 1960) but after the addition of sperm in *T. transversa* (LONG, 1964) and *Calloria* (PERCIVAL, 1944). Only after fertilization, however, does the first polar body form in *T. coreanica, Coptothyris* (HIRAI & FUKUSHI, 1960), *Hemithiris,* and *T. transversa* (LONG, 1964). In *Terebratulina septentrionalis* (CONKLIN, 1902), *T. retusa* (JAMES & others,

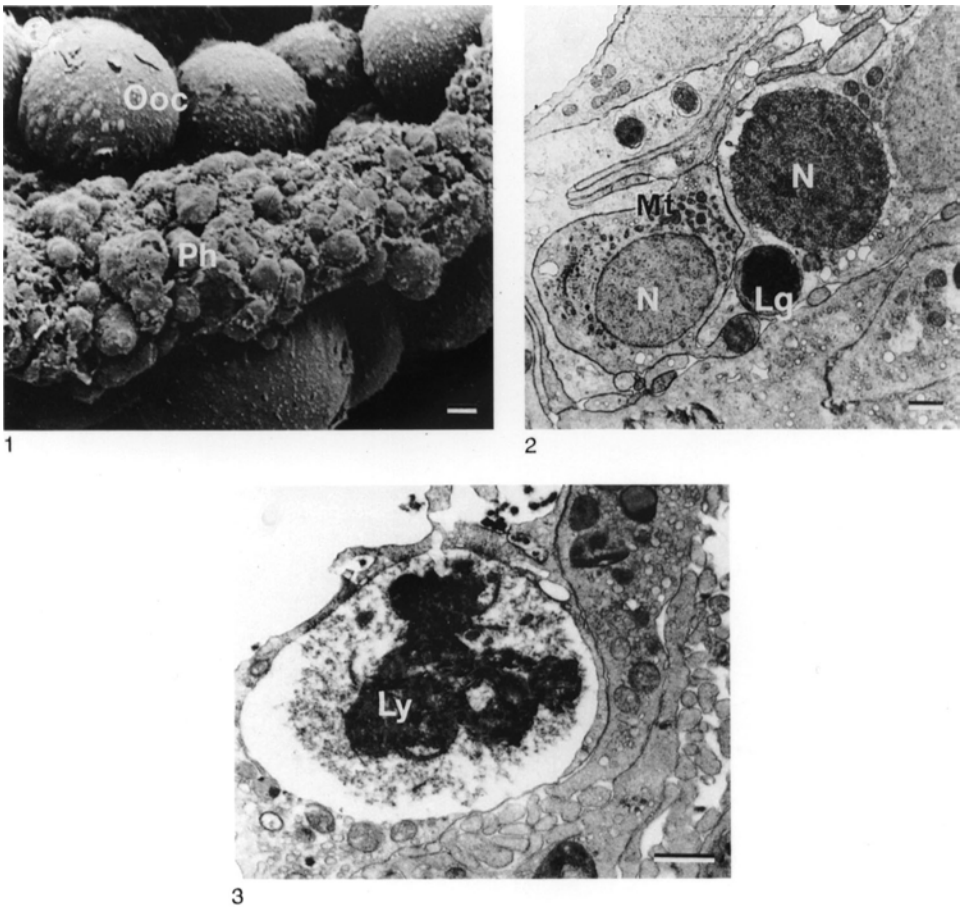

FIG. 155. SEM and TEM micrographs of coelomocytes of *Terebratulina retusa; 1,* the distal margin of the genital lamella in a recently spawned female showing vitellogenic oocytes (*Ooc*) and globular material that probably consists of phagocytes (*Ph*), scale bar: 10 μm; *2,* phagocytic matrix showing lipid granules (*Lg*), mitochondria (*Mt*), and nucleus (*N*), scale bar: 1.0 μm; *3,* putative lysosome (*Ly*) in a phagocyte, scale bar: 10 μm (James, Ansell, & Curry, 1991b).

1992), and *Neocrania* (NIELSEN, 1991), two polar bodies are formed after fertilization; and in *Lingula* the first polar body may be produced while the oocyte is in the body cavity or immediately after spawning (YATSU, 1902a). The only report of the division of the first polar body is for *T. septentrionalis* in which the polar bodies do not remain attached to the blastula after the 16-blastomere stage (CONKLIN, 1902).

In *Lingula* (YATSU, 1902a), *Terebratalia* (LONG, 1964), and *Terebratulina* (JAMES, ANSELL, & CURRY, 1991c) the follicular cells are shed sometime after spawning. The follicular cells of *Calloria* reportedly are not lost until fertilization has occurred and the fertilization membrane has formed (PERCIVAL, 1944). In *Neocrania* the follicular cells are shed prior to spawning (NIELSEN, 1991). Loss of the follicular cells that constitute the follicular envelope in *Terebratulina* reveals the highly convoluted and microvillous surface topography of the oocyte. The follicular cells retreat from the pole of the oocyte, which is diametrically opposite the region of accessory cell proliferation and the original

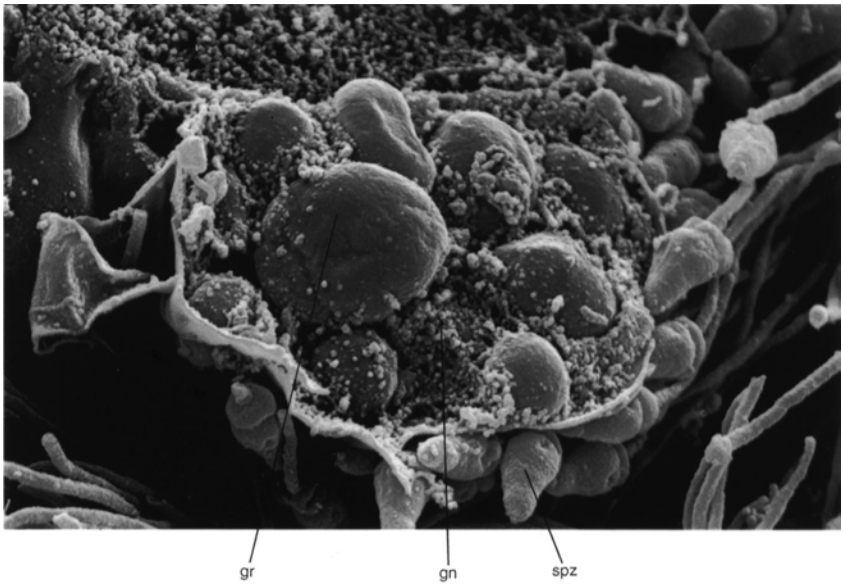

FIG. 156. SEM micrograph of a trophocyte in the gonad of *Calloria inconspicua,* which has been fractured to reveal glycogen granules (*gn*), large electron-dense granules (*gr*), and the heads of the spermatozoa (*spz*) touching the surface of the cell, ×5,800 (new).

point of attachment to the genital lamella (JAMES, ANSELL, & CURRY, 1991c).

Ultrastructural studies of the oocytes of *Lingula* (CHUANG, 1990) and *Terebratulina* (JAMES, ANSELL, & CURRY, 1991c) show that loss of the follicular cells exposes the surface of the oocyte, which retains its microvilli embedded in a filamentous or granular layer, probably some form of glycocalyx. The layer has been described in light microscopic studies as a mucoid (CHUANG, 1990) or a jelly layer (NIELSEN, 1991).

Typically, once an ovum has been fertilized, a fertilization membrane is formed to prevent penetration by other sperm. In *Lingula* and probably other brachiopods the observed increase in density of the filamentous and granular matrix surrounding the ovum and the production of large numbers of transversely striated, radial fibrous strands of varying diameter are assumed to indicate the development of a fertilization membrane (CHUANG, 1990). Formation of the fertilization membrane probably occurs rapidly after successful penetration by sperm. In *T. coreanica* and *Coptothyris* (HIRAI & FUKUSHI, 1960) and *Calloria* (PERCIVAL, 1944), the fertilization membrane is formed within 5 minutes of the addition of sperm.

Little information exists on the maturation of sperm in brachiopods. Spermatozoa appear to undergo no obvious morphological changes within the testes, although they probably become motile before being spawned. The acrosome filament, which is formed immediately prior to the penetration of the ovum, has been observed in *Hemithiris, Terebratulina unguicula,* and *Terebratalia* (LONG, 1964).

It is unknown whether any chemical stimulants are released by the ovum to attract sperm. Penetration by sperm has been observed only in *Lingula* in which the sperm enters the ovum at a point diametrically opposite the second polar body during the metaphase of the second meiotic division of the ovum (YATSU, 1902a). Typically, the ovum will respond to the penetration of the sperm by producing the fertilization membrane, thus excluding other sperm. In *Lin-*

gula, YATSU (1902a) reported the presence of a membrane prior to fertilization and assumed that a micropyle in the membrane facilitates penetration by sperm. The successful sperm sheds its tail, and, in *Lingula,* a thick nuclear membrane forms around the sperm nucleus and the female nucleus respectively, to form the (haploid) male and female pronuclei (YATSU, 1902a).

EMBRYOLOGY

In *Lingula* the male and female pronuclei migrate toward the center of the ovum, the pronuclear membranes break down, and the pronuclei fuse to form a zygote (Fig. 159.1; 160.1; YATSU, 1902a). Sperm penetration and fusion of the pronuclei have not been observed in detail for any other brachiopod.

The pattern of early cleavage of the zygote appears to be similar in all brachiopods. Cleavage into blastomeres is total (holoblastic), equal, and radial (Fig. 159.2–159.3; 160.2–160.3). Early reports of spiral cleavage are viewed with scepticism (NIELSEN, 1991). For all brachiopods studied, the first two divisions are meridional and at right angles to each other. Equal cleavage, relatively homogeneous distribution of ooplasm, and the loss or resorption of the polar bodies early in development have, however, confounded attempts to orient the blastomeres and trace the progress of a given cell lineage relative to any clearly recognizable cytological feature (YATSU, 1902a; CHUANG, 1990; LONG & STRICKER, 1991). Further descriptions of development will be divided into lingulids and discinids, craniids, and articulated groups.

Lingulids and Discinids

Nothing is known about the early stages of discinid development. Aspects of the early development of the lingulid *Glottidia* have been described (PAINE, 1963), but the most detailed account is that of YATSU (1902a) for *Lingula.* In *Lingula* the third cleavage is equatorial, and further cleavages tend to be biradial (KUME & DAN, 1968). According to YATSU (1902a) the fourth cleavage occurs simultaneously in two parallel planes, whose relationship to the previous plane has not been determined and gives rise to 16 blastomeres, which enclose a spaceous blastocoel (Fig. 159.4–159.5). The fourth cleavage may, however, be retarded, giving rise to a 12-blastomere stage. Cell division continues until a hollow, thin-walled, and ciliated blastula (coeloblastula) is formed (Fig. 159.7–159.8). A similar course of events produces the coeloblastula of *Glottidia* (PAINE, 1963).

Gastrulation in *Lingula* occurs at about the 30- to 40-cell stage and is initiated by flattening of the pole of the blastula that has the tallest blastomeres. These cells invaginate to form an endomesodermal cell mass that almost occludes the blastocoel. The invagination forms the archenteron and its communication with the exterior, the blastopore. Endomesodermal cell masses form two groups of mesodermal cell masses, one on either side of the archenteron. Each mesodermal cell mass hollows out to form a coelomic cavity, and the lining cells flatten out to line the endoderm on one side and the ectoderm on the other. The coelom of *Lingula* is thus formed by schizocoely (YATSU, 1902a; MALAKHOV, 1976). Soon after, the blastopore closes, and the anterior parts of the mesodermal masses become mesenchymetous and extend into the anterior part of the embryo, where the lophophore begins to develop (Fig. 159.11; YATSU, 1902a; LONG & STRICKER, 1991).

At this stage, proliferation of the ectoderm at the posterior end of the embryo forms a horizontal, ringlike mantle fold that grows forward to surround much of the remainder of the embryo, the anterior lobe (Fig. 159.12; LONG & STRICKER, 1991). The mantle lobe subsequently becomes constricted into a semicircular form with a straight, posterior margin separating the mantle into a dorsal and a ventral half. The shell appearing at this stage is a very thin cuticle (protegulum) secreted over the entire

TABLE 3. Table summarizing known brachiopod reproductive cycles; *BL,* brooding larvae; *GC,* gonad condition index; *PH,* plankton hauls; *PSP,* partially spawned; *RG,* ripe gonad; *RS,* recently spawned; *SF,* population size frequency analysis; *SP,* spawning (adapted from Long & Stricker, 1991; James & others, 1992).

Species	Author	Locality	Observation type	Month
Northern Hemisphere				
Inarticulated brachiopods				
Lingula anatina	Yatsu, 1902a	Japan	SP, PH	July–Aug
	Sewell, 1912	Southern Burma	PH	Feb–Mar; Dec–Jan
	Ashworth, 1915	Indian Ocean: Red Sea	PH	May–Sept
	Helmcke, 1940	West Africa; Indian Ocean	PH	Feb–Mar; Apr–May; Jun–Jul; Nov–Dec
	Kume, 1956	Japan	SP	June–Aug
	Chuang, 1959b	Singapore	SP	all year
	Sundarsan, 1968	Western India	PH	Jan–Feb
	Sundarsan, 1970	Western India	PH	Dec–Jan
	Chuang, 1973	Indian Ocean	PH	all year
Glottidia pyramidata	McCrady, 1860	South Carolina	PH	June–July
	Brooks, 1879	Chesapeake Bay, USA	PH	July–Aug
	Davis, 1949	Southern Florida	PH	all year
	Paine, 1963	Northern Florida	PH	Mar–Apr; May–July; Nov–Dec
Neocrania anomala	Joubin, 1886	Southern France	RG	Apr–Oct
	Rowell, 1960	Scotland	RS, RG, SF	April–Oct
Discinisca sp.	Chuang, 1968	Singapore	PH	May–Oct
D. sp.	Yamada, 1956	Western Japan	PH	
Articulated brachiopods				
Argyrotheca sp.	Atkins, 1960b	Mediterranean Sea	BL	Jan–Feb; Oct–Jan
A. jacksoni	Jackson, Goreau, & Hartman, 1971	West Indies	SF	all year
Coptothyris grayii	Hirai & Fukushi, 1960	Japan	SP	Oct–Nov
Dallina sp.	Lankester, 1873	Naples	RG	Nov–Dec
Frenulina sanguinolenta	Mano, 1960	Japan	BL	all year
Frieleia halli	Rokop, 1977	California	RG	Jan–Apr
Gryphus sp.	Lankester, 1873	Naples	RG	Dec–Jan
Hemithiris psittacea	Long, 1964	Washington	BL	Jan–Feb; Dec–Jan
Platidia spp.	Atkins, 1959	Western France	RG	Feb–Mar; Jun–Jul; Aug–Sept
Terebratalia coreanica	Hirai & Fukushi, 1960	Japan	SP	Oct–Nov
T. transversa	Long, 1964	Washington	SP	Jan–Feb; Nov–Dec
Terebratulina sp.	Morse, 1873	Maine	SP	April–Aug
T. unguis	Long, 1964	Washington	BL	Feb–Mar
T. septentrionalis	Webb, Logan,	Bay of Fundy, Canada & Noble, 1976	BL	Jan–Mar; Dec–Jan
T. retusa	Franzen, 1969	Western Sweden	RG	Nov–Dec
	Curry, 1982a	Scotland	SF	Apr–May; Oct–Dec
	James, Ansell, & Curry, 1991a	Scotland	GC, SP	Jan–Feb; Nov–Jan[1]
	James, 1991a & Curry, 1991a	Scotland	GC, SP	Jan–Feb; Apr; Jun; Nov–Jan[1]
Thecidellina barretti	Jackson, Goreau, & Hartman, 1971	Jamaica	SF	(single spawning)
T. congregata	Jackson, Goreau, & Hartman, 1971	Guam & Saipan	SF	(single spawning)

TABLE 3. Continued.

Species	Author	Locality	Observation type	Month
Southern Hemisphere				
Inarticulated brachiopods				
Lingula anatina	Kechington & Hammond, 1978	Queensland, Australia	RG, PH	Nov–Mar
Discinisca sp.	Hammond, 1980	Queensland, Australia	PH	Feb–May
Pelagodiscus sp.	Müller, 1860, 1861	Brazil	PH	Feb–Apr
	Blochmann, 1898	Indonesia	PH	July–Aug
	Eichler, 1911	Antarctic Ocean	PH	Feb–Apr
	Ashworth, 1915	Indian Ocean	PH	Oct–Nov
	Helmcke, 1940	Eastern Africa	PH	Dec–Jan; Feb–Mar
Articulated brachiopods				
Liothyrella sp.	Eichler, 1911	Antarctica	BL	Feb–Mar
L. neozelanica	Tortell, 1981	New Zealand	PSP	Feb–Mar
Neothyris lenticularis	Tortell, 1981	New Zealand	RG	Feb[2]–Mar
Notosaria nigricans	Percival, 1960	New Zealand	BL	Apr–Jul
	Tortell, 1981	New Zealand	RG	Feb[3]–Mar
Pumilus antiquatus	Rickwood, 1968	New Zealand	BL	Sept–Nov
Terebratella sanguinea	Tortell, 1981	New Zealand	RG	Apr–Jul[2]
Calloria inconspicua	Percival, 1944	New Zealand	BL	Apr–Jun[1]
	Doherty, 1979	New Zealand	SP	Jul–Sept[1]

[1]same species taken from different localities; [2]specimens collected between January and March; gonads appeared to be ripe but could not be induced to spawn; [3]specimens collected between January and March; males released sperm when water temperature was slightly increased.

external surface of the mantle (Fig. 159.13; YATSU, 1902a). The anterior lobe is formed from a central area of the gastrula that is raised into a mound subsequently giving rise to the lophophore. An invagination marks the future median part of the brachial (arm) ridge. Proceeding dorsally and posteriorly, it forms the stomodaeum (the embryonic mouth). Interrupted on the ventral side by this invagination, the brachial ridge adopts a dorsally directed U-shape. Eventually, the stomodaeum opens into the archenteron. The stomodaeum is believed to invaginate at the site where the blastopore closed, but the exact derivation of the mouth is uncertain. Meanwhile, the mantle lobes rapidly increase in size especially along the anterior margin, and the brachial ridge becomes densely ciliated (Fig. 159.13).

As development proceeds, the brachial ridge forms a circular disc and projects from the anterior. The mouth becomes clearly visible, and the brachial apparatus is raised up on a stalk (Fig. 159.14–159.15; YATSU, 1902a). The brachia assume a triangular outline with the two posterior angles forming the first pair of rudimentary tentacles and the anterior apex the earliest manifestation of the median tentacle. A second pair of tentacles are added on either side and adjacent to the median tentacle. At the same time the mouth shifts into a central position where it becomes flanked anteriorly by the epistome, arising as a preoral transverse ridge. Additional pairs of tentacles arise from the generative zones on either side of the median tentacle, eventually forming a trocholophe. Embryos with three pairs of tentacles bear the rudiments of the ventral muscle. A few muscle fibers are embedded among the mesenchyme cells of the brachial canal (arm-sinus). In addition, the archenteron also becomes differentiated into a thickly walled esophagus and a thinly walled stomach (Fig. 159.16; YATSU, 1902a).

At hatching, lingulid embryos are much more advanced in their development than the embryos of craniids and articulated

TABLE 4. Summary of known sizes of brachiopod eggs and reproductive strategies; *G,* gonochoristic; *H,* hermaphrodite; *L,* lecithotrophic; *P,* planktotrophic; *FS,* free spawning; *BL,* lophophore brooding; *BC,* brood chamber (new).

Species	Sex	Development type	Fecundity	Egg diameter (μm)	Strategy
Neocrania anomala	G	L		120[2,13] 125[11]	FS
N. californica					FS
Lingula anatina[1,21]	G	P	17,250[1]	95, 130[7]	FS
Glottidia pyramidata		P	60,000[12]		FS
Pumilus antiquatus	H	L	50–100[15]	200[15]	BL
Argyrotheca cuneata	H	L		95[18]	BC
A. cordata	H	L		100[18]	BC
A. jacksoni	G	L	3,000	90[8]	
Megathiris detruncata	H	L		90[18]	
Calloria inconspicua	H[8]	L	18,000[16] 22,000[5,9]	180[20,13]	BL
Terebratella sanguinea	G			100[20]	
Neothyris lenticularis	G			85[20]	
Gryphus vitreus	G			70[18]	
Lacazella sp.	H	L	150[8]	20[8]	BC
L. mediterranea	G[22]	L			BC
Thecidellina barretti	H	L	150[8]	20[8]	BC
Terebratulina unguicula	G			170[10]	BL
T. septentrionalis	G	L		160[4]	BL
T. retusa	G	L	8,000–15,000[8]	120[6] 130[8] 160[3]	FS
Laqueus californianus	G		35,000[9]	140[9] 170[19]	FS
Frieleia halli	G		<1,000[17]	112[17]	
Frenulina sanguinolenta				130[2]	
Terebratalia transversa	G	L		150[10,19]	FS
Notosaria nigricans	G	L	8,680[14] 14,000[21]	160[14] 200[20]	BL
Hemithiris psittacea	G	L		190[10]	BL
H. sp.			22,000[9]	90[9]	
Liothyrella antarctica		L			BL
Gwynia capsula		L			BC

[1]CHUANG, 1959a; [2]CHUANG, 1983a; [3]CLOUD, 1948; [4]CONKLIN, 1902; [5]DOHERTY, 1979; [6]FRANZEN, 1969; [7]HAMMOND, 1982; [8]JAMES, ANSELL, & CURRY, 1991a; JAMES, unpublished data, 1989; [9]LAW & THAYER, 1991; [10]LONG, 1964; [11]NIELSEN, 1991; [12]PAINE, 1962a; [13]PERCIVAL, 1944; [14]PERCIVAL, 1960; [15]RICKWOOD, 1968; [16]RICKWOOD, 1977; [17]ROKOP, 1977; [18]SENN, 1934; [19]REED, 1987; [20]TORTELL, 1981; [21]YATSU, 1902a; [22]LACAZE-DUTHIERS, 1861.

brachiopods. The embryo essentially forms two lobes; an anterior lobe from which the lophophore develops, and a posterior mantle lobe. These constrict to form the ventral and dorsal mantle lobes, which grow to envelop much of the anterior lobe. The mantle lobes secrete the protegulum before the embryo hatches from the fertilization membrane and becomes a free-swimming larva (Fig. 158.3; 159.13).

Craniids

After the first three cell divisions, the embryological development of *Neocrania* differs significantly from other inarticulated brachiopods, sharing similarities with the development of articulated groups (Fig. 161–162). The fourth cleavage results in two tiers of cells oriented perpendicular to each other, with the 16 blastomeres arranged as two, curved, double rows of cells forming a cross. Further cell divisions are irregular and asynchronous. The blastulae develop cilia and begin to swim. Gastrulation by invagination of the blastoporal pole occurs at about the 40- to 50-cell stage. In the postgastrulation stage, the larva of *Neocrania* remains fairly spherical even after the blastocoel has been occluded (Fig. 161.1; 162.1). Thereafter, it becomes somewhat flattened and elongate, with the blastopore located at the posterior end of the ventral side (Fig. 161.2; 162.2).

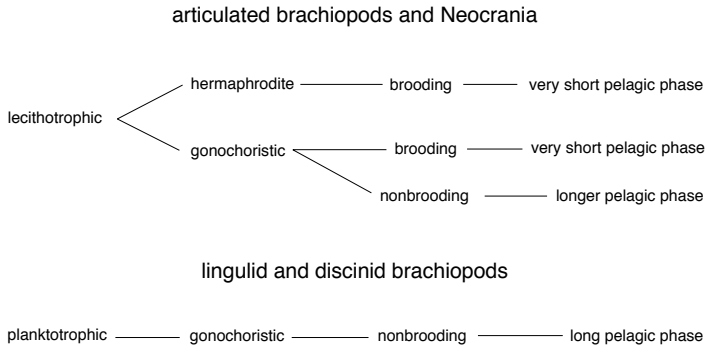

FIG. 157. Summary diagram of brachiopod reproductive strategies (new).

Endodermal and mesodermal cells occupy the anterodorsal and posteroventral sides of the archenteron wall respectively. The mesodermal layer expands anteriorly between the ectoderm and the endoderm as a single cell layer, while the endoderm elongates as a narrow sac (Fig. 161.3; 162.3). At a somewhat later stage while the blastopore is still open, mesoderm covers both lateral surfaces of the ectoderm and starts to differentiate into four plates on each side of the ectoderm. The periphery of each plate curls medially and constricts, creating a series of four pouches on each side of the larva and finally the

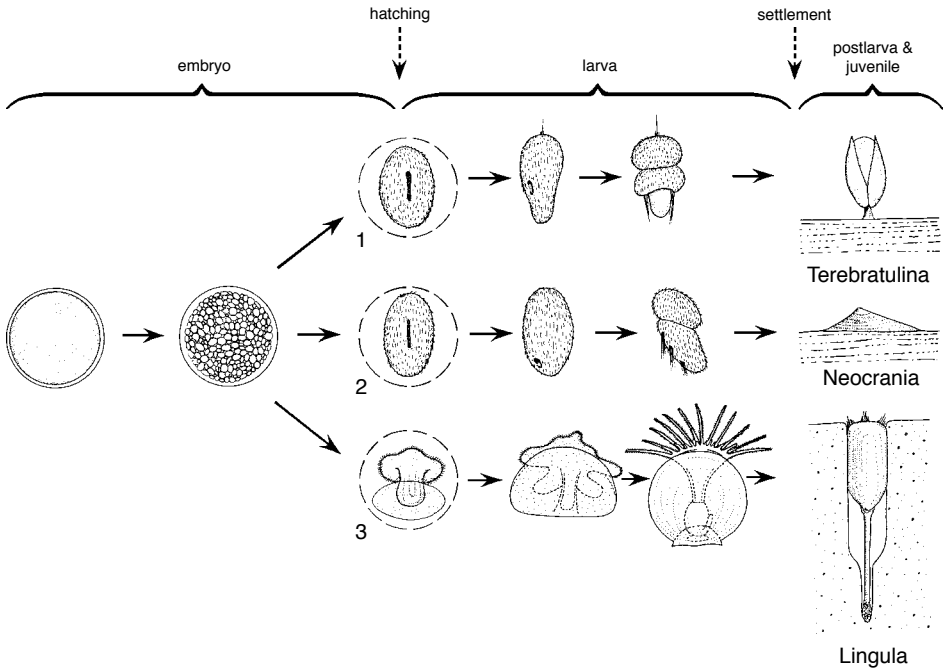

FIG. 158. Schematic diagram showing the approximate stages at which embryos of *1, Terebratulina retusa, 2, Neocrania anomala,* and *3, Lingula anatina* hatch from their fertilization membranes and become free-swimming larvae; the transition from the free-swimming larva to the postlarval (juvenile) stage occurs at settlement (new).

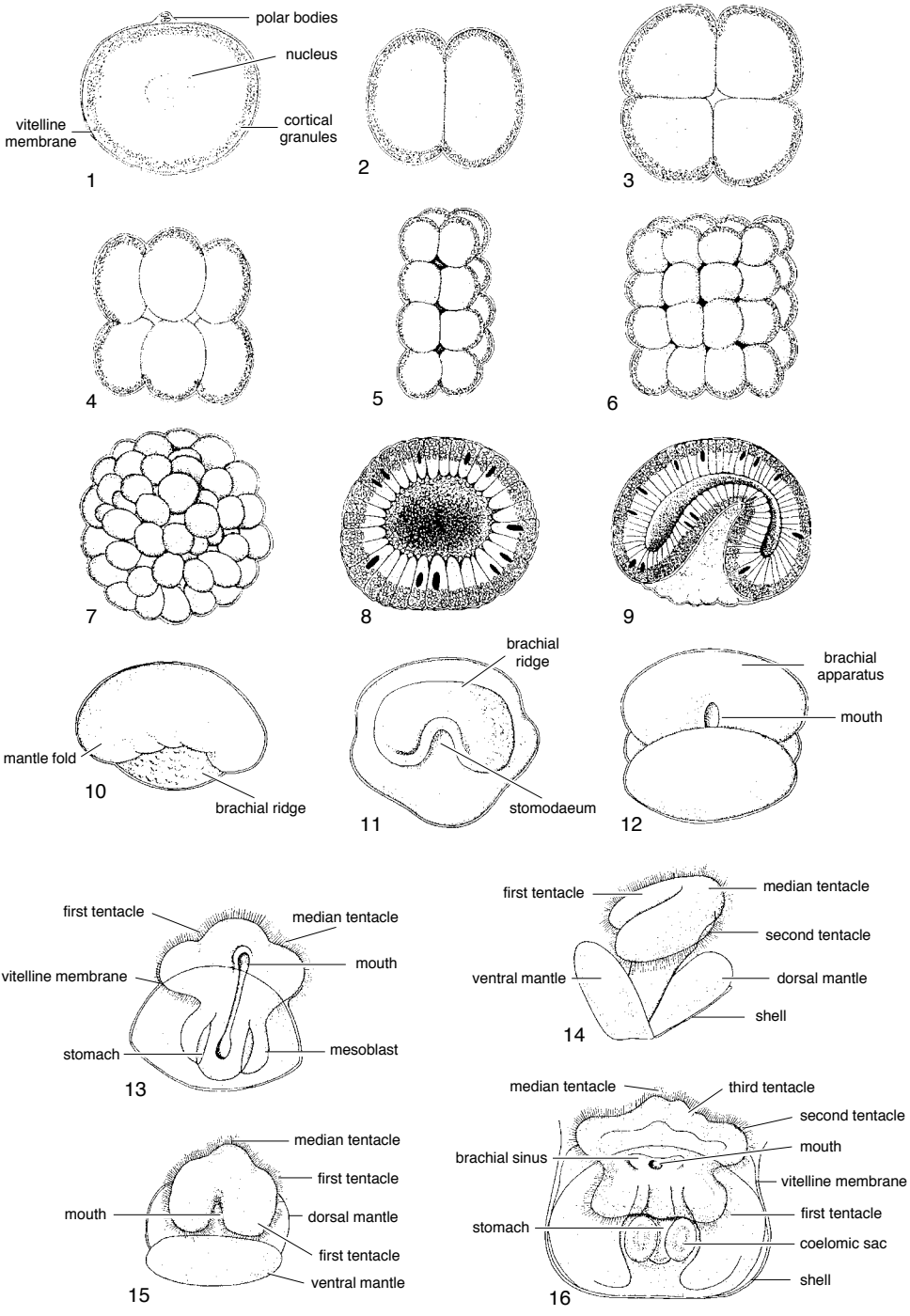

FIG. 159. *For explanation, see facing page.*

blastopore closes (Fig. 161.4; 162.4). Hence, the coleom of *Neocrania* is formed through modified enterocoely (Nielsen, 1991).

In the *Neocrania* larva only one major constriction is apparent, which separates the rounded anterior lobe from the rest of the dorsoventrally flattened larva (Fig. 163.3; Nielsen, 1991).

Articulated Groups

The development of the articulated brachiopods follows a similar course for all those species studied (Long & Stricker, 1991). The most detailed accounts are of *Terebratulina septentrionalis* (Conklin, 1902) and *Terebratalia transversa* (Long, 1964).

In *Terebratalia* the third cleavage is meridional or equatorial and forms a doughnut-shaped ring of eight cells or two tiers of four cells respectively (Fig. 160.6–160.7). The fourth division is equatorial or meridional, depending upon the previous cleavage, resulting in the formation of two tiers of eight cells (Long, 1964). As in *Neocrania,* beyond the stage of 16 cells further cell divisions are often irregular and asynchronous, eventually forming a hollow blastula (Fig. 160.8–160.9; Conklin, 1902; Long & Stricker, 1991). Cells at the presumptive blastoporal (vegetal) pole of the blastula (the point farthest from the position of the original egg nucleus) become columnar (Long & Stricker, 1991), and gastrulation occurs by invagination (emboly) of this thickened layer of cells (the gastral plate), thus forming a blastopore (Fig. 160.10–160.11). The invaginated cells form the endodermal anlage and eventually occlude the blastocoel. The chamber created by the process of invagination forms the archenteron. The only reported exception is in *Lacazella mediterranea* where gastrulation occurs by delamination (Kowalevsky, 1883).

Hatching of the embryo of articulated groups is not well documented, but rupture of the fertilization membrane and subsequent escape of larvae probably occur during the late blastula or early gastrula stage when embryos develop cilia and achieve motility (Fig. 158; Chuang, 1990). An apical tuft of long cilia forms, and the surface of the embryo is ciliated (Fig. 160.12; Long & Stricker, 1991). At this stage, the larvae of *Terebratalia, Terebratulina,* and probably other calcareous-shelled brachiopods are capable of swimming. Those of *Terebratalia* (Long & Stricker, 1991) and *Terebratulina* (James, unpublished, 1989) propel themselves through the water with their anterior end forward and in a clockwise direction, while the larva of *Notosaria* (Percival, 1960) spirals counterclockwise. The archenteron is elongated anteroposteriorly, and the anterior end of the embryonic gut forms a blind-ending pouch. More posteriorly, the archenteron opens ventrally via a blastopore that is elongated by the curvature of the larva.

It is generally agreed that the coelom of these larvae is formed by a modified form of enterocoely (Malakhov, 1976); reports of schizocoely in articulated groups have been largely discounted (Nielsen, 1991). With minor variations, the following description of coelomic formation applies to *Hemithiris, Terebratalia,* and *Terebratulina unguicula*

Fig. 159. Diagrammatic series illustrating the development of *Lingula anatina; 1,* mature ovum and polar bodies; *2,* 2-cell stage; *3,* 4-cell stage; *4,* 8-cell stage; *5,* 16-cell stage; *6,* 32-cell stage; *7,* blastula; *8,* cross section of late blastula prior to gastrulation; *9,* gastrula; *10,* embryo with brachial ridge and mantle fold; *11,* anterior view of a slightly more advanced embryo in which the stomodaeum has appeared; *12,* ventral view of a slightly older embryo in which the mantle lobes have formed; *13,* ventral view of embryo at the next stage with the rudiment of the median and first pair of tentacles; the mesodermal cell masses are also visible and the vitelline membrane has ruptured; *14,* ventral view of larva in which the rudiments of the second pair of tentacles have formed, the dorsal and ventral mantles are clearly divided, and the larval shell is visible; *15,* anterior view of previous example showing the brachial apparatus attached to the dorsal mantle; *16,* ventral view of a larva with a well-developed median tentacle and two pairs of tentacles; coelomic sacs are clearly visible (adapted from Yatsu, 1902a).

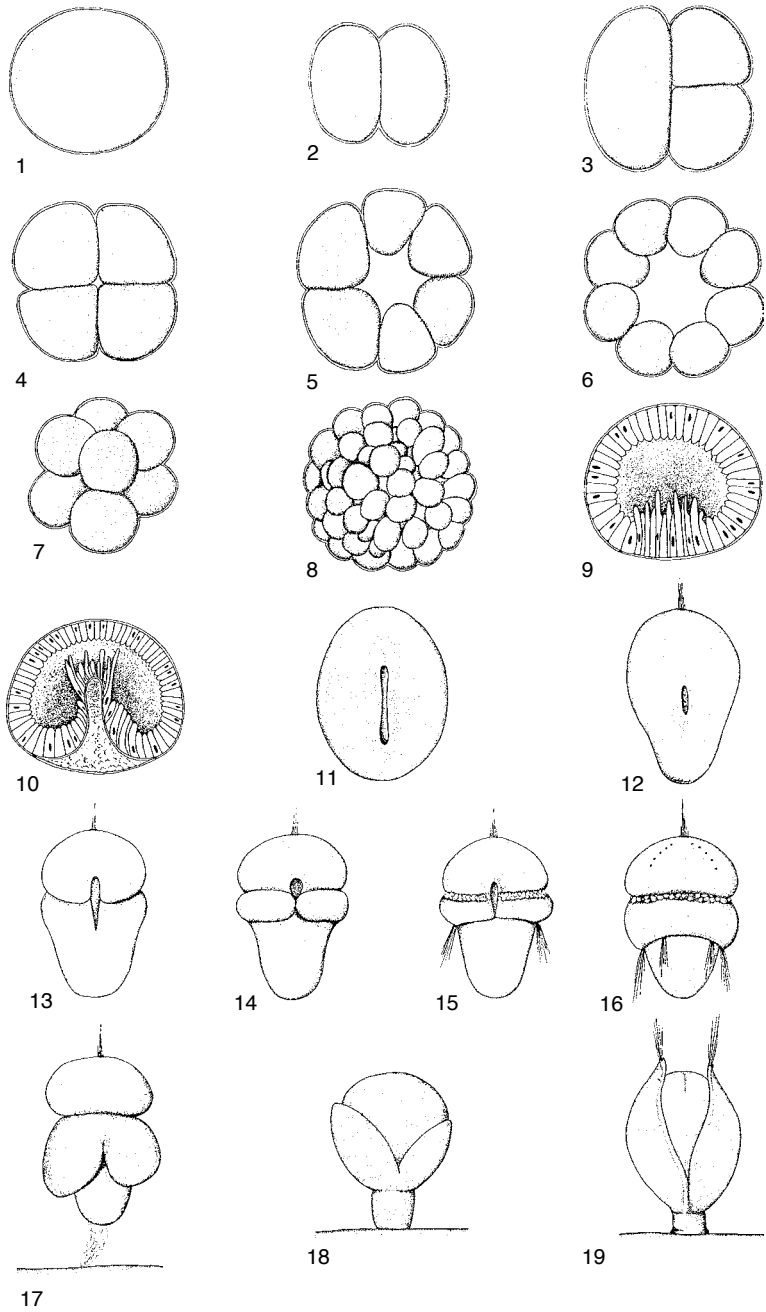

FIG. 160. Diagrammatic series illustrating the development of the articulated brachiopods; *1–16, Terebratalia transversa* and *17–19, Terebratulina retusa* in settlement and metamorphosis; *1,* zygote; *2,* 2-cell (blastomere) stage; *3,* 3-cell stage; *4,* 4-cell stage; *5,* 6-cell stage; *6,* 8-cell stage, flat ring; *7,* 8-cell stage, two tiers of four blastomeres; *8,* blastula; *9,* cross section of late blastula with thickened gastral plate prior to gastrulation; *10,* cross section of gastrulating blastula; *11,* ventral view of a 35-hour-old larva showing the elongated blastopore; hatching has probably occurred; *12,* ventral view of a slightly older larva with an apical tuft (adapted from Long & Stricker, 1991); *(Continued on facing page.)*

(Long, 1964), *T. septentrionalis* (Conklin, 1902), *Calloria* (Percival, 1944), *Notosaria* (Percival, 1960), and *Argyrotheca cordata* (Kowalevsky, 1883; Shipley, 1883; Plenk, 1913). The dorsal lining of the archenteron thickens, indicating the formation of mesoderm. Subsequently, a single layer of cells grows downward from the anterior and lateral parts of the roof of the archenteron to form a cellular curtain that eventually partitions elongated coelomic spaces (enterocoels) on either side of the archenteron. Almost simultaneously, the blastopore begins to close from its posterior end toward the anterior tip, but the exact manner in which the coelom becomes separated is unclear. Organogenesis in the larva of articulated brachiopods is heralded by a superficial, transverse constriction of the elongate gastrula into three lobes (Chuang, 1990).

Constrictions may occur in several ways in different species (Fig. 163). In some, the embryo is first constricted into two lobes, one of which is divided by a second constriction. In others, division is achieved by an ectodermal folding around the middle of the embryo, which has also been interpreted as a simultaneous occurrence of two constrictions in front of, and behind, the ectodermal fold. Constriction of the embryos of *Terebratalia* (Long, 1964) and *Argyrotheca* (Kowalevsky, 1883) first marks off the anterior lobe and then the mantle and pedicle lobe (Fig. 163.4). After marking off the anterior lobes in *Notosaria,* an ectodermal fold, first appearing on the dorsal side of the embryo, grows laterally downward on each side to encircle the embryo near the middle and forms the mantle lobe (Fig. 163.5; Percival, 1960). A fold, with or without constrictions, forms around approximately the middle of the embryos of *Coptothyris, Terebratalia coreanica* (Hirai & Fukushi, 1960), *Pumilus antiquatus* (Rickwood, 1968), *T. septentrionalis* (Conklin, 1902), and *Calloria* (Percival, 1944). The fold forms the mantle lobe between the anterior and the pedicle lobe (Fig. 163.6). In contrast, the first constriction in *T. septentrionalis* (Morse, 1873), *T. unguicula* (Long, 1964), *Argyrotheca* (Shipley, 1883), and *Lacazella* (Lacaze-Duthiers, 1861) delineates the pedicle lobe from the

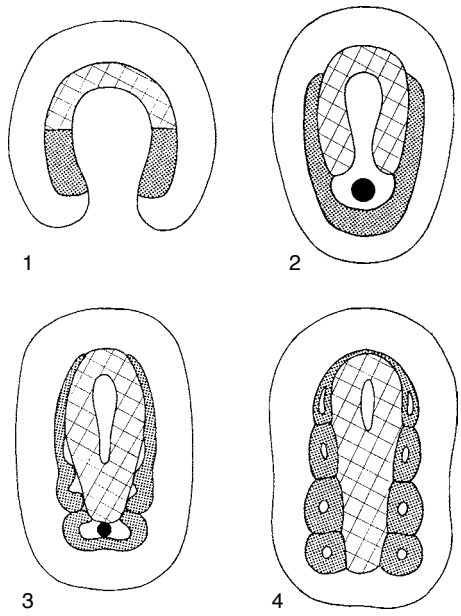

Fig. 161. Diagrams of four stages of development of the mesoderm (*shaded*) and the endoderm (*crosshatched*) of *Neocrania anomala; black dot* indicates position of the blastopore (adapted from Nielsen, 1991).

Fig. 160. *Continued from facing page.*
13, ventral view of a 40-hour-old larva in which the apical lobe has formed; *14,* ventral view of a 42-hour-old larva with the mantle lobe forming; *15,* ventral view of 48-hour-old larva; the blastopore is closing, the setal bundles have formed at the mantle margin, and vesicular bodies are evident at the base of the anterior lobe; *16,* dorsal view of larva at 70 hours, showing apical tuft, eye spots, vesicular bodies, setae, and a posterior band of cilia on the apical lobe (adapted from Long & Stricker, 1991); *17,* approximately 72-hour-old, trilobed *Terebratulina retusa* larva; separate ventral and dorsal mantle lobes are present and the pedicle lobe has secreted a mucous strand that adheres to the substrate; *18,* the pedicle attaches and metamorphosis takes place, the mantle lobes reverse to envelope the anterior lobe, and the apical tuft is lost; *19,* the shell is secreted and long marginal setae extend beyond the mantle of the postlarva (new).

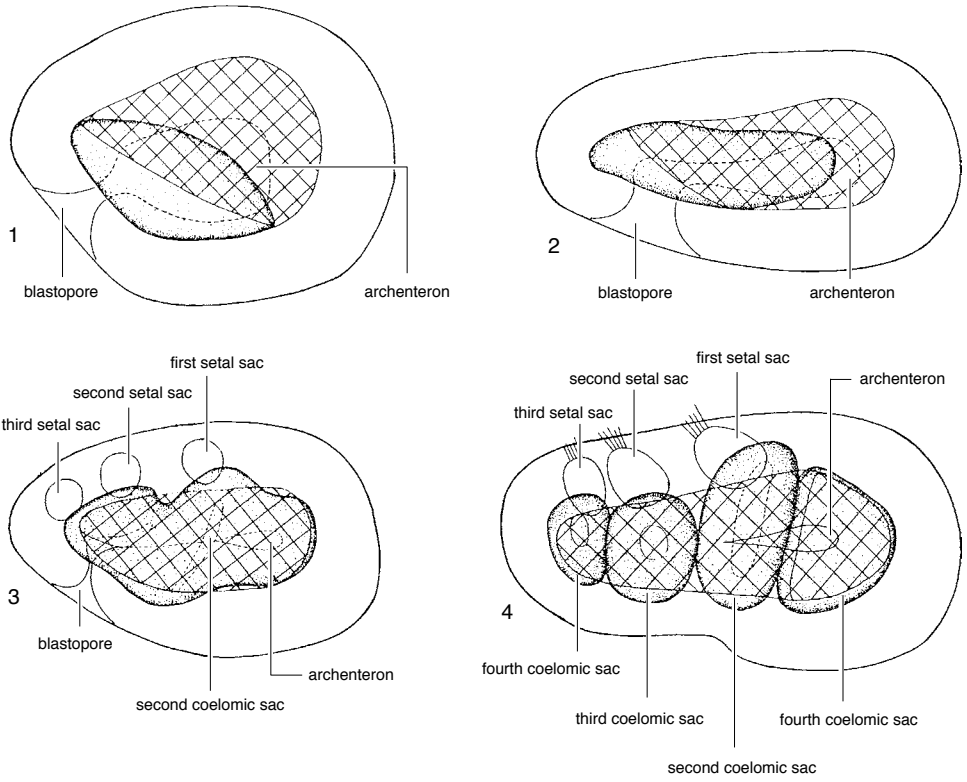

FIG. 162. Reconstructions of developmental stages of *Neocrania anomala* (based on serial sections) showing the differentiation of endoderm (*crosshatched*) and mesoderm (*stippled*); *1–4,* free-swimming larva; *1,* stage at 38 hours after fertilization; *2,* 46 hours after fertilization; *3,* 54 hours after fertilization; *4,* 67 hours after fertilization; *(Continued on facing page.)*

rest of the embryo, which is soon divided into the mantle lobe and the anterior lobe by a more anterior constriction (Fig. 163.7).

LARVAL DEVELOPMENT

Lingulids and Discinids

The free-swimming larvae of *Glottidia* (PAINE, 1963) and *Lingula* (YATSU, 1902a; SEWELL, 1912; ASHWORTH, 1915; CHUANG, 1959a, 1977) have been well described, as have discinid larvae, mainly of the cosmopolitan species *Pelagodiscus atlanticus* (WILLIAMS & ROWELL, 1965a). All are planktotrophic.

The trochophore of *Lingula* is first formed at the 3 p.t. stage and persists during the entire larval stage. Rupture of the fertilization membrane occurs at this stage; further extensions of the coelom and tentacular canals have also been formed; and myoepithelial cells are present in the tentacles.

A functional gut with rudimentary intestine and anus may differentiate in the embryo at the stage when the embryonic lophophore is only present as five lobes (YATSU, 1902a). The transition from the embryonic lecithotrophic to the larval planktotrophic mode of life disrupts secretion of the protegulum and results in a disturbance ring on the umbo of the larval shell (CHUANG, 1977). Further development of the gut occurs during the early larval stages. The intestine and statocysts may first appear at the 3 p.t. stage but in some larvae may not be differentiated until the 5 and 6 p.t. stages respectively.

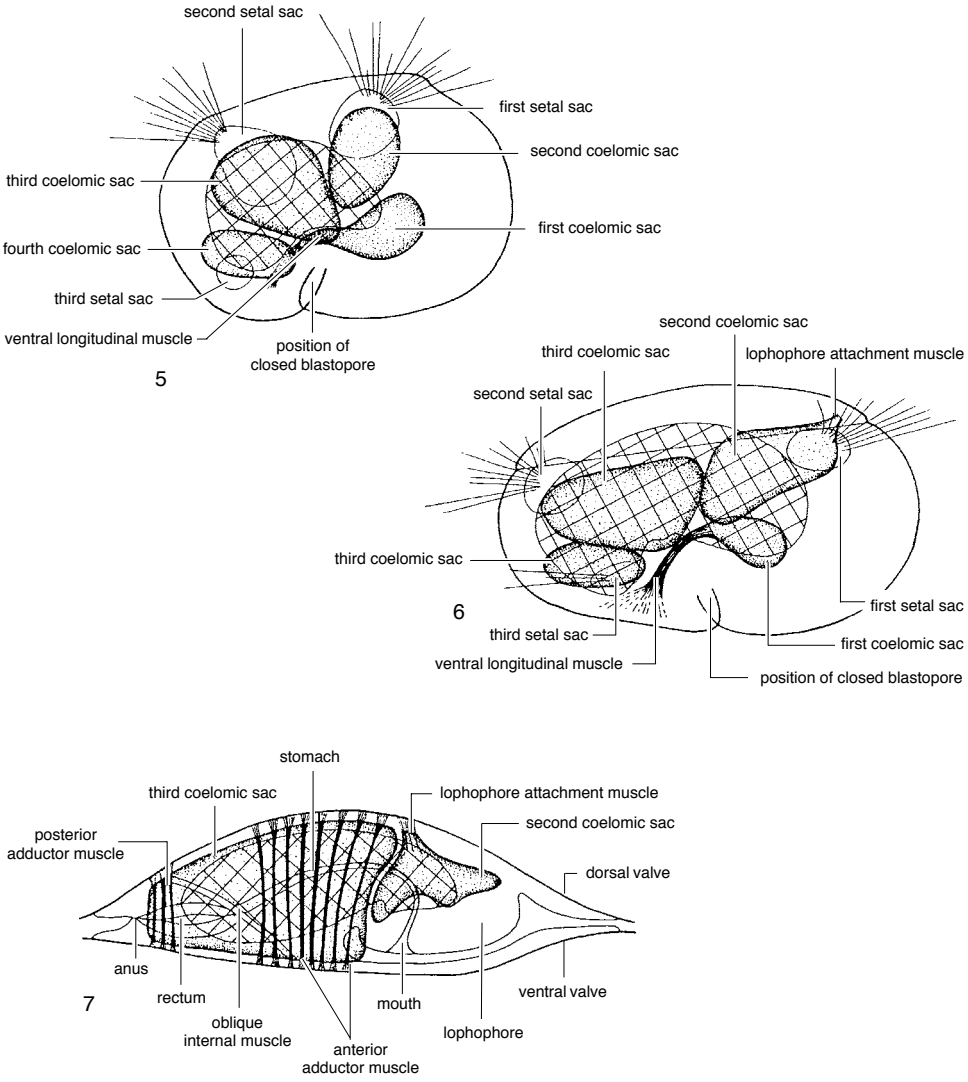

FIG. 162. *Continued from facing page.*

5, newly settled larva; *6,* a later metamprphosis stage; *7,* juvenile stage (adapted from Nielsen, 1991).

Rudimentary statocysts appear to be vesicular structures that, by the 6 p.t. stage, contain a few widely separated statoliths in rapid motion. The esophagus, digestive diverticula, stomach, and intestine begin to differentiate at about the 4 p.t. stage. Many of the main organ rudiments first become apparent at the 5 to 6 p.t. stage. Digestive diverticula become constricted into pouches; rudiments of the metanephridia are present; and the parietal muscle fibers and ganglia are formed. Four pairs of muscles are also found at this stage: the anterior occlusor; the internal oblique; the dorsal and ventral muscles. The ventral muscles are larval muscles and characteristic only of the free-swimming stage, since they degenerate after the animal becomes attached. External oblique muscles

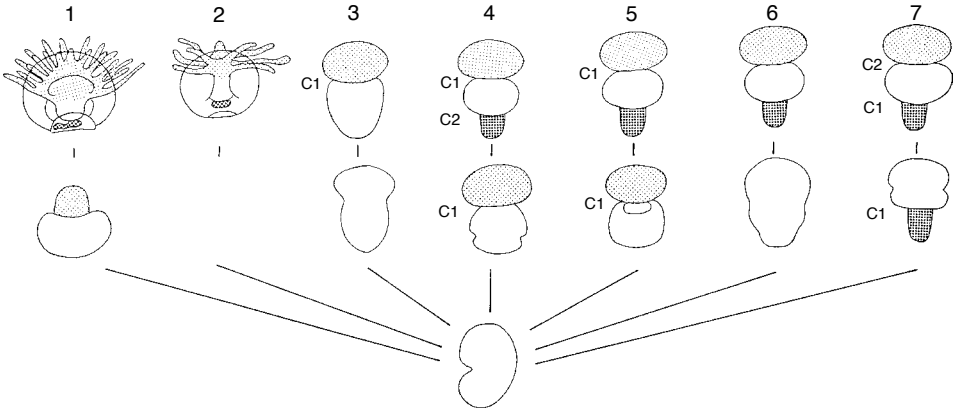

FIG. 163. Diagram of lobe formation during brachiopod development; *1,* lingulids; *2, Discinisca; 3, Neocrania; 4–7,* articulated groups identified in text; anterior lobe and lophophore, *stippled;* mantle lobe, *plain;* pedicle lobe and pedicle bud, *shaded; C1, C2,* first and second constriction respectively (adapted from Chuang, 1990).

appear at the 6 p.t. stage, and an unpaired posterior occlusor is formed at the beginning of the 7 p.t. stage (Fig. 164).

A pedicle appears at the 6 p.t. stage, developing as an outgrowth of the ventral mantle and containing an extension of the main body coelom. This is lined with coelomic epithelium underlain by a layer of slightly oblique longitudinal muscle that is one fiber in thickness (YATSU, 1902a). At the 7 p.t. stage, the pedicle is circular. With age, it increases in length, attaining the form of a twisted sausage at the 7 to 9 p.t. stage. In both lingulids and discinids, the pedicle is initiated as an evagination of the inner surface of the ventral mantle immediately behind the posterior body wall, the juvenile mantle continuing on the posterior side of the pedicle to the margin of the valve. Prior to settling of the juvenile, the pedicle assumes a position entirely posterior to the tissue that formed the posterior sector of the juvenile ventral mantle. The change in relative position is assumed to be associated with the transformation of the ventral mantle lobe of the juvenile, for in adults the tissue immediately in front of the pedicle comprises a single layer of outer epithelium lining the body cavity. After settling, the ventral mantle of discinids and lingulids is intact. With the loss of the posterior sector of the juvenile mantle, a flap of epithelium is developed that is continuous anterolaterally with the remainder of the ventral mantle. This sector of the adult mantle can only have developed from or have been proliferated by the tissues that initially formed the posterior body wall of the larva prior to settling. It is separated by the pedicle from the tissue that was involved in the corresponding sector of the juvenile mantle (Fig. 165). The secretory behavior of this posterior sector of the ventral mantle of the adult is considered to be of fundamental importance in determining the form of the adult shell (WILLIAMS & ROWELL, 1965a).

Considerable changes also affect the lophophore as it becomes a schizolophe, and a partition develops that divides the brachial canal into two canals: the future great canal and small brachial canals.

Increase in the size of the mantle and shell is continuous throughout these early developmental stages. At the 3 p.t. stage the two valves are semicircular and still joined together. The ends of the hinge line project laterally as a pair of small ears (the teeth in YATSU, 1902a). At the 7 p.t. stage, the shell is almost circular, becoming elongate by the 8 to 9 p.t. stage and elliptical by the 15 p.t. stage. Setae develop at the mantle margin by the 7 p.t. stage. The thin cuticle that initially joins the valves is ruptured along the hinge

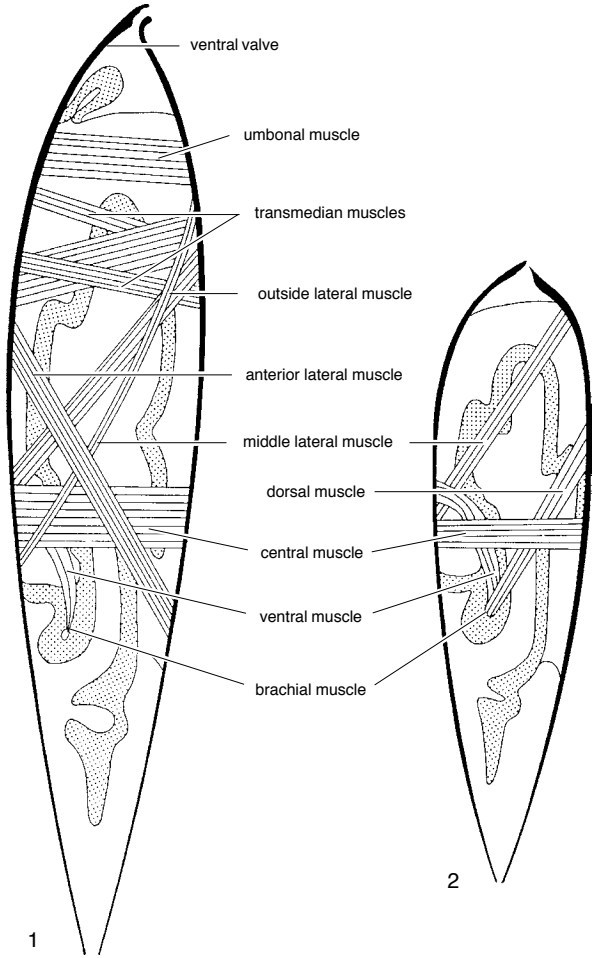

FIG. 164. Diagrammatic sections through *Lingula anatina* larva showing muscle development at *1,* 5 p.t. and *2,* 8 p.t. stages (adapted from Yatsu, 1902a).

line before the appearance of the 8 p.t. stage, and the transparent shell acquires a brownish tint along the margins. At the posterior end the superficial layers are bright green.

Statocysts at the 7 to 8 p.t. stage contain about 40 closely packed statoliths that move in unison within each enlarged statocyst. By the 8 to 9 p.t. stage, the digestive diverticula become progressively more lobulate, and the mantle canals start to appear.

The pedicle and setae develop during the later stages of the larva's planktonic life, unlike the differentiation of the gut, lophophore, and some elements of the muscular system and protegulum, which are presumed to be necessary for planktonic life stages. Initiation of pedicle and setal development seems to be dictated by the availability of suitable settlement substrate. Lack of suitable substrate may have the potential to delay formation of the pedicle. Hence, the pedicle has been reported to develop as early as the 6 p.t. stage (YATSU, 1902a) and as late as the 11 p.t. stage (ASHWORTH, 1915), with settlement occuring at the 10 p.t. (YATSU, 1902a) and 15 p.t. (ASHWORTH, 1915) stages respectively. Setae develop along the entire mantle margin but extend beyond the shell only in

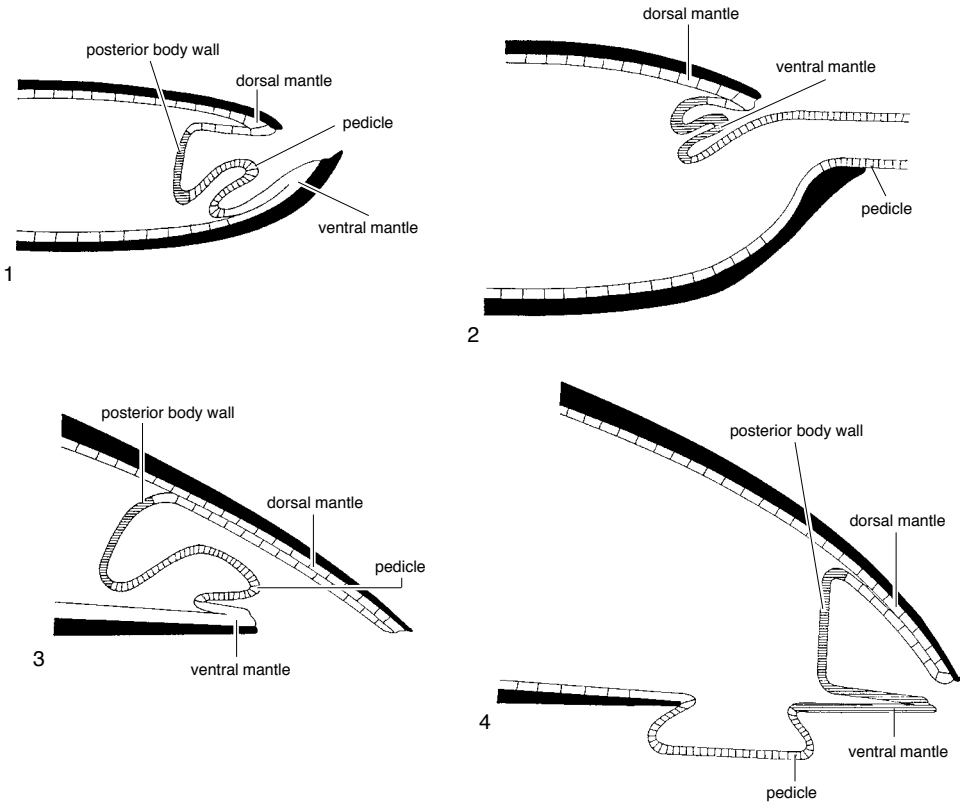

FIG. 165. Diagrammatic longitudinal sections; *1,* young lingulid prior to settling; *2,* adult lingulid; *3,* young discinid prior to settling; *4,* adult discinid (adapted from Williams & Rowell, 1965a).

posterolateral regions. In *Glottidia,* the pedicle is formed and the lophophore differentiated between the 2 and 9 p.t. stages (PAINE, 1963).

The earliest planktonic stage of *Discinisca lamellosa* is at the 2 p.t. stage and is characterized by two tufts of embryonic setae and a functional digestive system. The lophophoral tentacles are added in the same way as in *Lingula,* but the discinid larva is presumed to remain at the 4 p.t. stage throughout the planktonic phase, as no more developed, free-swimming stages have been observed. The shell is secreted at the 4 p.t. stage as a transparent, subcircular disc. Discinid larvae develop a complex succession of four different types of setae and may also possess statocysts and putative eyespots (Fig. 166; HAMMOND, 1980). The shell-less larva swims with its trocholophe, tentacles, and median tentacle fully extended and the tentacles bent slightly inward or outward near the tip (Fig. 167). Older *Discinisca* larvae shed their setae and swim like *Lingula,* rotating in a clockwise direction when viewed from the anterior end (CHUANG, 1968, 1977). The larvae propel themselves mainly with the beating of the lateral cilia of the lophophore and tentacle.

All larvae of *Pelagodiscus atlanticus* have been taken in water less than 200 m deep, well above the range of adult *Pelagodiscus;* and earlier stages probably remain in deeper water. There is little information about settling, but it is assumed that the larvae become attached at the 4 p.t. stage after a free-

swimming period that lasts about five or six days (MÜLLER, 1860).

The two thin valves of the larvae are roughly circular with a width of about 400 μm to 500 μm and are held together by the body wall and muscles. Characteristically, there are five pairs of principal setae (Fig. 168). The anterior four pairs are attached to the ventral valve; those placed further back are much broader and larger than the others. The fifth pair of principal setae occurs posteromedially in the dorsal mantle where it is associated with about 30 pairs of minor setae developing along the lateral and anterior margins. The lophophore, which at this stage contains coelomic spaces and associated musculature, is similar to that of *Lingula;* but the tentacles are relatively thicker, and the median tentacle is only a broad projection of the anterior margin. Within the body cavity, the alimentary canal is functional, and the intestine opens to the right side of the body wall through the anus. The digestive diverticula are not developed, but the wall of the gut is already differentiated. Metanephridia and statocysts are present, and the musculature is well developed, although the posterior adductor muscles are not yet formed. A pedicle rudiment occurs, confined within the valves, and, as in *Lingula,* it projects from the inner surface of the ventral mantle (Fig. 169). A pair of larval eyespots is also developed on the lateral body walls.

At settlement, the pedicle is protruded from the valves through the notch at the posterior margin of the ventral valve. The eyespots are lost, larval setae are replaced by adult ones, and the median tentacle is reduced in size shortly after settling. There is no detailed information on the postlarval development of *Pelagodiscus.* Very little is known about the larval stages of other discinids, but *Discinisca laevis* have been observed already attached at the 6 p.t. stage; and morphologically they are similar to recently settled *Pelagodiscus* (WILLIAMS & ROWELL, 1965a).

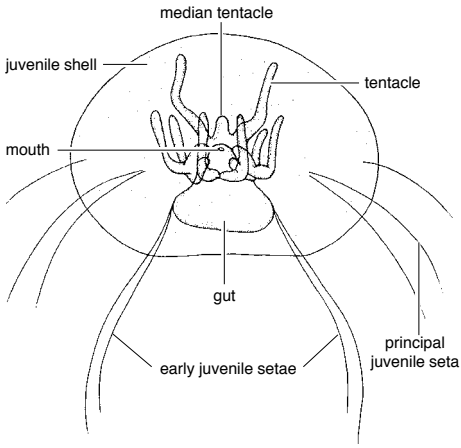

FIG. 166. Diagram of a free-swimming larva of *Discinisca* (adapted from Chuang, 1977).

Craniids

The larvae of *Neocrania* are lecithotrophic (NIELSEN, 1991). During the early, free-swimming stages of *Neocrania,* the endoderm occupies the anterodorsal part of the archenteron and the mesoderm occupies the posteroventral part (Fig. 162.1). The archenteron elongates with the blastopore at the posterior end of the ventral side. The endoderm elongates and narrows, while the mesoderm expands into a pair of lateral lobes (Fig. 162.2). Eventually, the endoderm constricts, and the archenteron persists anteriorly as a narrow lumen. Mesoderm still surrounds the narrow blastopore but extends to the anterior end of the endoderm and divides into a series of lateral plates. The setal sacs develop from three pairs of dorsal, ectodermal invaginations (Fig. 162.3). The posterior part of the endoderm becomes a solid cylinder, and the blastopore closes. Four pairs of coelomic sacs form from four pairs of plates of mesoderm, which fold up. The anterior pair of coelomic sacs surround the anterior part of the endoderm almost completely, while the three posterior pairs have a more restricted lateral position. In addition, small setae are formed from the setal sacs (Fig. 162.4; NIELSEN, 1991).

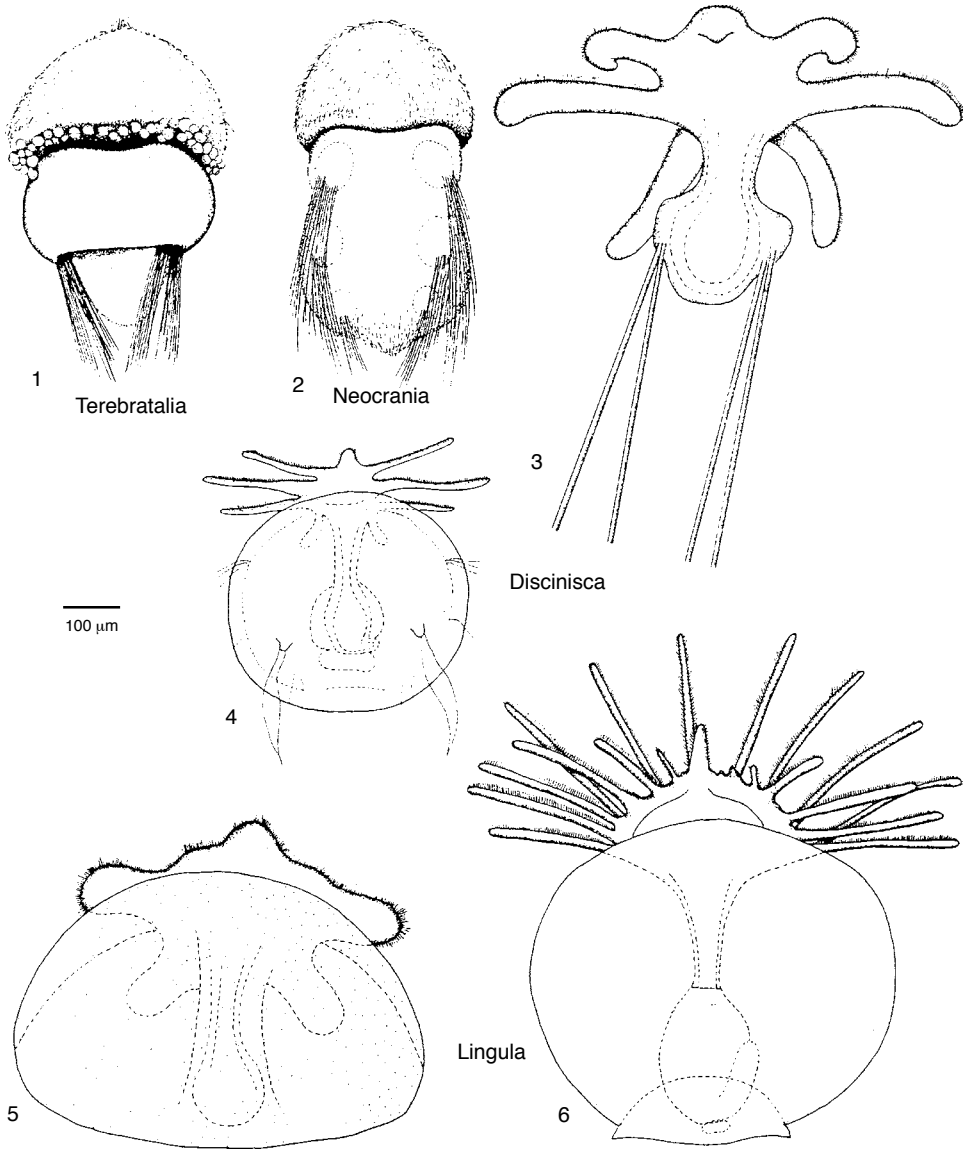

FIG. 167. Larvae of the four main types of brachiopods, dorsal views; *1, Terebratalia transversa; 2, Neocrania anomala; 3,* early *Discinisca* larva; *4,* full-grown *Discinisca* larva; *5,* early *Lingula* larva; *6,* the almost full-grown *Lingula* larva, scale bar: 100 μm (adapted from Nielsen, 1991).

Neocrania larvae, about 220 μm in length, appear to be fully developed approximately three days after fertilization (Fig. 170). The rounded anterior lobe and the lateral, ventral, and posterior sides are ciliated. Three pairs of long, setal bundles occur laterally on the dorsal side. The larvae are light brown and have a pair of reddish, anterolateral pigmented spots that have been interpreted as eyespots (NIELSEN, 1991).

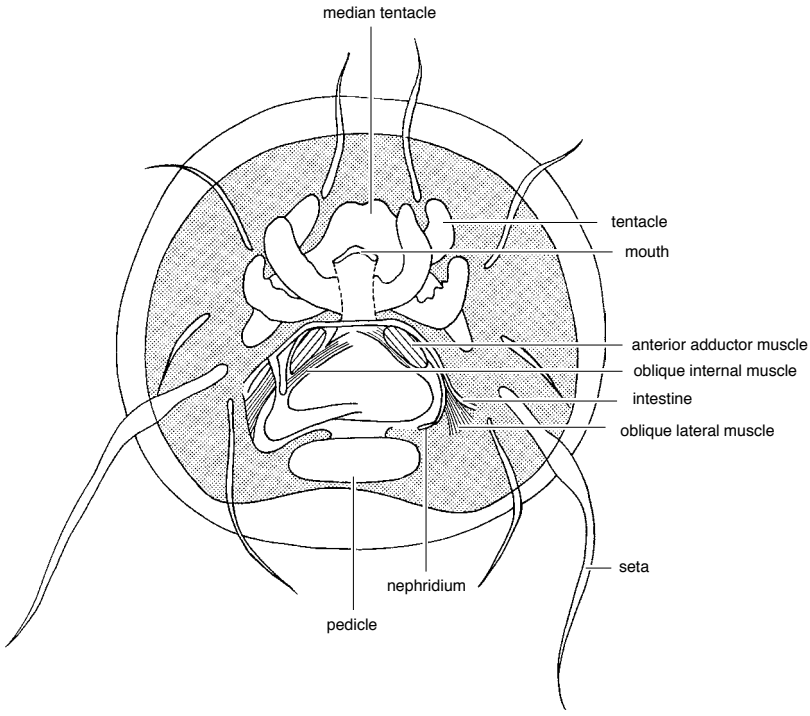

FIG. 168. Larval *Pelagodiscus* with 4 p.t. viewed ventrally, minor setae in dorsal valve omitted (adapted from Ashworth, 1915).

Articulated brachiopods

A fully developed, late stage larva of articulated brachiopods usually consists of the anterior, mantle, and pedicle lobes; it does not possess a functional gut and is lecithotrophic.

The anterior lobe is typically ciliated and bears a tuft of long apical cilia, supported on an apical plate. The apical cilia vary in length and in *Calloria* (PERCIVAL, 1944) and *Notosaria* (PERCIVAL, 1960) are lost prior to metamorphosis. In *Terebratalia,* the posterior margin of the anterior lobe supports a dense band of longer cilia (Fig. 171; LONG, 1964; STRICKER & REED, 1985a). The anterior lobe of many larvae possess putative eyespots (ocelli) or groups of small, usually red, pigment granules. Eyespots generally occur apically or subapically. *Argyrotheca* has four separate eyespots (KOWALEVSKY, 1883; SHIPLEY, 1883; PLENK, 1913); *Lacazella* has two or four (LACAZE-DUTHIERS, 1861; KOWALEVSKY, 1883); *Pumilus* has four groups of two (RICKWOOD, 1968); *T. transversa* has two groups of five to eight granules (LONG, 1964); *Coptothyris* and *T. coreanica* have two groups of about 10 (HIRAI & FUKUSHI, 1960); and *Frenulina sanguinolenta* has two groups of about 20 (MANO, 1960). Pigment granules usually occur as spherical protuberances (vesicular bodies; LONG & STRICKER, 1991). *T. transversa* has a number of these outgrowths (Fig. 167, 171), and *Calloria* has about 60; they are arranged along the posterior margin of the anterior lobe in both species. Eyespots and pigment granules do not occur in the larvae of *Hemithiris, Notosaria, Terebratulina unguicula, T. septentrionalis,* or *T. retusa* (CHUANG, 1990). Descriptions of eyespots and pigment granules are often confused, but it is likely that these features are

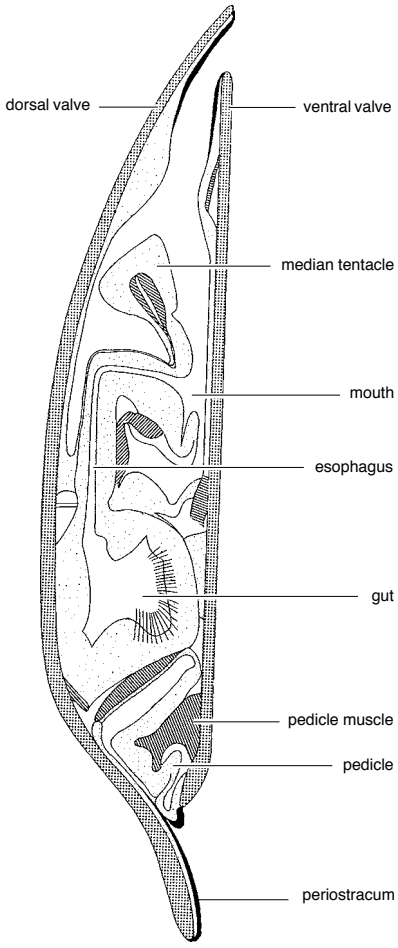

FIG. 169. Diagrammatic median longitudinal section of larval *Pelagodiscus* with four pairs of tentacles (not shown) located laterally from midline (adapted from Ashworth, 1915).

not homologous. Each of the eyespots of *Argyrotheca* consists of a cuplike invagination of the ectoderm with underlying nerve fibers and vitreous humor (PLENK, 1913), a neurological connection implying a sensory role. Pigment granules, however, lack any known connection with the nervous system and are assumed to be some form of metabolic waste (CHUANG, 1990).

The mantle lobes of the late-stage larva are clearly divisible into dorsal and ventral lobes. In *T. transversa* and probably other species a mantle lobe comprises an outer layer of thin, flattened, ectodermal cells and an inner layer of tall, columnar cells. These two layers enclose a space containing mesodermal cells also arranged in two sheets with a coelomic space in between. The mantle lobe grows until it almost completely encloses the pedicle lobe (LONG, 1964). Both lobes extend posteriorly from the midriff of the larvae, progressively enveloping the pedicle lobe. The ventral lobe is the larger and in *T. retusa* has been observed to extend beyond the distal tip of the pedicle lobe in specimens with delayed settlement (JAMES, unpublished, 1989). The outer, ectodermal layer contains large vacuoles (LONG, 1964). A longitudinal band of cilia on the ventral side of the mantle lobe enables the larva of *Notosaria* to creep along the substratum (PERCIVAL, 1960). Similarly, in *T. transversa* only a midventral band of cilia occurs on the mantle lobe (Fig. 171). Generally, two pairs of setal bundles are present and are formed in four separate ectodermal invaginations at the distal margin of the mantle lobe and disposed as two lateral and a pair of dorsal bundles. Each bundle contains from 4 to 20 setae in various larvae studied. The larva of *Lacazella* was reported as lacking setae (RUDWICK, 1970).

In the pedicle lobe, the ectoderm consists of a single layer of columnar cells that may be ciliated, although in *T. transversa* (LONG, 1964) and *T. retusa* (JAMES, unpublished, 1989) no cilia are present on the pedicle lobe. Some cells of the outer walls of the coelomic epithelium elongate and differentiate into smooth muscle cells to form a pair of pedicle adjustors. These extend from the base of the anterior (proximal) region of the mantle lobe into the pedicle lobe (FRANZEN, 1969; STRICKER & REED, 1985a, 1985b). Prior to settlement, the pedicle lobe of *T. transversa* develops a subequatorial constriction. The region to the posterior of the constriction tapers and eventually differentiates into the pedicle and the surrounding pedicle sheath of the metamorphosed juvenile. The anterior part of the pedicle is packed with

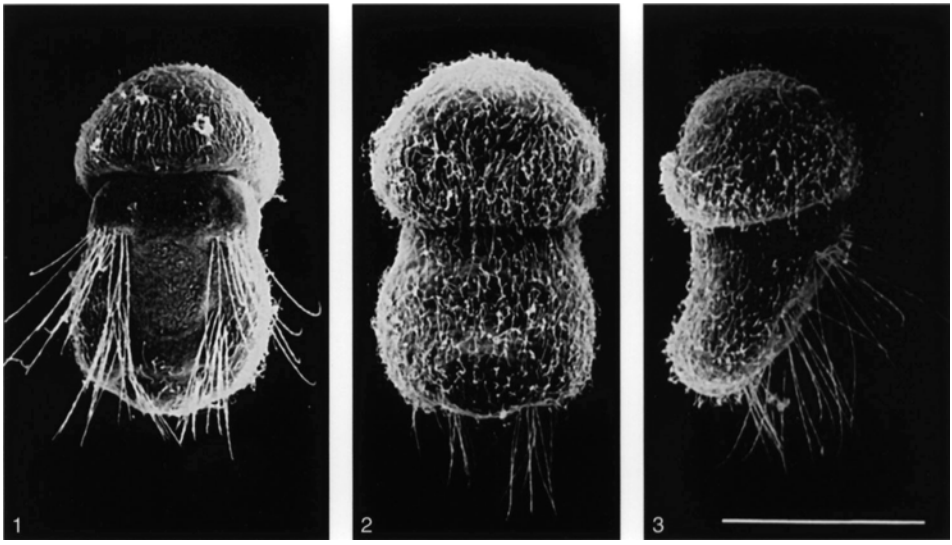

FIG. 170. SEM micrographs of full-grown larvae of *Neocrania; 1,* dorsal view, the circular dorsal area that will form the brachial valve recognizable; *2,* ventral view; *3,* lateral view, scale bar: 100 μm (Nielsen, 1991).

tissue that contains rudiments of some of the internal organs (see Fig. 63; LONG & STRICKER, 1991).

In contrast to the development of lingulids and discinids, the organs of the calcareous-shelled brachiopods are poorly differentiated during the free-swimming larval phase. Only the presumptive pedicle muscles, the incipient coelomic spaces, and the nonfunctional larval gut are present (Fig. 172.1; LONG & STRICKER, 1991). The presence of larval metanephridia, however, has been described in *Argyrotheca* (PLENK, 1913).

Larval Behavior

During the motile, planktonic larval phases, which may last from hours in articulated and craniid brachiopods to weeks in the lingulids and discinids, the larvae undergo morphological and behavioral changes. Accounts of larval behavior, particularly at settlement and metamorphosis, are rare (JAMES & others, 1992), and little information exists on the behavior of the planktonic larval stages of discinid and lingulid larvae.

When a brachiopod larva is capable of swimming freely, at hatching or upon liberation from a brood chamber, its behavior is likely to be influenced primarily by gravity or light. Positive phototaxis has been documented during the early, free-swimming larval stages of a number of articulated species, which become negatively phototactic prior to settlement.

The gametes of *T. retusa* are freely spawned, and the larvae first achieve motility at a stage that is presumed to be pregastrulation. The larvae, which are effectively revolving balls of cells, do not appear to move in a defined pattern until gastrulation has occurred. Postgastrulated larvae are slightly anteroposteriorly elongate and compressed dorsoventrally. Larvae at this stage rotate along the anteroposterior axis, usually in a clockwise direction when viewed anteriorly. Axial rotation and movement (anterior end forward) presumably allow the larvae to orient and swim in a trajectory. At this stage, larvae of *T. retusa* are negatively geotactic and swim away from the substrate. During early, free-swimming stages, such larvae exhibit no

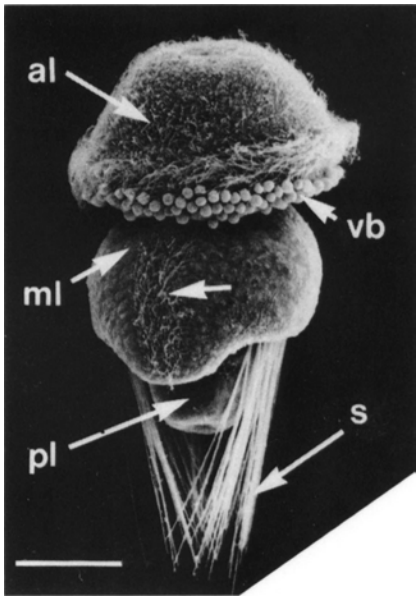

FIG. 171. SEM micrograph of a free-swimming larva of *Terebratalia* at 110 hours after fertilization; *arrows* mark an unlabeled band of cilia on the mantle lobe (*ml*), scale bar: 50 μm; *al,* apical lobe; *pl,* pedicle lobe; *s,* setae; *vb,* vesicular bodies (Stricker & Reed, 1985a).

response to light, although positive phototaxis may occur for a short period later in development. Eventually, they become positively geotactic, and negative phototaxis may also be involved. The now characteristically three-lobed larva swims toward the substrate with the anterior lobe flexing and sweeping in a lateral arc whenever it, or the apical cilia, make contact with the substratum (JAMES, unpublished, 1989; JAMES & others, 1992).

Brooded articulated larvae that emerge from the parent at a later stage of development may behave differently. The larvae of *Frenulina,* for example, just after emerging from the mantle cavity of the brooding parent, show positive phototaxis that becomes negative within a few hours (MANO, 1960).

Like that of *T. retusa* (JAMES & others, 1992), the *Frenulina* larva (MANO, 1960) sinks and rubs its anterior lobe against the substratum (CHUANG, 1990). Likewise, larvae of *Notosaria* glide along the surface of the substrate with the aid of a ventral band of cilia for several hours, the anterior lobe probing the substratum (PERCIVAL, 1960). *Neocrania* larvae that are competent to settle descend to the substrate and crawl, apparently seeking a suitable medium on which to settle (NIELSEN, 1991).

Most larvae possess a number of setal bundles that serve both a sensory and a defensive role. When the larva of *Argyrotheca,* for example, is disturbed, it contracts violently and projects its tufts of setae out in all directions (KOWALEVSKY, 1883). The larval setae of *Discinisca* are used in a similar defensive response (CHUANG, 1977). *T. transversa* larvae contract, bringing the anterior and posterior lobes closer together. The mantle lobe is raised from the pedicle lobe and the setae are erected perpendicular to the body to form a defensive circle around the middle of the body (LONG, 1964). The larva of *Neocrania* reacts in a similar manner. The undisturbed larva swims with the setae held close to the body. Irritation, however, stimulates contraction of the longitudinal ventral muscles, causing the body to curl up, bringing the anterior and posterior ends into contact and extending the setae in all directions (NIELSEN, 1991).

BROODING

Some articulated brachiopods brood their larvae in specialized pouches within the body cavity or in the mantle cavity. Species that brood are presumed either to draw sperm in with the inhalant current generated by the lophophore or, among simultaneous hermaphrodites, to effect self-fertilization (LONG & STRICKER, 1991). Fertilization probably occurs in the mantle cavity or within the brood pouch or chamber. Generally, small numbers of lecithotrophic embryos and larvae are brooded to an advanced state of motile larval development when settlement and metamorphosis may be possible soon after liberation from the parent.

Brooding within the mantle cavity occurs either by adherence of the larvae to the inner

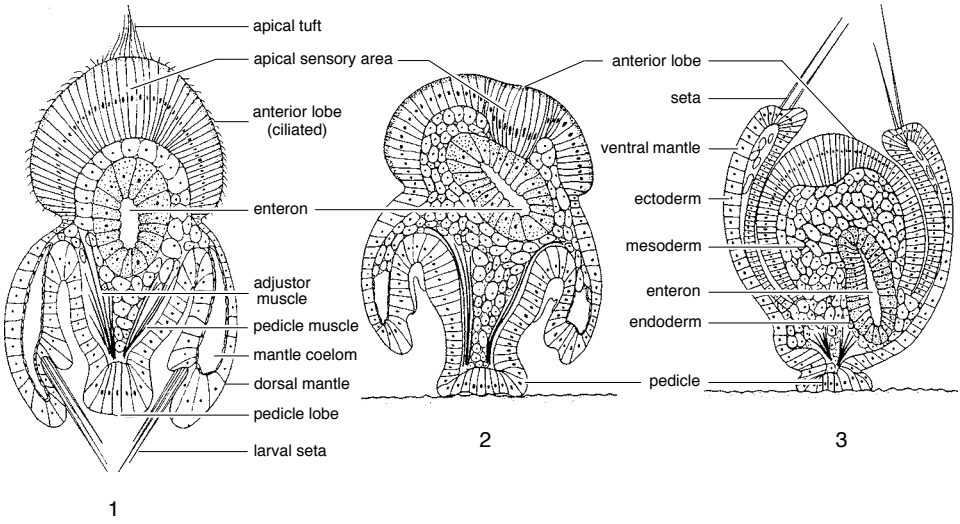

FIG. 172. Diagrams of longitudinal median sections of trilobed larva of *Terebratulina retusa; 1,* immediately prior to settlement; *2,* after settlement; *3,* after metamorphosis (adapted from Franzen, 1969).

mantle surface or within the confines of the tentacles of the lophophore. Early developmental stages of *Calloria* adhere to the mantle and develop into free-swimming larvae before discharge (PERCIVAL, 1944). The ova of *Frenulina* are spawned and adhere to longitudinal nurse ridges, one on each side of the midline of the dorsal mantle, where fertilization and development into free-swimming larvae take place (MANO, 1960).

Tentacles of the lophophore form a natural refuge in which a number of articulated species brood their larvae. *Pumilus* retains embryos and larvae within its schizolophe for at least nine days prior to the release of larvae, which are competent to settle (RICKWOOD, 1968). The rhynchonellids *Hemithiris* (LONG & STRICKER, 1991) and *Notosaria* (PERCIVAL, 1960) retain their shed ova in a basket created by curling the distal ends of the lophophore tentacles. Larvae develop at the base of the tentacles and the brachial lip and are generally oriented with their anterior ends toward the mouth (see Fig. 119; HOVERD, 1985). The larvae of *Liothyrella uva antarctica* are similarly sequestered in the spirals of the lophophore (BLOCHMANN, 1906). *T. unguicula* broods several thousand larvae within the lateral arms of its plectolophe (LONG, 1964) as does *T. septentrionalis.* The larvae are retained beneath the lophophoral tentacles that enclose them against the wall of the main body cavity and the floor of the dorsal mantle, thus forming a basket (WEBB, LOGAN, & NOBLE, 1976).

Lacazella possess two median, lophophore tentacles that are modified for the attachment of the embryos and larvae. The specialized tentacles are longer and larger than other tentacles and possess a collar of cells at the base of the swollen, pyriform, and glandular tentacle tip. A cellular suspensory filament attaches individual embryos to these tentacles. The embryos suspended on the distal parts of the modified tentacles are inserted into a single median brood pouch behind the mouth, embedded in the posteroventral portion of the body cavity (Fig. 173; LACAZE-DUTHIERS, 1861). *Argyrotheca* (KOWALEVSKY, 1883; SHIPLEY, 1883; SCHULGIN, 1885) as well as *Thecidellina* are known to deliver their eggs into brood pouches (WILLIAMS & ROWELL, 1965a). In *Argyrotheca* that brood, each -

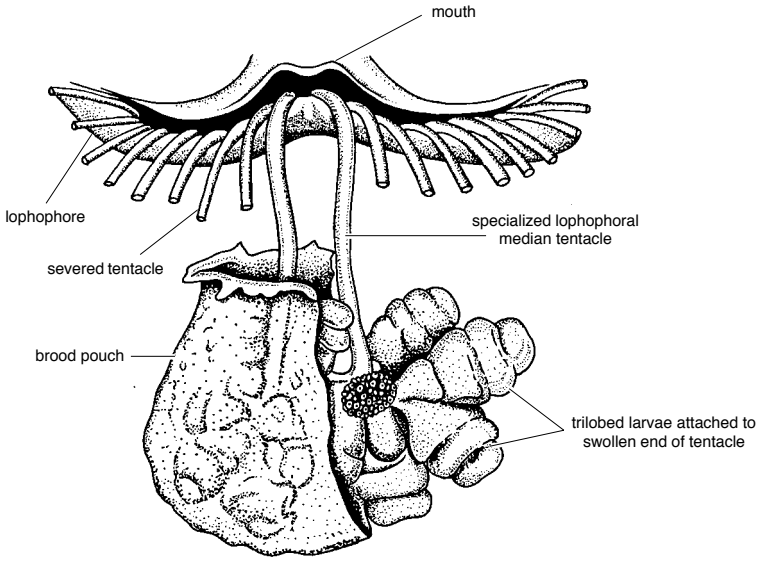

FIG. 173. Brood pouch and modified lophophoral tentacles of *Lacazella mediterranea;* part of the pouch has been removed to reveal the three-lobed larvae attached to a tentacle (adapted from Lacaze-Duthiers, 1861).

metanephridiopore opens to a separate brood pouch situated under the posterior border of the lophophore (SHIPLEY, 1883). Gametes are passed from the body cavity through the modified metanephridia directly into the brood pouches where the embryo develops, attached to the wall of the pouch by a fine filament (KOWALEVSKY, 1883; SHIPLEY, 1883). Brooding within the body cavity also occurs in *Gwynia capsula* where the larvae are retained to the three-lobed stage (SWEDMARK, 1967).

SETTLEMENT

Studies of substrate selection and the mechanisms involved in settlement and the subsequent survivial and growth of the sessile and juvenile stages facilitate an understanding of brachiopod life history and distribution patterns.

Some authors report rugophilic behavior, preferential settlement on a particular type of substratum and on or near members of the same species. Inferences on behavior drawn from patterns of juvenile settlement neglect the impact of other processes such as grazing, selective predation, substratum failure, and fluid dynamics near the substratum. Settlement of the larvae in the laboratory has been observed in *T. septentrionalis* (MORSE, 1873), *Argyrotheca* (SHIPLEY, 1883), *Calloria* (PERCIVAL, 1944; WISELY, 1969), *T. coreanica* and *Coptothyris* (HIRAI & FUKUSHI, 1960), *T. transversa* (LONG, 1964; STRICKER & REED, 1985a, 1985b), *Hemithiris* (LONG, 1964) and *Pumilus* (RICKWOOD, 1968). Data on selection of substrates are, however, sparse, and experimental evidence is inconclusive.

All brachiopod larvae are, to some degree, capable of delaying settlement until a suitable substratum has been located. For the planktotrophic lingulid and discinid larvae, competence to settle may last for several weeks; for the lecithotrophic larvae of articulated brachiopods and *Neocrania* the limit may be perhaps hours or a few days.

Lingulids and discinids

The larvae of lingulids and discinids, which pass through a relatively brief lecithotrophic embryonic phase before adopting a planktotrophic mode of life, may persist as

larvae for several weeks. Ambient water temperature, food, and suitable substrate availability may all have a profound influence on the rate of development of both embryo and larva. In temperate waters, it is estimated that the larvae of *Lingula* take approximately five to six days to achieve the 3 p.t. stage at which hatching occurs; and a further six weeks may be spent as plankton for the larva to reach the 15 p.t. stage (YATSU, 1902a). According to YATSU (1902a), in *Lingula* settlement is possible at the 10 p.t. stage. CHUANG (1959b) and BROOKS (1879), however, recorded settlement at the 9 p.t. stage in *Lingula* and *Glottidia* respectively. Given appropriate conditions it is estimated that *Lingula* may complete both embryonic and larval development in 31 to 32 days (CHUANG, 1990). The larval development of *Glottidia* is estimated to take 20 days at temperatures between 25 and 30°C (Table 5, p. 180; PAINE, 1963). The length of the larval stage in *Discinisca* is unknown, but the 4 p.t. stage is assumed to correspond to several p.t. stages in *Lingula* (CHUANG, 1990).

The pedicle protrudes from the valves, and the larvae burrow with the anterior end, using the setae to move the sand grains. The pedicle protrudes from between the valves, and the tip adheres to sand grains (PAINE, 1963). The larvae of *Discinisca* (CHUANG, 1977; HAMMOND, 1980) and *Pelagodiscus* (CHUANG, 1990) are presumed to settle at the 4 p.t. stage.

The larvae of lingulids and discinids can remain as plankton and become drift larvae. Drift larvae grow beyond the stage of development normally attained at settlement. In drift larvae of *Lingula,* the lophophore continues to grow by adding new pairs of tentacles, and the median tentacle persists. The epistome continues to enlarge and the shell valves continue to expand circumferentially. The mantle setae increase in number, and the pedicle increases in length but remains within the confines of the valves (CHUANG, 1990). Drift larvae of *Glottidia* also exhibit the characteristics of delayed settlement, with both the pedicle and the setae appearing in much larger larvae (PAINE, 1963). In drift larvae of *Discinisca,* the valves continue to grow, setae continue to increase in length but not number, and the pedicle continues to increase in size while remaining within the valves; the flexible mantle setae also increase in number (CHUANG, 1990). Lingulid and discinid larvae do not, however, undergo true metamorphosis at settlement.

Craniids

Lecithotrophic larval development in *Neocrania* takes approximately 70 hours (Table 5, p. 180).The larva attaches when it is about 200 μm to 300 μm long. Newly settled larvae possess ventral muscles that extend from the first pair of coelomic sacs to the posterior end of the larva. These muscles constrict, causing the larva to curl up ventrally (Fig. 174). Likewise, the muscles around the coelomic sacs contract, spreading out the setae of sacs 1 and 2 (those of sac 3 having been shed and the cilia having disappeared) (Fig. 162.5; NIELSEN, 1991). The posterior part of the body of the larva and the apical part of the anterior lobe make contact with and adhere to the substratum. During the days following settlement the larval body of *Neocrania* gradually flattens and becomes more rounded. Glandular cells on the dorsal surface secrete the dorsal valve, which grows radially pressing out the mantle setae along the sides of the body (Fig. 175; NIELSEN, 1991).

Articulated groups

The fully developed, lecithotrophic larvae of articulated brachiopods descend to the substrate after a variably long, demersal phase that may last from hours to a few days in different species (Table 5, p. 180). Although substrate selection has not been demonstrated, accounts describe larvae exploring and probing the substrate, particularly with their anterior lobes. Eventually, the pedicle lobe secretes a sticky sheet (STRICKER &

TABLE 5. Times of appearance of identifiable embryological features during the development of brachiopods; (adapted from James & others, 1992).

Species	Egg diameter (μm)	Temperature (°C)	Time (h)	Developmental stage	Authority
Hemithiris psittacea	190	10	23	blastula	Reed, 1987
			71	gastrula	
			117	mantle lobe appears	
			151	coelomic spaces present	
			187	setae develop	
			200	metamorphosis	
Terebratalia transversa	150	12	2–3	first cleavage	Reed, 1987
			4	second cleavage	
			18–14	blastula	
			22	gastrulation	
			33	coelomic partitioning	
			40	mantle lobe appears	
			48	setae appear	
			61	blastopore closes	
			92	mature larva	
			100	metamorphosis	
Terebratulina unguicula	170	10	3	second cleavage	Reed, 1987
			20	blastula	
			42	gastrulation	
			48	coelomic partitioning	
			66	mantle lobe present	
			102	short chaetae present	
			118	metamorphosis	
Terebratulina retusa	130	10	2	first cleavage	James, unpublished data, 1989
			3	second cleavage	
			19–20	blastula	
			28–30	gastrula	
			50	mantle lobes present	
			60	short mantle	
			72	metamorphosis	
Neocrania anomala	125	*	2	first cleavage	Nielson, 1991
			3	second cleavage	
			4	third cleavage	
			5	fourth cleavage	
			15	blastula (ciliated motile)	
			72	fully developed larva	
Glottidia pyramidata		27	0.5	first cleavage	Paine, 1963
			0.75	second cleavage	
			1	third cleavage	
			1.3	fourth cleavage	
			1.5	fifth cleavage	
			13	mantle lobes formed	
			19	cilia developed	
			24	median tentacle of lophophore formed	
			144–168	free-swimming 3 p.t. stage	
			264–408	5–8 p.t. stage	
			480 (20 days)	9 p.t. stage; settlement	

*larvae cultured at ambient sea temperature (±1°C).

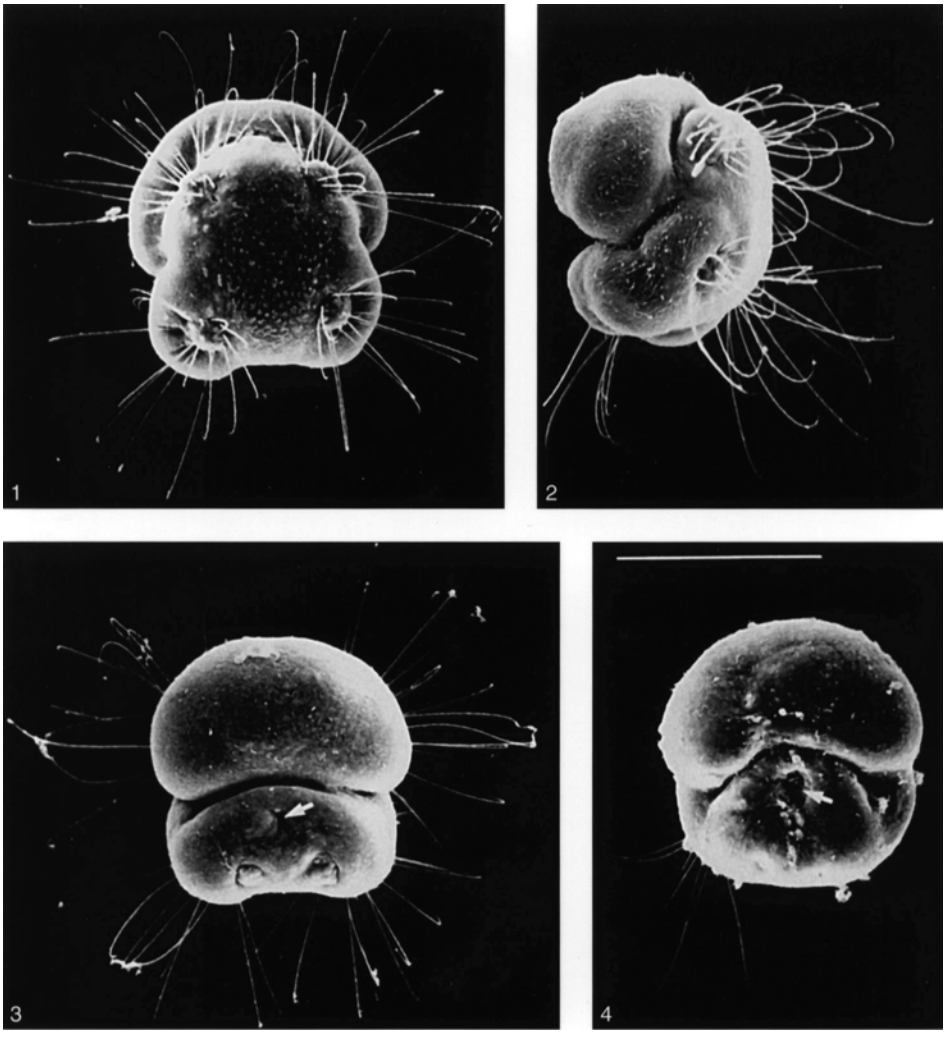

FIG. 174. SEM micrographs of contracted larvae and early settling stage of *Neocrania; 1–3,* contracted larvae in dorsal, lateral, and ventral views, respectively; *4,* ventral view of the newly settled larva; *arrows* point to the retracted attachment areas, scale bar: 100 μm (Nielsen, 1991).

REED, 1985c) or mucous strand (KOWALEVSKY, 1883; JAMES & others, 1992) from the distal tip of the pedicle lobe (Fig. 160.17). By adopting an orientation perpendicular to the substrate, the mucous strand adheres to the substrate, anchoring the larva. The larvae of *T. retusa* displaced at this stage of settlement are capable of reattachment. Once attached, these larvae continue their axial rotation, twisting the strand, effectively reducing its length and bringing the distal tip of the pedicle lobe into contact with the substrate (JAMES, unpublished, 1989). Subsequently, the pedicle lobe initiates a more stable form of substrate attachment.

When the larva of *T. retusa* is deprived of a suitable substrate, the mantle lobes continue to grow and may eventually extend

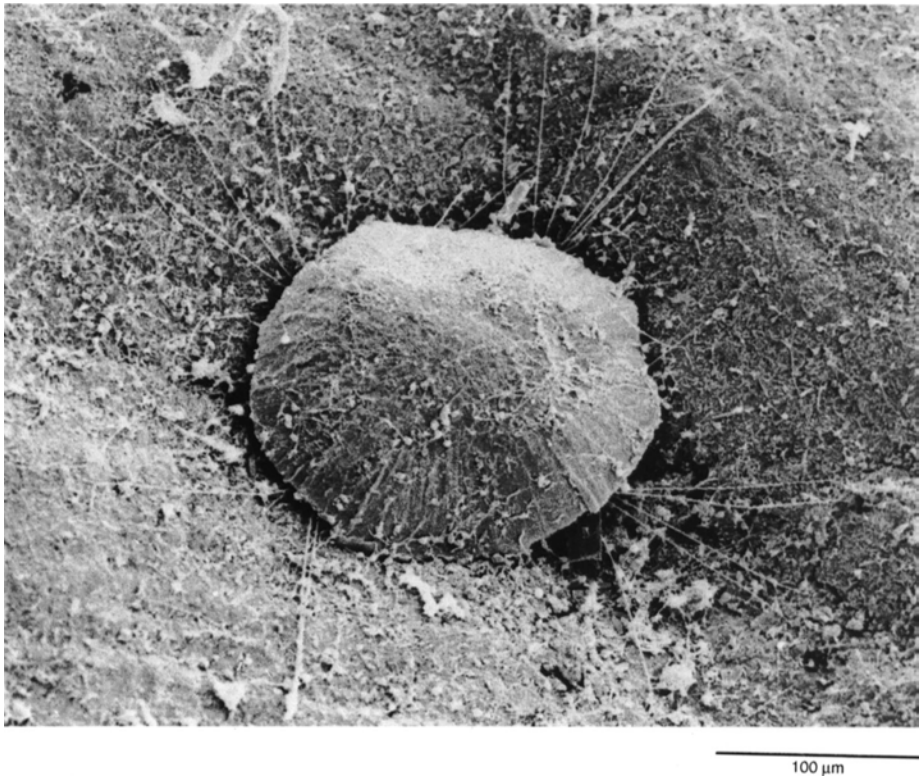

FIG. 175. SEM micrographs of a juvenile *Neocrania* about three days after settling, scale bar: 100 µm (Nielsen, 1991).

below the pedicle lobe. It is unknown if larvae in this condition remain competent to settle and metamorphose, but motile larvae were observed seven days after fertilization (JAMES, unpublished, 1989).

The process of metamorphosis has been described in detail for the terebratulides *T. retusa* (FRANZEN, 1969), *T. transversa* (STRICKER & REED, 1985a, 1985b), and *Calloria* (PERCIVAL, 1944). The general pattern of events appears to be similar in all articulated groups. Following attachment of the pedicle, the pedicle adjustor muscles contract and thereby reverse the position of the mantle lobe, causing it to envelop the anterior lobe (Fig. 160.18–160.19). In addition, fluid pressure generated from the coelom (FRANZEN, 1969) and violent spasmodic contractions of the anterior lobe (PERCIVAL, 1944) may also facilitate reversal of the mantle (CHUANG, 1990). Reversal of the mantle in the larva of *T. transversa* appears to be very rapid (LONG, 1964; STRICKER & REED, 1985a) but may require more than a day in other species (RICKWOOD, 1968). In the larva of *Calloria* the mantle lobe begins reversal at its base, forming a circular fold around the base of the anterior lobe, the free margin of the mantle lobe rolling anteriorly to envelop the anterior lobe (PERCIVAL, 1944). *Frenulina* combines settlement and metamorphosis. It stops swimming, lies on its side on the substrate, suddenly spreads the dorsal tuft of setae, and slowly lifts the dorsal mantle lobe. Simultaneously, the pedicle lobe protrudes and attaches to the substratum with a mucous secretion (MANO, 1960). As no reports exist of metamorphosis in unsettled larvae, it is assumed that settlement is a prerequisite of metamorphosis.

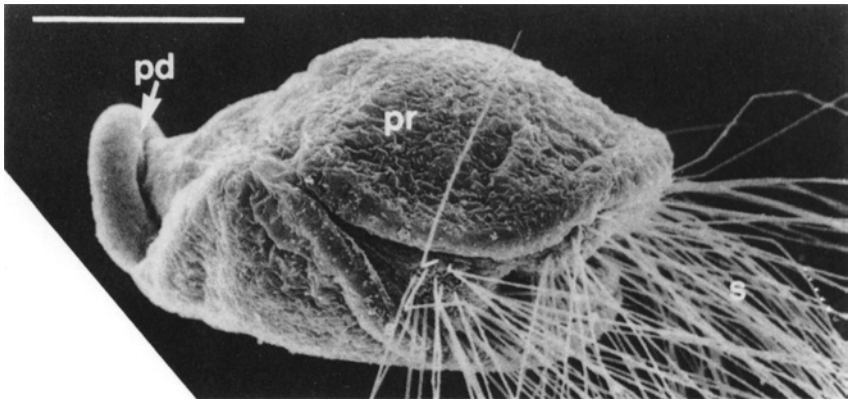

FIG. 176. SEM micrograph of a juvenile *Terebratalia* one day after metamorphosis, scale bar: 50 μm; *pd,* pedicle; *pr,* protegulum; *s,* setae (Stricker & Reed, 1985b).

In the larva of *T. transversa,* the setae on the mantle lobe project anteriorly and are retained, at least during the early part of the juvenile stage. Although formation of the periostracum begins prior to reversal of the mantle in the larva of *T. transversa,* no larval or embryonic shell is deposited until metamorphosis has taken place (STRICKER & REED, 1985a). In the larva of *Calloria,* however, formation of the shell is initiated before the mantle lobe is reversed (PERCIVAL, 1944), and externally the metamorphosed juvenile resembles a small adult (Fig. 160.19; 176; STRICKER & REED, 1985a).

POSTLARVAL AND EARLY JUVENILE DEVELOPMENT

Lingulids and Discinids

Lingulid and discinid postlarval forms are effectively miniature adults at the time of settlement with most of the postlarval organs formed (Fig. 177; CHUANG, 1990).

During the entire larval stage of *Lingula* (YATSU, 1902a; CHUANG, 1959b), *Glottidia* (BROOKS, 1879; PAINE, 1963) and *Discinisca* (CHUANG, 1968, 1977), the trocholophe persists (CHUANG, 1990). After settlement at about the 9 p.t. stage (or later) in *Lingula* (CHUANG, 1959b) and *Glottidia* (BROOKS, 1879; CHUANG, 1959b) and at the 4 p.t. stage in *Discinisca* (CHUANG, 1977), the median tentacle diminishes in size, becomes a small prominence in the epistome, and finally disappears. The two anterior, generative tips of the trocholophe, one on each side of the median tentacle, diverge, each developing into a curved brachium and giving rise to a series of tentacles. The lophophore is now a schizolophe, a condition that persists in the adult lophophore of *Pelagodiscus.*

In *Lingula, Glottidia,* and *Discinisca,* the trocholophe loses its locomotor function at settlement and is solely devoted to the role of circulating water through the mantle cavity for ventilation and feeding. For *Lingula,* this change in function coincides with atrophy of the two larval, lophophore retractor muscles before the 7 p.t. stage and the end of the larval stage respectively (YATSU, 1902a). An epistome forms, enlarges, and differentiates into the brachial fold to cover the mouth and the brachial groove.

The two generative zones at the tips of the pair of brachia of the trocholophe gradually move apart to define a median indentation, and the lophophore becomes a schizolophe. The epistome then undergoes lateral expansion concentric with the tentacle bases to form the juvenile brachial lip, which covers the brachial groove along its entire length. With further growth of the lophophore, the

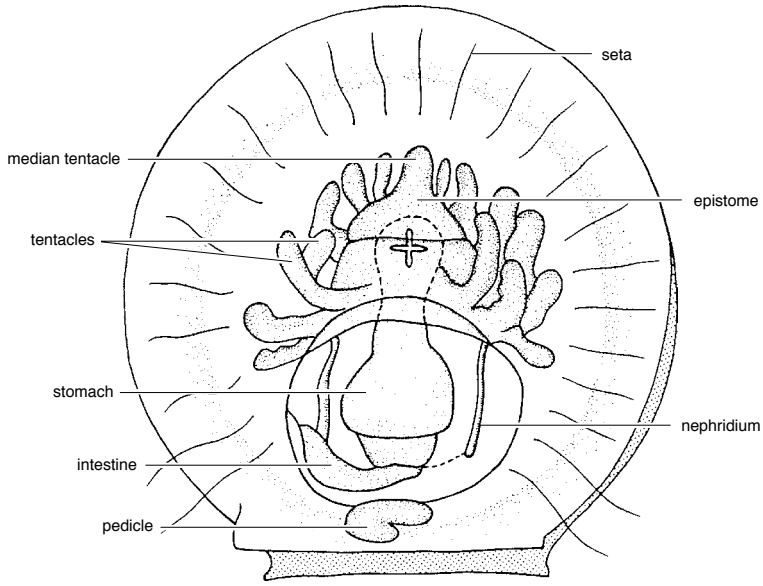

FIG. 177. Larval *Lingula anatina* with 8 p.t. viewed ventrally (musculature omitted) (adapted from Yatsu, 1902a).

generative zones are pushed away as the apices of the two ever-increasing spires, medially in the lingulids, ventrally in the discinids. Thus, the brachia form a series of whorls, eventually transforming the lophophore into a spirolophe; a chitinous brachial skeleton and the turgidity of the brachial canals provide the necessary support for the lophophore.

Craniids

Neocrania larvae are ciliated on the anterior lobe and the dorsal side of the body. At settlement, the cilia disappear, and the posterior pair of setal bundles are shed (NIELSEN, 1991). The newly settled *Neocrania* larva does not possess a functional gut, lophophore, or main organ rudiments and, like articulated forms, undergoes the most radical changes in morphology at settlement, adapting from a free-swimming, lecithotrophic larva to a sessile, suspension feeder. The dorsal valve forms within the first few days of settlement, and some of the attendant musculature appears to be present, as the valve can be pulled down to the substratum when the animal is disturbed (NIELSEN, 1991).

A *Neocrania* juvenile at approximately two days after settlement possesses ventral muscles that extend from the first pair of coelomic sacs to the thickened posterior epithelium, which is, in turn, attached to the substratum (Fig. 162.6). The second and third pairs of coelomic sacs stretch longitudinally, and each sac of the second pair develops a small, dorsal extension that forms the attachment of the sac to the epithelium in the anterior region of the expanding valve. During the later stages of metamorphosis the growing valve also pushes the setae aside (Fig. 162.6). The fourth pair of sacs is situated below the expanding third pair. None of the coelomic sacs is fused in the midline, and at this stage the endoderm is compact with no trace of mouth or anus. Eventually the two valves completely cover the body. After about a month after settlement, three pairs of tentacles are present but there is no well-defined median tentacle. An open gut with a mouth has formed at the bottom of the un-

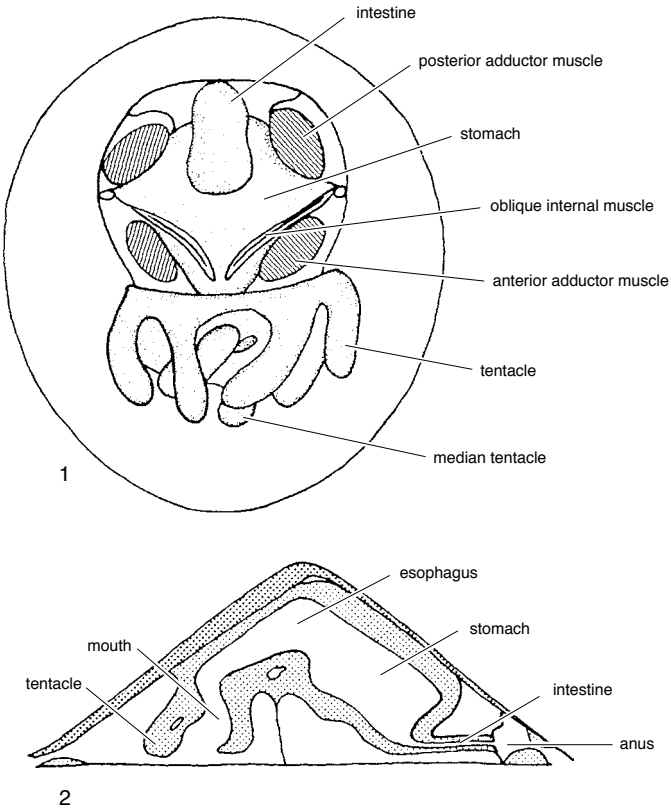

FIG. 178. Young *Neocrania anomala* recently attached, with 3 p.t. *1,* viewed ventrally and *2,* in diagrammatic median section (adapted from Rowell, 1960).

derside of the larval head, and the intestine is presumed to terminate at an anus at this stage (Fig. 162.7; NIELSEN, 1991).

At this stage the mantle has already secreted a thin calcareous shell covered by periostracum, but the ventral mantle is invested only in a periostracal layer that cements the animal to the substratum (WILLIAMS & WRIGHT, 1970). With the exception of the lophophore protractor and anal muscles, the adult muscle system is already present (Fig. 178).

The first and fourth pairs of coelomic sacs are no longer distinguishable, and the second pair fuses dorsally and ventrally, forming a ring around the secondary opening between the ectoderm and endoderm. Muscle filaments are present in two extensions, which attach the coelomic sacs to the epithelium of the dorsal valve. The third pair of coelomic sacs extends and makes contact dorsally and ventrally to form thin mesentaria, dorsal and ventral to the stomach. There is a large anterior adductor muscle on either side of the anterior part of the stomach; each muscle cell is attached to the shell epithelia. A much smaller pair of posterior adductors develops somewhat later, lateral to the posterior end of the stomach. At the same time a pair of oblique, internal muscles develops (Fig. 162.7; NIELSEN, 1991).

Digestive diverticula first appear at about the 10 p.t. stage as pouchlike outgrowths of the anterodorsal stomach wall. The anus

originates at the 5 p.t. stage. Metanephridia first appear at the 9 p.t. stage as two rows of cells embedded in the lateral body walls. They do not develop a lumen or become fully functional until the 16 p.t. stage. At earlier stages of development, the lophophore possesses a median tentacle and is rather like that of juvenile *Lingula.* The median tentacle of the lophophore was reported as being lost during the 5 to 6 p.t. stage (Rowell, 1960), the 10 p.t. stage, and as late as the 18 p.t. stage (Chuang, 1974) in the postlarva of *Neocrania.* The brachia form a series of whorls, transforming the lophophore into a spirolophe; the turgidity of the brachial canals provides the necessary support for the lophophore.

Articulated groups

Articulated brachiopods have few specialized larval organs. The apical tuft of long cilia found on the anterior lobe of articulated larva is presumed to be sensory and is usually lost soon after or immediately before settlement. The eyespots of *Frenulina* disappear by the 2 p.t. stage and bundles of larval setae are replaced along the entire mantle margin by postlarval setae (Mano, 1960).

Externally, the settled, postmetamorphic juvenile of articulated brachiopods resembles a miniature adult. Internally, however, only the pedicle retractor muscles, an enclosed gut rudiment, and incipient coelomic spaces have been reported in early juveniles. In *T. transversa,* a bivalved protegulum is secreted over the entire surface of the mantle within the first 24 hours of metamorphosis. The protegulum is calcified, and by four days after metamorphosis the rudiments of a juvenile shell have been added to the anterior and lateral edges of the protegulum (Stricker & Reed, 1985b). An ectodermal invagination near the posterior margin of the apical lobe, assumed to be the former site of the blastopore, forms the stomodaeum (mouth) and the esophagus, which communicate with the anterior part of the gut rudiment. The gut rudiment differentiates into two chambers. The anterior chamber forms the stomach, which gives rise to the digestive diverticula and is connected to the stomodaeum by the esophagus. The posterior chamber forms the blind-ending pylorus, as articulated brachiopods lack an anus or the equivalent of the intestine of inarticulated brachiopods (Rudwick, 1970; Chuang, 1990; Long & Stricker, 1991).

Little information exists on the formation of the excretory organs of articulated brachiopods, but strands of mesodermal cells near the inner surface of the body wall in postmetamorphic juveniles of *T. retusa* at about the 2 p.t. stage hollow out to form part of the metanephridia (Franzen, 1969).

In *T. transversa,* the pedicle adjustors are inserted into a solid core of connective tissue in the pedicle. Cartilage-like tissue occurs within the pedicle at later stages of development (Stricker & Reed, 1985c).

The lophophore of the articulated brachiopods is a postmetamorphic development of the anterior lobe (Long, 1964) and is the best documented organogenesis of juvenile forms. After reversal of the mantle and following settlement, the anterior lobe flattens and fuses with the dorsal valve (Chuang, 1990). The pattern of early development of the lophophore, however, varies. In *Calloria* (Percival, 1944), *Frenulina* (Mano, 1960), *T. transversa,* and *Hemithiris* (Long, 1964; Long & Stricker, 1991) a subapical groove forms along the midline of the anterior lobe. Anteriorly, an ectodermal infolding forms the stomodaeum, and the lophophoral tentacles develop as two protrusions lateral to the stomodaeum. The tentacle rudiments form a crescent, to which subsequent tentacles are added anteriorly (dorsally) as bilateral pairs, thus forming the taxolophe (Chuang, 1990; Long & Stricker, 1991). In *Frenulina* a thin fold or epistome appears anterior to the stomodaeum at the 4 p.t. stage (Mano, 1960). A number of juveniles of articulated species appear to bypass the

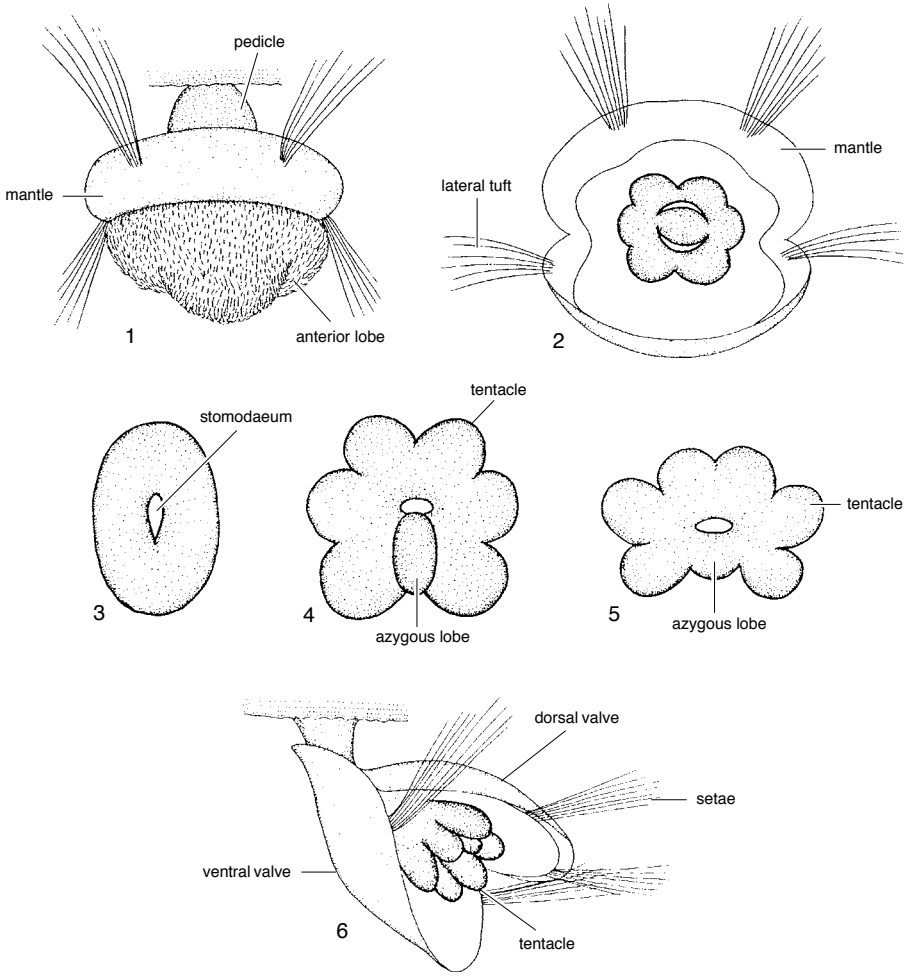

FIG. 179. Stages in the development of the lophophore of *Notosaria nigricans,* showing *1–4,* the differentiation and migration of the azygous lobe, *3–4,* breakthrough of the stomodaeum, and *2, 4–5,* definition of the tentacle rudiments; *6,* young adult viewed dorsally (adapted from Percival, 1960).

taxolophous stage of the trocholophe by the simultaneous development of two or more pairs of tentacles. Four tentacles develop simultaneously in *Lacazella* (LACAZE-DUTHIERS, 1861), and *Argyrotheca* (KOWALEVSKY, 1883) and six develop in *Notosaria* (PERCIVAL, 1960).

In the juvenile of *Notosaria,* the surface of the apical lobe becomes modified into a low, central mound surrounded by a broad margin (Fig. 179). The outline of the margin becomes hexagonal as the rudiments of the first three pairs of tentacles differentiate. The central mound becomes depressed, forming the stomodaeum; and an azygous lobe, which moves into a gap formed at the margin, forms the rudiment of the brachial lip. Additional tentacles are formed simultaneously at both ends of the row of tentacles on each side of the azygous lobe, and the brachial lip enlarges toward the tentacles to form a crescentic flap partially covering the

mouth. Meanwhile, the anterior lobe gradually shortens, flattens dorsoventrally, and spreads itself on the inner surface of the dorsal valve (PERCIVAL, 1960).

The first pair of tentacle rudiments of juvenile *T. retusa* are formed at about the same time as the stomodaeum connects with the stomach. A second pair of tentacles develops dorsally to the first and, when four pairs of tentacles are present, they are arranged in a ring around the mouth to form the trocholophe (FRANZEN, 1969).

Although a few small articulated brachiopods retain the trocholophe in adult stages of growth, the lophophore of most articulated species develops into more complex structures (see the section on the lophophore, p. 98).